Re: May 30th

From: **Mike Hansen** (Mike_Hansen@fd.org)
Sent: Fri 4/04/08 6:15 AM
To: RM Fleming (rmfmd7@hotmail.com)

Dr. Fleming,
That May 30 date was set to get the matter off the trial calender. I am still in negotiations with the government and have received no offer from them on the "general proposal" that I discussed with Mr. Everett. That is what my efforts are geared toward at the present moment. After I receive something, I will forward it to you for your review and gear my efforts to determining the viability of your claims on the fraud count.

Thank you, Mike Hansen

RM Fleming <rmfmd7@hotmail.com>
04/04/2008 07:38 AM

To: Mike Hansen PD corrected <mike_hansen@fd.org>
cc:
Subject: May 30th

Dear Mike,

I hear from the boys that after talking with their mother, I will not be going to prison and that there is a court date for May 30th. PTS in Reno confirms the May 30th date.

Yours,

Dr. Fleming

FW: May 30th

From: **RM Fleming** (rmfmd7@hotmail.com)
Sent: Fri 4/04/08 1:30 PM
To: Mike Hansen PD corrected (mike_hansen@fd.org)
Thank you Mike.

I hope you have a great weekend and have no doubt that my efforts and those of Dr. Harringtons shows there is no basis for fraud.

Yours,

Dr. Fleming

> Subject: Re: May 30th
> To: rmfmd7@hotmail.com
> From: Mike_Hansen@fd.org
> Date: Fri, 4 Apr 2008 08:17:37 -0500
>
> Dr. Fleming,
> That May 30 date was set to get the matter off the trial calender. I
> am still in negotiations with the government and have received no offer
> from them on the "general proposal" that I discussed with Mr. Everett.
> That is what my efforts are geared toward at the present moment. After I
> receive something, I will forward it to you for your review and gear my
> efforts to determining the viability of your claims on the fraud count.
>
> Thank you, Mike Hansen
>
>
>
> RM Fleming
> <rmfmd7@hotmail.c
> om> To
> Mike Hansen PD corrected
> 04/04/2008 07:38 <mike_hansen@fd.org>
> AM cc
>
> Subject
> May 30th
>
>
>
>
>
> Dear Mike,
>
> I hear from the boys that after talking with their mother, I will not be
> going to prison and that there is a court date for May 30th. PTS in Reno
> confirms the May 30th date.
>
> Yours,

>
> Dr. Fleming

Re: Proposed agreements

From: **Mike Hansen** (Mike_Hansen@fd.org)
Sent: Wed 5/14/08 10:40 AM
To: RM Fleming (rmfmd7@hotmail.com)
2 attachments
RF plea a...pdf (245.8 KB), RF Excl. ...pdf (266.1 KB)

Dr. Fleming,
Please review these documents and we will discuss them Monday, May 19
at 9am in the Hruska Courthouse in Omaha.
(See attached file: RF plea agrmt.pdf)(See attached file: RF Excl. agrmt.pdf)

Thanks, Mike Hansen

Re: confidential information-challenging Vickie's dates of employment

From: **Mike Hansen** (Mike_Hansen@fd.org)
Sent: Tue 5/05/09 7:00 AM
To: RM Fleming (rmfmd7@hotmail.com)

With all due respect, you are out of your mind. You need psychological help. I have an appointment out of the office in a jail most of the day. Seriously, we need to talk about getting you some counseling to help you get a grip on reality. You obviously are going to need to see a mental health professional. Take care of yourself, please. You may not think this is legal advice. It is. Your inability to stick with a choice you made, whether it is going to trial or trying to avoid going to prison is a clear sign of mental instability. If you do not do something about this now, there is no way you are going to successfully complete probation. We can discuss what you need to do tomorrow. In the meantime, just relax and try not to think of the Nebraska case.

Mike Hansen

Re: no contest

From: **Mike Hansen** (Mike_Hansen@fd.org)
Sent: Thu 5/14/09 9:29 AM
To: RM Fleming (rmfmd7@hotmail.com)
Judge Kopf will not accept a no contest plea.

If you would have waited for the jury to return a verdict, you would have been convicted of counts 11, 12, and 13. I believe you would have been sent to prison if you would have refused to acknowledge your guilt. Even if you finally came around and admitted that you went into the soy chip study with the best of intentions, but were unable to get 60 participants, panicked and then defrauded Tabor, there is no guarantee that you could have avoided prison. Most everyone that goes to trial and loses goes to prison. At the time you decided to plead guilty, the deal you made with the government was the only real way to avoid going to prison. My understanding is that fact was your key motivator in accepting the deal.

I hope this answers your questions.

Mike Hansen

RM Fleming <rmfmd7@hotmail.com> 05/13/2009 05:48 PM

To: Mike Hansen PD corrected <mike_hansen@fd.org>
cc:
Subject: no contest

Dear Mike,

Am I correct that you told me that Judge Kopf does not accept no contest pleas?

I also understood that if guilty on counts 11-13, that there would definitely have been jail time without a plea deal. Is that also correct?

Dr. Fleming

RE: soy numbers

From: **Mike Hansen** (Mike_Hansen@fd.org)
Sent: Wed 3/18/09 8:46 AM
To: RM Fleming (rmfmd7@hotmail.com)

3 attachments

Maublant.pdf (683.2 KB), Li.pdf (978.8 KB), Eur J Nuc...pdf (432.7 KB)

I have been speaking to Dr. Jay this morning and I think he will be brilliant. Do not contact him!

To answer "Why?": That information will not aid the trier of fact sufficiently to overcome the risk of any statistical opinion blowing up in our face. The jury will only understand "Statistical examination of a set of data cannot 'prove' or 'disprove' falsification of data records" and they will tune the rest out. This information would only be presented to confuse, not clarify anything. A good trial lawyer like the two prosecutors in your case could destroy Kaiser without batting an eye. (I know I could). This would cause the jury to think that all our experts are not credible and you are probably going to get convicted of everything. I have no confidence in this evidence to do anything but be a catalist for conviction.

That being said. We need to figure out what our defense is on the soy counts. My advice is still for you to finally admit that there were not 60 participants and stop this charade. Losing this at trial may cost you everything, while taking this out of play may porvide an opportunity for you to continue to practice medicine. The jury will believe Vicki that there were around 12 participants involved when she stopped working for you. That is nowhere near the 52 that you represented had to have begun the study while Vicki was there most of the day. This the jury will understand and that's enough. Even if Calkins or Rydberg lost your materials. Vicki's testimony along with Tabor getting your exel attachment in from 2-25-04 sinks you.

If you really want to help, print out the attached articles and pinpoint for me the relevant portions (I know I have missed some) that show that the authors believe that the pharmadynamic properties of sestamibi change over time. That mibi does not stick. I want to make sure I haven't missed any relevant passages to impeach their experts.

I also want your opinion if we should share the patient images for the first 10 counts that you sent to me.
(See attached file: Maublant.pdf)(See attached file: Li.pdf)(See attached file: Eur J Nucl Med Article - Crane.pdf)
Mike

RM Fleming
<rmfmd7@hotmail.com>
03/18/2009 10:09 AM

To
Mike Hansen PD corrected <mike_hansen@fd.org>
cc

Subject
RE: soy numbers

Mike,

Why?

Dr. Fleming

> Subject: RE: soy numbers
> To: rmfmd7@hotmail.com
> From: Mike_Hansen@fd.org
> Date: Wed, 18 Mar 2009 09:35:30 -0500
>
> After reading the report, I stand by my position that we are not presenting
> any statistical evidence in our defense on the last three counts. If you
> disagree, hire your our lawyer to present whatever statistical evidence you
> want. End of story.
>
> Mike
>
>

Victoria

From: **RM Fleming** (rmfmd7@hotmail.com)
Sent: Fri 6/06/08 2:50 PM
To: Mike Hansen PD corrected (mike_hansen@fd.org)
Mike,

If I haven't already mentioned it, I think we should get payroll information from the Podiatrist Vickie went to work for after FHHI. Who knows, maybe she was even working two jobs when she was with me. At any rate, since she always complained about needing money, I doubt she waited between jobs and her podiatry payroll checks should dovetail mine.

Dr. Fleming

RE: missing, follow up

From: **RM Fleming** (rmfmd7@hotmail.com)
Sent: Thu 6/05/08 4:25 PM
To: Mike Hansen (mike_hansen@fd.org)
Thank you. I trust you received the information regarding payroll proof of Vicki and Angela's dates of employment.

Soy

From: **RM Fleming** (rmfmd7@hotmail.com)
Sent: Tue 6/24/08 5:07 PM
To: Mike Hansen PD corrected (mike_hansen@fd.org)
Dear Mike,

I understand that you have not meet with Vickie or her daughter yet. I understand the prosecution states both Vickie and her daughter will testify they did not see the patients. That testimony would be true, since they could not have seen the patients since they were not working for me during most of the study. I have sent you payroll information confirming that they did not work at FHHI during most of the study and as suggested this payroll information can also be obtained from the bank. You can demonstrate that Vickie was working elsewhere at the time by verifying her payroll information from her employer. I see no reason to plea guilty simply because the prosecuter made false assumptions about where Vickie and her daughter were employed at the time the study was going on.

Yours,

Dr. Fleming

(No Subject)

From: **RM Fleming** (rmfmd7@hotmail.com)
Sent: Wed 7/16/08 4:59 PM
To: Mike Hansen PD corrected (mike_hansen@fd.org)
Mike,

The simple questions for Victoria and her daughter are as follows:

1) What dates did you work for Dr. Fleming?

2) Where did you work next?

3) What dates did you work there?

Have you obtained the payroll information yet?

Yours,

Dr. Fleming

Perjury

From: **RM Fleming** (rmfmd7@hotmail.com)
Sent: Wed 7/16/08 5:09 PM
To: Mike Hansen PD corrected (mike_hansen@fd.org)
Dear Mike,

Since I have payroll information proving neither Victoria nor her daughter where there for the majority of the soy study, how do you plan to handle any perjured testimony from them?

Dr. Fleming

Tarascio

From: **RM Fleming** (rmfmd7@hotmail.com)
Sent: Sun 12/21/08 5:29 PM
To: Mike Hansen PD corrected (mike_hansen@fd.org)
Mike,

When you get to Vicki, you should ask how the soy issue ever came up. I remember standing in the office with Vicki on the telephone. During the conversation Vicki became more and more shaken up. After she hung up the telephone, I asked her what was up and she said it was Kathy Palmer and Palmer told her that they were either going to get me of Vicki. Vicki's husband had been in jail and the FBI visiting their home made him very nervous. Coercion, coercion, coercion! Vicki tried to give them something to get them off her back. I think this is important along with noting checks were paid bi-weekly and getting Vicki's next employer payroll information. I doubt Angela went immediately to work, but she might have.

Dr. Fleming

Fw: Fleming Exclusion

From: **Mike Hansen** (Mike_Hansen@fd.org)
Sent: Thu 5/21/09 11:56 AM
To: rmfmd7@hotmail.com

1 attachment

Fleming L...pdf (144.1 KB)

----- Forwarded by Mike Hansen/NEF/08/FDO on 05/21/2009 01:55 PM -----

	"Palmer, Kathy M (OIG/OI)" <Kathy.Palmer@oig	
To	.hhs.gov>	"Everett, Alan (USANE)" <Alan.Everett@usdoj.gov>, "Mike Hansen" <Mike_Hansen@fd.org>
	05/20/2009 11:20 AM	
cc		
Subject		FW: Fleming Exclusion

The exclusion agreement was signed on 5/11/09. It is attached. Dr. Fleming will be receiving more detailed information from the office.

Thanks,
Kathy
(See attached file: Fleming Exclusion Agreement 5-11-09.pdf)

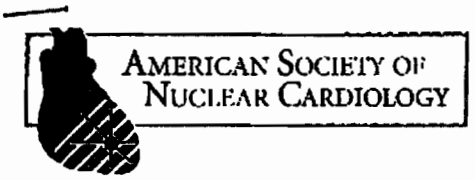

4550 Montgomery Avenue
Suite 780 North
Bethesda, Maryland 20814-3304
Telephone: 301-215-7575
Website: www.asnc.org
Email: admin@asnc.org
Fax: 301-215-7113

June 17, 2009

Richard Fleming, M.D.
6850 Sharlands
#A2001
Reno, NV 89523

Re: American Society of Nuclear Cardiology

Dear Dr. Fleming:

This Notice is to inform you that the Ethics and Discipline Committee of the American Society of Nuclear Cardiology ("ASNC") met on June 8, 2009 and voted to expel you from membership pursuant to Article VI, Section 1(a) of the Bylaws (copy enclosed). The reason for the action is your conviction of the felonies of health care fraud and mail fraud as reflected in the Plea Agreement enclosed with this letter.

Under the Bylaws, you have a right to request a hearing. If you fail to request a hearing by Friday, July 10, 2009, the action of the Ethics and Discipline Committee will become final.

Once the action becomes final, your name will be removed from the membership roles, and you may no longer hold yourself out as, or pretend to be, a member of ASNC.

If you have any questions about this Notice or your right to request a hearing, you or your legal counsel may contact the attorney for ASNC, Mr. James Lynch. He can be reached at (618) 465-1264.

Sincerely,

Steven D. Carter

Steven D. Carter
Executive Director

cc: James B. Lynch, Esq.

Enclosures: (1) ASNC Bylaws
(2) Plea Agreement

RE: further question

From: **RM Fleming** (rmfmd7@hotmail.com)
Sent: Mon 7/20/09 3:35 PM
To: Mike Hansen PD corrected (mike_hansen@fd.org)
Mike,

I still don't understand what you did to fake your data from my real data and why the Judge was upset with you and what he was talking about when he said he wasn't going to let you become a witness nor withdraw from the case. How did you fake the data and why would you have had to withdraw from the case as my attorney?

Dr. Fleming

> Subject: Re: further question
> To: rmfmd7@hotmail.com
> From: Mike_Hansen@fd.org
> Date: Mon, 20 Jul 2009 08:49:31 -0500
>
> Here are the top three:
>
> 3. The draft report totally impeached the credibility of Dr. Carriquiry
> effectively eliminating any possibility of complete aquital.
> 2. The draft report showed that anyone could create valid data from a
> valid representative sample.
> and the number 1 reason why I was upset
> 1. YOU gave the draft report to the government and they would have never
> gotten it but for your exceptional arrogance and ignorance.
>
> I hope this clarifies the matter for you.
>
> Mike
>
>
>
> From: RM Fleming <rmfmd7@hotmail.com>
>
> To: Mike Hansen PD corrected <mike_hansen@fd.org>
>
> Date: 07/17/2009 04:36 PM
>
> Subject: further question
>
>
> Dear Mike,
>
> What was the issue and why were you upset that the Judge called you before
> the bench when he discovered that you had made falsified data using my real
> soy data?
>
> Dr. Fleming
>

May 13 02 02:50p Goracke Ritterbush & Pio (402)896-1726 p.1

Goracke, Ritterbush & Piotrowski, L.L.P.
Certified Public Accountants
5010 South 118th Street, Suite 100 • Omaha, Nebraska 68137-2208
Telephone (402)-896-1500
Fax (402)-896-1726

Fax No. (402) 896-1726

FACSIMILE TRANSMITTAL

TO: Vicky
FROM: Clare
DATE: 5-13-02
RE: Payroll
NO. OF PAGES (INCLUDING THIS PAGE) 3
MESSAGE:
Vicky, Enclosed is your payroll report for the period ended April 26, 2002 The second page is a summary of your future payroll checks Call if you have questions Clare.

IF YOU HAVE ANY PROBLEMS RECEIVING ALL PAGES, PLEASE CALL (402) 896-1500. THANK YOU.

Fleming Heart & Health Institute Payroll
5/13/2002

	Kim	Vicky	John
Gross Wages	$ 1,680.00	$ 461.52	$90.00
Insurance	$ 202.75	$ -	-
FICA	113.00	35.30	6.88
Fed w/h	160.00	22.00	0.00
State w/h	48.00	6.60	0.00
Net payroll	$ 1,359.00	$ 397.62	$83.12
	Married 0 dependents	Married 0 dependents	Single 0 dependents

Fleming Heart & Health Institute
Pay History - Victoria M Terescio

	Per Pay Period			Totals	
Date Effective	Cash	Medical Insurance	Per Pay Period (26 pay periods)	Per Annum (2,080 hours)	Per Hour
5/8/2002	1,538.46	-	1538.46	40,000.00	19.23

FICA	117.69
Fed W/H	169.00
State	50.70
Net payroll	$1,201.07

						BALANCE 831762
1997	2-8-01	Meyer Der Blum	500			826762
1998	"	Hy-Vee	57870			
1999	"	[illegible]	6000			
	2-9-01	[illegible]	600.00			
2000	"	Aquila	50000			202892
2001	2-12-01	Pablo	1800			
[illegible]	"	3-04 Dist			36424	235516
2002	2-13-01	IRS	3500			
2003	"	[illegible]	2500			
2004	"	[illegible]	480 09			
2005	"	[illegible]	840			
[illegible]	"	[illegible]	8000			411 07
2006	2-14-01	Nicole	3800			
2007	"	Wal-Mart	31 55			
2008	2-15-01	Meyer Der Qu	500			

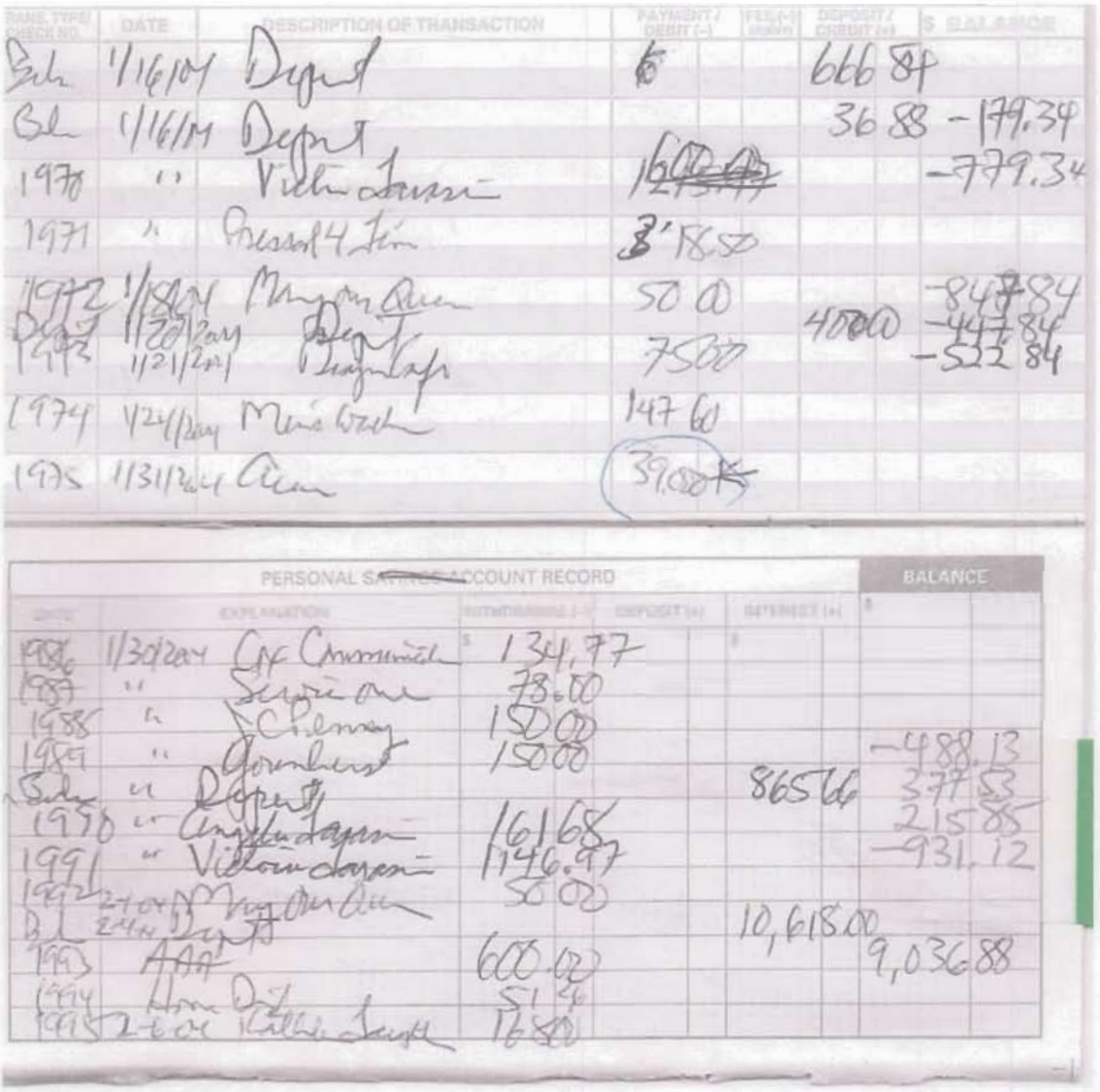

Subject: Re: Soy chip shipment
Date: Wednesday, January 7, 2004 11:54 AM
From: rfmd1@fhhi.omhcoxmail.com <rfmd1@fhhi.omhcoxmail.com>
Reply-To: "rfmd1@fhhi.omhcoxmail.com" <rfmd1@fhhi.omhcoxmail.com>
To: Dr Tabor <drtabor@soy.MD>

Yes and we are ready to go.

-------*Original Message*-------

From: Dr Tabor <mailto:drtabor@soy.MD>
Date: Wednesday, January 07, 2004 10:42:36
To: Richard Fleming MD <mailto:rfmd1@fhhi.omhcoxmail.com>
Cc: Tod Dauler <mailto:toddauler@revivalsoy.com>
Subject: Soy chip shipment

Dr. Fleming: Is this where we ship the soy chips?

The Camelot Foundation

9290 West Dodge Road, Suite 204

Omaha, NE 68114

Tele: (402) 343-0800

Fax: (402) 343-0900

Rfmd1@fhhi.omhcoxmail.com

Subject: Re: Soy chip shipment
Date: Wednesday, January 7, 2004 11:48 AM
From: Dr Tabor <drtabor@soy.MD>
To: Richard Fleming MD <rfmd1@fhhi.omhcoxmail.com>

Good -- start recruiting heavily -- we can give them the "healthy diet" advice at the second visit when they pick up their soy chips — Avon may want other advice than just "avoid sugar drinks and reduce fat" -- we really need to show a good weight loss with this, so if we choose based on the right inclusion criteria I think the weight loss will be substantial -- you can go ahead with the 1 week load in chips will be to you by Monday morning! We will send a pallet or two -- let us know as you need more (3 day turnaround shipping). Thanks!!

Yes and we are ready to go.

-------*Original Message*-------

From: Dr Tabor <mailto:drtabor@soy.MD>
Date: Wednesday, January 07, 2004 10:42:36
To: Richard Fleming MD <mailto:rfmd1@fhhi.omhcoxmail.com>
Cc: Tod Dauler <mailto:toddauler@revivalsoy.com>
Subject: Soy chip shipment

Dr. Fleming: Is this where we ship the soy chips?

The Camelot Foundation

9290 West Dodge Road, Suite 204

Omaha, NE 68114

Tele: (402) 343-0800

Fax: (402) 343-0900

Rfmd1@fhhi.omhcoxmail.com

10 - ICD-9-CM Diagnosis and Procedure Codes
(Rev. 1472, Issued: 03-06-08, Effective: 05-23-07, Implementation: 04-07-08)

ICD-9-CM and its "Official ICD-9-CM Guidelines for Coding and Reporting" have been selected as the approved coding set for entities covered under the Health Insurance Portability and Accountability Act (HIPAA) for reporting diagnoses and inpatient procedures. This requires the use of ICD-9-CM and its official coding and reporting guidelines by most health plans (including Medicare) by October 16, 2002. The Administrative Simplification Act of 2001, however, permits plans and providers to apply for an extension until October 16, 2003.

The "Official ICD-9-CM Guidelines for Coding and Reporting" provides guidance on coding. The "ICD-9-CM Coding Guidelines for Outpatient Services," which is part of the "Official ICD-9-CM Guidelines for Coding and Reporting," provides guidance on diagnosis coding specific to outpatient facilities and physician offices.

Proper coding is necessary on Medicare claims because codes are generally used to assist in determining coverage and payment amounts.

A ICD-9-CM Diagnosis Codes

The CMS accepts only ICD-9-CM diagnostic and procedural codes that use definitions contained in DHHS Publication No. (PHS) 89-1260 or CMS approved errata and supplements to this publication. The CMS approves only changes issued by the Federal ICD-9-CM Coordination and Maintenance Committee. Diagnosis codes must be full ICD-9-CM diagnoses codes, including all five digits where applicable.

Diagnosis coding changes for Volume 1 and 2 are approved annually by a Federal committee. The changes take effect each year October 1. Volume 3 is revised annually by CMS. Updates include:

- Addition of new codes;
- Deletion of old codes; and
- Revisions to descriptions of codes.

Rules for reporting diagnosis codes on the claim are:

- Use the ICD-9-CM code that describes the patient's diagnosis, symptom, complaint, condition or problem. Do not code suspected diagnosis.

- Use the ICD-9-CM code that is chiefly responsible for the item or service provided.

- Assign codes to the highest level of specificity. Use the fourth and fifth digits where applicable.

- Code a chronic condition as often as applicable to the patient's treatment.

- Code all documented conditions that coexist at the time of the visit that require or affect patient care or treatment. (Do not code conditions that no longer exist.)

Claims submitted to the carrier on Form CMS-1500 or its electronic equivalent must have a diagnosis code to identify the patient's diagnosis/condition (item 21). All physician and nonphysician specialties (e.g., PA, NP, CNS, CRNA) must use an ICD-9-CM code number and code to the highest level of specificity. Up to four codes may be submitted
in priority order (primary, secondary condition). An independent laboratory is required to enter a diagnosis only for limited coverage procedures.

All narrative diagnoses for nonphysician specialties must be submitted on an attachment.

Inpatient claims submitted to the intermediary on Form CMS-1450 or its electronic equivalent must have a principal diagnosis. For inpatient claims, the provider reports the principal diagnosis in the appropriate form locator. The principal diagnosis is the condition established after study to be chiefly responsible for the admission. Even though another diagnosis may be more severe than the principal diagnosis, the principal diagnosis, as defined above, is entered. Entering any other diagnosis may result in incorrect assignment of a DRG and an overpayment to a hospital under PPS.

The physician should code the ICD-9-CM code that provides the highest degree of accuracy and completeness. In the context of ICD-9-CM coding, the "highest degree of specificity" refers to assigning the most precise ICD-9-CM code that most fully explains the narrative description of the symptom or diagnosis. Concerning level of specificity, ICD-9-CM codes contain either 3, 4, or 5-digits. If a 3-digit code has 4-digit codes which further describe it, then the 3-digit code is not acceptable for claim submission. If a 4-digit code has 5-digit codes which further describe it, then the 4-digit code is not acceptable for claim submission.

For electronically submitted DMEPOS claims, a valid diagnosis code, which most fully explains the patient's diagnosis, is required. The CMS understands that physicians may not always provide suppliers of DMEPOS with the most specific diagnosis code, and may provide only a narrative description. In those cases, suppliers may choose to utilize a variety of sources to determine the most specific diagnosis code to include on the individual line items of the claim. These sources may include, but are not limited to: coding books and resources, contact with physicians or other health professionals, documentation contained in the patient's medical record, or verbally from the patient's physician or other healthcare professional.

Beneficiaries are not required to submit ICD-9 codes on beneficiary-submitted claims. Beneficiary-submitted claims are filed on Form CMS-1490S. For beneficiary-submitted claims, the carrier must develop the claim to determine a current and valid ICD-9 code and may enter the code on the claim.

EXAMPLE: A patient is referred to a radiologist for a chest x-ray because of a cough. The result of the chest x-ray indicates the patient has pneumonia. During the performance of the diagnostic test, it was determined that the patient has hypertension and diabetes mellitus. The interpreting physician reports a primary diagnosis of pneumonia. The interpreting physician may report the hypertension and diabetes mellitus as secondary diagnoses.

10.1.5 - Diagnostic Tests Ordered in the Absence of Signs and/or Symptoms

(Rev. 1, 10-01-03)

When a diagnostic test is ordered in the absence of signs/symptoms or other evidence of illness or injury, the testing facility or the physician interpreting the diagnostic test should report the screening code as the primary diagnosis code. Any condition discovered during the screening should be reported as a secondary diagnoses.

10.1.6 - Use of ICD-9-CM to the Greatest Degree of Accuracy and Completeness

(Rev. 1, 10-01-03)

The following longstanding coding guidelines are part of "Official ICD-9-CM Guidelines for Coding and Reporting."

The testing facility or the interpreting physician should code the ICD-9-CM code that provides the highest degree of accuracy and completeness for the diagnosis resulting from test, or for the sign(s)/ symptom(s) that prompted the ordering of the test.

The "highest degree of specificity means assigning the most precise ICD-9-CM code that most fully explains the narrative description in the medical chart of the symptom or diagnosis.

EXAMPLE 1: A chest x-ray reveals a primary lung cancer in the left lower lobe. The interpreting physician should report the ICD-9-CM code as 162.5 for malignancy of the left "lower lobe, bronchus or lung," not the code for a malignancy of "other parts of bronchus or lung" (162.8) or the code for "bronchus and lung unspecified" (162.9).

EXAMPLE 2: If a sputum specimen is sent to a pathologist and the pathologist confirms growth of "streptococcus, type B" which is indicated in the patient's medical record, the pathologist should report a primary diagnosis as 482.32 (Pneumonia due to streptococcus, Group B). However, if the pathologist is unable to specify the organism, then the

pathologist should report the primary diagnosis as 486 (Pneumonia, organism unspecified).

Technetium-99m-Sestamibi Myocardial Perfusion Imaging in Detection of Coronary Artery Disease: Comparison Between Initial (1-Hour) and Delayed (3-Hour) Postexercise Images

Raymond Taillefer, Marie Primeau, Paolo Costi, Raymond Lambert, Jean Léveillé, and Yves Latour

Department of Nuclear Medicine and Division of Cardiology, Hôpital Hôtel-Dieu de Montréal, Université de Montréal, Canada

Technetium-99m-sestamibi, a new myocardial perfusion imaging agent, does not show significant or rapid myocardial redistribution following its intravenous injection at stress. The purpose of this study was to evaluate the myocardial clearance of ^{99m}Tc-sestamibi and ischemic/normal wall ratios at 1 hr and at 3 hr after injection at stress in patients with significant coronary artery disease. Twenty-five patients with ischemic defects on ^{201}Tl scans (n = 15) and/or significant disease on coronary angiogram (n = 18) were prospectively studied. Planar images were obtained at 65 and at 190 min after an injection at stress of 20–25 mCi of ^{99m}Tc-sestamibi. A rest study was performed 1–6 days later. Ischemic/normal wall ratios were 0.73 ± 0.10 and 0.83 ± 0.12 ($p < 0.05$) at 1 and 3 hr, respectively (0.98 ± 0.15 at rest). Myocardial washout was 26% ± 12% for normal walls and 15% ± 8% for ischemic walls ($p < 0.001$). Segmental analysis showed 48 and 46 ischemic segments at 1 and 3 hr, respectively. In conclusion, although only a few ischemic segments were missed at 3 hr, significantly lower ischemic/normal wall ratios were found at 1 hr. Faster myocardial washout from normal walls is responsible for the partial reduction of this ratio.

J Nucl Med 1991; 32:1961–1965

Thallium-201 myocardial perfusion scintigraphy is recognized as a useful clinical procedure for the evaluation of patients with coronary artery disease (*1–4*). However, although its value as a diagnostic test has been well established, ^{201}Tl-chloride presents some disadvantages. Its physical and biologic characteristics are not ideal for imaging purposes. The development of a myocardial perfusion agent labeled with ^{99m}Tc is attractive because of the physical advantages of ^{99m}Tc over ^{201}Tl. The ^{99m}Tc-hexakisaliphatic isonitriles (*5*) have shown interesting properties as myocardial perfusion agents. At the present time, three isonitriles analogs have been the subject of more detailed evaluation in humans: ^{99m}Tc-TBI (t-butyl isonitrile) (*6*), ^{99m}Tc-CPI (carbomethoxy isopropyl isonitrile) (*7–8*) and ^{99m}Tc-sestamibi (methoxy isobutyl isonitrile) (*9–18*). Because of more favorable biologic characteristics, including rapid lung and liver clearance and slow myocardial washout, ^{99m}Tc-sestamibi is the most interesting of these agents.

Like ^{201}Tl, the myocardial distribution of ^{99m}Tc-sestamibi reflects the coronary blood flow (*19–25*). Besides advantages related to the physical characteristics of ^{99m}Tc, one interesting property of ^{99m}Tc-sestamibi is that there is no significant myocardial redistribution after its administration. This property gives a good scheduling flexibility for imaging which is particularly useful in the evaluation of acute conditions such as thrombolysis for acute myocardial infarction (*26*) or unstable angina (*27*). Patients can be stabilized before diagnostic imaging. Previous studies have reported a time interval between ^{99m}Tc-sestamibi injection and myocardial imaging varying from 30 min to 6 hr (*28–30*). However, there are few data available on the difference between early and late ^{99m}Tc-sestamibi imaging for detection of ischemic disease (*31*). The purpose of this study was to evaluate the myocardial clearance of both normal and abnormal walls and ischemic/normal wall ratios at 1 hr and 3 hr after ^{99m}Tc-sestamibi injection at stress in patients with coronary artery disease.

METHODS

Patient Population

Twenty-five patients (23 males, 2 females) with ischemic defects on ^{201}Tl myocardial perfusion imaging and/or significant coronary artery disease on coronary angiography were prospectively studied. The mean age was 57 yr (with a range from 36 to 75 yr). Since it is reported that ^{99m}Tc-sestamibi does not significantly redistribute, all patients were submitted to two separate injections, one at stress and one at rest a few days later. Written informed consent, approved by the ethics committee of our institution, was obtained from each patient. Patients with recent

Received Jan. 23, 1991; revision accepted Apr. 4, 1991.
For reprints contact: Dr. Raymond Taillefer, MD, Nuclear Medicine Department, Hôtel-Dieu de Montréal, 3840 St. Urbain St., Montreal, Quebec, Canada H2W 1T8.

myocardial infarction (less than 4 wk), unstable angina, congestive heart failure or symptomatic known valvular heart disease were excluded from the study.

Technetium-99m-Sestamibi Myocardial Study

Within a week, all patients had two ^{99m}Tc-sestamibi injections, the first with injection at stress and the second at rest. There was an interval of at least 24 hr between the two injections. Cardiovascular drugs were discontinued 24–48 hr prior to the injection. Patients were asked to fast after midnight. An intravenous line with NaCl 0.9% solution was started in an antecubital vein. Patients were exercised on a treadmill according to the Bruce protocol until they reached 85% of the age-predicted maximal heart rate or developed angina, shortness of breath, hypotension or arrhythmias. One minute before the end of the stress test, a dose of 20 mCi of ^{99m}Tc-sestamibi per 70 kg of body weight was injected. Patients drank two glasses of whole milk within 45 min after the ^{99m}Tc-sestamibi injection to accelerate hepatobiliary clearance.

The rest injection was performed after the patient rested for at least 15 min, with a dose of 25 mCi of ^{99m}Tc-sestamibi flushed with 10 cc of NaCl 0.9% solution.

Technetium-99m-Sestamibi Data Acquisition

Myocardial planar imaging was performed 1 and 3 hr after ^{99m}Tc-sestamibi stress injection with a small field of view scintillation camera using a low-energy, high-resolution parallel-hole collimator. The camera was interfaced to a medical data system (MDS) computer. The first image acquired was the best septal view (usually the 45° left anterior oblique view) followed by the anterior and left lateral view right decubitus. Ten-minute images were acquired for each view with the photopeak set at 140 keV with a 15% energy window. Digital images were recorded using 128 × 128 matrix. The same acquisition parameters were used for delayed (3-hr) imaging. Special care was taken to obtain exactly the same views and angles acquired for the 1-hr images. Imaging at rest was performed 90 min following ^{99m}Tc-sestamibi injection. The same gamma camera and acquisition parameters were used for the rest study. Again, the same views as the stress study were obtained.

Data Analysis

Qualitative Analysis. All myocardial ^{99m}Tc-sestamibi studies were analyzed by three experienced observers without prior knowledge of the patient's history, stress electrocardiogram, ^{201}Tl scan result or coronary anatomy. Disagreements in interpretation were resolved by consensus. Sets of rest-stress (1-hr) and rest-stress (3-hr) ^{99m}Tc-sestamibi images were interpreted separately. For the initial reading, observers did not know which images were performed at 1 or 3 hr following stress ^{99m}Tc-sestamibi injection. On the second reading, both stress studies (1 and 3 hr) were placed side by side for comparative analysis. The left ventricle was divided into three segments in each image. Segments were characterized as normal, ischemic or scar based on a normal myocardial distribution, transient defect or fixed defect, respectively. The observers also attempted to compare subjectively the diagnostic information of the 1-hr and the 3-hr stress images. This comparison takes into consideration only the subjective evaluation of normal-to-abnormal myocardial wall ratios and the diagnostic certainty of the images. The three sets of images (stress 1-hr, stress 3-hr, and rest study) were normalized to the maximal myocardial activity.

Quantitative Analysis. After visual analysis of ^{99m}Tc-sestamibi images and correlation with ^{201}Tl scan and/or coronary angiography results, ischemic/normal wall ratios were determined from the best view showing the ischemic defect. Regions of interest on normal and ischemic myocardial segments were drawn on the computer screen. The same regions (location and surface) and the same walls were chosen for each of the three studies (rest, stress 1-hr and stress 3-hr) in a given patient. A region of interest for the background was chosen over the left lung. Fixed myocardial defects were not included for analysis.

Segmental myocardial time-activity curves were obtained for both ischemic and normal walls and corrected for ^{99m}Tc physical decay. Myocardial washout between 1 and 3 hr was determined from these curves for both normal and abnormal walls.

Statistical Analysis

All data are presented as the mean ± 1 s.d. The Student's t-test for paired measures was used to assess differences between data.

RESULTS

Patient Population

Out of the 25 patients, 15 had a previous ^{201}Tl study with at least one ischemic segment and 18 had a coronary angiogram with significant coronary artery disease defined as a ≥70% reduction in the luminal diameter of one or more major coronary arteries. Eight patients had both ^{201}Tl testing and a coronary angiogram. The mean time interval between ^{99m}Tc-sestamibi scintigraphy and coronary angiogram was 12 days (with a range of 1–32 days) and the mean time interval between the ^{99m}Tc-sestamibi imaging and ^{201}Tl study was 14 days (with a range of 1–34 days). The mean time between both rest and stress ^{99m}Tc-sestamibi injection was 2.2 ± 1.6 days (with a range of 1–6 days).

The hemodynamic parameters during the treadmill stress test with ^{99m}Tc-sestamibi injection were the following: maximal heart rate: 130 ± 22 bpm, maximal systolic blood pressure: 162 ± 28 mmHg, double product: 21,000 ± 6,100. Patients reached 79% ± 11% of the maximal predicted heart rate. Eight patients had a previous myocardial infarction. On coronary angiogram, 5 patients had single-vessel disease, 11 had double-vessel disease and 2 had triple-vessel disease.

The stress ^{99m}Tc-sestamibi images were obtained at 66 ± 10 min (initial imaging) and at 192 ± 12 min (delayed imaging) following the injection performed 60 sec before the end of exercise. Imaging was done at 90 ± 20 min after the ^{99m}Tc-sestamibi rest injection.

Qualitative Analysis

Two qualitative readings were performed by the three observers. The first blinded reading involved the segmental comparison between initial and delayed post-exercise images. The 1-hr postexercise imaging showed 48 ischemic, 12 scar and 165 normal segments, while the 3-hr post-exercise images detected 46 ischemic, 12 scar and 167 normal segments. There was no significant statistical difference between these values. Following the initial reading,

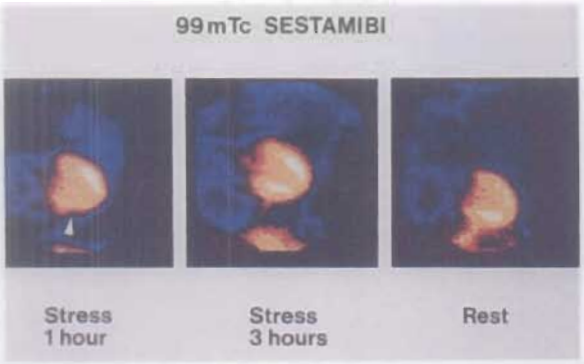

FIGURE 1. Three planar anterior views (stress 1-hr, stress 3-hr and at rest) obtained in a pateint with a 95% stenosis of the right coronary artery. Images were normalized to the maximal myocardial activity. One hour after the injection of ^{99m}Tc-sestamibi at stress, there is a defect involving the inferior wall (arrow). Two hr later (stress 3-hr image) there is a redistribution of ^{99m}Tc-sestamibi, the myocardial defect being almost completely corrected. The rest study shows a normal inferior wall radionuclide uptake.

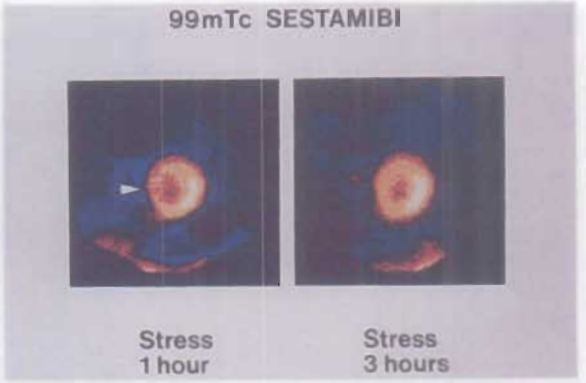

FIGURE 3. These two 45° left anterior oblique images were obtained in a patient with a 95% stenosis of the left anterior descending artery. The septal wall defect (arrow) clearly seen at 1 hr after ^{99m}Tc-sestamibi injection at stress shows a mild partial correction at 3 hr.

the 1 and 3-hr postexercise and rest images were placed side by side for subjective comparison on the diagnostic quality of the images. This comparison showed that the 1-hr postexercise images were superior to the 3-hr images in 15 patients, while they were judged to be similar in 10 patients (Figs. 1–3). In no cases were the 3-hr postexercise images judged to be better than the images obtained at 1 hr after the injection at stress.

Quantitative Analysis

Figure 4 shows the ischemic/normal wall ratios obtained for the same myocardial regions of interest at 1 and 3 hr after stress ^{99m}Tc-sestamibi injection and at 90 min after injection at rest. Fixed defects were excluded from this analysis. The mean ratio at 1 hr and at 3 hr after stress injection was 0.73 ± 0.10 and 0.83 ± 0.12, respectively. This difference was statistically significant ($p < 0.05$). These two postexercise ischemic/normal wall ratios were also statistically different from the ischemic/normal wall ratio at rest which was 0.98 ± 0.15 ($p < 0.05$). The rate of clearance of ^{99m}Tc-sestamibi between the 1-hr and the 3-hr stress images was determined for both normal and ischemic myocardial walls. The net clearance was 26% ± 12% for myocardial walls with normal perfusion and 15% ± 8% for ischemic walls ($p < 0.001$).

DISCUSSION

For many years, the relatively rapid myocardial redistribution of ^{201}Tl has been considered to be an advantage since difference between ischemia and scar may be

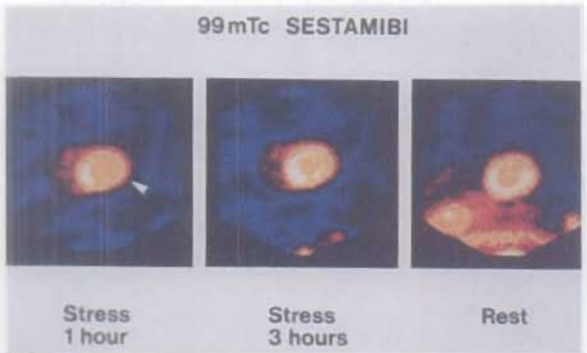

FIGURE 2. Patient with a 90% stenosis of the left circumflex artery. On the 45° left anterior oblique view, there is a significant perfusion defect of the lateral wall (arrow) 1 hr after the injection of ^{99m}Tc-sestamibi at stress. This defect is partially corrected 2 hr later (stress 3 hr). Normal myocardial uptake of ^{99m}Tc-sestamibi at rest.

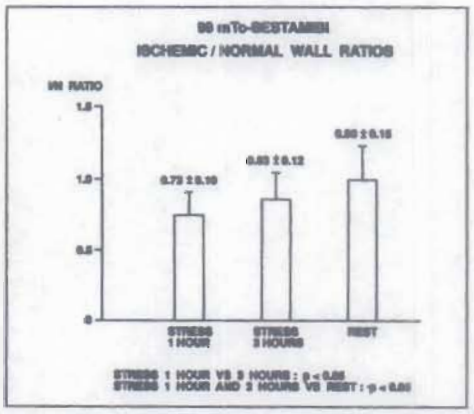

FIGURE 4. Ischemic/normal wall ratios obtained for the same myocardial regions of interest at 1 and 3 hr after injection of ^{99m}Tc-sestamibi at stress and at 90 min after injection at rest.

achieved with a single injection of the radionuclide. However, recent data showed that reinjection at rest or 24-hr delayed imaging is necessary in a significant number of patients in order to obtain better results in myocardial viability assessment (*32–35*). Although ^{201}Tl and ^{99m}Tc-sestamibi have a myocardial distribution which is proportional to coronary blood flow, all other biologic and physical characteristics are different. One of the most important differences in the pharmacokinetics of the two radiopharmaceuticals is the lack of significant or rapid myocardial redistribution of ^{99m}Tc-sestamibi following its intravenous injection at stress. This characteristic offers interesting advantages. Timing of imaging after the injection is not as critical as with ^{201}Tl. This property is particularly well suited for radionuclide imaging in the evaluation of acute conditions such as thrombolysis for acute myocardial infarction or unstable angina. Following ^{99m}Tc-sestamibi administration and usual medical therapy, imaging is performed when the patient's condition is stabilized. Furthermore, the absence of significant change in the myocardial activity during acquisition is preferable for optimal SPECT imaging.

According to data obtained in a Phase II clinical trial with ^{99m}Tc-sestamibi (*18*), the best compromise between a high myocardial count rate and low background activity (decreased liver and lung uptake) is achieved between 1 and 2 hr following the injection of ^{99m}Tc-sestamibi at stress. Most of the clinical studies using this new radiopharmaceutical have reported a time interval with a range from 1 to 3 hr between injection and imaging, although some others have used an interval up to 6 hr (*28–30*). This has been particularly reported in the evaluation of thrombolysis or unstable angina where stabilization of the patient's condition is a critical factor.

The results of our study showed that although there was no significant statistical difference in the diagnostic accuracy between the 1- and 3-hr post-stress images, the ischemic/normal wall ratios were statistically higher at 3 hr (0.84) than at 1 hr (0.73). This may affect the diagnostic certainty and possibly the sensitivity of coronary artery disease detection in cases where the ischemic defect is slight or mild. This partial correction of the ischemic/normal wall ratio over time is related to a differential myocardial net clearance, the normally perfused walls showing a significantly faster clearance (26%) than the ischemic myocardial walls (15%) at 3 hr after the injection at stress. Although the time-activity myocardial curves obtained in this study represented a global myocardial washout over time, it was impossible to determine the presence or the relative role of a washin compartment. The net clearance is thus probably more appropriate than the term myocardial washout in this condition. In an animal model of myocardial ischemia, Okada et al. (*24*) reported a similar rate of ^{99m}Tc-sestamibi washout from both normal and ischemic areas. The ischemic/normal wall activity ratio was the same over a 4-hr period. Our results differ from that study probably because a permanent occlusion model has been used instead of a transient ischemia as seen in our patient population.

Franceschi et al. (*31*), reported similar findings in a group of nine patients studied with SPECT imaging at 20 min, 1, 2, 4 and 6 hr after injection of 25–30 mCi of ^{99m}Tc-sestamibi at stress. They have found significant differences between the clearance rates from normal and ischemic myocardium. The ^{99m}Tc-sestamibi washout from normal myocardium was 27% ± 8% at 6 hr after injection and 16% for ischemic myocardial defects. The ischemic/normal wall ratio increased with time for both mild and severe defects: 0.70 at 20 min, 0.80 at 4 hr and 0.84 at 6 hr. Reperfusion was more obvious at 4–6 hr. Their data, however, did not indicate if the sensitivity of coronary artery disease detection was decreased by late imaging. Their data were acquired on slices of the heart obtained with SPECT imaging, which provides better contrast resolution. Our study was performed with planar imaging. Because of the inherent limitations related to planar acquisition ("shine-through" and "overlapping" activity secondary to hyperemic response surrounding the ischemic defect), the effects of redistribution can possibly be more obvious than with SPECT imaging.

Based on the above-mentioned results, ^{99m}Tc-sestamibi imaging should be performed no later than 1–1.5 hr following the injection at stress in order to avoid the effect of myocardial redistribution on the diagnosis of coronary artery disease. This limitation does not represent a significant drawback in clinical practice for stress test imaging. However, the impact of ^{99m}Tc-sestamibi myocardial redistribution should be evaluated when this agent is used in the risk assessment and effect of thrombolytic therapy in patients with acute myocardial infarction. Some studies have reported a time interval of up to 6 hr between ^{99m}Tc-sestamibi injection and imaging in this acute condition, mainly for practical (injection performed during the night) and medical (patient's stabilization) considerations. Theoretically, in the presence of myocardial redistribution, such delay may cause an underestimation of the myocardium at risk (initial defect).

This study has used a time interval of 1 hr between ^{99m}Tc-sestamibi injection at stress and imaging as the reference. Although most of the clinical studies have reported a time interval varying from 1 to 2 hr (which offers the best compromise between good count rate and low background activity), it should be useful to evaluate the diagnostic impact and compare images performed at 15–30 min to images obtained later after the injection.

In conclusion, although only a few ischemic segments were missed at 3 hr, significantly lower ischemic/normal wall ratios were found at 1 hr. Faster myocardial washout from normal walls is responsible for the partial correction of this ratio. It is thus preferable to image earlier after ^{99m}Tc-sestamibi injection at stress in order to improve detection of coronary artery disease.

ACKNOWLEDGMENTS

The authors gratefully acknowledge the valuable help of Anne-Marie Dufort, Marc Dumont, the audiovisual service, and the nuclear medicine technologists of Hôtel-Dieu de Montréal.

REFERENCES

1. Pohost GM, Zir LM, Moore RM, McKusik KA, Guiney TE, Beller GAA. Differentiation of transiently ischemic from infarcted myocardium by serial imaging after a single dose of thallium-201. *Circulation* 1979;55:294–302.
2. Okada RD, Boucher CA, Strauss HW, Pohost GM. Exercise radionuclide imaging approaches to coronary artery disease. *Am J Cardiol* 1980;46:1188–1204.
3. Brown KA, Boucher CA, Okada RD, et al. Prognostic value of exercise thallium-201 imaging in patients presenting for evaluation of chest pain. *J Am Coll Cardiol* 1983;4:994–1001.
4. Gibson RS, Watson DD, Craddock GB, et al. Prediction of cardiac events after uncomplicated myocardial infarction: a prospective study comparing predischarge exercise thallium-201 scintigraphy and coronary angiography. *Circulation* 1983;68:321–336.
5. Jones AG, Abrams MJ, Davison A, et al. Biological studies of a new class of technetium complexes: the hexakis (alkylisonitrile) technetium (I) cations. *Int J Nucl Med Biol* 1984;11:225–234.
6. Holman BL, Jones AG, Lister-James J, et al. A new Tc-99m-labeled myocardial imaging agent, hexakis (T-butyl-isonitrile), technetium (I) (Tc-99m-TBI): initial experience in the human. *J Nucl Med* 1984;25:1350–1355.
7. Holman BL, Sporn V, Jones AG, et al. Myocardial imaging with technetium-99m-CPI: initial experience in the human. *J Nucl Med* 1987;28:13–18.
8. Sia STB, Holman BL, Campbell S, et al. The utilization of technetium-99m-CPI as a myocardial perfusion imaging agent in exercise studies. *Clin Nucl Med* 1987;12:681–687.
9. Kahn J, McGhie I, Akers M, et al. Quantitative rotational tomography with ^{201}Tl and ^{99m}Tc-2-methoxy-isobutyl isonitrile: a direct comparison in normal individuals and patients with coronary artery disease. *Circulation* 1989;79:1282–1293.
10. Iskandrian A, Heo J, Kong B, Lyons E, Marsh S. Use of technetium-99m-isonitrile (RP-30A) in assessing left ventricular perfusion and function at rest and during exercise in coronary artery disease and comparison with coronary arteriography and exercise thallium-201 SPECT images. *Am J Cardiol* 1989;64:270–275.
11. Kiat H, Maddahi J, Roy L, et al. Comparison of technetium-99m-methoxy-isobutyl-isonitrile and thallium-201 for evaluation of coronary artery disease by planar and tomographic methods. *Am Heart J* 1989;117:1–11.
12. Larock MP, Cantineau R, Legrand V, Kulbertus H, Rigo P. ^{99m}Tc-MIBI (RP-30) to define the extent of myocardial ischemia and evaluate ventricular function. *Eur J Nucl Med* 1990;16:223–230.
13. Najm YC, Maisey MN, Clarme SM, Fogelman I, Curry PVL, Sowton E. Exercise myocardial perfusion scintigraphy with technetium-99m-methoxy isobutyl isonitrile: a comparative study with thallium-201. *Int J Cardiol* 1990;26:93–102.
14. Sinusas AJ, Beller GA, Smith WH, Vinson EL, Brookeman V, Watson DD. Quantitative planar imaging with technetium-99m-methoxy isobutyl isonitrile: comparison of uptake patterns with thallium-201. *J Nucl Med* 1989;30:1456–1463.
15. Stirner H, Buell V, Kleinhaus E, Bares R, Grosse W. Myocardial kinetics of ^{99m}Tc-hexakis - (2-methoxy-isobutyl-isonitrile) (HMIBI) in patients with coronary heart disease: a comparative study versus ^{201}Tl with SPECT. *Nucl Med Commun* 1988;9:15–23.
16. Taillefer R, Dupras G, Sporn V, et al. Myocardial perfusion imaging with a new radiotracer, technetium-99m-hexamibi (methoxy isobutyl isonitrile): comparison with thallium-201 imaging. *Clin Nucl Med* 1989;14:89–96.
17. Taillefer R, Lambert R, Dupras G, et al. Clinical comparison between thallium-201 and Tc-99m-methoxy isobutyl isonitrile (hexamibi) myocardial perfusion imaging for detection for of coronary artery disease. *Eur J Nucl Med* 1989;15:280–286.
18. Wackers FJ, Berman DJ, Maddahi J, et al. Technetium-99m-hexakis-2-methoxyisobutyl isonitrile: human biodistribution, dosimetry, safety and preliminary comparison to thallium-201 for myocardial perfusion imaging. *J Nucl Med* 1989;30:301–311.
19. Canby RC, Silber S, Pohost GM. Relations of the myocardial imaging agents Tc-99m-MIBI and Tl-201 to myocardial blood flow in a canine model of myocardial ischemic insult. *Circulation* 1990;81:289–296.
20. Glover DK, Okada RD. Myocardial kinetics of Tc-MIBI in canine myocardium after dipyridamole. *Circulation* 1990;81:628–636.
21. Leppo JA, Meerdink DJ. Comparison of the myocardial uptake of a technetium-labeled isonitrile analogue and thallium. *Circ Res* 1989;65:632–639.
22. Meerdink DJ, Leppo JA. Myocardial transport of hexakis (2-methoxyisobutylisonitrile) and thallium before and after coronary reperfusion. *Circ Res* 1990;66:1738–1746.
23. Mousa SA, Cooney JM, Williams SJ. Relationship between regional myocardial blood flow and the distribution of ^{99m}Tc-sestamibi in the presence of total coronary artery occlusion. *Am Heart J* 1990;119:842–847.
24. Okada RD, Glover D, Gaffney T, Williams S. Myocardial kinetics of technetium-99m-hexakis-2-methoxy-2-methylpropylisonitrile. *Circulation* 1988;77:491–498.
25. Sinusas AJ, Watson DD, Cannon JM, Beller GA. Effect of ischemia and postischemic dysfunction on myocardial uptake of technetium-99m-labeled methoxyisobutyl isonitrile and thallium-201. *J Am Coll Cardiol* 1989;14:1785–1793.
26. Wackers FJT. Thrombolytic therapy for myocardial infarction assessment of efficacy by myocardial perfusion imaging with technetium-99m-sestamibi. *Am J Cardiol* 1990;66:36–41.
27. Grégoire J, Théroux P. Detection and assessment of unstable angina using myocardial perfusion imaging: comparison between technetium-99m-sestamibi SPECT and 12-lead electrocardiogram. *Am J Cardiol* 1990;66:42–46.
28. Santoro G, Bisi G, Sciagra R, Leoncini M, Fazzini P, Meldolesi U. Single-photon emission computed tomography with technetium-99m-hexakis-2-methoxyisobutyl isonitrile in acute myocardial infarction before and after thrombolytic treatment: assessment of salvaged myocardium and prediction of late functional recovery. *J Am Coll Cardiol* 1990;15:301–314.
29. Gibbons RJ, Verani MS, Behrenbeck T, et al. Feasability of tomographic ^{99m}Tc-hexakis-2-methoxy-2-methylpropylisonitrile imaging for the risk assessment of myocardial area at risk and the effect of treatment in acute myocardial infarction. *Circulation* 1989;80:1277–1286.
30. Wackers FJ, Gibbons RJ, Verani MS, et al. Serial quantitative planar technetium-99m-isonitrile imaging in acute myocardial infarction: efficacy for noninvasive assessment of thrombolytic therapy. *J Am Coll Cardiol* 1989;14:869–873.
31. Franceschi M, Guimond J, Zimmerman RE, et al. Myocardial clearance of Tc-99m-hexakis-2-methoxy-2-methylpropyl isonitrile (MIBI) in patients with coronary artery disease. *Clin Nucl Med* 1990;15:307–312.
32. Tamaki N, Ohtani Y, Yonekura Y, et al. Significance of fill-in after thallium-201 reinjection following delayed imaging: comparison with regional wall motion and angiographic findings. *J Nucl Med* 1990;31:1617–1623.
33. Gutman J, Berman DS, Freeman M, et al. Time to complete redistribution of thallium-201 in exercise myocardial scintigraphy: relationship to the degree of coronary artery stenosis. *Am Heart J* 1983;106:989–995.
34. Cloninger KG, DePuey EG, Garcia EV, et al. Incomplete redistribution delayed thallium-201 single photon emission computed tomographic (SPECT) images: an overestimation of myocardial scarring. *J Am Coll Cardiol* 1988;12:9545–9963.
35. Kiat H, Berman DS, Maddahi J, et al. Late reversibility of tomographic myocardial thallium-201 defects: an accurate marker of myocardial viability. *J Am Coll Cardiol* 1988;12:1456–1463.

Pulmonary Uptake of Technetium-99m-Sestamibi Induced by Dipyridamole-Based Stress or Exercise

Gilbert A. Hurwitz, Samia K. Ghali, Mariwan Husni, Piotr J. Slomka, Adel G. Mattar, Robert H. Reid and Neville M. Lefcoe
Departments of Diagnostic Radiology, Nuclear Medicine and Medicine, University of Western Ontario; and Department of Nuclear Medicine, Victoria Hospital, London, Ontario, Canada

On poststress images with ^{99m}Tc-sestamibi (MIBI), increased lung uptake of the radiotracer may reflect severe or multivessel coronary artery disease. **Methods:** We measured pulmonary/myocardial ratios of MIBI at standardized times on immediate poststress acquisitions and on delayed tomographic acquisitions. In 1500 sequential patients referred for rest and stress myocardial tomography, ancillary planar images were obtained 4 min postinjection at peak stress with exercise, either alone (exercise, n = 674), or after intravenous dipyridamole (dipyridamole, n = 826). **Results:** Based on 95% confidence limits in the angiographic normals, high values for immediate acquisitions were found in 17% of dipyridamole studies and 15% of exercise studies. High values for delayed acquisitions were found in 10% of dipyridamole studies and 9% of exercise studies. For both stress modes, increased values were related ($p < 0.001$) to ischemic perfusion defects for immediate images, to fixed defects for delayed images, and to ventricular dilation in both cases. By logistic regression analysis, body weight and history of infarction were also minor independent determinants ($p < 0.01$) of delayed acquisitions. In a subset of 250 cases with angiographic correlation (163 with dipyridamole; 87 with exercise), immediate lung uptake was highly correlated with ventricular dysfunction and with coronary stenoses ($p < 0.0001$). Relationships were similar to those in a historic control series imaged with ^{201}Tl. Values for delayed poststress images, and for corresponding rest images, showed strong relationships to ventricular dysfunction but not to stenosis severity. **Conclusion:** The relationships of immediate lung uptake to scintigraphic and angiographic disease patterns suggest its possible diagnostic use as an indicator of stress-induced ventricular decompensation.

Key Words: technetium-99m-sestamibi; lung uptake; tomographic acquisitions; dipyridamole

J Nucl Med 1998; 39:339–345

In using technetium-based agents for myocardial imaging (*1,2*), a potential drawback is the decreased value of pulmonary uptake of the perfusion agent. With ^{201}Tl, the classic radionuclide used for this purpose, lung uptake can be assessed as an ancillary aspect of interpretation of planar or tomographic imaging. Increased poststress lung uptake of ^{201}Tl has considerable diagnostic value because it correlates with multivessel or severe coronary artery disease (*3–5*). Major prognostic value has been attributed to this ancillary imaging sign (*5–8*). The diagnostic relevance of stress-induced lung uptake of ^{201}Tl has been shown after a variety of stress modalities (*9,10*), but relationships to gender, peak exercise heart rate and other factors may modify its interpretation (*4,5*). Although ^{99m}Tc-sestamibi (MIBI) has been in widespread use for several years, there is only limited information (*11–15*) concerning the potential value of pulmonary uptake with it. This probably derives from the standard imaging protocols with MIBI in which imaging is usually not performed until at least 30 min after stress injection.

Published studies leave unanswered questions about the usefulness of lung uptake measurements with MIBI. On conventional MIBI images obtained 1 hr after stress, the value of lung uptake as an ancillary diagnostic sign has been reported as absent (*14*), reduced in comparison to ^{201}Tl (*12,13*) or possibly as helpful as those of ^{201}Tl (*11*). Most previous studies have focused on exercise rather than on pharmacological stress. Recently, Giubbini et al. (*15*) found that lung uptake on images acquired 1 hr after ergometric exercise correlated well with left ventricular dysfunction but not with the number of stenosed coronary arteries.

A few studies (*12,13*) have suggested that lung uptake of MIBI may be a more useful sign of disease when measured on immediate poststress images compared to standard acquisitions at 1 hr after injection. We reviewed the routine use of early poststress MIBI images (*16*) and evaluated images performed after dipyridamole-based tests as well as after ergometric stress.

MATERIALS AND METHODS

Sequential MIBI Imaging Series

From April 1992 to September 1993, 1500 sequential referrals were made to the nuclear medicine department at Victoria Hospital for diagnostic stress myocardial scintigraphy. These studies involved 1445 patients (evaluations were performed on two separate occasions in 53 patients and on three occasions in 1 patient) and were ordered by referring physicians for the usual clinical indications (*16*). Tomographic imaging with MIBI was used as the standard laboratory procedure to assess myocardial perfusion. Starting in April 1992, all patients had ancillary images taken starting at 4 min after peak stress with a mobile camera situated beside the stress table (*13,16*). These images were acquired in the left anterior oblique 40° projection for 2 min in the electrocardiogram (ECG)-gated mode with 16 frames synchronized to the R-wave. As part of routine image interpretation, these images were displayed in cinematic mode and used for visual rating of ventricular contractile function including left ventricular size (*17*). With all frames added together for better count statistics, these images also were used to assess abdominal background (*16*). Although relative lung uptake was observed on these images, quantitation of lung uptake was not included routinely.

Routine MIBI Perfusion Studies

Patients were assigned to supine bicycle ergometry stress alone if a brief clinical assessment suggested that would allow them to reach a diagnostic stress level (*16,18*). If exercise capacity was considered limited, stress was performed with vasodilatation with dipyridamole combined with either bicycle exercise or repeated isometric exercise, as appropriate. In this series, 674 patients (45% of the 1500 patients) were studied with exercise stress alone, and 826 patients (55%) were studied with dipyridamole-based tests. At peak exercise, MIBI was injected in a dose of 12 MBq/kg body weight. To ensure MIBI uptake by the myocardium (*19*), exercise

Received Dec. 12, 1996; revision accepted Apr. 1, 1997.
For correspondence or reprints contact: Gilbert A. Hurwitz, MD, Department of Nuclear Medicine, Victoria Hospital, 375 South St., London, Ontario, N6A 4G5, Canada.

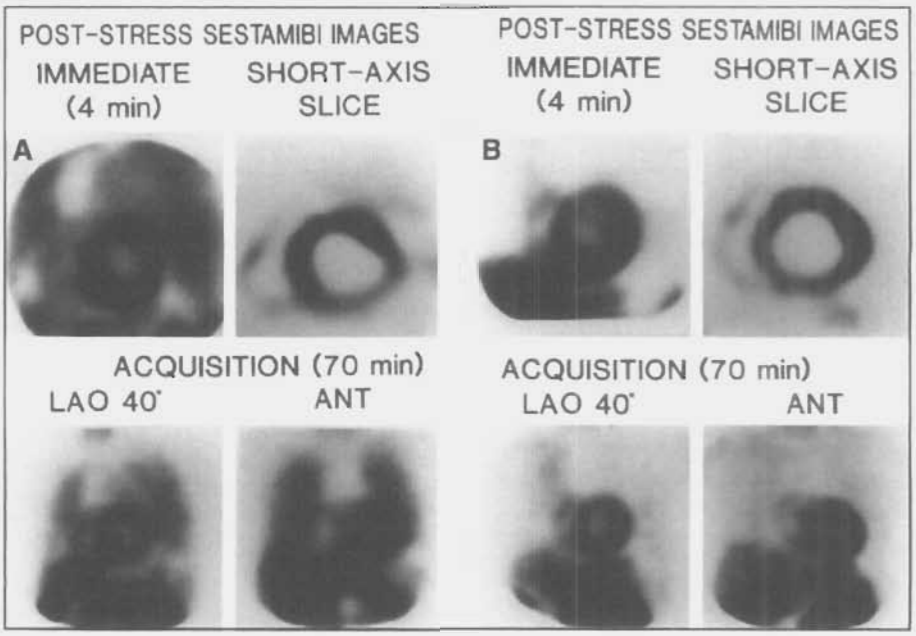

FIGURE 1. (A) MIBI images with stress-induced lung uptake of MIBI. This 62-yr-old man with remote bypass grafting had poor left ventricular function (ejection fraction of 36%). Upper left panel shows immediate image obtained with a mobile camera 4 min after exercise stress (6 metabolic equivalents). Ventricular dilation and increased uptake in both lungs is obvious. Lower panels (left anterior oblique 40° on left and anterior on right) show 30-sec acquisitions obtained starting 60 min after tracer injection as part of stress tomography. Upper right panel shows midventricular short-axis slice reconstructed from 32 acquisition images. Tomography showed anteroapical and infero-lateral infarcts with adjacent ischemia in a dilated left ventricle. On a subsequent study 1 yr later, performed with dipyridamole-exercise stress, lung uptake was similarly increased. (B) MIBI images in patient with normal pulmonary uptake. Image arrangement corresponds to Figure 1A. Left ventricular dilation is present, but lung uptake of tracer is not present, and no perfusion defects were detected. ECG-gated blood-pool scintigraphy 5 days later showed the ejection fraction to be 24%. This 65-yr-old man with atypical chest pain and left bundle branch block exercised to a peak heart rate of 140 bpm. Correlating cardiac catheterization was consistent with idiopathic cardiomyopathy (no coronary stenoses, Grade 5 ventriculogram).

was continued after radiotracer bolus appeared in the heart as assessed on the persistence scope of the adjacent mobile camera. The peak workload was continued for 1 min followed by a wind-down period of 1.5 min. The peak exercise workload was translated into metabolic equivalents by the equation:

$$METs = (kpm \times 2 + 300)/(3.5 \times kg),$$

where kpm is the peak ergometric workload attained (*16*) and kg is body weight in kilograms.

Poststress tomographic imaging was performed by 180° tomography (32 stops of 30 sec) on a large field-of-view camera with stress acquisition started 1 hr after radiotracer injection. Corresponding tomographic rest images were preferentially performed on a separate day, n = 661 (44%), or, if required, on the same day as the stress procedure with a dose of 3 MBq/kg. After reconstruction, rest and stress images were observed in dual-display mode, cine images (*17*) were assessed along with relevant clinical and ECG data, and reports were generated by nuclear medicine physicians. Images were archived on optical laser disks for subsequent review.

Correlating Cardiac Catheterization

Cardiac catheterization studies were ordered by referring clinicians on clinical grounds usually after perfusion scanning. A single cardiovascular radiologist has independently reported all of our angiographic studies. Coronary stenoses were rated as a percent of luminal diameter and classified as to their position in the three main coronary arteries or branches. Left ventricular function was rated on biplane contrast ventriculography on a scale from 1 (normal) to 5 (globally hypokinetic) based on the number, site and severity of hypokinetic segments (*9,20,21*). On retrospective review, catheterization studies correlated to perfusion scans if (a) there was no previous revascularization, (b) infarction or revascularization did not occur between the two studies and (c) the two diagnostic studies were performed within 4 mo of each other. Of the 1500 MIBI perfusion scans reviewed, 250 had correlating catheterization studies by these criteria.

Historical Comparison with Thallium-201 Planar Imaging

A series of 550 planar ^{201}Tl perfusion studies with correlating angiography has been described previously (*16*). This historical comparison series was similar to the MIBI cases with respect to selection and performance of stress tests and interpretation of correlating angiography. Angiographically correlated cases with the two agents were similar in clinical characteristics, stress-test results and incidence and severity of coronary artery disease.

Quantitation of Lung Uptake

After completing the 1500 MIBI studies, images (Fig. 1) were retrieved batch-wise from the optical disk to calculate pulmonary/myocardial ratios. ECG-gated images were initially formatted by adding all frames of the study. For MIBI images, it was essential to overcome the problem of scaling counts to variable abdominal activity (*16*) by finding the area of peak myocardial counts and saturating the images. Image processing was performed by two of the authors.

Regions were delineated in the myocardium and the left lung as described originally for ^{201}Tl images (*18*) and subsequently used for ^{201}Tl (*9,20*) and MIBI (*13*). The operator outlined a transmural segment of myocardium containing the area of peak counts (Region A) and a crescentic region over the left lung (Region B). Lung uptake was calculated as the ratios of count densities (B/A) and expressed as a percentage (Fig. 2).

In a small number of cases, images were not available or suitable for retrospective processing of lung uptake. Eleven studies were associated with low counts. Partially interstitial injection was noted during the stress procedure in five of these. In three other studies, neither immediate nor delayed poststress images were correctly

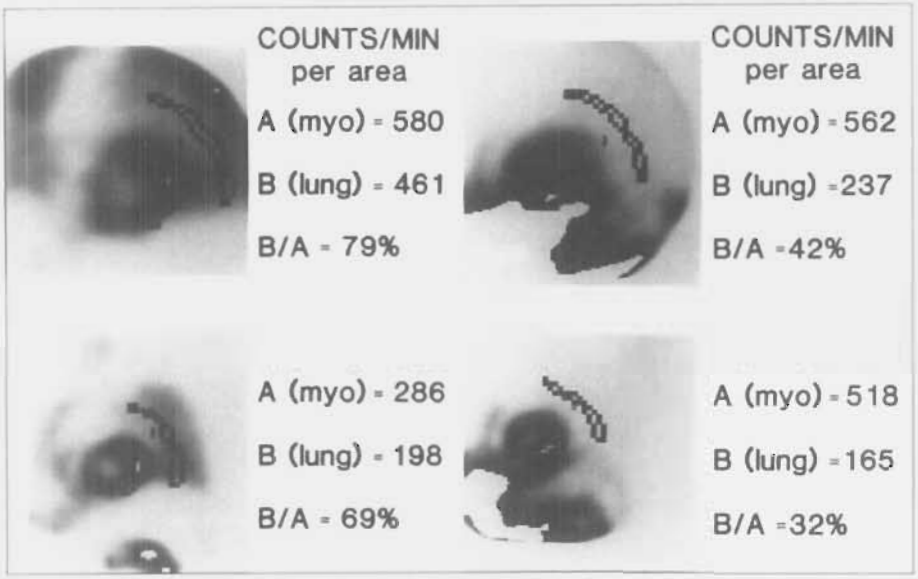

FIGURE 2. Quantitation of lung uptake of MIBI using pulmonary/myocardial ratios (P/M) in two men who had previous infarctions followed by angioplasty. Upper panels show immediate left anterior oblique 40° images and lower panels show corresponding SPECT tomoacquisitions obtained 70 min after stress. Patient shown in left panels performed exercise to a peak heart rate of 162 bpm and had increased uptake on immediate image (P/M = 79%) and on delayed tomographic acquisition (P/M = 69%). Patient on right was stressed with dipyridamole followed by a low level of exercise limited by knee pain (arthritis) and chest pain. Because of high abdominal uptake, saturation of images was necessary to visualize the myocardium, and values were within normal range on both immediate (P/M = 42%) and delayed images (P/M = 32%).

archived, and patient symptoms precluded further imaging in one. Thus, 1485 studies were suitable for further analysis:

1. Early poststress MIBI images: Of the 1485 studies, camera malfunction precluded image acquisition in six; positioning was poor in two; early poststress images were not correctly archived in five. Appropriate images could be assessed in 1472 cases.
2. Stress MIBI tomographic acquisitions: Quantitation was performed using the left anterior projection, which matched the early poststress view. The myocardium could be easily delineated on these 30-sec acquisitions, but appropriate scaling of the images was critical. Before delineation of myocardial and pulmonary regions, the left ventricle was centered in a box measuring 19 × 19 cm or 22% of the field of view. Planar delayed imaging, rather than tomography, was performed in four patients (due to technical or clinical limitation). Archiving deficiencies precluded data availability in 20 further studies and appropriate measurements were obtained in 1461 cases.
3. Rest MIBI tomographic acquisitions: Quantitation was performed in a similar fashion to the quantitation of stress images, but only the angiographically-correlated cases were assessed. Archived studies were available for 244 of these cases.
4. Immediate poststress ^{201}Tl images: Lung/myocardial ratios were assessed in these studies as previously described (*9,20*).

Review of Scintigraphic and Angiographic Data

For all studies, scintigraphic reports and hard copy of tomographic images were reviewed by one of the authors. The results of stress scintigraphic imaging studies were characterized as defect, showing a definite perfusion abnormality, dilation, showing definite left ventricular dilation on the tomograms, or normal. After a comparison of stress and rest tomograms, cases with focally abnormal perfusion were characterized further as having ischemic defects (stress > rest), fixed defects (stress = rest) or both types. Findings likely to be attributed to causes other than coronary artery disease, such as attenuation artifact or abnormal conduction (isolated septal hypoperfusion associated with left bundle branch block), were construed as normal. Although quantitation of tomographic images was not routinely performed, this evaluation was performed in a setting in which a direct method of quantitating myocardial perfusion and left ventricular size on clinical tomograms was under development (*22*).

Angiographic studies were categorized according to the site and number of stenoses. For binary classification, significant disease was taken as the presence of a stenosis of at least 50% luminal diameter in one of the three main arteries (left anterior descending, right coronary and left circumflex arteries) or their branches. To calculate the number of diseased arteries, left mainstem disease was regarded as equivalent to left anterior descending plus left circumflex. A more detailed system was used to compare the effect of various arterial sites of disease to the scintigraphic findings (*20*). For this formulation, the left mainstem was considered a separate site, and stenoses in the left mainstem and each of the three arteries were rated on a continuous scale according to the percent of stenosis giving branch lesions half the weight of a lesion in the main arterial trunk.

Statistical Methods

Normal values for pulmonary/myocardial ratios with MIBI were calculated on the basis of catheterization data; 25 studies (11 involving dipyridamole and 14 with exercise alone) had contrast ventriculography scores of 1 (normal) and had no significant coronary artery stenoses. Upper limits of normal (95% confidence, one-tailed) were calculated for pulmonary/myocardial (P/M) ratios on immediate images and delayed images. These values were applied to the patients stressed with dipyridamole-based and exercise tests (Table 1). Characteristics of the patients having high values on the immediate images were contrasted with those having normal values. Univariate comparisons were made by paired Student's *t*-tests or by chi-squared tests where appropriate (Tables 2 and 3). To assess which factors might contribute independently to increased lung uptake, multivariate analysis was performed using factors identified as significant from the univariate analysis. Logistic regression analysis was performed for both stress modes and for both poststress intervals (Table 4).

In the subset of angiographically correlated cases, lung uptake values on immediate and delayed images were related to the principal angiographic findings by analysis of variance (Fig. 3). Coronary disease was tabulated as the number of diseased coronary arteries and ventricular dysfunction by the grading of contrast ventriculography. Comparison of means of specific groups was evaluated by Newman-Keuls tests.

TABLE 1
Incidence of Increased P/M Ratios on Immediate and Delayed Poststress Images*

Abnormal value	Immediate ≥57% Incidence	p	Delayed ≥46% Incidence	p
Scan findings				
Normal	6% (43/753)	—	2% (14/746)	—
Single findings				
Ischemic defects (I)	19% (40/209)	‡	9% (18/205)	‡
Fixed degects (F)	14% (18/127)	†	10% (13/127)	‡
Dilated ventricle (D)	21% (7/34)	†	9% (3/35)	†
Combined findings				
I + F	24% (29/122)	‡	20% (25/123)	‡
I + D	33% (9/27)	‡	11% (3/27)	†
F + D	41% (33/80)	‡	34% (27/79)	‡
I + F + D	46% (55/120)	‡	34% (41/119)	‡

*These images are the results of rest/stress per fusion tomography.
†$p < 0.01$.
‡$p < 0.001$ by chi-squared tests in comparison with the group with normal perfusion tomography.
P/M = pulmonary/myocardial ratio.

Further modeling of the angiographic correlates of pulmonary/myocardial ratios was then performed. As similar values and influences were previously shown for the two stress-mode groups (Fig. 3), they were pooled for this purpose. Multilinear relationships were derived for dependence on the severity of stenoses at four sites (the left mainstem and each of the three principal coronary arteries) and on contractile dysfunction (Table 5). The resulting coefficients for sites of stenosis indicate the magnitude and statistical significance of the effect of a 100% stenosis at each site. The coefficient for contractile dysfunction indicates the effect of the poorest level of function (Grade 5 by contrast ventriculography) on pulmonary/myocardial ratios. As the effect of stenoses on flow likely was related to obstructed arterial area, the square of the obstructed luminal diameter was used for modeling. Use of this function improved correlations in comparison to a linear model or to several nonlinear models. Similar analyses were performed for the rest MIBI studies and for the historic ^{201}Tl controls.

RESULTS

Increased lung uptake was found on early poststress MIBI images relatively frequently in our referred population (Table 1). Values greater than 56% on the immediate images were found in 16% of the evaluable images. There was no difference between the test modes in this regard ($p = 0.8$ by chi-squared testing). High values were associated with ischemic defects, with fixed defects and left ventricular dilation, but they were most common when several of these abnormal findings were present. In contrast, among those with normal tomograms, the incidence of high lung ratios (6%) was similar to that among the angiographically-defined normals.

On delayed images, values for lung uptake were lower and generally correlated with immediate values (delayed = 0.69 × immediate; $r = 0.814$, $p < 0.0001$). Increased values for lung uptake on the delayed images were less frequent than for the immediate poststress images (234/1472 versus 144/1461, $p < 0.0001$) across the spectrum of tomographic results (Table 1); in

TABLE 2
Dipyridamole-Based Scintigraphic Studies: Characteristics of Patients According to the Value of Immediate Poststress Lung Uptake (normal ≤ 56%)

Characteristic	High P/M	Normal P/M	P value*
	n=139	n=678	
Gender (male)—%	71%	52%	<0.001
Age (yr)—mean ± s.d.	61 ± 10	61 ± 11	0.9
Weight (kg)—mean ± s.d.	86 ± 17	79 ± 16	<0.001
Revascularization—%	25%	22%	0.4
Infarction (by history)—%	65%	34%	<0.001
Hypertension—%	53%	46%	0.3
Workload (METs)—mean ± s.d.	3.8 ± 1.6	4.2 ± 1.9	0.04
Peak heart rate (bpm)—mean ± s.d.	107 ± 20	112 ± 20	0.01
Protocol (same day)—%	55%	57%	0.7
Scan findings†—%			
Ischemic defects	61%	33%	<0.001
Fixed defects	65%	29%	<0.001
Ventricular dilation	51%	15%	<0.001

*Chi-squared or t-tests as appropriate.
†Presence of findings either alone or in combination.
P/M = pulmonary/myocardial ratio.

TABLE 3
Exercise Scintigraphic Studies: Characteristics of Patients According to the Value of Immediate Poststress Lung Uptake

Characteristic	High P/M	Normal P/M	P value*
	n = 95	n = 560	
Gender (male)—%	79%	69%	0.05
Age (yr)—mean ± s.d.	56 ± 9	56 ± 11	0.9
Weight (kg)—mean ± s.d.	85 ± 14	80 ± 15	0.01
Revascularization—%	29%	24%	0.3
Infarction (by history)—%	43%	26%	<0.001
Hypertension—%	29%	31%	0.7
Workload (METs)—mean ± s.d.	6.4 ± 1.8	7.1 ± 1.9	<0.001
Peak heart rate (bpm)—mean ± s.d.	134 ± 20	139 ± 20	0.04
Protocol (same day)—%	57%	55%	0.7
Scan findings†—%			
Ischemic defects	51%	22%	<0.001
Fixed defects	47%	22%	<0.001
Ventricular dilation	35%	9%	<0.001

*Chi-squared or t-tests as appropriate.
†Presence of findings either alone or in combination.
P/M = pulmonary/myocardial ratio.

TABLE 4
Factors Contributing to Increased Lung Uptake on Immediate Poststress and Delayed Tomographic Images

Images	Dipyridamole-based		Exercise alone	
Immediate	Ischemic defect	‡	Ischemic defect	‡
	Dilation	‡	Dilation	‡
	Body weight	‡		
Delayed	Fixed defect	‡	Fixed defect	‡
	Dilation	‡	Dilation	‡
	Body weight	†	Ischemic defect	†
	Infarction	†		

*These table findings are the results of multifactorial logistic regression analysis.
†$p < 0.01$.
‡$p < 0.001$.

particular, a weaker association with ischemic defects was suggested. Figure 1A shows concordant elevated values for the immediate and delayed images (80% and 64%, respectively), and Figure 1B shows concordant normal values (48% and 37%, respectively).

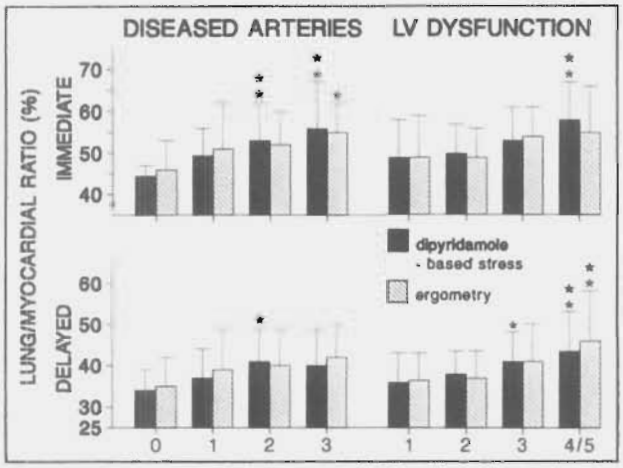

FIGURE 3. Lung/myocardial ratios (mean ± s.d.) on immediate and delayed poststress images according to dipyridamole use in scintigraphic stress imaging protocol and angiographic findings. Studies were grouped according to number of diseased coronary arteries (minimum 50% stenosis) in left panel, and according to grading of ventricular function on biplane contrast ventriculography (1 = normal, 5 = globally hypokinetic) in right panel. Increased values are shown compared to normal group (no coronary stenoses or normal ventricular function): * $p < 0.05$; ** $p < 0.01$.

High initial lung uptake (Tables 2 and 3) was found more often in those with a history of infarction and in those showing significant abnormalities on subsequent tomographic images. Such studies were not distinguished from those with normal values by age, frequency of prior revascularization or by hypertension. These relationships of increased lung uptake were generally similar on exercise and on dipyridamole-based tests. However, the association of increased lung uptake with male gender and with increased body weight seemed more prominent on the pharmacological stress tests. The relationship with attained workload was more prominent on the exercise tests. Multivariate analysis suggested (Table 4) that tomographic imaging findings were the major determinants of increased lung uptake and that clinical and stress-mode factors played minor roles. Obesity seemed to be a factor independently associated with increased lung uptake, as it was observed in some cases with presumed false-positive lung uptake measurements i.e. normal tomographic results.

Table 4 displays the contrasts between immediate and delayed lung uptake measurements with respect to associated scintigraphic findings. For the immediate images, ischemic defects provided a major independent contribution. In contrast, fixed defects were noncontributory. For the delayed images, fixed defects contributed to a much greater extent than did ischemic defects. Ventricular dilation played a major role as a synergistic contributor in both circumstances. There was a notable similarity of findings in this regard between the pharmacologically enhanced and exercise stress modes.

In the angiographic series (Fig. 3), mean values for immediate lung uptake reflected the extent of coronary artery disease increasing from 46% in those without significant stenoses to 56% in those with triple-vessel disease. Values also increased in relation to dysfunction shown on contrast ventriculography. By analysis of variance, the overall effect on the immediate ratio of coronary stenosis extent ($F = 10$, $p < 0.0001$) was greater than that of ventricular dysfunction ($F = 7$, $p = 0.0002$). The effect on the delayed ratio was greater for ventricular dysfunction ($F = 11$, $p < 0.0001$) than for extent of stenosis ($F = 6$, $p = 0.0004$). The pattern was similar for dipyridamole-based and for ergometric stress tests as substantiated by analysis of interaction terms. Despite these consistent patterns for group means, there was considerable variation among individuals. Figure 4 shows the range of immediate lung uptake values in men with significant coronary stenoses and normal ventricular function.

TABLE 5
Multivariate Regression Equations Linking Lung Uptake of Myocardial Perfusion Agents with Angiographic Features

Agent	State	Time	Equation
MIBI*		Immediate	P/M = 45 + 14**LM** + 8**LAD** + 3**RCA** + 2LCX + 5**CD**
MIBI	Stress	Delayed	P/M = 34 + 15**LM** + 4**LAD** + 2RCA + 2LCX + 8**CD**
MIBI	Rest	Delayed	P/M = 38 + 1LM + 0LAD + 2RCA + 0LCX + 6**CD**
^{201}Tl†	Stress	Immediate	P/M = 43 + 11**LM** + 7**LAD** + 2RCA + 1LCX + 9**CD**

*N = 250 for MIBI.
†N = 550 for ^{201}Tl.
Statistically significant contribution indicated by bold where $p < 0.05$ and by underline where $p < 0.001$. Angiographic features are scaled from 0 (no disease) to 1 (100% stenosis, grade 5/5 ventricular dysfunction); stenosis severity is entered as the square of the obstructed luminal diameter. P/M = pulmonary/myocardial ratio (%); LM = left mainstem stenosis; LAD = left anterior descending artery stenosis; RCA = right coronary artery stenosis; LCX = left circumflex artery stenosis; CD = contractile dysfunction by ventriculography.

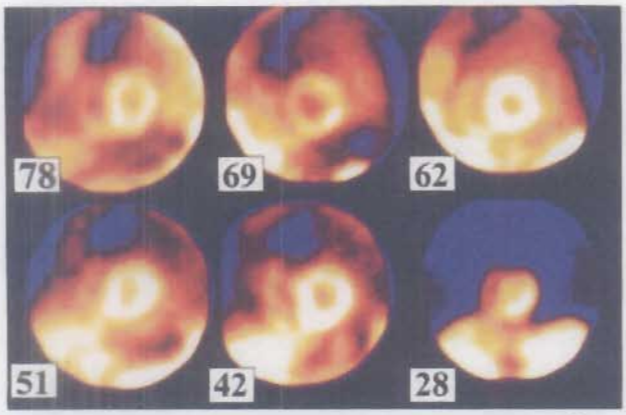

FIGURE 4. Examples of immediate (4-min) poststress images with ^{99m}Tc-MIBI in angiographically correlated studies showing the range of lung uptake. All cases were men with normal biplane contrast ventriculograms and significant coronary artery lesions (all had at least 70% stenosis in left anterior descending artery). To show relative lung uptake, each image is saturated to peak activity in myocardium. Lung uptake values (lung/myocardial ratios) are shown in lower left corner.

In these same cases, delayed images gave lung uptake values ranging from 62% (upper left) to 19% (lower right).

The multifactorial regression models shown in Table 5 indicate the relationship of lung uptake ratios, measured under differing physiological and imaging conditions, to specific sites of arterial stenosis as well as to ventricular dysfunction. Relationships of lung uptake on early poststress MIBI images were similar to those of ^{201}Tl. With both perfusion agents, left mainstem and left anterior descending artery stenoses were the main lesions contributing to pulmonary uptake modified by left ventricular function. Other sites of stenosis provided only minor contributions to lung uptake ratios in this paradigm. On the corresponding rest tomographic acquisitions, left ventricular dysfunction contributed to lung uptake whereas coronary stenoses did not. The delayed poststress images were influenced to a greater extent by ventricular dysfunction than by stenosis severity.

DISCUSSION

Our study suggests the feasibility and potential diagnostic value of routine assessment of lung uptake of MIBI on immediate poststress images. Imaging was started 2.5 min after completion of the wind-down phase of the stress procedure (*16,19*) with satisfactory data obtained in over 98% of cases. The allocation of a mobile gamma camera to acquire these ancillary images in the stress laboratory may have other advantages. Such a camera may be used to obtain first-pass ventriculographic studies (*15,23*) and to ensure adequate myocardial uptake of the radiotracer from the blood pool before exercise is stopped (*19*). With the patient connected to monitoring leads in the immediate poststress period, electrocardiographic gating of the early poststress images can be accomplished easily (*17,21*) and ventricular contractile function assessed. In cases with severe coronary artery disease, such images may reveal stress-induced ventricular dilation or dyskinesis (*24*) as well as stress-induced lung uptake.

Analysis of the frequency and relationships of data derived from early and delayed poststress imaging (Tables 1 and 5, Fig. 3) confirms that lung uptake with MIBI may have important diagnostic value when measured on immediate poststress images (*12,13*). Some investigators have found relatively poor relationships between lung uptake and coronary stenoses when measured on MIBI tomographic acquisitions at 1 hr after stress injection (*13–15*). Giubbini et al. (*15*) found inverse relationships between left ventricular ejection fraction measured on first-pass studies and delayed measurements. This study (Fig. 3 and Table 5) supports the findings of Giubbini et al. (*15*) by documenting a strong relationship of delayed lung uptake measurements (both rest and stress) to left ventricular dysfunction as assessed by contrast ventriculography. Measurements obtained early poststress in our study, but not those obtained under other physiologic conditions, were strongly correlated with the extent and severity of coronary disease. These findings are not unexpected given the tendency for rapid clearance from the lung of both ^{201}Tl (*25*) and MIBI (*13*). Depending on the diagnostic objectives and the equipment available, quantitation of lung uptake on either immediate or delayed MIBI images could be of value.

The angiographic relationships of early poststress lung uptake of MIBI, including the importance of coronary stenoses, parallel those with ^{201}Tl. Although others have emphasized the relationship of increased lung uptake to multivessel disease, our results show the predominance of stenoses along the left axis (*20*), left mainstem or left anterior descending arteries with both radiotracers (Table 5) in induction. Our results (Fig. 3) suggest a similar interpretation of lung uptake for MIBI whether stress is performed with vasodilators or with exercise alone. Our results in normal patients differ from that of the Montreal group (*26*), which is probably due to the nature of our subjects..

The findings of our study may not apply uniformly to other laboratories performing rest or stress perfusion studies with MIBI. As initial and delayed MIBI images frequently show high abdominal uptake (*16*), proper scaling of the digitized images (to the peak area of uptake in myocardium) needs to be performed. Duplication of our results by other centers will require attention to this preliminary step in processing. In our laboratory, the particular stress modality used did not significantly affect the frequency of increased lung uptake, but this finding requires verification by centers where stress is performed with other protocols. Our experience suggests that outlining the inferior myocardium may be difficult and may lead to errors in assessing lung uptake ratios when dipyridamole is used without supplementary exercise. When upright exercise on a treadmill or bicycle is used, P/M ratios may well have lower values. Earlier acquisition of tomographic images (30 min poststress) might improve the relationship of lung uptake to coronary stenoses.

Further limitations of our study need to be addressed before recommending routine assessment of immediate poststress MIBI images. In the minutes after injection, MIBI undergoes more dynamic change than is the case with ^{201}Tl (*13,19*). The optimal window for assessing lung activity of MIBI might best be determined with a high-count multicrystal camera, which also would allow careful simultaneous definition of the relation with parameters of left ventricular function. The prognostic implications of increased MIBI lung uptake will need to be evaluated and compared to those of ^{201}Tl. Lung uptake varies widely among patients who are similar with respect to left ventricular function (Fig. 1, reduced function; Fig. 4, normal function). A larger number of patients will need to be evaluated to compare lung uptake with other prognostic indicators.

CONCLUSION

Increased lung uptake on immediate (4-min) poststress images with MIBI is seen in a significant portion of studies with abnormalities on perfusion tomograms. This potential ancillary diagnostic sign appears related to ischemic perfusion defects,

may be induced with exercise alone or with dipyridamole-based stress, and it is seen more frequently with severe disease. In a subset of MIBI studies with correlating angiograms, relationships to coronary artery stenoses were similar to those of ^{201}Tl. By comparison, lung uptake on delayed (1-hr) MIBI images is less frequent, and it appears related to fixed defects and to poor ventricular function. Further investigation of the potential value of early poststress MIBI images may result in the recovery of an important ancillary diagnostic sign, which appears to have been lost with the transition from ^{201}Tl- to ^{99m}Tc-based perfusion agents.

ACKNOWLEDGMENTS

We thank the Visual Services Department of Victoria Hospital for preparing the figures, Ms. Soraya Ali, Ms. Judy Smith and Mrs. Jo-Anne Quann for secretarial support. We also thank Dr. Craig A. MacDonald, who, until his retirement in December 1995, reported all cardiac catheterization studies at our hospital.

REFERENCES

1. Wackers FJT, Berman DS, Maddahi J, et al. Technetium-99m hexakis 2-methoxyisobutyl isonitrile: human biodistribution, dosimetry, safety and preliminary comparison to thallium-201 for myocardial perfusion imaging. *J Nucl Med* 1989;30:302–311.
2. Leppo JA, DePuey EG, Johnson LL. A review of cardiac imaging with sestamibi and teboroxime. *J Nucl Med* 1991;32:2012–2022.
3. Boucher CA, Zir LM, Beller GA, et al. Increased lung uptake of thallium-201 during exercise myocardial imaging: clinical hemodynamic and angiographic implications in patients with coronary artery disease. *Am J Cardiol* 1980;46:189–196.
4. Kaul S, Chesler DA, Boucher CA, Okada RD. Quantitative aspects of myocardial perfusion imaging. *Semin Nucl Med* 1987;17:131–144.
5. Mahmood S, Buscombe JR, Ell PJ. The use of thallium-201 lung/heart ratios. *Eur J Nucl Med* 1992;19:807–814.
6. Gill JB, Ruddy TD, Newell JB, Finkelstein DM, Strauss HW, Boucher CA. Prognostic importance of thallium uptake by the lungs during exercise in coronary artery disease. *N Engl J Med* 1987;317:1486–1489.
7. Miller DD, Kaul S, Strauss HW, Newell JB, Okada RD, Boucher CA. Increased exercise thallium-201 lung uptake: a non-invasive prognostic index in two-vessel coronary artery disease. *Can J Cardiol* 1988;4:270–276.
8. Pollock SG, Abbott RD, Boucher CA, Beller GA, Kaul S. Independent and incremental prognostic value of tests performed in hierarchical order to evaluate patients with suspected coronary artery disease. *Circulation* 1992;85:237–248.
9. Hurwitz GA, O'Donoghue JP, Powe JE, Gravelle DR, MacDonald AC, Finnie KJC. Pulmonary thallium-201 uptake following dipyridamole-exercise combination compared with single modality stress-testing. *Am J Cardiol* 1992;69:320–326.
10. Villanueva FS, Kaul S, Smith WH, Watson DD, Varma SK, Beller GA. Prevalence and correlates of increased lung/heart ratio of thallium-201 during dipyridamole stress imaging for suspected coronary artery disease. *Am J Cardiol* 1990;66:1324–1328.
11. Maisey MN, Mistry R, Sowton E. Planar imaging techniques used with technetium-99m sestamibi to evaluate chronic myocardial ischemia. *Am J Cardiol* 1990;66:47E–54E.
12. Taillefer R, Costi P, Jarry M, Benjamin C, Leveille J, Lambert R. Increased ^{99m}Tc-sestamibi (MIBI) lung uptake in diagnosis of coronary artery disease: comparison between early (5 min) and delayed (60 min) post-stress MIBI and ^{201}Tl planar imaging [Abstract]. *J Nucl Med* 1993;34(suppl):121P.
13. Hurwitz GA, Fox SP, Driedger AA, Willems C, Powe JE. Pulmonary uptake of sestamibi on early post-stress images: angiographic relationships, incidence and kinetics. *Nucl Med Commun* 1993;14:15–22.
14. Saha M, Forrest, TF, Brown KA. Lung uptake of technetium-99m sestamibi: relation to clinical, exercise, hemodynamic, and left ventricular function variables. *J Nucl Cardiol* 1994;1:52–56.
15. Giubbini R, Campini R, Milan E, et al. Evaluation of technetium-99m-sestamibi lung uptake: correlation with left ventricular function. *J Nucl Med* 1995;36:58–63.
16. Hurwitz GA, Saddy S, O'Donoghue JP, et al. The VEX-test for myocardial scintigraphy with Tl-201 and sestamibi: effect on abdominal background activity. *J Nucl Med* 1995;36:914–920.
17. Hurwitz GA, Powe JE, Melendez L, Ali SA, Lim RK, Miller DB. Equilibrium wall motion studies with sestamibi: evaluation of parameters for routine acquisition [Abstract]. *Clin Nucl Med* 1995;20:656.
18. Hurwitz GA, Powe JE, Driedger AA, Finnie KJC, Laurin NR, MacDonald AC. Dipyridamole combined with symptom-limited exercise for myocardial perfusion scintigraphy: image characteristics and clinical role. *Eur J Nucl Med* 1990;17:61–68.
19. Hurwitz GA, Blais M, Powe JE, Champagne CL. Stress/injection protocols for myocardial scintigraphy with sestamibi and thallium-201: implications of early post-stress kinetics. *Nucl Med Commun* 1996;17:400–409.
20. Hurwitz GA, MacDonald AC. Stenoses of the left anterior descending artery: predominant role in stress-induced pulmonary uptake of thallium-201. *Can J Cardiol* 1994;10:982–988.
21. Hurwitz GA, Laurin NR, Powe JE, Driedger AA, MacDonald AC. Ischemic left ventricular dysfunction assessed on ECG-gated thallium-201 myocardial perfusion images. *Can J Cardiol* 1990;6:198–204.
22. Slomka PJ, Hurwitz GA, St Clement G, Stephenson J. Three-dimensional demarcation of perfusion zones corresponding to specific coronary arteries: application for automated interpretation of myocardial SPECT. *J Nucl Med* 1995;36:2120–2126.
23. Hurwitz GA, Babensee SE, Cradduck TD, Powe JE, Driedger A Simplified first-pass technique for left ventricular ejection fraction with rest/stress myocardial perfusion imaging [Abstract]. *Eur J Nucl Med* 1990;16:S5.
24. Hurwitz GA, O'Donoghue JP, MacDonald AC, Laurin NR, Powe JE. Markers of left ventricular dysfunction induced by exercise, dipyridamole or combined stress on ECG-gated myocardial perfusion scans. *Nucl Med Commun* 1993;14:318–327.
25. Rothendler JA, Boucher CA, Strauss HW, Pohost GM, Okada RD. Decrease in the ability to detect elevated lung thallium due to delay in commencing imaging after exercise. *Am Heart J* 1985;110:830–835.
26. Primeau M, Taillefer R, Essiambre R, Lambert R, Honos G. Technetium-99m sestamibi myocardial perfusion imaging: comparison between treadmill, dipyridamole and trans-oesophageal atrial pacing "stress" tests in normal subjects. *Eur J Nucl Med* 1991;18:247–251.

ORIGINAL ARTICLE

Annals of Nuclear Medicine Vol. 17, No. 5, 393–398, 2003

Enhanced regional washout of technetium-99m-sestamibi in patients with coronary spastic angina

Souichi ONO,* Yasuchika TAKEISHI,** Hiroyuki YAMAGUCHI,* Shigeru ABE,*
Hidetada TACHIBANA,* Takayuki SATO* and Isao KUBOTA**

*Departments of Radiology and Cardiology, Yamagata Prefectural Shinjo Hospital
**First Department of Internal Medicine, Yamagata University School of Medicine

Background: Reverse redistribution and rapid washout of ^{99m}Tc-sestamibi are observed in patients with acute myocardial infarction and may indicate viable myocardium. However, the clinical significance of this phenomenon has not been rigorously examined in other cardiac diseases. Thus, we investigated whether reverse redistribution and washout of ^{99m}Tc-sestamibi could be used in the diagnosis and follow-up of patients with coronary spastic angina. ***Methods:*** Thirty patients diagnosed as coronary spastic angina were examined. During coronary arteriography, spasm was induced by provocation test with ergonovine, and only total or subtotal occlusion was considered positive. Myocardial perfusion tomography was obtained 45 min (early) and 3 hr (delayed) after ^{99m}Tc-sestamibi injection. Segmental defect score was visually graded from 0 (normal) to 4 (defect), and a total defect score was determined as the sum of defect scores for all segments. Washout rate of ^{99m}Tc-sestamibi from the myocardium was calculated for each segment. After medical treatment with calcium antagonists and nitrates for 3 months, ^{99m}Tc-sestamibi imaging was repeated. ***Results:*** Out of 30 patients, on the early images 17 (57%) patients demonstrated decreased ^{99m}Tc-sestamibi uptake in spastic segments; on the other hand, 24 (80%) patients did decreased ^{99m}Tc-sestamibi uptake in spastic segments on delayed images. Total defect scores in delayed images were higher than those in early images (6.9 ± 0.3 vs. 3.6 ± 0.4, $p < 0.01$). Reverse redistribution of ^{99m}Tc-sestamibi was observed in 17 out of 30 patients (57%) with coronary spastic angina. Washout rate of ^{99m}Tc-sestamibi from spastic segments was higher than that from non-spastic segments ($16 \pm 2\%$ vs. $11 \pm 5\%$, $p < 0.01$). After medical treatment, washout rate from spastic segments was decreased to 10 ± 4 ($p < 0.01$), and left ventricular ejection fraction was increased from $63 \pm 8\%$ to $73 \pm 4\%$ ($p < 0.01$). ***Conclusion:*** Rapid washout of ^{99m}Tc-sestamibi was observed in patients with coronary spastic angina and might indicate that the ability of myocyte to retain the tracer was impaired due to repetitive brief ischemia by coronary spasm. The early and delayed ^{99m}Tc-sestamibi imaging provides useful information for the diagnosis and responses to the treatment in patients with coronary spastic angina.

Key words: ^{99m}Tc-sestamibi, reverse redistribution, washout, spastic angina

ORIGINAL ARTICLE

Annals of Nuclear Medicine Vol. 17, No. 5, 393–398, 2003

Enhanced regional washout of technetium-99m-sestamibi in patients with coronary spastic angina

Souichi ONO,* Yasuchika TAKEISHI,** Hiroyuki YAMAGUCHI,* Shigeru ABE,* Hidetada TACHIBANA,* Takayuki SATO* and Isao KUBOTA**

*Departments of Radiology and Cardiology, Yamagata Prefectural Shinjo Hospital
**First Department of Internal Medicine, Yamagata University School of Medicine

Background: Reverse redistribution and rapid washout of ^{99m}Tc-sestamibi are observed in patients with acute myocardial infarction and may indicate viable myocardium. However, the clinical significance of this phenomenon has not been rigorously examined in other cardiac diseases. Thus, we investigated whether reverse redistribution and washout of ^{99m}Tc-sestamibi could be used in the diagnosis and follow-up of patients with coronary spastic angina. ***Methods:*** Thirty patients diagnosed as coronary spastic angina were examined. During coronary arteriography, spasm was induced by provocation test with ergonovine, and only total or subtotal occlusion was considered positive. Myocardial perfusion tomography was obtained 45 min (early) and 3 hr (delayed) after ^{99m}Tc-sestamibi injection. Segmental defect score was visually graded from 0 (normal) to 4 (defect), and a total defect score was determined as the sum of defect scores for all segments. Washout rate of ^{99m}Tc-sestamibi from the myocardium was calculated for each segment. After medical treatment with calcium antagonists and nitrates for 3 months, ^{99m}Tc-sestamibi imaging was repeated. ***Results:*** Out of 30 patients, on the early images 17 (57%) patients demonstrated decreased ^{99m}Tc-sestamibi uptake in spastic segments; on the other hand, 24 (80%) patients did decreased ^{99m}Tc-sestamibi uptake in spastic segments on delayed images. Total defect scores in delayed images were higher than those in early images (6.9 ± 0.3 vs. 3.6 ± 0.4, $p < 0.01$). Reverse redistribution of ^{99m}Tc-sestamibi was observed in 17 out of 30 patients (57%) with coronary spastic angina. Washout rate of ^{99m}Tc-sestamibi from spastic segments was higher than that from non-spastic segments ($16 \pm 2\%$ vs. $11 \pm 5\%$, $p < 0.01$). After medical treatment, washout rate from spastic segments was decreased to 10 ± 4 ($p < 0.01$), and left ventricular ejection fraction was increased from $63 \pm 8\%$ to $73 \pm 4\%$ ($p < 0.01$). ***Conclusion:*** Rapid washout of ^{99m}Tc-sestamibi was observed in patients with coronary spastic angina and might indicate that the ability of myocyte to retain the tracer was impaired due to repetitive brief ischemia by coronary spasm. The early and delayed ^{99m}Tc-sestamibi imaging provides useful information for the diagnosis and responses to the treatment in patients with coronary spastic angina.

Key words: ^{99m}Tc-sestamibi, reverse redistribution, washout, spastic angina

Feasibility and Diagnostic Accuracy of a Gated SPECT Early-Imaging Protocol: A Multicenter Study of the Myoview Imaging Optimization Group

Assuero Giorgetti, Massimiliano Rossi, Mario Stanislao, Guido Valle, Pietro Bertolaccini, Alberto Maneschi, Raffaele Giubbini, Maria Luisa De Rimini, Marco Mazzanti, Mario Cappagli, Elisa Milan, Duccio Volterrani, and Paolo Marzullo, on behalf of the Myoview Imaging Optimization group

CNR Institute of Clinical Physiology, Pisa, Italy

The aim of this study was to investigate whether early (time 1, or T1) myocardial tetrofosmin imaging is feasible and as accurate in detecting coronary artery disease as is standard delayed (time 2, or T2) imaging. **Methods:** One hundred twenty patients (100 men and 20 women; mean age ± SD, 61 ± 10 y) with anginal symptoms underwent tetrofosmin gated SPECT. Stress/rest T1 imaging was performed at 15 min and T2 at 45 min after injection. Image quality was visually evaluated using a 4-point scale (from 0 = poor to 3 = optimal). Myocardial perfusion analysis was performed on a 20-segment model using quantitative perfusion SPECT software, and reversible ischemia was scored as a summed difference score (SDS). Coronary angiography was performed within 1 mo on all patients, and stenosis of more than 50% of the diameter was considered significant. **Results:** Overall, quality was scored as optimal or good for 94% of T1 images and 95% of T2 images (P = not statistically significant). Heart, lung, liver, and subdiaphragmatic counts did not differ for stress and rest T1 and T2 imaging. A good linear relationship was seen between T1 and T2 SDS ($r = 0.69$; $P < 0.0001$), and Bland–Altman analysis showed good agreement between the 2 conditions. In terms of global diagnostic accuracy, areas under the receiver-operating-characteristic curve were comparable between T1 and T2 (0.80 vs. 0.81, P = not statistically significant). Discrepancies between T1 and T2 SDS were observed in 44% of patients (T1 − T2 SDS > 2). Linear regression analysis showed a good correlation between T1 and T2 SDS ($r = 0.67$; $P < 0.0001$), whereas the Bland–Altman method showed a shift in the mean value of the difference of +2.67 ± 2.73. In patients with a T1 − T2 SDS of more than 2, areas under the receiver-operating-characteristic curves were significantly higher for T1 than for T2 images (0.79 vs. 0.70, $P < 0.001$). **Conclusion:** T1 imaging is feasible and as accurate as T2 imaging in identifying coronary artery disease. However, in a discrete subset of patients, early acquisition strengthens the clinical message of defect reversibility by permitting earlier, more accurate identification of more severe myocardial ischemia.

Received Feb. 13, 2007; revision accepted Jun. 27, 2007.
For correspondence or reprints contact: Assuero Giorgetti, MD, CNR Institute of Clinical Physiology, Via Moruzzi 1, 56124, Pisa, Italy.
E-mail: asso@ifc.cnr.it

Key Words: tetrofosmin; gated SPECT; myocardial imaging; early imaging; delayed imaging; coronary artery disease

J Nucl Med 2007; 48:1670–1675
DOI: 10.2967/jnumed.106.039107

Sestamibi and tetrofosmin represent reliable alternative tracers to ^{201}Tl for detecting coronary artery disease and viable myocardium (*1–3*). Unlike sestamibi, tetrofosmin has a more favorable biodistribution, and theoretically, its rapid accumulation in the myocardium and the relatively fast liver kinetic (*4,5*) allow early imaging. Such early imaging could result in shorter waiting times for patients and could be important in some clinical situations, such as suspected acute coronary syndromes, in which time is critical for therapeutic interventions. As previously reported, one important factor limiting early and fast imaging protocols with ^{99m}Tc-compounds is a possible increase in the number of artifactual defects in the inferior wall due to high subdiaphragmatic uptake (*6–8*).

Therefore, the aim of the present study was to investigate whether early (time 1, or T1) myocardial tetrofosmin gated SPECT is technically feasible and as clinically accurate as standard delayed (time 2, or T2) imaging in subjects with known coronary anatomy.

MATERIALS AND METHODS

Patient Population

The study population included 120 patients (100 men and 20 women; mean age ± SD, 61 ± 10 y; range, 23–83 y) referred to 9 Italian nuclear medicine departments from January 2005 to March 2006 for stress/rest tetrofosmin gated SPECT. All patients had a known coronary anatomy at the time of the study or underwent coronary angiography within 2 wk of that time.

The patients were studied after fasting overnight and were asked to avoid foods containing phylline derivates for 48 h before the stress. Nitrates, β-blockers, and calcium-channel blockers were

discontinued 5 plasma half-lives before gated SPECT, whereas other drugs such as angiotensin-converting enzyme inhibitors were maintained.

Scintigraphic Protocol

Each patient underwent stress/rest tetrofosmin gated SPECT in a 1- or 2-d protocol as previously described (*9*). Seventy-eight patients (65%) underwent a bicycle stress test, whereas 42 patients (35%) had pharmacologic stress induced using a low-dose dipyridamole infusion (0.56 mg/kg in 4 min).

In the 1-d protocol, tetrofosmin (296–370 MBq) was administered intravenously at peak stress. Immediately after the end of the stress, the patients ate a fatty meal to accelerate hepatobiliary clearance of the tracer. Within 15 min (T1), gated SPECT was performed using a double-head γ-camera (Millennium; GE, or ECAM; Siemens) equipped with high-resolution collimators. The protocol included a 64 × 64 matrix, 32 projections, 40-s projections, and 8 frames per cycle used in association with a 15% window centered on the 140-keV photopeak of ^{99m}Tc. Then, within a range of 45 min to 1 h after radiotracer injection (T2), the stress study was repeated using the same acquisition protocol to obtain standard gated SPECT images. The studies were reconstructed using filtered backprojection without attenuation or scatter correction.

Immediately after completion of the stress study, 740–830 MBq of tetrofosmin were administered under resting conditions, and both T1 and T2 gated SPECT scans were obtained as for the stress imaging.

In the 2-d protocol, 370–600 MBq of tetrofosmin were injected and the T1 and T2 gated SPECT scans were obtained on separate days.

In no patient did the total dose administered in the 2 protocols exceed 1,200 MBq.

When indicated by a history of previous myocardial infarction, tetrofosmin at rest was injected after nitrate administration (sublingual isosorbide mononitrate, 5 or 10 mg according to body weight).

Analysis of Scintigraphic Data

Qualitative and quantitative analysis of scintigraphic data was performed at a core laboratory (CNR Pisa).

Determining the feasibility of the study required evaluation of the overall quality of the gated SPECT images. Two independent observers visually analyzed the quality using a 4-point scale (from 0 = poor to 3 = optimal). Quantitative analysis was performed on anterior raw images by drawing irregular regions of interest on the heart, lungs, liver, and subdiaphragmatic area including the liver. Counts obtained in each region were normalized to the number of pixels and compared for both stress and rest T1 and T2 images. Washout rates were calculated according to the formula 100 × (early – delayed/early counts).

The presence and extent of perfusion defects and their reversibility were evaluated on a 20-segment model by an operator-independent analysis of regional myocardial perfusion and wall motion using previously validated software for gated SPECT analysis (quantitative gated SPECT and quantitative perfusion SPECT (*10*)). Summed stress score, summed rest score, and summed difference score (SDS) were automatically measured according to the clinical conditions of the acquisition.

Agreement between the 2 sets of scans was analyzed using SDS as an integrative parameter reflecting the presence and the extent or severity of perfusion defects.

Analysis of myocardial function between T1 and T2 scans was performed using ejection fraction (EF) and summed motion score as parameters reflecting the degree of global and regional left ventricular dysfunction.

Coronary Angiography

All angiograms were quantitatively evaluated using GE Medical Systems software by physicians who were unaware of the protocol. Stenosis of more than 50% of the vessel diameter was considered significant.

Statistical Analysis

Continuous variables are presented as mean ± SD. Where indicated, differences were assessed by the Student *t* test for paired or unpaired data. In the evaluation of quality between T1 and T2 images, the χ^2 test was used for comparison of proportions. When the total number of observations was fewer than 20, the Fisher exact test was applied.

The significance of the relationship between T1 and T2 perfusion data and functional indices after stress and at rest was assessed by linear regression analysis. Agreement was also analyzed using the Bland–Altman method (*11*). Accuracy in coronary stenosis detection was estimated by analysis of receiver-operating-characteristic (ROC) curves, using MedCalc software (version 9.3.0.0). κ-Values were used as previously described (*12*). Statistical significance for all analyses was assessed at a *P* value of less than 0.05.

RESULTS

Clinical Results

Of the 120 study patients, 34 had a clinical history of previous myocardial infarction; 61 had been previously revascularized (16 with a coronary artery bypass graft and 45 with percutaneous coronary angioplasty); 53 had single-, 22 double-, and 9 triple-vessel disease; and 36 did not have significant coronary artery stenosis.

Scintigraphic Results

Analysis of Image Quality. All patients except one had gated SPECT images of a quality suitable for qualitative clinical interpretation. In particular, the quality of stress/rest gated SPECT images was rated as optimal in 38 patients at T1 versus 42 at T2, good in 76 at T1 versus 73 at T2, fair in 5 at T1 versus 4 at T2, and poor in 1 patient at both T1 and T2 (*P* = not statistically significant [NS] for all values). The only patient with poor-quality images at both T1 and T2 showed obvious motion artifacts, which were corrected with software.

Heart, lung, liver, and subdiaphragmatic counts did not differ between stress T1 and T2 and averaged 76 ± 21, 43 ± 14, 115 ± 64, and 76 ± 39 counts per pixel, respectively, at T1 and 77 ± 26, 42 ± 17, 104 ± 43, and 81 ± 36 counts per pixel, respectively, at T2 (*P* = NS for all values). Heart, lung, and subdiaphragmatic washouts were negligible, whereas the liver showed a 5% washout from stress T1 to T2. Rest T1 and T2 did not show appreciable differences, and washouts were comparable.

Semiquantitative Analysis of Perfusion Imaging. The mean T1 SDS results were slightly but statistically significantly higher than the mean T2 results (4.15 ± 3.72 vs.

3.67 ± 3.72, $P < 0.05$). Linear regression analysis showed a good relationship between T1 and T2 SDS ($y = 0.689x + 799$; $r = 0.69$; SEE = 0.06; $P < 0.0001$) (Fig. 1). The Bland–Altman method showed a shift in the mean value of the difference (T1 − T2 SDS) of +0.50 ± 2.92 (range, −9.0 to +18.0), with 96% of the results enclosed inside the 95% confidence interval of –5.34 to 6.34 (Fig. 1).

ROC curve analysis identified cutoffs of 2.5 for T1 SDS and 1.5 for T2 SDS as the best for separating patients with from those without coronary artery disease (Fig. 1). With these thresholds, T1 imaging predicted coronary artery disease in 66 of 84 patients (79% sensitivity) and excluded it in 26 of 36 patients (72% specificity). T2 imaging predicted coronary artery disease in 67 of 84 patients (80% sensitivity) and excluded it in 24 of 36 patients (67% specificity). Areas under the ROC curves were similar between T1 and T2 images (0.80 vs. 0.81, P = NS) (Fig. 1). The κ-statistic showed good agreement between T1 and T2 imaging results ($\kappa = 0.68$; SE = 0.07).

In the 78 patients undergoing exercise stress testing, ROC curve analysis showed that areas under the curves were similar between T1 and T2 images (0.83 vs. 0.79, P = NS). Similarly, in the 42 patients who underwent dipyridamole stress testing, areas under the ROC curves were similar between T1 and T2 images (0.87 vs. 0.84, P = NS).

Myocardial Perfusion in Patients with Discrepancies Between T1 and T2 Results. We found discrepancies between T1 and T2 (T1 − T2 SDS > 2) in 53 (44%) of 120 patients. No significant differences in clinical data were found between these patients and the general study population. Mean T1 SDS was significantly higher than mean T2 SDS (5.26 ± 3.71 vs. 2.63 ± 2.82, $P < 0.0001$) (Fig. 2). Linear regression analysis showed a good correlation between T1 and T2 SDS ($y = 0.89x + 2.98$; $r = 0.67$; SEE = 0.1; $P < 0.0001$. The Bland–Altman method showed a shift in the mean value of the difference (T1 − T2 SDS) of +2.67 ± 2.73 (range, +1 to +18.0). ROC curve analysis identified cutoffs of 3.0 for T1 and 2.0 for T2 SDS as the best for separating patients with from those without coronary artery disease. With these thresholds, T1 imaging predicted coronary artery disease in 33 of 38 patients (88% sensitivity) and excluded it in 10 of 15 patients (75% specificity). On the other hand, T2 imaging predicted coronary artery disease in 23 of 38 patients (72% sensitivity) and excluded it in 10 of 15 (75% specificity). Areas under the ROC curves were significantly higher for T1 than for T2 images (0.79 vs. 0.70, $P < 0.001$) (Fig. 2). An example of a patient with perfusion discrepancies is shown in Figure 3.

Semiquantitative Analysis of Myocardial Function. Mean poststress EFs were similar in T1 and T2 imaging (0.53 ± 0.12 vs. 0.53 ± 0.13, P = NS). Linear regression analysis showed a good correlation between T1 and T2 poststress EFs ($y = 0.968x + 1.428$; $r = 0.95$; SEE = 0.03; $P < 0.0001$) (Fig. 4). The Bland–Altman method showed a shift in the mean value of the difference (T1 − T2 EF) of +0.29 ± 4.22 (range, −11.0 to 11.0, 95% confidence interval, –8.1 to +8.7) (Fig. 4).

Mean EFs at rest were similar between T1 and T2 imaging (0.54 ± 0.12 vs. 0.53 ± 0.12, P = NS). Linear regression analysis showed a good correlation between T1 and T2 resting EFs ($y = 0.961x + 1.641$; $r = 0.94$; SEE = 0.03; $P < 0.0001$). The Bland–Altman method showed a shift in the mean value of the difference (T1 − T2 EF) of +0.51 ± 4.13 (range, −11.0 to 22.0, 95% confidence interval, –7.76 to +8.76) (Fig. 4).

Myocardial Function in Patients with Discrepancies Between T1 and T2 SDS. In patients with differences between T1 and T2 SDS, mean poststress EF was similar

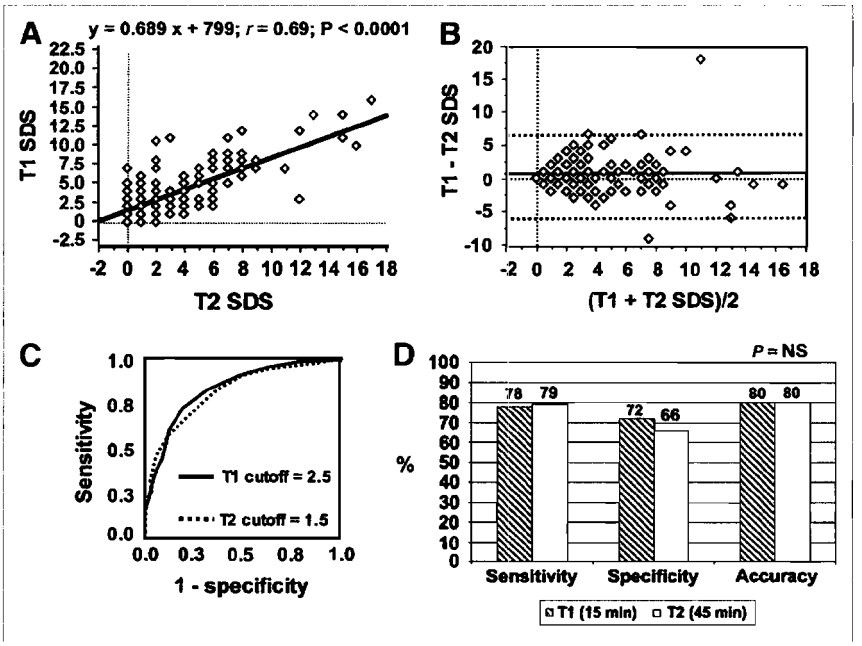

FIGURE 1. (A) Linear regression analysis showed good relationship between T1 and T2 SDS ($y = 0.689x + 799$; $r = 0.69$; SEE = 0.06; $P < 0.0001$). (B) Bland–Altman analysis showed good agreement between T1 and T2 SDS. (C) ROC curve analysis identified cutoffs of 2.5 for T1 and 1.5 for T2 SDS as best separating patients with from those without coronary artery disease. (D) With these thresholds, global diagnostic accuracy was identical between T1 and T2 (0.80 vs. 0.81, P = NS).

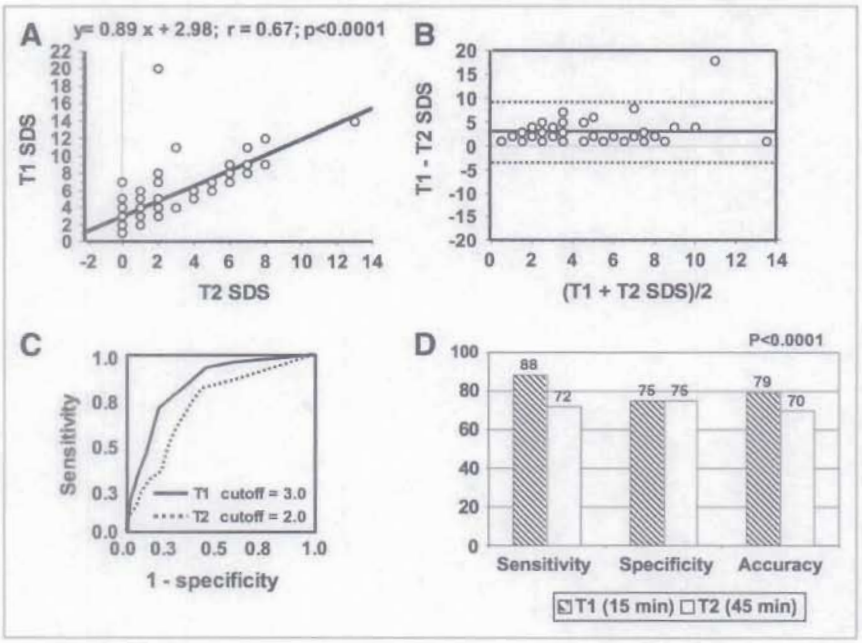

FIGURE 2. (A and B) In patients with T1 − T2 SDS of more than 2, linear regression analysis (A) showed good correlation between T1 and T2 SDS ($y = 0.89x + 2.98$; $r = 0.67$; SEE = 0.1; $P < 0.0001$), whereas Bland–Altman method (B) showed shift in mean value of difference of +2.67 ± 2.73. (C) ROC curve analysis identified cutoffs of 3.0 for T1 and 2.0 for T2 SDS as best separating patients with and without coronary artery disease. (D) With these thresholds, T1 resulted in global diagnostic accuracy significantly higher than that of T2 imaging (0.79 vs. 0.70, $P < 0.001$).

under the 2 conditions (0.54 ± 0.12 vs. 0.53 ± 0.13, P = NS). However, mean poststress summed motion score was significantly higher in T1 than in T2 scans (11 ± 13 vs. 8 ± 11, $P < 0.001$). In this subgroup of patients, neither mean EF nor summed motion score at rest was statistically different (P = NS).

DISCUSSION

To our knowledge, this was the first study exploring the feasibility and clinical accuracy of a tetrofosmin gated SPECT early-imaging protocol. Early acquisition provided clinical information the same as, and in a discrete subset of patients more accurate than, that provided by the standard delayed protocol, suggesting the possibility of significantly reducing imaging time while increasing diagnostic accuracy.

Comparison of Early and Delayed Perfusion Imaging

The idea of performing early myocardial imaging with tetrofosmin is not new (*8,13*). Matsunary et al. (*8*) tested the feasibility of early SPECT at rest in 13 healthy volunteers and concluded that, to avoid technical artifacts that could

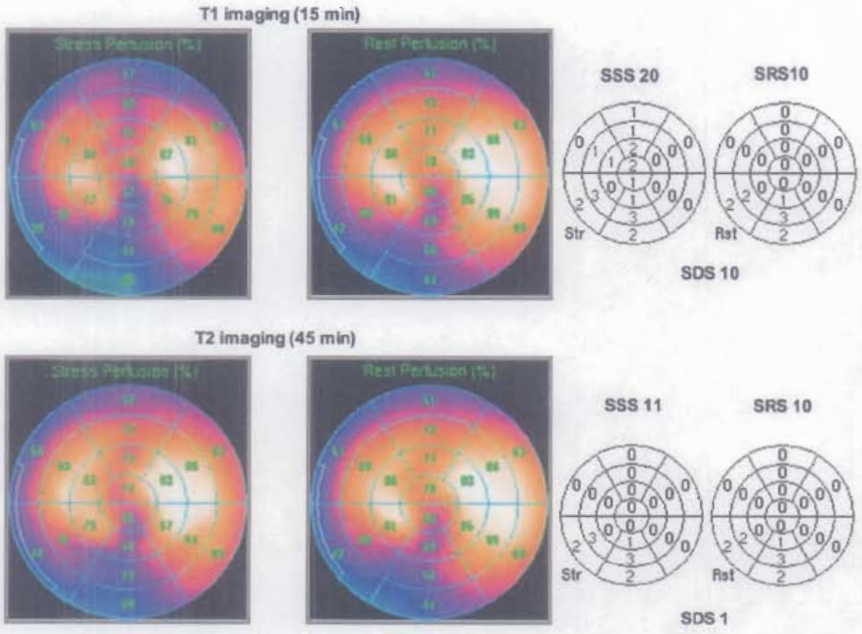

FIGURE 3. Perfusion bull's eyes (left) and relative quantitative perfusion SPECT scores (right) in patient with previous myocardial infarction and double-vessel disease. (Top) Early imaging identified fixed perfusion defect of inferior wall and reversible defect of anterior and anteroseptal walls, resulting in SDS of 10. (Bottom) Standard delayed imaging failed to identify reversible defect in territory of left anterior descending coronary artery, resulting in SDS of 1. Therefore, 2 different clinical messages were obtained from same patient: previous inferior myocardial infarction plus anterior myocardial ischemia using early imaging and previous inferior infarction without ischemia using standard delayed scans.

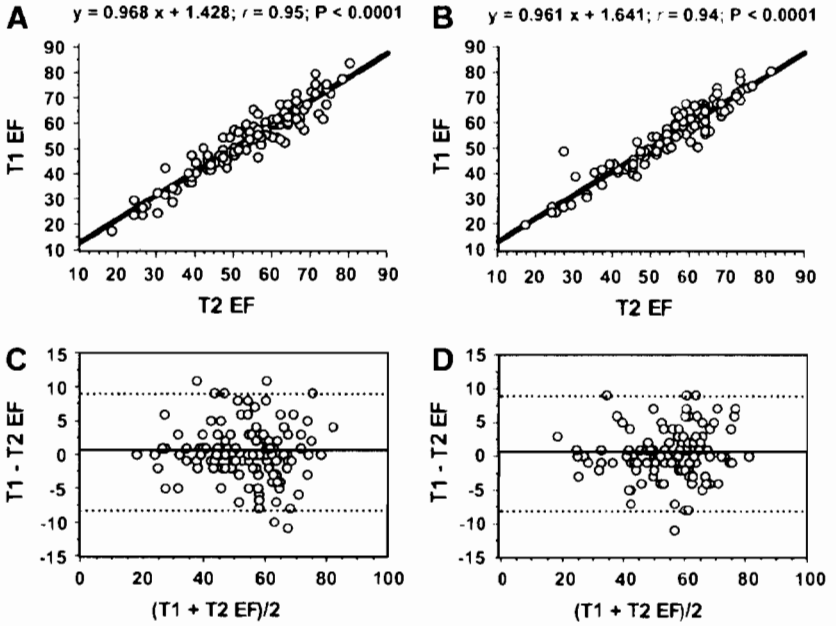

FIGURE 4. (A and C) Linear regression analysis (A) showed good correlation between T1 and T2 poststress EFs ($y = 0.968x + 1.428$; $r = 0.95$; SEE = 0.03; $P < 0.0001$), whereas Bland–Altman method (C) showed good agreement between the 2 sets of measures. (B) Similarly, linear regression analysis showed good correlation between T1 and T2 resting EFs ($y = 0.961x + 1.641$; $r = 0.94$; SEE = 0.03; $P < 0.0001$). (D) Bland–Altman method showed shift in mean value of difference of +0.51 ± 4.13.

result in false-positive findings, performing delayed scans was better. Important limitations of this study included the relatively small number of patients, the impossibility of extending the conclusions to stress imaging, and the absence of any data on subjects with known coronary anatomy. Indeed, the presence of intense liver activity adjacent to the inferior wall could cause an oversubtraction of radiotracer counts from the inferior wall when filtered backprojection is applied but could also result in an inverse relationship with the subtracted counts in the reconstructed images (*7*). It is conceivable that attenuation correction algorithms or iterative reconstruction could reduce the influence of background activity on actual count density in the inferior wall (*14*). In our study, we performed neither attenuation correction nor iterative reconstruction. Additionally, images were suitable for clinical interpretation, and changes in subdiaphragmatic activity from T1 to T2 did not alter the global count density in the heart. Furthermore, we performed a clinically oriented evaluation demonstrating that a tetrofosmin gated SPECT early-imaging protocol is technically feasible and as clinically accurate as standard delayed imaging in subjects with known coronary anatomy.

Pathophysiologic Implications of Early Myocardial Perfusion Imaging

In our study, we found consistent discrepancies between T1 and T2 SDS in 44% of patients. This finding could have some pathophysiologic explanations. In fact, the regulation of regional perfusion is dependent on many variables, but the ischemic event is closely and inversely related to the time from its induction by stress. Theoretically, the earlier the scintigraphic acquisition, the higher the probability of defining the severity and extent of ischemia. It is conceivable that near the time of the stress, ischemia induces a more pronounced wall thinning that could determine, through the partial-volume effect, a more evident perfusion defect.

Additionally, tetrofosmin could also become partially redistributed with time. Schulz et al. reported that the relative washout fraction per hour for tetrofosmin was 8.3% ± 9.9% in areas with a stress-induced defect (*15*). Ito et al. found that tetrofosmin showed a kinetic behavior similar to that of ^{201}Tl and that the optimal imaging time was within 10–35 min after exercise (*16*). Although we did not perform any regional measure of radiotracer washout, our data were in indirect agreement with those reported above demonstrating differences between early and delayed distribution of radiotracer (SDS difference) that could be attributed to a more severe poststress defect in T1 imaging. Thus, our data suggested that early tetrofosmin imaging could have an important clinical impact, identifying ischemia more accurately in terms of severity and extension.

Comparison of Left Ventricular Function on Early and Delayed Imaging

Our data showed a similar mean EF in T1 and T2 imaging both after stress and at rest. However, in patients with discrepancies in myocardial perfusion between the 2 sets of scans, the analysis of regional wall motion resulted in higher T1 poststress summed motion scores.

Transient ischemia can produce perfusion defects associated with left ventricular contractile dysfunction, and one third of patients show persistent dysfunction (*17,18*). The association between perfusion defects and wall motion abnormalities could have important pathophysiologic and clinical implications. It has been shown that poststress stunning

is more sensitive than a resting abnormality of regional wall motion and is highly specific to severe angiographic stenosis (*19*). Because this phenomenon is time-dependent, in some patients standard delayed imaging could miss this information, reducing the potential diagnostic power of gated SPECT.

Study Limitations

We performed an automatic analysis of myocardial perfusion imaging. Because quantitative perfusion SPECT software does not include reference data files for early acquisitions, either poststress or at rest, early imaging was compared with the available standard database, possibly generating apparent perfusion defects. However, this possibility is not in keeping with the higher diagnostic accuracy demonstrated by T1 imaging, when compared with T2 imaging. Future application of early imaging should include a more appropriate database of healthy individuals studied at 15 min, or at least a specific reference group for normal findings on tetrofosmin gated SPECT.

CONCLUSION

Early stress and rest tetrofosmin imaging is feasible and does not lessen image quality. Globally, early scans show accuracy identical to that of standard delayed scans in identifying coronary artery disease. In a discrete subset of patients, early acquisition allowed the identification of more severe myocardial ischemia associated with regional wall motion abnormalities. Therefore, our data demonstrate that early myocardial imaging with tetrofosmin can provide clinical information the same as, and in some cases even more accurate than, that provided by the standard delayed scan, reducing total imaging time. Reduction of imaging time is mandatory for improving both patient compliance with the study and the logistics of nuclear cardiology laboratories.

ACKNOWLEDGMENTS

We are indebted to Ilaria Citti and to Adrian Holden, MD, for their expert review of the manuscript and to Laura Bruselli, MD, and all the Myoview Imaging Optimization study investigators from the 9 Italian centers (CNR Pisa, 22 patients; nuclear medicine departments from Pisa, 11 patients; S. Giovanni Rotondo, 21 patients; Massa-Carrara, 10 patients; Brescia, 12 patients; Napoli, 20 patients; Ancona, 7 patients; La Spezia, 5 patients; and Castelfranco Veneto, 12 patients) who helped us in the examination of the study subjects.

REFERENCES

1. Underwood SR, Anagnostopoulos C, Cerqueira M, et al. Myocardial perfusion scintigraphy: the evidence. *Eur J Nucl Med Mol Imaging.* 2004;31:261–291.
2. Tamaki N, Morita K. SPET in cardiology: diagnosis, prognosis, and management of patients with coronary artery disease. *Q J Nucl Med Mol Imaging.* 2005;49: 193–203.
3. Travin MI, Bergmann SR. Assessment of myocardial viability. *Semin Nucl Med.* 2005;35:2–16.
4. Jain D, Wackers FJT, Mattera J, McMahon M, Sinusas AJ, Zaret BL. Biokinetics of technetium-99m-tetrofosmin myocardial perfusion imaging agent: implication for one-day imaging protocol. *J Nucl Med.* 1993;34:1254–1259.
5. Higley B, Smith FW, Smith T, et al. Technetium-99m-1,2 bis (bis(2-ethoxyethyl) phosphino) ethane: human biodistribution, dosimetry and safety of a new myocardial perfusion imaging agent. *J Nucl Med.* 1993;34:30–38.
6. Germano G, Chua T, Kiat H, Areeda JS, Berman DS. A quantitative phantom analysis of artifacts due to hepatic activity in technetium-99m myocardial perfusion SPECT studies. *J Nucl Med.* 1994;35:356–359.
7. Nuyts J, Dupont P, Van den Maegdenbergh V, Vleugels S, Suetens P, Mortelmans L. A study of the liver-heart artifact in emission tomography. *J Nucl Med.* 1995; 36:133–139.
8. Matsunari I, Tanishima Y, Taki J, et al. Early and delayed technetium-99m-tetrofosmin myocardial SPECT compared in normal volunteers. *J Nucl Med.* 1996;37:1622–1626.
9. Hesse B, Tagil K, Cuocolo A, et al. EANM/ESC procedural guidelines for myocardial perfusion imaging in nuclear cardiology. *Eur J Nucl Med Mol Imaging.* 2005;32:855–897.
10. Germano G, Berman DS. *Clinical Gated Cardiac SPECT.* Armhonk, NY: Futura Publishing Company; 1999.
11. Bland JM, Altman DG. Statistical methods for assessing agreement between two methods of clinical assessment. *Lancet.* 1986;1:307–310.
12. Fleiss J. *Statistical Methods for Rates and Proportions.* 2nd ed. New York, NY: Wiley and Sons; 1981.
13. Ferreira M, Ferrer-Antunes AI, Lima J. Fast ninety minute Tc-99m-tetrofosmin stress-rest imaging protocol: results on a small sample [abstract]. *J Nucl Cardiol.* 1999;part 2, 15:59.
14. Bateman TM, Cullom SJ. Attenuation correction single-photon emission computed tomography myocardial perfusion imaging. *Semin Nucl Med.* 2005;35: 37–51.
15. Schulz G, Ostwald E, Kaiser HJ, wom Dahl J, Kleinhans E, Buell E. Cardiac stress-rest single-photon emission computed tomography with technetium 99m-labeled tetrofosmin: influence of washout kinetics on regional myocardial uptake values of the rest study with a 1-day protocol. *J Nucl Cardiol.* 1997;4:298–301.
16. Ito Y, Uehara T, Fukuchi K, Tsujimura E, Hasegawa S, Nishimura T. Comparison of dual-isotope acquisition of ^{201}Tl and 99Tcm-tetrofosmin for the detection of ischaemic heart disease and determination of the optimal imaging time of 99Tcm-tetrofosmin. *Nucl Med Commun.* 1998;19:119–126.
17. Ambrosio G, Betocchi S, Pace L, et al. Prolonged impairment of regional contractile function after resolution of exercise-induce angina: evidence of myocardial stunning in patients with coronary artery disease. *Circulation.* 1996;94: 2455–2466.
18. Paul AK, Hasegawa S, Yoshioka J, et al. Characteristics of regional myocardial stunning after exercise in gated myocardial SPECT. *J Nucl Cardiol.* 2002;9: 388–394.
19. Emmett L, Iwanochko RM, Freeman MR, Barolet A, Lee DS, Husain M. Reversible regional wall motion abnormalities on exercise technetium-99m-gated cardiac single photon emission computed tomography predict high-grade angiographic stenoses. *J Am Coll Cardiol.* 2002;39:991–998.

Case Reports

The Significance of Incidental Noncardiac Findings

in Tc-99m Sestamibi Myocardial Perfusion Imaging: Illustrated by a Case

Sofia N. Chatziioannou, MD, PhD
Carina Alfaro-Franco, MD
Warren H. Moore, MD
Leticia Alanis-Williams, CNMT
Ramesh D. Dhekne, MD
Patrick V. Ford, MD

Technetium 99m sestamibi is widely used in the evaluation of myocardial perfusion imaging. Although the aim of such imaging is cardiac evaluation, numerous other organs are included in the imaging field. Failure to identify incidental abnormal findings in these organs delays diagnosis and treatment. In common with other radiopharmaceutical agents, technetium 99m sestamibi is distributed throughout the body and accumulates in multiple tissues. When interpreting studies that involve this radiotracer, the physician must be aware of its physiologic distribution, in order to recognize abnormal uptake. We present an illustrative case in which areas of decreased tracer activity were noted incidentally during the evaluation of unprocessed single photon emission computed tomography data. These findings were due to metastasis of colon cancer to the liver. ***(Tex Heart Inst J 1999;26:229-31)***

Key words: *Heart/radionuclide imaging; liver neoplasms/radionuclide imaging; myocardial perfusion; sestamibi; technetium Tc 99m sestamibi/diagnostic use; tomography, emission-computed, single-photon*

From: *The Department of Radiology, Baylor College of Medicine (Drs. Chatziioannou, Moore, Dhekne, and Ford); and the departments of Nuclear Medicine (Drs. Chatziioannou, Moore, Dhekne, and Ford; and Ms Alanis-Williams) and Cardiology (Dr. Alfaro-Franco), St. Luke's Episcopal Hospital, Houston, Texas*

Address for reprints: *Sofia N. Chatziioannou, MD, PhD, Department of Nuclear Medicine, St. Luke's Episcopal Hospital, 6720 Bertner Avenue, MC 3-261, Houston, TX 77030*

The radiopharmaceutical agent technetium 99m (Tc-99m) sestamibi is used routinely for myocardial perfusion imaging in reaching diagnoses and prognoses in coronary artery disease.[1-5] The mechanism of cellular uptake is not entirely clear, but it seems to be related to the concentration of mitochondria inside the cells and the electrochemical gradient across the cell membrane.[6] Recently, there has been increasing evidence that Tc-99m sestamibi is concentrated by a variety of tumors.[7-19]

After intravenous administration, Tc-99m sestamibi is physiologically taken up by the salivary glands, thyroid, heart, liver, and spleen. There is physiologic hepatobiliary and renal clearance.

The field of view of unprocessed single photon emission computed tomographic (SPECT) data varies, in accordance with the size of the camera crystal and the size of the patient, but it usually includes the entire chest, the liver, the spleen, and part of the bowel; occasionally, the thyroid gland and the kidneys are also included. Therefore, the interpreting physician has the opportunity to evaluate other organs and should take advantage of it.

A case with incidental abnormality in the liver is discussed below.

Case Report

In June of 1998, a 71-year-old man with a history of hypertension, hypercholesterolemia, coronary artery disease, myocardial infarction, and L4-L5 laminectomy and diskectomy presented with acute onset of severe lower back pain radiating to the left leg. Magnetic resonance imaging of the lumbar spine showed foraminal stenosis at the level L4-L5. There was no evidence of any neoplastic process involving the spine.

Physical examination revealed mild neurological findings in the distal lower extremity. The chest and abdomen were normal.

Hospital Course. The patient was admitted for ventral and left-sided decompression laminectomy of L4-L5 and L5-S1. A routine electrocardiogram revealed a "new" right bundle branch block and a left anterior fascicular block. Because

of this finding and the patient's history of coronary artery disease, stress myocardial perfusion imaging with SPECT was performed; it showed a fixed perfusion defect in the posterior wall consistent with scar tissue. A review of the unprocessed data revealed multiple photopenic defects in both lobes of the liver (Fig. 1). Subsequent ultrasonography of the abdomen demonstrated multiple hypoechoic lesions in both lobes of the liver, consistent with metastatic disease. Computed tomography (CT) of the abdomen confirmed the presence of multiple metastatic lesions in the liver (Fig. 2). A CT-guided needle biopsy of the liver was performed and metastatic adenocarcinoma, mucin positive, favoring an intestinal primary tumor, was diagnosed. Gastrointestinal evaluation, including colonoscopy, uncovered a large (4- to 7-cm) ulcerated mass in the mid-ascending colon, and biopsy confirmed adenocarcinoma.

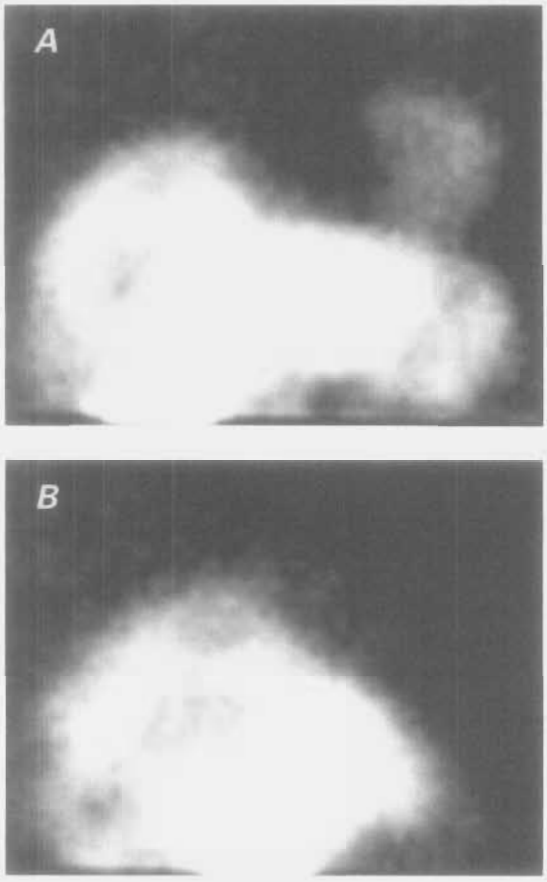

Fig. 1 Anterior (A) and lateral (B) projections of the lower thorax and upper abdomen from the unprocessed data of single photon emission computed tomographic myocardial perfusion, which demonstrate multiple areas of photopenia in the liver. The heart is also visualized.

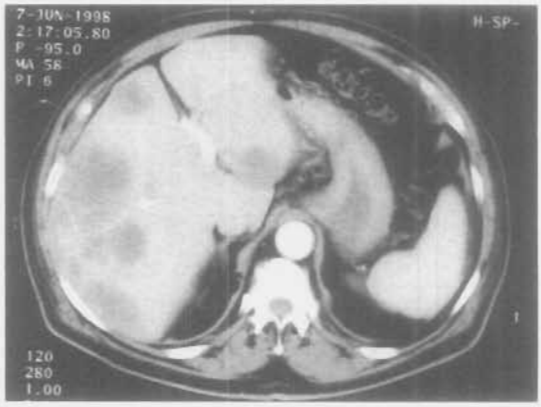

Fig. 2 Computed tomogram of the abdomen demonstrating metastatic lesions in the liver.

Discussion

Myocardial perfusion imaging is a diagnostic technique that is widely used in evaluating myocardial perfusion. In the case described above, we used Tc-99m sestamibi, which, in common with any other radiopharmaceutical agent, is distributed throughout the body, with increased concentration in the salivary and thyroid glands and in the heart, liver, hepatobiliary system, spleen, bowel, kidneys, and urinary tract. Its use, other than in the evaluation of myocardial perfusion, has expanded to include tumor imaging. Of course the primary aim of myocardial perfusion imaging is the evaluation of myocardial perfusion, so processed tomographic slices typically include only the heart and small parts of adjacent organs. However, because the unprocessed data include the physiologic or pathologic radiopharmaceutical uptake in the rest of the imaged body, it is important that the interpreting physician evaluate all the information available; incidental findings in the other organs may lead to an earlier diagnosis of pathologic conditions that require treatment. In the case discussed above, sestamibi led to the uncovering of metastatic cancer of the colon and to earlier treatment of this disease.

Unfortunately, there are no specific characteristics of the photopenic defects in the liver in a Tc-99m sestamibi scan that can differentiate between benign and malignant disease. Therefore, the interpreting physician should report any such findings and state the potential of their malignancy. Further investigation by clinical, laboratory, and other diagnostic means should then be undertaken. It should be pointed out that areas of increased tracer uptake in the liver are likely to represent malignancy, because cysts have decreased sestamibi uptake, and hepatocellu-

lar carcinoma has been reported to demonstrate increased uptake.[16] However, areas of increased tracer uptake in the liver can be difficult to ascertain because liver uptake of sestamibi is normally high.

The interpreting physician should also be aware that other abnormalities might be revealed in a Tc-99m sestamibi scan. Abnormalities with increased tracer uptake are: thyroid nodules (benign or malignant);[17,18] parathyroid adenomas,[7] adjacent to the thyroid gland or anywhere in the mediastinum, for which sestamibi imaging is the procedure of choice; lung malignancies;[10-11] breast malignancies,[8-9] for which sestamibi has been approved by the Food and Drug Administration both for detection and for differentiation from benign processes;[19] metastases of breast malignancies to the axillary lymph nodes;[19] lymphomas;[12,13] brain tumors;[14] sarcomas;[15] and infectious processes and granulomas.[20]

Abnormalities with decreased tracer activity are: renal photopenic defects suggestive of cysts or possible malignancy (since normal cortical uptake of sestamibi is relatively high[21]); and, finally, acute cholecystitis, in the event that the gallbladder cannot be visualized.[22]

In conclusion, the interpretation of myocardial perfusion imaging should not be limited to the heart, because it can reveal other pathologic conditions. Because the ultimate goal is the well-being of the patient, any available information should be examined and interpreted.

References

1. Maddahi J, Kiat H, Van Train KF, Prigent F, Friedman J, Garcia EV, et al. Myocardial perfusion imaging with technetium-99m sestamibi SPECT in the evaluation of coronary artery disease. Am J Cardiol 1990;66:55E-62E.
2. Iskandrian AS, Heo J, Kong B, Lyons E, Marsch S. Use of technetium-99m isonitrile (RP-30A) in assessing left ventricular perfusion and function at rest and during exercise in coronary artery disease, and comparison with coronary arteriography and exercise thallium-201 SPECT imaging. Am J Cardiol 1989;64:270-5.
3. Chatziioannou SN, Moore WH, Ford PV, Fisher RE, Lee VV, Alfaro-Franco C, et al. Prognostic value of myocardial perfusion imaging in patients with high exercise tolerance. Circulation 1999;99:867-72.
4. Brown KA, Atland E, Rowen M. Prognostic value of normal technetium-99m-sestamibi cardiac imaging. J Nucl Med 1994;35:554-7.
5. Berman DS, Hachamovitch R, Kiat H, Cohen I, Cabico JA, Wang FP, et al. Incremental value of prognostic testing in patients with known or suspected ischemic heart disease: a basis for optimal utilization of exercise technetium-99m sestamibi myocardial perfusion single-photon emission computed tomography. J Am Coll Cardiol 1995;26:639-47.
6. Piwnica-Worms DP, Kronauge JF, LeFurgey A, Backus M, Hockett D, Ingram P, et al. Mitochondrial localization and characterization of 99Tc-SESTAMIBI in heart cells by electron probe X-ray microanalysis and 99Tc-NMR spectroscopy. Magn Reson Imaging 1994;12:641-52.
7. Hindie E, Melliere D, Perlemuter L, Jeanguillaume C, Galle P. Primary hyperparathyroidism: higher success rate of first surgery after preoperative Tc-99m sestamibi-I-123 subtraction scanning. Radiology 1997;204:221-8.
8. Waxman AD. The role of (99m)Tc methoxyisobutylisonitrile in imaging breast cancer. Semin Nucl Med 1997; 27:40-54.
9. Khalkhali I, Cutrone J, Mena I, Diggles L, Venegas R, Vargas H, et al. Technetium-99m-sestamibi scintimammography of breast lesions: clinical and pathological follow-up. J Nucl Med 1995;36:1784-9.
10. Nishiyama Y, Kawasaki Y, Yamamoto Y, Fukunaga K, Satoh K, Takashima H, et al. Technetium-99m-MIBI and thallium-201 scintigraphy of primary lung cancer. J Nucl Med 1997;38:1358-61.
11. Bom HS, Kim YC, Song HC, Min JJ, Kim JY, Park KO. Technetium-99m-MIBI uptake in small cell lung cancer. J Nucl Med 1998;39:91-4.
12. Nishiyama Y, Yamamoto Y, Kawasaki Y, Satoh K, Takashima H, Ohkawa M, et al. Accumulation of Tc-99m MIBI in breast lymphoma: comparison with Ga-67 citrate. Ann Nucl Med 1996;10:429-32.
13. Matsui R, Komori T, Narabayashi I, Namba R, Nakata Y, Tabuchi K, et al. Tc-99m sestamibi uptake by malignant lymphoma and slow washout. Clin Nucl Med 1995;20: 352-6.
14. Baillet G, Albuquerque L, Chen Q, Poisson M, Delattre JY. Evaluation of single-photon emission tomography imaging of supratentorial brain gliomas with technetium-99m sestamibi. Eur J Nucl Med 1994;21:1061-6.
15. Soderlund V, Jonsson C, Bauer HC, Brosjo O, Jacobsson H. Comparison of technetium-99m-MIBI and technetium-99m-tetrofosmin uptake by musculoskeletal sarcomas. J Nucl Med 1997;38:682-6.
16. Fukushima K, Kono M, Ishii K, Sakai E, Hirota S, Yuri H. Technetium-99m methoxyisobutylisonitrile single-photon emission tomography in hepatocellular carcinoma. Eur J Nucl Med 1997;24:1426-8.
17. Alonso O, Lago G, Mut F, Hermida JC, Nunez M, De Palma G, et al. Thyroid imaging with Tc-99m MIBI in patients with solitary cold single nodules on pertechnetate imaging. Clin Nucl Med 1996;21:363-7.
18. Sundram FX, Mack P. Evaluation of thyroid nodules for malignancy using 99Tcm-sestamibi. Nucl Med Commun 1995;16:687-93.
19. Taillefer R, Robidoux A, Turpin S, Lambert R, Cantin J, Leveille J. Metastatic axillary lymph node technetium-99m-MIBI imaging in primary breast cancer. J Nucl Med 1998;39:459-64.
20. Onsel C, Sonmezoglu K, Camsari G, Atay S, Cetin S, Erdil YT, et al. Technetium-99m-MIBI scintigraphy in pulmonary tuberculosis. J Nucl Med 1996;37:233-8.
21. Hurwitz GA, Duan HY, Blais M, Mattar AG, Gravelle DR. An atlas of renography with Tc-99m sestamibi: comparison with Tc-99m DTPA. Clin Nucl Med 1995; 20: 821-9.
22. Lamont AE, Joyce JM, Grossman SJ. Acute cholecystitis detected on a Tc-99m sestamibi myocardial imaging. Clin Nucl Med 1996;21:879.

STUDIES ON THE VELOCITY OF BLOOD FLOW

XIII. The Circulatory Response to Thyrotoxicosis[1]

By HERRMAN L. BLUMGART, SAMUEL L. GARGILL and DOROTHY ROURKE GILLIGAN

(From the Research Laboratories of the Beth Israel Hospital, The Thorndike Memorial Laboratory of the Boston City Hospital, and the Department of Medicine, Harvard Medical School, Boston)

(Received for publication January 20, 1930)

Parry in 1815 (1) originally described exophthalmic goitre as a form of heart disease, beginning the chapter on "Diseases of the Heart" with the following words: "There is one malady which I have in five cases seen coincident with what appeared to be enlargement of the heart, and which, so far as I know, has not been noticed, in that connection, by medical writers. The malady to which I allude is enlargement of the thyroid gland." Ever since then the importance of cardiac damage in patients with thyrotoxicosis has impressed students of this disease.

Various aspects of the circulation in thyrotoxicosis have been studied to gain more adequate insight into the pathologic physiology of this condition so as to provide a rational basis for treatment. The minute volume output of the heart has been measured by several investigators, but information regarding the velocity of blood flow has not been hitherto available. The purpose of the present investigation was to learn the degree to which the blood flow is accelerated in thyrotoxicosis and to study the relation of such measurements to other aspects of the circulation.

[1] This investigation was aided in part by a grant from the DeLamar Mobile Research Fund of Harvard University.

RÉSUMÉ OF THE LITERATURE

Pulse rate and pulse pressure. In general, investigators have found that there is a definite, though inexact, correspondence between the elevation in the basal metabolic rate and the increase in pulse rate. Sturgis and Tompkins (2), in a study of 154 patients with thyrotoxicosis, found a fairly constant relationship between the resting pulse rate and the basal metabolism. They state that "a basal pulse rate below 90 per minute is seldom, and below 80 per minute is rarely associated with an increased metabolism." The rise in pulse rate is due, presumably, to increased metabolism for Minot and Means (3) observed that the degree of pulse elevation for a given metabolic rate was essentially the same in thyrotoxicosis and in chronic leukemia. Read (4), and Davies and Eason (5) corroborated the observations of Sturgis and Tompkins, finding, in spite of numerous exceptions, a general relation between the pulse rate and the basal metabolic rate. Davies and Eason also observed that as the basal metabolic rate increased, the pulse pressure likewise tended to increase. An increased pulse rate usually signifies an increased blood flow although blood flow may be actually diminished if a great reduction in the stroke volume occurs (6, 7). In brief, the pulse rate and the pulse pressure tend to be elevated with increase in minute volume output, but the relation is a varying one.

Vital capacity of the lungs. Rabinowitch (8) studied the vital capacity of the lungs in a series of patients with thyrotoxicosis and observed that it became lower as the basal metabolic rate increased. McKinlay (9) likewise found a reduction in the vital capacity of the lungs to below 70 per cent of the normal in a great majority of severely toxic cases of thyroid disease. He observed that the minute volume of pulmonary ventilation at rest was not related to the diminution in the vital capaciy of the lungs. Lemon and Moersch (10) compared the vital capacity of the lungs and basal metabolic rate in 85 subjects. They found a tendency toward decreased vital capacity with increased metabolic rates, but stated that there was no precise relationship between the two measurements in a given individual.

Minute volume output of the heart. Plesch (11) studied the minute volume output of the heart in one case of exophthalmic goitre, using an ingenious but rather crude gasometric method. He found that the minute volume output of the heart was 5,288 cc. as contrasted with 4,359 cc. in one normal subject. The pulse rate of the patient with exophthalmic goitre averaged 97, that of the normal subject 72 per minute, while the oxygen consumption was 6.47 cc. per kilo per minute as compared to 3.52 cc. for the normal subject. Rabinowitch and Bazin (12) studied the venous oxygen unsaturation of the arm blood in patients with thyrotoxicosis, and inferred that no significant increase occurred in the minute volume output of the heart or in the output per beat. Liljestrand and Stenström (13) carefully studied the minute volume output of the heart in ten healthy subjects and in eleven patients with exophthalmic goitre, using the nitrous oxide method of Krogh and Lindhard (30). Eight female patients with an average increase in the

basal metabolic rate of 58 per cent above the normal showed an increase of 80 per cent in the minute volume output of the heart, while three male patients with an increase in the basal metabolic rate of 66 per cent showed an increase of 100 per cent in the minute volume output of the heart. Davies, Meakins and Sands (14), and Blalock and Harrison (27) likewise observed that the minute volume output of the heart was increased roughly in proportion to the increased basal metabolic rate although an exact parallelism between the two measurements could not be traced in every instance. Similar results were obtained in several patients with exophthalmic goitre by Kininmonth (15) using the ethyl iodide method of Henderson and Haggard. Robinson (16), Liljestrand and Stenström (13), and Burwell, Smith and Neighbors (17) found the output of the heart increased to such an extent that the oxygen demands of the body were supplied without diminishing the oxygen tension of the mixed venous blood.

METHODS

The velocity of blood flow was measured by means of the radium active deposit method (18, 19, 20, 21). The active deposit was injected into the right antecubital vein, and the times of its arrival in the right chambers of the heart and in the arteries about the elbow of the left arm were recorded. The time that elapses between the injection of the active deposit into the antecubital vein and the arrival of the active deposit in the right chambers of the heart has been termed "the arm to heart time" for it is a measure of the velocity of venous blood flow from the arm to the heart. The time that elapses between the arrival of the active deposit of radium in the right chambers of the heart and its arrival in the arteries about the elbow of the arm has been called "the crude pulmonary circulation time" and provides an estimate of the velocity of blood flow through the lungs.

The venous pressure was measured according to the direct venipuncture method of Moritz and Tabora (22), and the vital capacity of the lungs by means of a Collins spirometer. The basal metabolic rate was measured with a Benedict-Roth apparatus. The tests were carried out under strictly basal conditions. The Aub-DuBois standard was used. All measurements were made in duplicate and did not differ by more than 5 per cent. The basal metabolic rate and the velocity of blood flow were measured on the same day in one-half of the cases, while in the rest the measurements were made on successive days. Particular care was taken to gain the confidence and coöperation of the patient so that the velocity of blood flow measurements could be made

under as nearly basal conditions as possible. The pulse rate was counted several times before and after each test. Whenever feasible, observations were repeated after the basal metabolic rate had returned to normal in order to study the effect of treatment.

RESULTS

Twenty-seven measurements of the pulmonary circulation time and related aspects of the circulation were made in thirteen patients. In studying the data it seemed desirable to divide the patients into two groups. The first group includes nine patients who showed no clinical evidence of circulatory insufficiency; the second group consists of four patients who showed signs of cardiovascular disease.

I. Thyrotoxic patients with no clinical evidence of cardiovascular disease

Table 1 presents the results of twenty measurements of the pulmonary circulation time and related aspects of the circulation in the nine patients of this group, all of whom had exophthalmic goitre. In all but one of the patients, (D. A.), observations were repeated when the basal metabolic rate had been lowered by treatment. The diagnoses were established by the clinical findings and by microscopic examination of the excised thyroid tissue, the results of which are given in the appended case summaries. The clinical condition of the patients varied considerably. Some individuals were very toxic and had experienced symptoms for many years, while in others the disease was less severe and of shorter duration. Six of the nine patients were females, and three patients were males. The ages of the patients varied from 18 to 45 years.

Blood. In all patients the hemoglobin and red blood cell concentration in the peripheral blood were within the limits of normal.

Pulse rate. The pulse rates before treatment were usually elevated but became normal with lowering of the basal metabolic rate. There was a general relation between the degree of elevation of the pulse rate and the increase in the basal metabolic rate. In a given case, however, the relation was not always evident. Patient W. F., for instance, with a basal metabolic rate of 35 per cent above the normal, had a pulse rate of 68 and 80 on two occasions before treatment, while

the pulse rate was 76 after subtotal thyroidectomy when the basal metabolic rate was only 13 per cent above the normal.

Venous pressure. No significant deviations from the normal were observed in the venous blood pressures before or after treatment.

Vital capacity of the lungs and respiratory minute volume. The vital capacity of the lungs was diminished in five of the nine patients in the absence of any evidence of circulatory failure. The diminution was an inconstant finding and was not related to the degree of elevation in the basal metabolic rate. With a decrease in the basal metabolic rate toward normal the vital capacity of the lungs tended to increase although this was not apparent in every instance. Before treatment when the basal metabolic rate averaged 33 per cent above normal, the average vital capacity of the lungs was 1870 cc. per square meter of body surface. After compound solution of iodine had been given, the average basal metabolic rate decreased to 22 per cent above normal, but the vital capacity of the lungs failed to increase. After operation, however, the average basal metabolic rate was one per cent above normal and the average vital capacity increased to 2010 cc. per square meter of body surface.

In a few patients the respiratory minute volume was measured while the basal metabolic rate was elevated and again following appropriate treatment. While there was slight diminution in the respiratory minute volume with a return of the basal metabolic rate to normal, the magnitude of the respiratory minute volume before treatment and its decrease after treatment bore no direct relation to the oxygen consumption.

Velocity of blood flow. The velocity of blood flow was strikingly increased, the pulmonary circulation time in some cases being the most rapid observed in any condition up to this time. As in our previous studies, the velocity of blood flow from the arm to the heart showed considerable variation, although in most patients it was definitely increased above the normal. The variability of the arm to heart circulation time was unusually great, due, probably, to the vasomotor instability of these thyrotoxic patients. The extent of the increase in the velocity of blood flow through the lungs was closely related to the extent of increase in the basal metabolic rate. This relationship was present in each individual case and is shown by the average results.

TABLE 1

Circulatory measurements and related aspects in patients with thyrotoxicosis who showed no clinical evidence of cardiovascular disease

Date	Name	Sex	Age	Clinical diagnosis	Pulse rate	Arterial pressure		Vital capacity		Circulation time			Pulmonary circulation velocity, percentage of normal	Basal metabolic rate, percentage variation from normal	Remarks
						Systolic	Diastolic	Observed	Per square meter	Arm to heart	Arm to arm	Pulmonary			
			years			mm. Hg	mm. Hg	cc.	cc.	seconds	seconds	seconds	per cent	per cent	
April 13, 1928	E. B.	F.	32	Thyrotoxicosis	108	140	80	2,500	1,610	3.5	7.5	4.0	270	+60	Before treatment. Lugol's solution M.X. t.i.d begun April 15, 1928, and ended April 24, 1928. Subtotal thyroidectomy April 25, 1928. Pathological diagnosis: Hyperplasia of thyroid
June 1, 1928	E. B.	F.	32		78	100	70	2,700	1,720	5.5	15.0	9.5	114	+9	
November 15, 1927	G. O.	F.	25	Exophthalmic goitre	98	110	70	2,800	1,730	4.5	8.5	4.0	270	+24	Before treatment. Lugol's solution M.X. t.i.d. begun November 15, 1927, and ended November 18, 1927. Subtotal thyroidectomy November 19, 1927. Pathological diagnosis: Hyperplasia of thyroid
March 21, 1928	G. O.	F.	25		68	105	70	3,400	2,090	10.0	30.0	20.0	54	−3	
May 17, 1928	G. O.	F.	25		66	118	75	3,300	2,000	6.0	18.0	12.0	90	±0	
January 9, 1928	D. S.	M.	45	Exophthalmic goitre	105	115	40	3,200	1,960	2.5	8.0	5.5	196	+35	Before treatment. Lugol's solution M.X. t.i.d. begun January 21, 1928, and ended February 3, 1928. Subtotal thyroidectomy February 4, 1928. Pathological diagnosis: Hyperplasia of thyroid
June 16, 1928	D. S.	M.	45		60	124	80	3,700	2,200	11.0	29.0	18.0	60	−9	
October 6, 1927	D. A.	F.	30	Exophthalmic goitre, myasthenia gravis	120	140	92	1,800	1,190	2.0	8.0	6.0	180	+33	Before treatment

November 15, 1927	M. C.	F.	23	Exophthalmic goitre	94	120	80	2,800	1,590	11.0	17.5	6.5	166	+24	Before treatment. Lugol's solution M.V. t.i.d. begun April 2, 1928 and ended April 15, 1928. Subtotal thyroidectomy April 16, 1928. Pathological diagnosis: Hyperplasia of thyroid
March 27, 1928	M. C.	F.	23		124	110	75	2,000	1,240	5.0	11.0	6.0	180	+26	
May 29, 1928	M. C.	F.	23		76	110	70	2,500	1,600	8.0	23.0	15.0	72	−13	
January 8, 1929	I. B.	M.	45	Exophthalmic goitre	92	140	80	4,200	2,700	8.0	14.0	6.0	180	+27	Before treatment. Lugol's solution M.X. t.i.d. begun January 11, 1929 and ended January 21, 1929. Right hemithyroidectomy January 22, 1929. Left hemithyroidectomy March 18, 1929. Pathological diagnosis: Hyperplasia of thyroid
May 20, 1929	I. B.	M.	45		68	130	90	4,100	2,400	10.0	21.5	11.5	94	+3	
March 6, 1928	Y. A.	F.	21	Exophthalmic goitre	94	110	70	3,200	2,010	3.0	9.5	6.5	166	+29	Before treatment. Lugol's solution M.X. t.i.d. begun March 22, 1928
March 23, 1928	Y. A.	F.	21		82	105	70	2,600	1,630	7.0	15.0	8.0	135	+20	
April 14, 1928	W. F.	M.	38	Thyrotoxicosis	68	110	60	3,600	2,320	8.0	16.5	8.5	127	+35	Before treatment. Lugol's solution M.X. t.i.d. begun April 15, 1928 and ended April 26, 1928. Subtotal thyroidectomy April 27, 1928. Pathological diagnosis: Hyperplasia of thyroid
April 24, 1928	W. F.	M.	38		80	115	70	3,400	2,260	3.0	10.5	7.5	144	+35	
June 16, 1928	W. F.	M.	38		76	90	40	3,500	2,170	8.0	19.0	11.0	98	+13	
October 7, 1927	F. R.	F.	18	Exophthalmic goitre	88	130	70	1,900	1,370	7.5	16.5	9.0	120	+11	Lugol's solution M.X. t.i.d. begun October 5, 1927 and ended October 14, 1927. Subtotal thyroidectomy October 15, 1927. Pathological diagnosis: Hyperplasia of thyroid
April 15, 1928	F. R.	F.	18		80	115	75	2,700	1,940	8.0	19.0	11.0	98	+7	
Average before treatment					99	123	74	2,960	1,870	4.9	10.8	5.9	183	+33	
Average after Lugol's solution					83	117	70	2,630	1,753	5.8	14.0	8.2	132	+22	
Average after operation					72	112	71	3,220	2,010	8.4	21.5	13.1	83	+1	
Normal average					76	120	80		2,250	6.6	17.4	10.8	100	±0	

In a previous study of fifty-eight normal persons, the arm to heart circulation time averaged 6.6 seconds, and the crude pulmonary circulation time 10.8 seconds. In these patients with thyrotoxicosis in whom the basal metabolic rate averaged 33 per cent above normal, the arm to heart circulation time averaged 4.9 seconds and the crude pulmonary circulation time 5.9 seconds. These results signify an in-

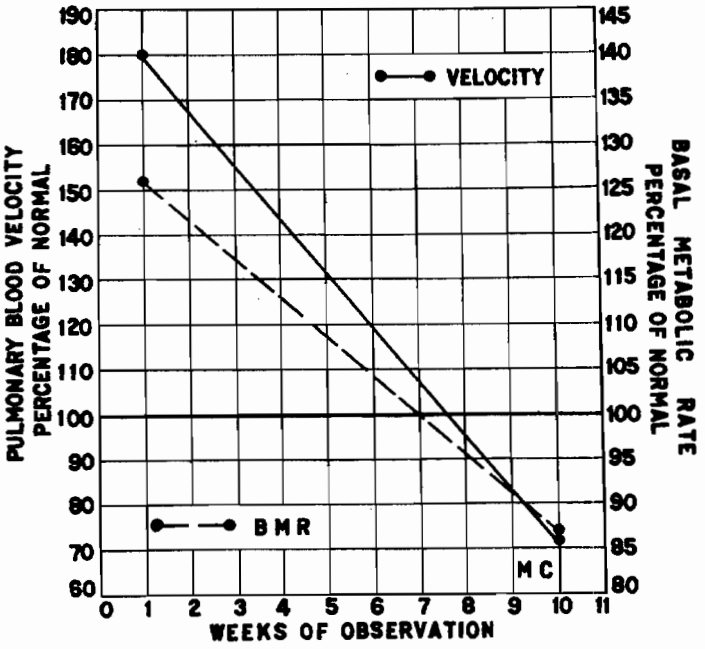

FIG. 1. RELATION OF THE VELOCITY OF BLOOD FLOW THROUGH THE LUNGS AND BASAL METABOLIC RATE IN PATIENT M. C. SUBTOTAL THYROIDECTOMY WAS PERFORMED DURING THE FOURTH WEEK OF OBSERVATION

creased velocity of blood flow from the arm to the heart of 34 per cent and an increased speed of blood flow through the lungs of 83 per cent above the average of normal.

As the basal metabolic rate became lower, the velocity of blood flow likewise approached normal. This is shown graphically in figure 1, as well as by the results in table 1. The slowing in blood flow toward normal as the basal metabolic rate was lowered by Lugol's solution

TABLE 2

Circulatory measurements and related aspects in patients with thyrotoxicosis who showed clinical evidence of cardiovascular disease

Date	Name	Sex	Age	Clinical diagnosis	Pulse rate	Arterial pressure		Vital capacity		Circulation time			Pulmonary circulation velocity, percentage of normal	Basal metabolic rate, percentage variation from normal	Remarks
						Systolic	Diastolic	Observed	Per square meter	Arm to heart	Arm to arm	Pulmonary			
			years			mm. Hg	mm. Hg	cc.	cc.	seconds	seconds	seconds	per cent	per cent	
January 8, 1929	L. R.	M.	36	Thyrotoxicosis, thyrotoxic heart	90	135	72	3,100	1,970	4.0	10.0	6.0	180	+33	Before treatment
February 13, 1928	M. B.	F.	61	Thyrotoxicosis	116	195	110	1,500	960	7.0	13.0	6.0	180	+50	Before treatment. Lugol's solution
March 26, 1928	M. B.	F.	61	Hypertension	88	200	110	2,000	1,340	6.5	16.5	10.0	108	+41	M.X. t.i.d. begun on February 13,
May 10, 1928	M. B.	F.	61		90	225	120	2,000	1,250	9.0	23.0	14.0	77	+28	1928, and ended on February 20, 1928. Subtotal thyroidectomy on February 21, 1928. Pathological diagnosis: Toxic adenoma of thyroid
February 13, 1928	R. N.	F.	45	Thyrotoxicosis	94	118	65	1,700	1,080	5.0	12.0	7.0	154	+24	Lugol's solution M.X. t.i.d. begun on
April 17, 1928	R. N.	F.	45	Thyrotoxic heart, auricular fibrillation	69	115	70	3,200	1,950	11.0	26.5	15.5	70	+7	February 12, 1928, and ended on February 14, 1928. Subtotal thyroidectomy on February 15, 1928. Pathological diagnosis: Hyperplasia of thyroid
December 6, 1927	P. F.	M.	66	? Toxic adenoma, arteriosclerosis, thyrotoxic heart	88	120	80	2,500	1,690	7.5	17.0	9.5	114	+40	Before treatment
Average before operation					97			2,200	1,430	5.9	13.0	7.2	150	+37	
Average after operation					80			2,600	1,600	10.0	24.8	14.8	73	+18	
Normal average					76				2,250	6.6	17.4	10.8	100	±0	

affords additional rational basis for the preoperative administration of compound solution of iodine.

II. Patients with thyrotoxicosis and clinical evidences of cardiovascular disease

Seven measurements of the velocity of blood flow and related aspects of the circulation were made in the four patients of this group (table 2). Signs or symptoms of circulatory insufficiency had previously been present but were absent at the time of the test, although in one patient, R. N., auricular fibrillation was present at the time of the first, but not at the time of the second series of measurements. The vital capacity of the lungs was lowered in all patients, while the venous pressure was within the upper limits of normal. The velocity of blood flow through the lungs, although conspicuously increased, was slightly slower than the average velocity observed in the group of patients without cardiovascular disease but with similar basal metabolic rates. The pulse rate was generally increased in proportion to the elevation in the basal metabolic rate as in the preceding group of patients.

DISCUSSION

The work done by the heart consists mainly in expelling the blood into the aorta and into the pulmonary artery against the existing pressures, and in imparting to the blood a certain velocity. The conspicuously increased velocity of blood flow found in patients with thyrotoxicosis emphasizes the strain under which the heart labors even when the body is under basal metabolic conditions.

Certain facts assume increased significance when considered in relation to our results. The hot, flushed, salmon-colored skin, the tendency to perspire, the increased pulse pressure, the tendency to increased blood volume (23) and the diminution in the vital capacity of the lungs observed clinically suggest that considerable vasodilatation is present in thyrotoxicosis and that the functional cross sectional diameter of the peripheral and pulmonary vascular bed is increased. The relation between volume flow and velocity flow through tubes of known diameter is a simple one and is expressed by the equation

$v = \frac{a}{\pi r^2}$ where v = velocity expressed in seconds, a = volume per second and r is the radius of the tube. If other factors remain equal, an increase in the functional cross sectional area of the vascular bed would tend to diminish the speed of blood flow. The fact that the velocity of blood flow is so strikingly increased in spite of the existence of considerable vasodilatation is further evidence of the extreme strain under which the heart labors (24).

Although the second group of patients experienced dyspnoea on the slightest exertion, the velocity of blood flow was only slightly slower than that observed in similar patients (group I) without cardiovascular disease. This fact emphasizes the close interdependence of the circulatory-respiratory-metabolic mechanism. Increased tissue metabolism cannot take place unless there is a proportionate increase both in blood flow and in effective pulmonary ventilation. The observations on the velocity of blood flow in the patients of group I, in whom there was no evidence of cardiovasulcar disease, indicate the degree to which the velocity of blood flow was increased to satisfy the increased metabolic demands of the tissues. A blood flow less rapid than this in the patients of group II was evidently inadequate and was accompanied by dyspnoea on the slightest exertion. This finding is of interest for while the velocity of blood flow was slightly slower in the patients of group II than in the patients of group I, it was nevertheless much more rapid than that found in normal subjects. The question of whether a given velocity of blood flow is adequate, therefore, cannot be decided in any absolute terms but only in relation to the metabolic rate of that patient. According to this concept the term "normal velocity of blood flow" denotes the velocity of blood flow found in normal subjects with a normal basal metabolic rate.

The extremely rapid velocity of blood flow observed in patients with thyrotoxicosis affords additional information as to why such individuals experience signs and symptoms of circulatory insufficiency on but relatively slight exertion. Plummer and Boothby (25) have shown that a given amount of work by thyrotoxic patients is accompanied by a disproportionate rise in the basal metabolic rate requiring a similar disproportionate rise in ventilation and in blood flow. Rabinowitch (8) and others have shown that the vital capacity of thyrotoxic

patients is greatly diminished, thereby imposing a limitation on the degree to which the ventilation can be increased. The work of Liljestrand and Stenström (13), Bock and Field (26), Kininmonth (15), Burwell, Smith, and Neighbors (17), Means and Newburgh (29) and others indicates that the minute volume output of the heart in thyrotoxic patients at rest corresponds to that in normal individuals doing light work. This indicates that the "reserve" in the minute volume output of the heart is utilized by thyrotoxic patients even while at rest. The extremely rapid blood flow found in the present studies indicates similarly that what may be termed the "reserve" in the velocity of blood flow has been seriously encroached upon. In brief, a thyrotoxic individual experiences dyspnoea more readily than a normal one because: (1) an increased gaseous exchange is necessary; (2) a greater expenditure of energy and hence a relatively greater degree of hyperpnea is necessary to accomplish a given task; (3) the pulmonary bellows are much less efficient; (4) the "reserve" in the minute volume output has been moderately, and the "reserve" in the velocity of blood flow has been greatly encroached upon even while the patient is at rest.

The greatly increased work of the heart even under basal conditions serves to explain the frequency of circulatory insufficiency in thyrotoxicosis. Whether the frequency of cardiac damage in this condition is due partly to a specific toxic effect on the heart cannot be stated on the basis of present knowledge.

The increased velocity of blood flow in thyrotoxicosis probably occurs to meet the demands of the elevated metabolic rate and not as a result of a toxic effect on the heart. We have observed several patients with essential hypertension in whom the basal metabolic rate was elevated as high as plus 33 per cent without the clinical evidence of thyrotoxicosis. Measurements demonstrate that in these subjects the increase in the velocity of blood flow through the lungs is similar to that observed in thyrotoxic patients with equally high metabolic rates but without hypertension. The findings are in accord with certain observations on the minute volume output of the heart (14, 28). The increased burden imposed by this elevation of basal metabolic rate is of serious import to the already overworked heart and indicates the advisability of reducing the basal metabolic rate in such patients

by appropriate means. Such reduction of the basal metabolic rate while tending to lessen the amount of the cardiac work, could not be expected to affect the degree of the arterial hypertension. Similar considerations probably apply to other states such as leukemia and fever in which the metabolic rate is elevated. These observations, again demonstrate that alteration of one fundamental physiological function is accompanied by changes which tend to keep constant the various relationships within the internal environment.

SUMMARY

1. Twenty-seven series of measurements were made in thirteen patients with thyrotoxicosis in order to correlate the clinical manifestations with changes in the velocity of blood flow through the lungs, the basal metabolic rate, pulse rate, venous and arterial pressures and vital capacity of the lungs. Measurements made when the basal metabolic rate was elevated were compared with subsequent measurements when the rate was reduced.

2. There was a general but inexact relation between the degree of elevation of the pulse rate and the increase in the basal metabolic rate.

3. No significant deviations from the normal were observed in the venous blood pressure before or after treatment.

4. Diminution in the vital capacity of the lungs was an inconstant finding. With a decrease in the basal metabolic rate, the vital capacity of the lungs tended to increase.

5. The velocity of blood flow was strikingly increased so that the pulmonary circulation time was the fastest yet recorded in man. The increase in velocity of blood flow through the lungs was proportional to the degree of elevation in the basal metabolic rate. This emphasizes the strain under which the heart labors in thyrotoxicosis.

6. In nine patients with thyrotoxicosis but without circulatory failure, the basal metabolic rate averaged 33 per cent above the normal, while the velocity of blood flow through the lungs averaged 83 per cent above the normal. In four thyrotoxic patients with similar basal metabolic rates but with cardiovascular disease, the velocity of blood flow was slightly slower. The fact that the latter group of patients experienced dyspnoea on slight exertion emphasizes the close interdependence of the circulatory-respiratory-metabolic mechanism.

7. When the basal metabolic rate was lowered by the administration of compound solution of iodine or by operation, the velocity of blood flow was correspondingly slowed.

ABSTRACTS OF HISTORIES AND PHYSICAL EXAMINATIONS OF PATIENTS WITH THYROTOXICOSIS

E. B. entered the hospital because of nervousness and loss of weight. She had become increasingly nervous during the four years before admission. One year before admission she became distinctly irritable and noted an undue tendency to perspire. Six months before admission a swelling appeared in the front of the neck. During the three weeks preceding her entry to the hospital she had occasional dyspnoea and palpitation. There had been a loss of 17 lbs. in weight during the last six months. *Physical examination* showed marked nervousness; a moist, warm skin; a flushed face; symmetrical enlargement of the thyroid gland with systolic bruit over it; the heart not enlarged, with rate of 100 per minute; fine tremor of fingers and hyperactive reflexes. The blood pressure was 140 mm. Hg systolic and 80 mm. Hg diastolic. The basal metabolic rate was plus 60 per cent on April 12. Ten minims of Lugol's solution were given three times daily from April 15 to April 24. Subtotal thyroidectomy was performed on April 25. The pathological report was "Marked chronic inflammation, with marked follicular hyperplasia, and no colloid distention; hyperplasia of thyroid."

G. O'M. entered the hospital because of nervousness, fatigue and swelling of the neck. For eighteen months before admission she had noticed easy fatigability, restlessness and tremor of the hands. One year before admission she began to perspire unduly and noted a swelling at the base of the neck. She experienced palpitation on slight exertion during the two months before admission. She lost 20 lbs. within the six months preceding her entry to the hospital, although her appetite remained very good. *Physical examination* showed restlessness; quick, jerky movements; warm, moist skin; slight exophthalmos; symmetrical enlargement of the thyroid gland, with a bruit over the isthmus. Her heart was not enlarged, the rate was 94 per minute. The blood pressure was 120 mm. Hg systolic, 70 mm. Hg diastolic. The reflexes were hyperactive and there was a fine tremor of the fingers. The basal metabolic rate was plus 24, plus 22 and plus 24 per cent on October 12, November 10 and November 16, respectively. Ten minims of Lugol's solution were given three times a day from November 15 to November 18. A subtotal thyroidectomy was performed on November 19. The pathological report was—"Sections show marked chronic inflammation, with very marked follicular hyperplasia, the epithelium being columnar in type, and showing retrograde changes. There is no colloid distention; hyperplasia of thyroid."

D. S. came to the hospital because of nervousness, easy fatigability, and trembling of hands, two months in duration. In spite of increased food intake, he had

lost 15 pounds in the two months preceding his entry into the hospital. *Physical examination* showed nervousness; flushed facies; warm, moist skin; slight exophthalmos with definite stare; no thyroid gland enlargement; normal sized heart, with rate of 90 per minute. The blood pressure was 115 mm. Hg systolic and 40 mm. Hg diastolic. There was fine tremor of both hands. The basal metabolic rate was plus 40 and plus 35 per cent on December 28 and January 7, respectively. Ten minims of Lugol's solution were given three times a day from January 21 to February 3. Subtotal thyroidectomy was performed on February 4. The pathological report was "Moderate chronic inflammation with very marked follicular hyperplasia, showing retrograde changes; hyperplasia of thyroid."

D. A. had had a right hemithyroidectomy in 1915, twelve years before the present admission to the hospital. Three years previously drooping of the eyelids was first noted. Four months before admission she had to give up her work on account of increasing weakness and nervousness. Dysphagia and dysarthria gradually developed. Food seemed to lodge in her throat, and her voice became nasal in quality. Two months before admission diplopia was noted, especially on fatigue. She had lost 20 pounds during the four months preceding admission. She reentered now because of nervousness, weakness, difficulty in talking and swallowing, and drooping of the eyelids. *Physical examination* showed complete ptosis of the upper eyelids; limitation of ocular movements laterally and upward; weakness of facial muscles without atrophy; nasal quality to speech; well-healed, semi-circular scar at base of neck; small, hard mass moving with deglutition to the right of the hyoid bone; normal sized heart, with rate of 120 per minute; warm, moist skin and marked tremor of fingers. The blood pressure was 140 mm. Hg systolic and 90 mm. Hg diastolic. The basal metabolic rate was plus 23, plus 32 and plus 31 per cent on September 27, October 10 and 11, 1927, respectively. The clinical diagnosis was not only exophthalmic goitre but also myasthenia gravis. Ten minims of Lugol's solution were given three times daily from October 11 to October 23. Left hemithyroidectomy was performed on October 24. She died October 26. The pathological report was "Moderate chronic inflammation with moderate follicular hyperplasia, the epithelium being columnar in type; hyperplasia of thyroid."

M. C. entered the hospital because of swelling in her neck, palpitation, nervousness and difficult breathing. Four months before admission increased nervousness, voracious appetite and a tendency to perspire freely were noted. Six weeks before admission a swelling in the neck and tremor of the hands appeared. During the month before entry she had experienced palpitation and dyspnoea, especially on lying down. *Physical examination* showed a warm, moist skin; fine tremor of extended hands; moderate exophthalmos with bilateral lid-lag, symmetrical enlargement of thyroid gland with bruit; heart of normal size with rate of 120 per minute and a soft blowing systolic murmur over the apex. The blood pressure

was 136 mm. Hg systolic, 98 mm. Hg diastolic. The basal metabolic rate was plus 28 and plus 24 per cent on November 11 and 16, 1927, respectively. Treatment was delayed because the patient developed an upper respiratory tract infection and an acute purulent otitis media. Ten minims of Lugol's solution were given three times daily from April 2 to April 15, 1928. Subtotal thyroidectomy was done the next day. The pathological report was "Sections show marked chronic inflammation, with marked follicular hyperplasia, the epithelium being columnar in type, and no colloid distention. Parenchymatous hyperplasia of thyroid."

I. B. had suffered from nervousness, loss of weight, tremor of hands, and palpitation for one year before admission to the hospital. During the two months preceding his entry, eight to ten attacks of palpitation occurred daily. He perspired unduly and fatigued easily. *Physical examination* showed nervousness and restlessness. The skin was moist, warm and salmon-colored. There was moderate exophthalmos; an enlarged thyroid gland with a bruit and thrill over it; a normal sized heart with rate of 100 per minute; and marked tremor of fingers. The blood pressure was 148 mm. Hg systolic, 68 mm. Hg diastolic. The basal metabolic rate was plus 44, plus 22 and plus 27 per cent on January 3, 5 and 9, respectively. Ten minims of Lugol's solution were given three times a day from January 11 to January 21. Right hemithyroidectomy was performed on January 22 and left hemithyroidectomy on March 18. The pathological report was "Sections show marked follicular hyperplasia, with marked chronic inflammation. There is no colloid distention of acini. Parenchymatous hyperplasia of thyroid gland."

Y. A. entered the hospital because of increasing nervousness, perspiration and swelling in her neck. A swelling first appeared in the neck seven years before admission. For two years before admission she had been markedly nervous and had suffered from disturbed sleep, and profuse perspiration. *Physical examination* showed a nervous, restless girl with flushed, moist skin; slight exophthalmos with lid-lag; symmetrical enlargement of the thyroid gland with systolic and diastolic bruit over it; normal sized heart with rate of 90 per minute; and a coarse tremor of extended hands. The blood pressure was 120 mm. Hg systolic, 70 mm. Hg diastolic. The basal metabolic rate was plus 31 and plus 29 per cent on March 1 and 5, respectively. Ten minims of Lugol's solution were given three times daily from March 22 to April 3. Subtotal thyroidectomy was performed April 4. The pathological report was "Marked chronic inflammation, with marked follicular hyperplasia, but no colloid distention. Hyperplasia of thyroid."

W. F. entered the hospital because of nervousness and loss of weight. For one year before admission he had tired easily, had become irritable and nervous, and had developed a tremor of the hands. In spite of greatly increased food intake

he had lost 20 pounds in the three months before admission. *Physical examination* revealed a flushed, moist skin; marked tremor of extended hands; heart not enlarged with rate of 120 per minute. The blood pressure was 120 mm. Hg systolic, 60 mm. Hg diastolic. There was no exophthalmos or enlargement of the thyroid gland. The basal metabolic rate was plus 36 and plus 34 per cent on April 12 and 16, respectively. Ten minims of Lugol's solution were given three times daily from April 15 to April 26. Subtotal thyroidectomy was performed on April 27. The pathological report was "Sections show moderate follicular hyperplasia, with slight chronic inflammation. There was no colloid distention. Hyperplasia of thyroid (moderate.)"

F. R. entered the hospital because of tremor of hands and nervousness. Two years before admission undue irritability and nervousness developed and one year before admission she noted tremor of hands and voracious appetite. *Physical examination* showed trembling of lips and chin; a warm, moist skin with pigmented areas under chin and in right axilla; slight exophthalmos; a palpable thyroid gland; normal heart with rate of 90 per minute; and fine and coarse tremor of both hands. The blood pressure was 130 mm. Hg systolic, 70 mm. Hg diastolic. The basal metabolic rate was plus 35 per cent on September 20 and plus 10 per cent on October 7. Thirty minims of Lugol's solution were given daily from October 5 to October 14. Subtotal thyroidectomy was performed on October 15, 1927. The pathological report was "Marked chronic inflammation, with moderate follicular hyperplasia. Epithelium columnar in type, and there are retrograde changes in acini. Hyperplasia of thyroid."

L. R. entered the hospital because of attacks of palpitation, dyspnoea and loss of weight. One year before admission attacks of palpitation gradually increasing in severity appeared. About five months before admission he began to suffer from dyspnoea on exertion with occasional attacks of severe palpitation. *Physical examination* showed a young man with a flushed, moist, salmon-colored skin, and tremor of hands. There was no exophthalmos. The thyroid gland was uniformly enlarged. The heart showed moderate enlargement to the left, action regular, rate 85 per minute. The first sound was accentuated and a systolic murmur was heard over the apex and base. The blood pressure was 135 mm. Hg systolic and 65 mm. Hg diastolic. Electrocardiographic tracings on admission showed normal rhythm, a week later, auricular fibrillation. The basal metabolic rate was plus 68 and plus 33 per cent on December 14, 1928 and January 8, 1929, respectively. Thirty minims of Lugol's solution were given daily from January 10 to January 21. Right hemithyroidectomy was performed on January 22 and and left hemithyroidectomy on March 26, 1929. The pathological diagnosis, was "Parenchymatous hyperplasia of thyroid gland."

M. B. had suffered from nervousness, dizziness and trembling of hands for one year and marked weakness for six months. During these six months she perspired

profusely and lost 25 pounds. *Physical examination* showed flushed skin and face, moderate exophthalmos with lid-lag, symmetrical enlargement of thyroid gland and fine tremor of extended hands. The heart was moderately enlarged to the left, the rate, 110 per minute. No murmurs were heard. The peripheral vessels were sclerosed and the blood pressure was 210 mm. Hg systolic and 110 mm. Hg diastolic. There were no signs of congestive heart failure. Electrocardiographic tracings showed left ventricular predominance with slurring of R_1 and S_3. The basal metabolic rate was plus 50 per cent on February 14. Lugol's solution, ten minims, three times a day, was given from February 13 to February 21. A subtotal thyroidectomy was performed February 21. The pathological report was "Sections show marked colloid distention of acini, with slight chronic inflammation. There is no evidence of hyperplasia. Toxic adenoma of thyroid gland." On March 26 she complained of weakness and trembling of hands, the blood pressure was 200 mm. Hg systolic and 110 mm. Hg diastolic, and there was slight pitting edema of lower extremities. The lungs were clear. The basal metabolic rate was plus 41 per cent. On May 10 she felt much better, had gained 22 pounds and was no longer nervous. The blood pressure was 225 mm. Hg systolic and 120 mm. Hg diastolic. The basal metabolic rate was plus 28 per cent.

R. N. entered the hospital because of attacks of palpitation, nervousness and easy fatigability, one year in duration. She had lost about 60 pounds during the year before admission, in spite of increased food intake. *Physical examination* showed a prematurely gray-haired woman; with flushed, moist skin; moderately enlarged thyroid gland; normal sized heart with rate of 94 per minute and absolutely irregular rhythm; a pulse deficit of 12; and fine tremor of extended hands. There was no exophthalmos, lid-lag, or peripheral edema. Electrocardiogram on February 13 showed auricular fibrillation. The basal metabolic rate was plus 22 and plus 24 per cent on February 10 and 14, respectively. Lugol's solution, ten minims, three times daily, was given from February 12 to February 14. Subtotal thyroidectomy was performed February 15. The pathological report was "Moderate to marked chronic inflammation. Follicular hyperplasia is very marked and the epithelium shows retrograde changes. There is no colloid distention. Hyperplasia of thyroid."

P. F. entered the hospital because of cough, dyspnoea and edema of feet. For many years he had suffered from "asthma." Three years before admission increasing nervousness developed. One month before admission sensation of pressure over the precordium, cough, and nocturnal dyspnoea appeared. Three days before admission he noticed swelling of his feet and palpitation on the slightest exertion. In spite of increased food intake, he had lost weight steadily. *Physical examination* showed a poorly nourished, elderly white man, restless and apprehensive; with marked exophthalmos; a warm, moist skin;

palpable thyroid gland with a hard nodule in the right lobe. The heart was definitely enlarged with systolic murmur over apex, rate of 90 per minute, and absolutely irregular rhythm. Peripheral vessels were markedly sclerosed. Auscultation of lungs showed prolonged expiratory phase accompanied by musical squeaks. There was pitting edema of both legs up to the knees. The blood pressure was 120 mm. Hg systolic and 80 mm. Hg diastolic. With full doses of digitalis, the edema disappeared and normal sinus rhythm was restored by the administration of quinidine sulphate. The basal metabolic rate was plus 29 and plus 40 per cent on November 5 and December 3, respectively. Ten minims of Lugol's solution were given three times daily from December 14 to December 22, 1927. Right hemithyroidectomy was performed December 23, 1927 and left hemithyroidectomy on February 9, 1928. The pathological report was "Sections show moderate chronic inflammation but marked follicular hyperplasia with columnar epithelium, showing retrograde changes. No colloid distention seen. Hyperplasia of thyroid."

BIBLIOGRAPHY

1. Parry, C. H., Vol. II, Page 111. London, 1825. Collections from the Unpublished Medical Writings of the late Caleb Hillier Parry.
2. Sturgis, C. C. and Tompkins, E. H., Arch. Int. Med., 1920, xxvi, 467. A Study of the Correlation of the Basal Metabolism and Pulse Rate in Patients with Hyperthyroidism.
3. Minot, G. R. and Means, J. H., Arch. Int. Med., 1924, xxxiii, 576. The Metabolism-Pulse Ratio in Exophthalmic Goiter and in Leukemia.
4. Read, J. M., Arch. Int. Med., 1924, xxxiv, 553. Basal Pulse Rate and Pulse Pressure Changes Accompanying Variations in the Basal Metabolic Rate.
5. Davies, H. W. and Eason, J., Quart. J. Med., 1924, xviii, 36. The Relation between the Basal Metabolic Rate and the Pulse-Pressure in Conditions of Disturbed Thyroid Function.
6. Meakins, J., Dautrebande, L. and Fetter, W. J., Heart, 1923, x, 153. The Influence of Circulatory Disturbances on the Gaseous Exchange of the Blood. IV. The Blood Gases and Circulation Rate in Cases of Mitral Stenosis.
7. Barcroft, J., Bock, A. V. and Roughton, F. J., Heart, 1922, ix, 7. Observations on the Circulation and Respiration in a Case of Paroxysmal Tachycardia.
8. Rabinowitch, I. M., Arch. Int. Med., 1923, xxxi, 910. The Vital Capacity in Hyperthyroidism with a Study of the Influence of Posture.
9. McKinlay, C. A., Arch. Int. Med. 1924, xxxiv, 168. The Vital Capacity of the Lungs and Its Significance in Hyperthyroidism.
10. Lemon, W. S. and Moersch, H. J., Arch. Int. Med., 1924, xxxiii, 130. Basal Metabolism and Vital Capacity.

11. Plesch, J., Ztschr. f. exper. Path. u. Therap., 1909, vi, 380. Hämodynamische Studien.
12. Rabinowitch, I. M. and Bazin, E. V., Arch. Int. Med., 1926; xxxviii, 566. The Output of the Heart per Beat in Hyperthyroidism.
13. Liljestrand, G. and Stenström, N., Acta Med. Scandinav,. 1925, lxiii, 99. Clinical Studies on the Work of the Heart during Rest. I. Blood Flow and Blood Pressure in Exophthalmic Goiter.
14. Davies, H. W., Meakins, J. and Sands, J., Heart, 1924, xi, 299. The Influence of Circulatory Disturbances on the Gaseous Exchange of the Blood. V. The Blood Gases and Circulation Rate in Hyperthyroidism.
15. Kininmonth, J. G., Quart. J. Med., 1928, xxi, 277. The Circulation Rate in Some Pathological States with Observations on the Effect of Digitalis.
16. Robinson, G. C., J. Am. Med. Assoc., 1926, lxxxvii, 314. The Measurement of the Cardiac Output in Man and Its Variations.
17. Burwell, C. S., Smith, W. C. and Neighbors, DeW., Am. J. Med. Sci., 1929, clxxviii, 157. The Output of the Heart in Thyrotoxicosis, with the Report of a Case of Thyrotoxicosis Combined with Primary Pernicious Anemia.
18. Blumgart, H. L. and Yens, O. C., J. Clin. Invest., 1927, iv, 1. Studies on the Velocity of Blood Flow. I. The Method Utilized.
19. Blumgart, H. L. and Weiss, S., J. Clin. Invest., 1927, iv, 15. Studies on the Velocity of Blood Flow. II. The Velocity of Blood Flow in Normal Resting Individuals, and a Critique of the Method Used.
20. Blumgart, H. L., and Weiss, S., J. Clin. Invest., 1927, iv, 389. Studies on the Velocity of Blood Flow. VI. The Method of Collecting the Active Deposit of Radium and Its Preparation for Intravenous Injection.
21. Blumgart, H. L. and Weiss, S., J. Clin. Invest., 1927, iv, 399. Studies on the Velocity of Blood Flow. VII. The Pulmonary Circulation Time in Normal Resting Individuals.
22. Moritz, F. and Tabora, D. V., Deutsch. Arch. f. klin. Med., 1910, xcviii, 475. Ueber eine Methode, beim Menschen den Druck in Oberflächlichen Venen exakt zu bestimmen.
23. Thompson, W. O., J. Clin. Invest., 1926, ii, 477. Studies in Blood Volume. I. The Blood Volume in Myxedema with a Comparison of Plasma Volume Changes in Myxedema and Cardiac Edema.
24. Evans, C. L., J. Physiol., 1919, lii, 6. The Velocity Factor in Cardiac Work.
25. Plummer, H. S. and Boothby, W. M., Am. J. Physiol., 1922, lxiii, 406. The Cost of Work in Exophthalmic Goiter.
26. Bock, A. V. and Field, H., Jr., Quoted by Means, J. H., Endocrinology, 1925, ix, 192. Circulatory Diseases in Diseases of Glands of Internal Secretion.
27. Blalock, A. and Harrison, T. R., Surg. Gyn. Obst., 1927, xliv, 617. Study Number Four on the Regulation of Circulation. The Effects of Thyroidectomy and Thyroid Feeding on the Cardiac Output.

28. Liljestrand, G. and Stenström, N., Acta. Med. Scandinav., 1925, lxiii, 142. Clinical Studies on the Work of the Heart during Rest. III. Blood Flow in Cases of Increased Arterial Blood Pressure with Observations on the Influence of Pregnancy on the Blood Flow.
29. Means, J. H. and Newburgh, L. H., Tr. Ass. Am. Phys., 1915, xxx, 51. Studies of the Blood Flow by the Method of Krogh and Lindhard.
30. Krogh, A. and Lindhard, J., Skand. Archiv. f. Physiol., 1912, xxvii, 100. Measurements of the Blood Flow Through the Lungs of Man.


R. Fleming, M.D.

THE EVOLUTION OF NUCLEAR CARDIOLOGY TAKES US BACK TO THE BEGINNING TO DEVELOP TODAY'S "NEW STANDARD OF CARE" FOR CARDIAC IMAGING: HOW QUANTIFYING REGIONAL RADIOACTIVE COUNTS AT FIVE AND 60 MINUTES POST-STRESS UNMASKS HIDDEN ISCHEMIA

Richard M. Fleming, M.D., FACP, FASNC; Gordon M. Harrington, Ph.D.; Riaz Baqir, M.D.; Scott Jay, M.D.; Sridevi Challapalli, M.D.; Kayla Avery, M.D.; Jim Green, M.D.
Reno Nevada Cardiology, Reno, Nevada

Introduction

In 1926, Blumgart[1] published the first paper on nuclear cardiology. He demonstrated that a radioactive isotope injected into the venous system of the right arm could be sequentially measured over the next several minutes by calculating the amount of radioactivity in the arterial system of the left arm. This was termed "circulation time," and the longer the time required for detection, the weaker the heart muscle. It also established the need for multiple images under the same state of stress. By 1959, Gorlin[2] demonstrated that resting studies could not be used to evaluate ischemia,[3,4] which later proved to be the result of coronary flow reserve, a phenomenon associated with vasodilatory capacity of coronary arteries under stress and not under resting conditions.

The prognosis for nuclear cardiology was critical by the mid 1960s, when Love[5] pointed out that there were no useful isotopes available to clinically evaluate the patient. This was remedied with the introduction of thallium-201 in 1975. By the late 1980s, the search for better imaging agents lead to the production of several compounds using the isotope technetium-99m. Despite the promise of rapid uptake and release, some of these agents[6] would prove to be difficult to use in everyday practice. By contrast, the more lipophilic compound, sestamibi, would prove to be easier to use. Unfortunately, most clinical studies were being performed with rest-stress imaging for comparison despite the teachings of Blumgart and Gorlin.

By 1993, Crane[7] established that sestamibi did not merely enter cells and remain there but underwent uptake and release dependent upon the level of ischemia present, which influenced mitochondrial calcium. In recent years, this understanding has been applied extensively in other areas of nuclear medicine to better detect disease and in some instances to better understand the responses of certain cancers to treatment.[8-10] This knowledge of cellular and subcellular organelle (mitochondrial) uptake and release (washout) has yielded a better understanding and detection of congestive heart failure.[11-14] cardiomyopathies,[15-17] Prinzmetal's angina,[18,19] and ischemia.[11, 13, 20-23]

Recently, our group completed work demonstrating improved detection of ischemia and vulnerable plaque,[24-26] which had been impossible to detect when comparing resting images to stress images. This report shares both a description of this new standard of care in cardiac imaging and an example of its contribution to clinical cardiology.

Case Example

Mr. P is a 58-year-old Caucasian male who was admitted to the hospital for further evaluation of exertional chest discomfort. His evaluation had included a history and physical, electrocardiogram (ECG), exercise stress test, echocardiogram, and an echocardiographic stress test. His diagnostic studies found no evidence of ST changes by ECG or by treadmill stress. The echocardiogram revealed no regional wall motion abnormalities, and stressing the patient by treadmill did not revealed exertional wall motion problems. His internist wanted to avoid a cardiac catheterization given these "normal" findings. Concerned with the patient's description of exertional discomfort, a myocardial perfusion imaging study (MPI) was ordered. The results of comparing rest to stress images are shown in Figure 1. In an effort to exclude tissue attenuation artifacts, the institution also employed attenuation correction, which is also shown in Figure 1. The conclusion of this study was that the patient did not have ischemia. The patient returned to his telemetry bed to prepare for hospital discharge, at which time he demonstrated ST elevations on the monitor.

In addition to the use of resting and stress images, we had obtained a second set of post-stress images at five minutes post stress using the protocol shown in Figure 2. The findings from this study were completely different and pointed to disease in his left anterior descending artery system. The five-minute post stress imaging results are shown in Figure 3. The results of the findings at five minutes post stress were then compared with results obtained at 60 minutes post stress. The difference (redistribution/washout) is the difference or the change that has occurred over time.

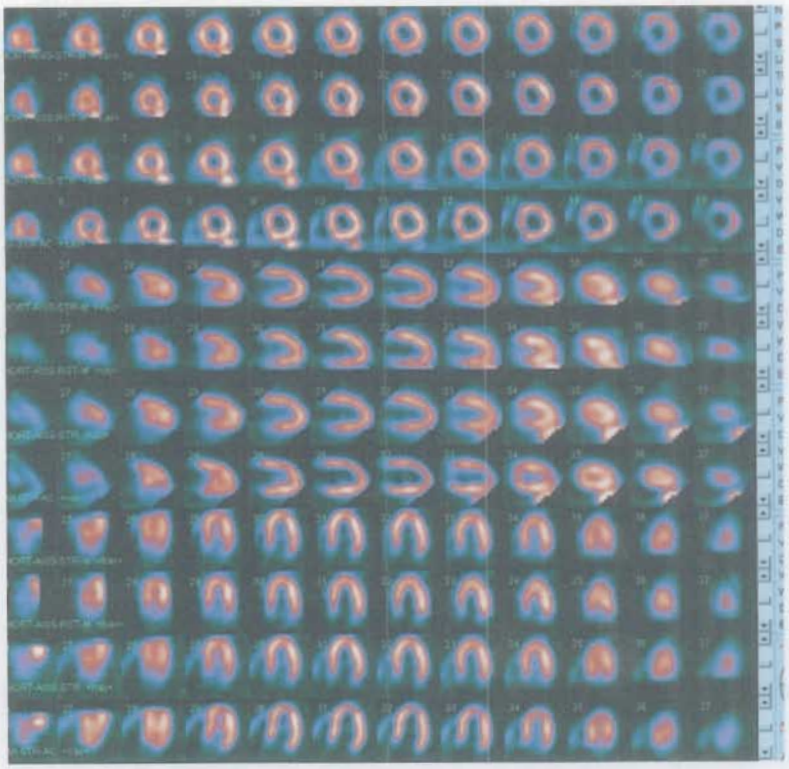

Figure 1. Dynamic resting image to assess myocardial damage (MII) and dynamic stress image to assess ischemia with and without attenuation correction (AC).
The same patient shown in figures 2, 3, 5 and 6 is displayed using coronal short axis (top 4 rows), vertical long axis (rows 5-8) and the horizontal long axis (rows 9-12). Rows 1-2, 5-6, and 9-10 show images using nonattenuation-corrected images. Rows 3-4, 7-8, and 11-12 show the same regions using AC. Rows 2, 4, 6, 8, 10 and 12 show resting images providing information regarding myocardial (MII) infarction/injury (infarction, stunned or hibernating) while rows 1, 3, 5, 7, 9 and 11 reveal the same regions of myocardium following pharmacologic stress, in this case adenosine. These images were interpreted as "normal," showing no evidence of infarction or ischemia.

As shown in Figure 2, the amount of technetium that should be present in an area if there was the same amount of isotope in that region at both five and 60 minutes would be 10% less. This means that, if there is no disease, the isotope count for the entire heart at five minutes (374,930) (Figure 3) should reduce by 10% of this amount 55 minutes later. This would have yielded a count of 337,437 (90% of 374,930) at 60 minutes. Instead, the total heart count was actually 216,886. Clearly, the isotope does not simply get delivered to the heart and "stick" there like glue. Rather, there is a constant delivery, uptake, and release that depends on ischemia and cellular health, which is itself dependent upon the level of ischemia present.

Given the 10% decay of technetium 99-m, the actual loss of isotope from five minutes to 60 minutes was 42%. This shows that the patient had considerable disease, which was missed using only a single stress image result obtained at 60 minutes post stress. A quick observation shows that the inferior region

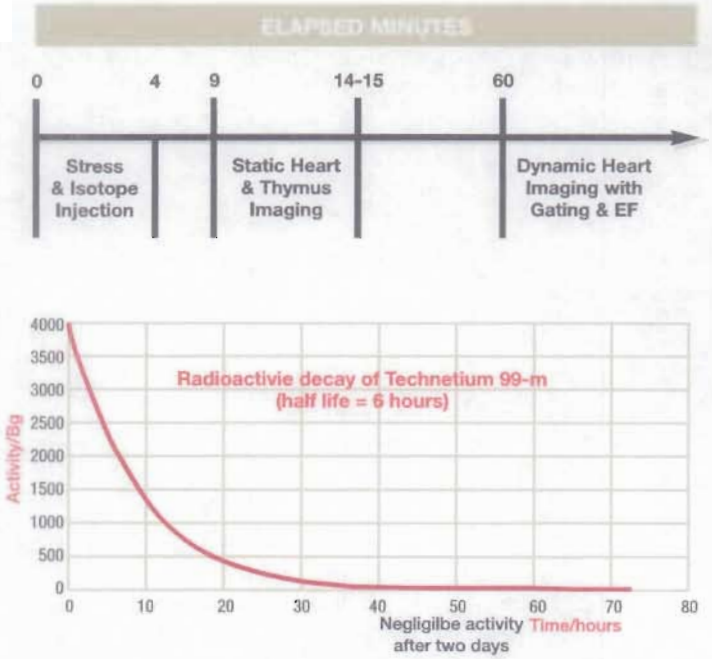

Figure 2. Multiple imaging protocol following stress to calculate quantitative change in sestamibi.

Patients are brought for imaging and undergo stress and isotope injection. While this varies depending upon the type of stress[27] used, the injection of technetium-99m isotope is performed per institutional standards. Five minutes after the injection of technetium isotope, a static (planar) image of the heart is performed[28] to look for evidence of inflammation and to obtain information about tracer activity at five minutes. A second image (tomographic) is obtained 55 minutes later where dynamic images are obtained which can be processed to obtain comparison information regarding tracer activity. Identical regions of interest (ROIs) from the five and 60 minute images are compared. The additional dynamic information can be used to determine wall motion abnormalities and ejection (EF) fraction which is billed for separately. The second part of the figure shows the radioactive decay curves for technetium-99m-isotopes. Between the first and second set of images, there is a 55 minute period of time, which is associated with a 10% decay in isotope. Any additional change is a reflection of ischemia.

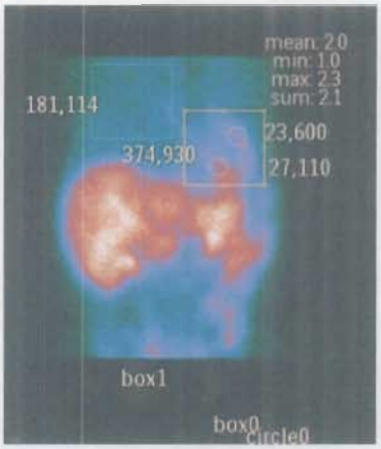

Figure 3. Static image taken at five-minutes post stress with regions of interest defined and quantified.

Static imaging at five minutes with regions of interest (ROI) showing total heart count of 374,930 and total lung count of 181,114, with a calculated heart-to-lung (H:L) ratio of 2.0. The anterior ROI shows a 23,600 count and the inferior ROI shows 27,110.

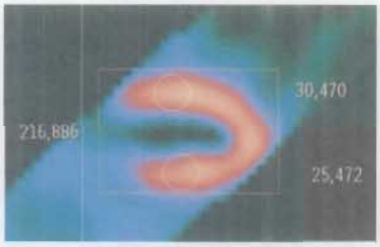

Figure 4. Regions of interest for assessment of washin/washout (WR) at 60 minutes.

Reconstruction of the same myocardial region noted in Figure 3, this time taken from the dynamic image result obtained at 60-minutes post stress. This shows a total heart count of 216,886 in this single plane with total heart counts greater than 1 million, revealing total heart washin. The anterior ROI shows an increase in count activity (washin) of 30,470 compared with the activity of 23,600 (Figure 3) obtained at 5 minutes. The inferior ROI shows a count of 25,472 compared with the count activity of 27,110 (Figure 2) obtained five minutes post stress.

(right coronary artery/RCA) had a five-minute value of 27,110 and a 60-minute value of 25,472 (6% washout). The RCA was not the site of disease.

When the anterior region supplied by the left anterior descending artery (LAD) was studied, the five-minute count was 23,600. Instead of decreasing by 10% to 21,240, the count actually increased to 30,470. This increased amount of radioactive counts over time revealed a delay in delivery and uptake of the isotope to a region supplied by a critically narrowed artery and in this case one with a vulnerable plaque. Such arteries are not able to vasodilate on demand[3,4] and show a delay in isotope delivery. Since the inferior region did not have arterial narrowing and the LAD did, the 60-minute images appear to have equal amounts of tracer activity, leading to the "false normal"-appearing images shown in Figure 1.

The information acquired from the five- and 60-minute images revealed ischemia in the LAD

system that was shown on coronary angiography (Figures 5 and 6). Following stent placement, the patient showed normalization of his ST elevation in the cardiac catheterization laboratory.

Discussion

The sensitivity and specificity of single-photon emission computed tomography has been limited to 65-90% over the last four decades despite improvements in isotopes, nuclear cameras and computers, attenuation correction algorithms, and attenuation rings/bars. One of the first lessons as a medical student is to determine which test to run to diagnose a patient's problem. We are all taught that the results are then compared to what is presumed to be normal. "Normal" is determined by whether or not you have prior studies to compare with. If not, one takes the information obtained from a patient's test and compares it with what is expected. A classic example is poor R-wave progression (PRWP) on an ECG. While this doesn't define damage to the heart's septum, the question is raised in one's mind: Does the PRWP reflect lead placement, body habitus, or actual myocardial damage with loss of myocardium and subsequently electrical activity? The answer is easy to solve if one has a prior ECG of the patient to use as comparison. If R-waves were present the week before but are absent or reduced now, the level of suspicion for myocardial damage increases.

Much of this limitation in nuclear imaging comes from the comparison of rest to stress images. Despite the teachings of Blumgart and Gorlin, physicians have mistakenly concluded that comparing resting images ("apples") to stress images ("oranges") are the way to look for ischemia. However, the knowledge acquired by multiple investigators has demonstrated that this simply isn't true.[7-26] The real genius behind nuclear imaging is that it provides a physiologic measure of what is going on in the body. This can be used to differentiate benign versus cancerous cells, to determine how cancer will respond to treatment, or, as we have seen here, to find hidden disease that appears nonexistent if one waits too long to look for it. Coronary arteries with critically diseased arterial regions — due to almost complete occlusion of the coronary lumen or to vulnerable plaques, both of which impair stenosis flow reserve — will produce a delay in final delivery and equilibration of isotope and subsequently a "false negative" finding on the MPI. Similarly, using our five- and 60-minute multi-imaging protocol, regional problems with attenuation artifacts are eliminated since a region of the heart is being compared with itself over time, much like the PRWP from one ECG to another. Unless there is a change in breast tissue or abdominal girth, septal wall hypertrophy,

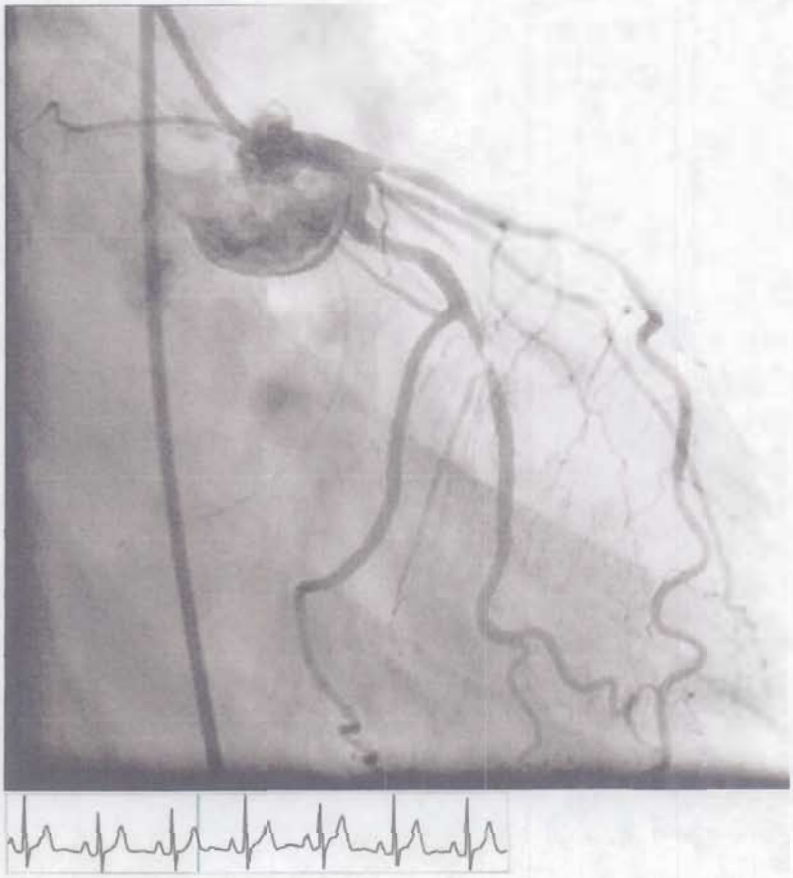

Figure 5. Critically diseased left anterior descending, first diagonal and first obtuse marginal arteries matching washout (WR) data prior to stenting.
Cardiac catheterization revealed a "normal" left main (LM) and right coronary artery (RCA). The left anterior descending (LAD) had an 80% diameter stenosis (DS) ostial (beginning) lesion in addition to a 75% "long segmental" proximal lesion. The first diagonal had a 60% DS lesion at the ostium. The proximal left circumflex (LCx) had a 40% DS proximal and an 80% DS ostial lesion of the first obtuse marginal (OM1).

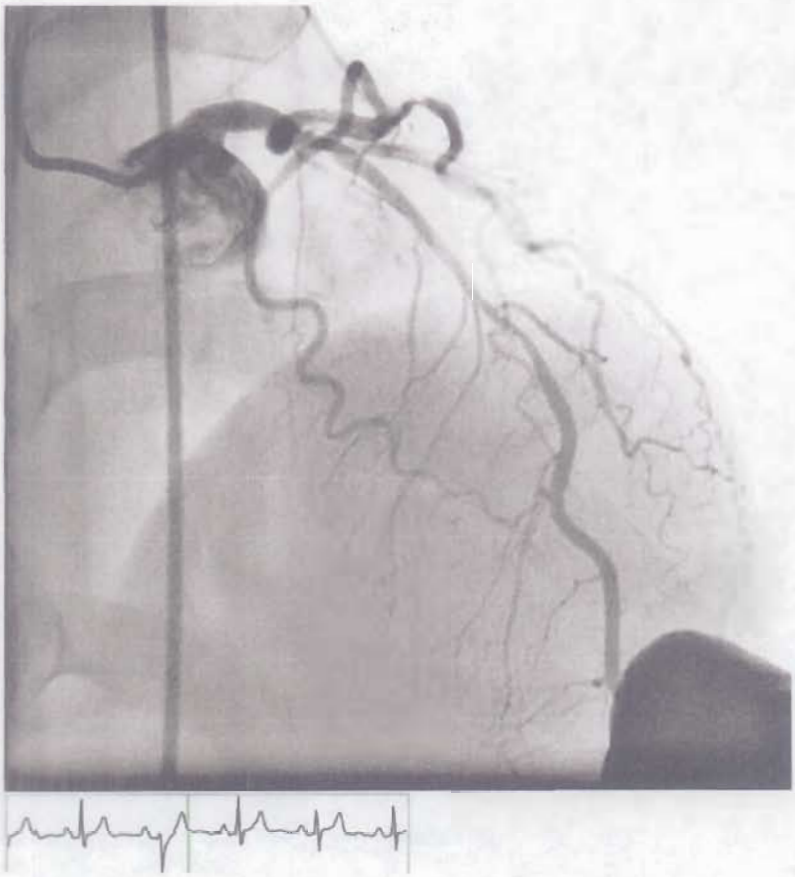

Figure 6. Critically diseased left anterior descending, first diagonal and first obtuse marginal arteries after stenting.
Cardiac catheterization of same arteries shown in Figure 5 following insertion of a Cypher RX drug-eluting 3.5 x 8 mm stent for the 80% DS ostial lesion of the LAD, a Cypher RX drug-eluting 3.0 x 33 mm stent for the 75% DS proximal LAD lesion, and a Cypher RX drug-eluting 3.0 x 13 mm stent for the 80% DS ostial lesion of OM1.

or formation of a bundle branch during the study, the comparison of the amount of radioactive counts in a region of the heart to itself will not be altered over the 55 minutes between the first image and second image, minus the expected 10% decay of sestamibi.

Studies currently underway (Figure 7) are demonstrating that the use of FH (Fleming-Harrington) redistribution/washout/washin can also be used to determine treatment intervention for individuals presenting with acute coronary syndrome.

Conclusion

Upon entering medical school and throughout my education as a cardiologist in Houston, I was trained by great teachers who repeatedly taught us to question how we could best diagnose and treat heart disease. "Based upon the numbers of people whose heart disease is missed using rest-stress imaging (18%), this new FH Redistribution/Washout protocol will detect 40-60,000 individuals who would otherwise be told they have no heart disease, yet have "vulnerable plaques" or "critical lessions" and would subsequently experience an adverse cardiac event (MI, death). Similarly, using the numbers of people who have no disease but are reported to have ischemia by rest-stress imaging[29] and who subsequently experience an unnecessary complication, this new protocol could reduce this number by 4,400 to 8,800 people annually in the United States. As a result, we have now changed the *Standard of Care for Cardiac Imaging*. We now know that multiple sequential imaging of the heart at five and again at 60-minutes post stress using sestambi provides information, which cannot be obtained by comparing rest and stress images. The unmasking of this disease has provided us with the method necessary to find "vulnerable" plaques, unmask critically narrowed arteries that would not be detected using a single 60 minute stress image and more importantly provides the excellence in cardiac care emphasized by our teachers, Drs. DeBakey and Cooley. As they taught us, "average isn't good enough", "excellence is to be strived for." This new standard of care provides this excellence they and their predecessors (Blumgart and Gorlin) called for.

References

1. Blumgart HL, Yens OC. Studies on the velocity of blood flow: I. The Method Utilized. J Clin Invest. 1927 Apr;4(1):1-13.
2. Gorlin R, Brachfeld N, MacLeod C, Bopp P. Effect of nitroglycerin on the coronary circulation in patients with coronary artery disease or increased left ventricular work. Circulation. 1959 May;19(5):705-18.
3. Fleming RM, Harrington GM. Quantitative coronary arteriography and its assessment of atherosclerosis. Part 1. Examining the

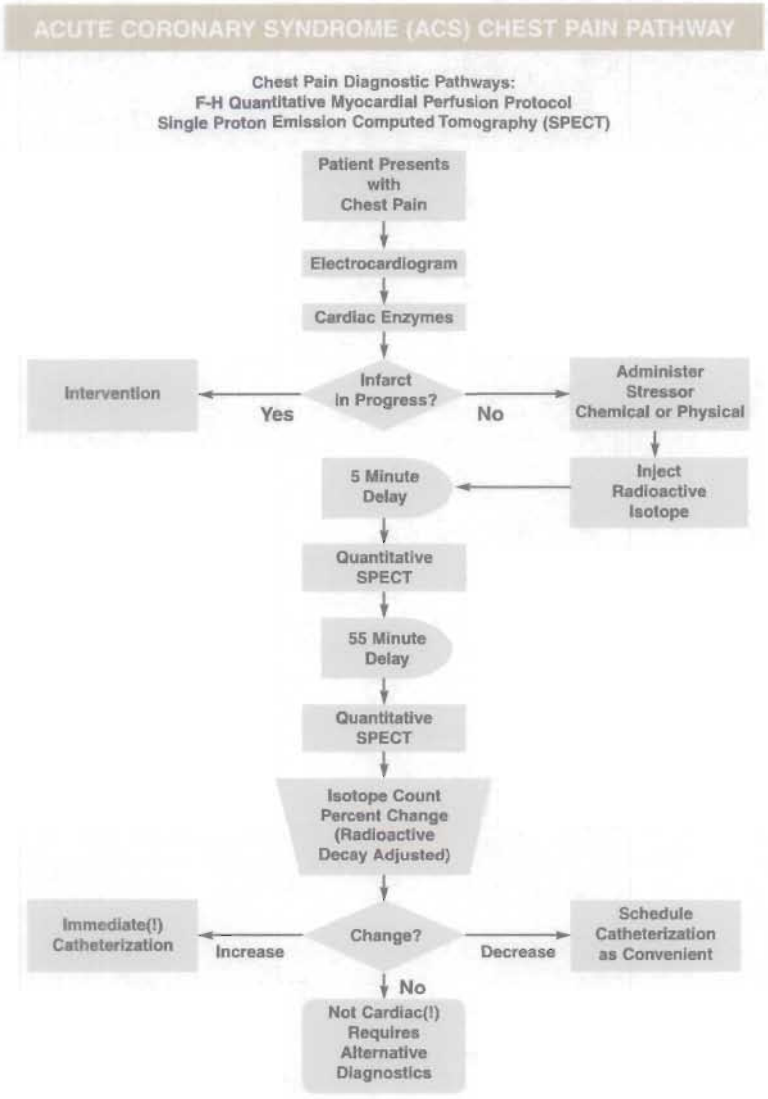

Figure 7. Acute coronary syndrome (ACS) chest pain pathway.
Ongoing research has demonstrated that the use of FH (Fleming-Harrington) washout can also be used in the acute coronary syndrome setting to differentiate treatment intervention.

independent variables. Angiology. 1994 Oct;45(10):829-33.

4. Fleming RM, Harrington GM. Quantitative coronary arteriography and its assessment of atherosclerosis. Part 2. Calculating stenosis flow reserve directly from percent diameter stenosis. Angiology.1994 Oct;45(10):835-40.
5. Love WD. Isotope Technics in Clinical Cardiology. Circulation. 1965 Aug;32:309-15.
6. Fleming RM, Kirkeeide RL, Taegtmeyer H, Adyanthaya A, Cassidy DB, Goldstein R. A comparison of technetium-99m teboroxime tomography with automated quantitative coronary arteriography and thallium-201 tomographic imaging. J Am Coll Cardiol. 1991 May;17(6):1297-302.
7. Crane P, Laliberte R, Heminway S, Thoolen M, Orlandi C. Effect of mitochondrial viability and metabolism on technetium-99m-sestamibi myocardial retention. Eur J Nucl Med. 1993 Jan;20(1):20-5.
8. Sciuto R, Pasqualoni R, Bergomi S, Petrilli G, Vici P, Belli F, Botti C, Mottolese M, Maini CL. Prognostic value of (99m)Tc-sestamibi washout in predicting response of locally advanced breast cancer to neoadjuvant chemotherapy. J Nucl Med. 2002 Jun;43(6):745-51.
9. Gupta Y, Ahmed R, Happerfield L, Pinder SE, Balan KK, Wishart GC. P-glycoprotein expression is associated with sestamibi washout in primary hyperparathyroidism. Br J Surg. 2007 Dec;94(12):1491-5.
10. Chatziioannou SN, Alfaro-Franco C, Moore WH, Alanis-Williams L, Dhekne RD, Ford PV. The significance of incidental noncardiac findings in Tc-99m sestamibi myocardial perfusion imaging: Illustrated by a case. Tex Heart Inst J. 1999;26(3):229-31.
11. Hurwitz GA, Ghali SK, Husni M, Slomka PJ, Mattar AG, Reid RH, Lefcoe NM. Pulmonary uptake of technetium-99m-sestamibi induced by dipyridamole-based stress or exercise. J Nucl Med. 1998 Feb;39(2):339-45.
12. Sugiura T, Takase H, Toriyama T, Goto T, Ueda R, Dohi Y. Usefulness of Tc-99m methoxyisobutylisonitrile scintigraphy for evaluating congestive heart failure. J Nucl Cardiol. 2006 Jan-Feb;13(1):64-8.
13. Kumita S, Seino Y, Cho K, Nakajo H, Toba M, Fukushima Y, Okamoto N, Takano T, Kumazaki T. Assessment of myocardial washout of Tc-99m-sestamibi in patients with chronic heart failure: comparison with normal control. Ann Nucl Med. 2002 Jun;16(4):237-42.
14. Matsuo S, Nakae I, Tsutamoto T, Okamoto N, Horie M. A novel clinical indicator using Tc-99m sestamibi for evaluating cardiac mitochondrial function in patients with cardio-

myopathies. J Nucl Cardiol. 2007 Apr;14(2):215-20.

15. Ikawa M, Kawai Y, Arakawa K, Tsuchida T, Miyamori I, Kuriyama M, Tanaka M, Yoneda M. Evaluation of respiratory chain failure in mitochondrial cardiomyopathy by assessments of 99mTc-MIBI washout and 123I-BMIPP/99mTc-MIBI mismatch. Mitochondrion. 2007 Feb-Apr;7(1-2):164-70.
16. Meissner K, Sperker B, Karsten C, Zu Schwabedissen HM, Seeland U, Böhm M, Bien S, Dazert P, Kunert-Keil C, Vogelgesang S, Warzok R, Siegmund W, Cascorbi I, Wendt M, Kroemer HK. Expression and localization of P-glycoprotein in human heart: effects of cardiomyopathy. J Histochem Cytochem. 2002 Oct;50(10):1351-6.
17. Kazumasa U, Isobe S, Izawa H, Kobayashi M, Hirashiki A, Yamada T, Ohshima S, Kato K, Murohara T, Yokota M. Increased 99m-Tc-sestamibi washout reflects impaired myocardial contractile reserve and prolonged relaxation in patients with nonobstructive hypertrophic cardiomyopathy. J Nucl Med. 2008;49(Suppl 1):189P.
18. Ono S, Yamaguchi H, Takayama S, Kurabe A, Heito T. [Rest delayed images on 99mTc-MIBI myocardial SPECT as a noninvasive screen for the diagnosis of vasospastic angina pectoris] Kaki Igaku. 2002 May;39(2):117-24.
19. Ono S, Takeishi Y, Yamaguchi H, Abe S, Tachibana H, Sato T, Kubota I. Enhanced regional washout of technetium-99m-sestamibi in patients with coronary spastic angina. Ann Nucl Med. 2003 Jul;17(5):393-8.
20. Fukushima K, Momose M, Kondo C, Kusakabe K, Kasanuki H. Myocardial kinetics of (201)Thallium, (99m)Tc-tetrofosmin, and (99m)Tc-sestamibi in an acute ischemia-reperfusion model using isolated rat heart. Ann Nucl Med. 2007 Jul;21(5):267-73.
21. VanBrocklin HF, Hanrahan SM, Enas JD, Nandanan E, O'Neil JP. Mitochondrial avid radioprobes. Preparation and evaluation of 7'(Z)-[125I]iodorotenone and 7'(Z)-[125I]iodorotenol. Nucl Med Biol. 2007 Jan;34(1):109-16.
22. Richter WS, Cordes M, Calder D, Eichstaedt H, Felix R. Washout and redistribution between immediate and two-hour myocardial images using technetium-99m sestamibi. Eur J Nucl Med. 1995 Jan;22(1):49-55.
23. Meerdink DJ, Aleppo JA. Myocardial transport of hexakis(2-methoxy-isobutylisonitrile) and thallium before and after coronary reperfusion. Circ Res. 1990 Jun;66(6):1738-46.
24. Fleming RM, Harrington GM, Baqir R. Use of parabolic model in Tomographic diagnosis of infarction and stenosis. Presented at: The 1st Congress on Controversies in Cardiovascular diseases: Diagnosis, treatment and intervention (C-Care); July 4, 2008; Berlin, Germany.
25. Fleming RM, Harrington GM, Baqir R, Jay S, Avery K, Wallenmeyer M. The clinical importance of multiple SPECT images following stress — A new standard of care. Presented at: 30th Annual Meeting and Educational Symposium Missouri Valley Chapter of Society of Nuclear Medicine; October 4, 2008; Omaha, NE.
26. Fleming RM, Harrington GM, Baqir R, Jay S, Avery K, Wallenmeyer M. Multiple post stress SPECT imaging unmasks hidden coronary artery disease and eliminates the need for unnecessary cardiac catheterization. It's all about detecting CHANGE! Validating Blumgart's work. Lancet. Forthcoming 2008.
27. Fleming RM. Textbook of Angiology. New York: Springer-Verlag; 1999. Chapter 31, Nuclear Cardiology: Its role in the detection and management of coronary artery disease; p. 397-406.
28. Fleming RM. The Fleming Unified Theory of Vascular Disease: a link between atherosclerosis, inflammation, and bacterially aggravated atherosclerosis (BAA). Angiology. 2000 Jan;51(1):87-9.
29. Fierens E. Outpatient coronary arteriography. Catheterization and Cardiovascular Diagnosis. 2005;10:27-32.

Noncardiac findings on dual-isotope myocardial perfusion SPECT

Kim A. Williams, MD,[a,b] Kalisha A. Hill, MD,[c] and Candace M. Sheridan, BS[a]

Background. **This study examined the frequency of reporting noncardiac findings (NCFs), such as malignancies from inspection of raw projection images with dual-isotope single photon emission computed tomography (SPECT) perfusion imaging, which could potentially be of greater clinical importance than myocardial perfusion imaging alone. Dual-isotope (ie, rest thallium 201 and stress technetium 99m sestamibi [MIBI] or Tc-99m tetrofosmin [TET]) SPECT myocardial perfusion imaging combines multipotential tracers for noncardiac purposes (Tl-201 for renal or splenic imaging, inflammation, or lymphoma and MIBI or TET for hepatobiliary imaging and detecting increased mitochondrial number or activity in neoplastic processes). These images are optimally interpreted with cinematic inspection of the raw projection data, but this may not be practiced uniformly in every laboratory.**

Methods and Results. **We reviewed 12,526 computer-generated text reports of dual-isotope perfusion SPECT studies from a 6-year period for NCFs. NCFs were categorized by organ and by probability of malignancy: high (eg, focal breast or lung uptake of MIBI or TET), intermediate (eg, lymph node uptake or thyroid abnormalities), or low (eg, filling defects in liver, kidney, spleen, or gall bladder; ascites; or pleural effusions). Confirmatory imaging studies or clinical confirmation for each NCF was sought. There were a total of 207 NCFs identified in 180 reports (1.7% of reports, ranging from 0% to 2.8% of reports of individual interpreters). Of these, 107 NCFs were unsuspected before SPECT; 24% were considered at high probability for malignancy, and 24% were considered intermediate in likelihood of malignancy. Follow-up data were available for 178 NCFs, confirming 88% of these findings, including 82% of breast foci, 62% of lung foci, 86% of hepatobiliary/spleen abnormalities, and 94% of renal abnormalities. The probability of malignancy was highest (82%) in breast or lung foci in which uptake of both Tl-201 and the Tc-99m–labeled agent was present.**

Conclusions. **In patients referred for evaluation of myocardial perfusion, NCFs are unusual and require systematic and careful inspection of projection images for their detection. With Tl-201, TET, MIBI, or dual-isotope imaging, detecting and reporting NCFs may occasionally result in life-saving early cancer identification. (J Nucl Cardiol 2003;10:395-402.)**

Key Words: Single photon emission computed tomography myocardial perfusion imaging • malignancy • noncardiac findings

Dual-isotope single photon emission computed tomography (SPECT) myocardial perfusion scintigraphy was introduced in 1993[1] with thallium 201 at rest and technetium 99m sestamibi (MIBI) at stress. Since that time, this protocol has become widely used for the diagnosis and assessment of prognosis in patients with known or suspected coronary artery disease in a wide variety of clinical settings.[1-5] In 1995 Tc-99m tetrofosmin (TET), an agent with characteristics similar to MIBI, was validated for SPECT myocardial perfusion imaging.[6]

Dual-isotope imaging with either Tl-201 with TET or Tl-201 with MIBI combines multifaceted tracers for noncardiac purposes. Tl-201 has an uptake pattern that could be useful for thyroid, renal, or splenic imaging but also accumulates in thyroid cancer, lymphoma, and areas of inflammation.[7-16] Both MIBI and TET are agents that have hepatobiliary uptake excretion and are used clinically for thyroid and parathyroid imaging. Possibly because of their uptake in mitochondria, these agents are also highly concentrated within neoplastic processes of several varieties.[15-36]

From the Departments of Medicine (Cardiology)[a] and Radiology (Nuclear Medicine),[b] University of Chicago, and Department of Pathology,[c] Northwestern University School of Medicine, Chicago, Ill.

Received for publication Nov 7, 2002; final revision accepted Feb 5, 2003.

Reprint requests: Kim A. Williams, MD, University of Chicago, Director, Nuclear Cardiology, 5758 S Maryland Ave, MC9025, Chicago, IL 60637; *kwilliam@medicine.bsd.uchicago.edu.*

1071-3581/2003/$30.00 + 0
doi:10.1016/S1071-3581(03)00524-5

To optimize visual detection of these foci of abnormal uptake, the interpreter should view a rotating cinematic display of the raw projection data.[37] This allows detection of soft-tissue attenuation, patient motion, and other cardiac and noncardiac abnormalities that may be evident during SPECT myocardial perfusion imaging. However, this practice of reviewing raw projection data may vary widely between interpreters, between commercial software presentations, and from laboratory to laboratory.

This retrospective study examined the frequency of detecting noncardiac findings (NCFs) (eg, malignancies) from inspection of raw projection images with dual-isotope SPECT myocardial perfusion imaging, which could potentially be of greater importance to the patient's prognosis and management than myocardial perfusion imaging alone.

METHODS

Study Population

We retrospectively reviewed 12,526 computer-generated text reports of patients who had undergone dual-isotope imaging with Tl-201 at rest and Tc-99m MIBI or TET stress perfusion SPECT over a 6-year period (1993 through 1999). Each report was inspected for a description of an "additional scintigraphic finding" that was noncardiac-related but seen on planar projection images viewed in cine format. Comments about attenuation artifacts (eg, breast shadowing, diaphragmatic attenuation, or pacemakers) and cardiac-related nonmyocardial findings (eg, pulmonary uptake of Tl-201) were excluded from analysis.

Data Analysis

NCFs were categorized by anatomic localization in an organ and by probability of malignancy as high, intermediate, or low. This probability of malignancy was synthesized from the differential diagnosis generated by the physician interpretation as reflected in the text of the conclusions of the report. Thus solitary nodules or foci of uptake in the lung or breast were considered to indicate high likelihood (reported as a "possible neoplastic process"). Thyroid nodules ("possibly a multinodular goiter, hyperfunctioning nodule, or malignancy") and lymph node uptake ("an inflammatory, infectious, or neoplastic process") were considered to indicate intermediate likelihood. Ascites, effusions, and filling defects were considered to indicate a low probability of malignancy.

Follow-up of NCFs

For examination of the accuracy and clinical importance of the NCFs, confirmatory imaging studies or clinical information for each NCF was sought through the patients' self-reported histories, radiology image files, primary physicians' clinic notes, and electronic medical records.

In addition, for each of the 6 physicians reporting findings during this time frame, the number of NCFs reported was compared with the total number of studies interpreted by that physician in order to determine the frequency with which these findings were reported.

Statistical Analysis

Continuity-corrected χ^2 analysis with 1 *df* was applied for comparison of frequency data. $P < .05$ was considered statistically significant for a single comparison.

RESULTS

Of the 12,526 reports, a total of 207 NCFs were identified in 180 reports (1.7% of total). The incidence of reporting NCFs varied among interpreters, ranging from 0% to 2.8% of reports, with the highest frequency occurring in the nuclear medicine/cardiology physician who read scans most frequently (56% of all studies) in the laboratory. The overall results are tabulated in Table 1.

Of the 207 NCFs, 45 (24%) were considered to have a high probability for malignancy (eg, focal breast or lung uptake of MIBI or TET), 10% were considered to have an intermediate probability for malignancy (eg, lymph node or axillary uptake or thyroid abnormalities), and the remainder were considered to have a low likelihood of malignancy (eg, filling defects in the liver, spleen, kidney, or gall bladder; ascites; or pleural effusions).

Follow-up over a 3- to 6-year period was available for 202 of 207 NCFs. In an additional 24 NCFs, the clinicians were aware of the findings but chose not to pursue the findings with correlative imaging. As shown in Table 1, this occurred most often with renal (n = 7), thyroid (n = 4), and breast (n = 4) lesions.

For the 178 lesions with correlative follow-up, 102 (57%) were known to the patients' clinicians before SPECT imaging and were considered as confirmed findings (eg, the presence of ascites and splenomegaly in patients undergoing preoperative SPECT before liver transplantation). The remaining 76 NCFs (43%) were not suspected before SPECT.

The follow-up information available for the 178 NCFs confirmed 156 (88%) of these findings, including 82% of breast lesions (ie, a benign or malignant abnormality noted at the location of tracer uptake) and 62% of lung foci. Benign conditions of the breast that had tracer uptake included postsurgical scarring (n = 1), microcalcification (n = 4), fibroadenoma (n = 1), a benign cyst

Table 1. Overall results

Suspected diagnosis	No.	No imaging follow-up	Imaging follow-up	% Follow-up	Correct lesion (No.)	% Correct	Known diagnosis (No.)
Ascites, peritoneal dialysis fluid	38	0	38	100%	38	100%	34
Axillary uptake	13	3	10	77%	7	70%	8
Breast uptake	37	4	33	89%	27	82%	8
Gastrointestinal activity in thorax	4	0	4	100%	3	75%	3
Hepatobiliary	18	4	14	78%	12	86%	5
Lung focal uptake	14	1	13	93%	8	62%	4
Bony or bone marrow uptake	3	1	2	67%	2	100%	2
Pericardial photolucency	8	2	6	75%	5	83%	3
Pleural photolucency	13	1	12	92%	11	92%	7
Renal abnormalities	23	7	16	70%	15	94%	4
Skin focus vs contamination	1	0	1	100%	0	0%	0
Splenic abnormalities	28	2	26	93%	25	96%	21
Thyroid abnormalities	7	4	3	43%	3	100%	3
Total	207	29	178	86%	156	88%	102

(n = 1), and nonspecific breast nodules that appeared to be clinically stable (n = 5).

Uptake of a single tracer was less specific for breast or lung cancers (Table 2), including 0 of 1 with Tl-201 alone, 2 of 7 (29%) with MIBI, and 4 of 23 (17%) with TET. However, if both tracers on a dual-isotope study were noted in a lung or breast lesion, there was a statistically significantly higher likelihood of the lesion being malignant (9/11 [82%] vs 6/31 [19%], $P = .0007$). In one case, however, the diagnosis of breast malignancy was made remotely from the SPECT scan, with negative mammography results 15 months before and 1 week after Tl-201 and TET were noted in the right breast. When this case was pursued with ultrasound imaging of the breast and biopsy, the diagnosis of infiltrating ductal carcinoma was made 4 months after the SPECT study.

With regard to the intermediate likelihood of malignant lesions—lymph node or axillary uptake (n = 10) and thyroid nodules (n = 3)—there was a malignancy rate of 14% (3/13, including 1 thyroid lymphoma and 2 axillary lymphomas). With regard to the low likelihood of malignant lesions (eg, filling defects, ascites, or pleural effusion), there was one occurrence of malignancy (renal cancer, 1/67 [1%]).

Of note, there was a high correlation between the finding of an abnormality in a subdiaphragmatic organ and confirmation of that abnormality, including 86% of hepatobiliary abnormalities, 81% of splenic abnormalities, and 94% of renal abnormalities (Table 1).

An example of TET uptake in breast cancer (and its subsequent use for following the tracer uptake in the malignancy) is shown in Figure 1. An example of a false-positive TET uptake result in the lung is shown in Figure 2.

DISCUSSION

SPECT myocardial perfusion imaging is a rapidly growing diagnostic technique that plays a pivotal role in the detection and management of patients with ischemic heart disease.[1-6] It is most often performed in older patients, obese subjects, and smokers, all of whom may be at increased risk for development of malignancy or other noncardiac abnormalities that could be detected by nuclear imaging techniques. A widely and increasingly performed SPECT technique, dual-isotope imaging with Tl-201 and the Tc-99m–labeled tracers MIBI (hexakis-2-methoxyisobutylisonitrile) or TET (1,2-bis-[bis(2-ethoxyethyl) phosphino]ethane), offers a pluripotential method of diagnosing abnormal foci of tracer uptake in the cardiac field of view. Detection of many of these subclinical disorders would have otherwise been delayed until symptoms supervened. The case detailed in this report with negative mammography results suggests that some of the cases categorized as having "false-positive" results in our study actually may have been falsely negative mammographic study results, as this technique has recently been reported to have a sensitivity possibly as low as 60%.[38]

Dual-isotope SPECT myocardial perfusion images are optimally interpreted with cinematic inspection of the raw projection data. These rotating planar projection images allow detection of both cardiac and noncardiac abnormalities in the cardiac field of view, such as patient

% Known	Thought malignant (No.)	% Thought malignant	Proven malignant (No.)	% Malignant	Known malignant	% Known	% Unknown
90%	0	0%	0	0%	—	—	—
80%	0	0%	2	20%	1	50%	50%
24%	30	91%	9	27%	2	22%	78%
75%	0	0%	0	0%	—	—	—
36%	2	14%	0	0%	0	0%	100%
31%	12	92%	6	46%	4	67%	33%
100%	0	0%	0	0%	—	—	—
50%	0	0%	0	0%	—	—	—
58%	0	0,m%	0	0%	—	—	—
25%	1	6%	1	6%	1	100%	0%
0%	1	100%	0	0%	—	—	—
81%	0	0%	0	0%	—	—	—
100%	0	0%	1	33%	0	0%	100%
57%	46	26%	19	11%	8	42%	58%

motion artifacts, soft-tissue and metallic attenuation artifacts (eg, pacemakers, coins, or medallions), interfering subdiaphragmatic activity, and abnormal injection-site activity, which may affect interpretation of the myocardial perfusion images. Important cardiac findings, such as the presence of large, severe perfusion defects, cardiac enlargement, or increased pulmonary tracer uptake, may also be apparent on inspection of projection data.[37]

This study provides a cross-sectional retrospective analysis of the frequency of detection of noncardiac abnormalities and suggests that this frequency may be as high as 2.8%, but another finding of this study was that the reporting rate may vary widely between interpreters. In addition, the frequency of detecting abnormalities will vary with the size of the field of view. The smaller detectors used specifically for cardiac imaging limit detection of NCFs, particularly those below the diaphragm.

Although the major impact of these findings seems to be detection of an occasional malignancy, recognition of other findings, such as ascites or effusions, may be critical for proper interpretation of the cardiac scan (as they may cause excessive attenuation artifacts) or may lead to important diagnoses, if they were unknown before the SPECT study. It is important to note that in this study, several non-neoplastic conditions were found to be foci of tracer uptake, especially in breast tissue.

Table 2. Results by tracer

Tracer	Suspected diagnosis (No.)	Final diagnosis (No.)	% Correct
Breast cancer			
Tl-201	1	0	0%
MIBI	5	1	20%
TET	17	2	12%
Tl-201/MIBI	2	1	50%
Tl-201/TET	5	5	100%
	30	9	30%
Lung cancer			
Tl-201	0	0	—
MIBI	2	1	50%
TET	6	2	33%
Tl-201/MIBI	3	2	67%
Tl-201/TET	1	1	100%
	12	6	50%
Tl-201	1	0	0%
MIBI	7	2	29%
TET	23	4	17%
Tl-201/MIBI	5	3	60%
Tl-201/TET	6	6	100%
Total	42	15	36%

Cardiac Tracers: Malignancies and Mechanisms

Review of the recent literature reveals over 200 publications on the use of these cardiac tracers as nonspecific tumor–searching compounds for detection or evaluation of malignancies. Examples include the use of Tl-201 scintigraphy to characterize metastatic thyroid carcinoma and to identify those patients with poorer

Journal of Nuclear Cardiology
Volume 10, Number 4;395-402

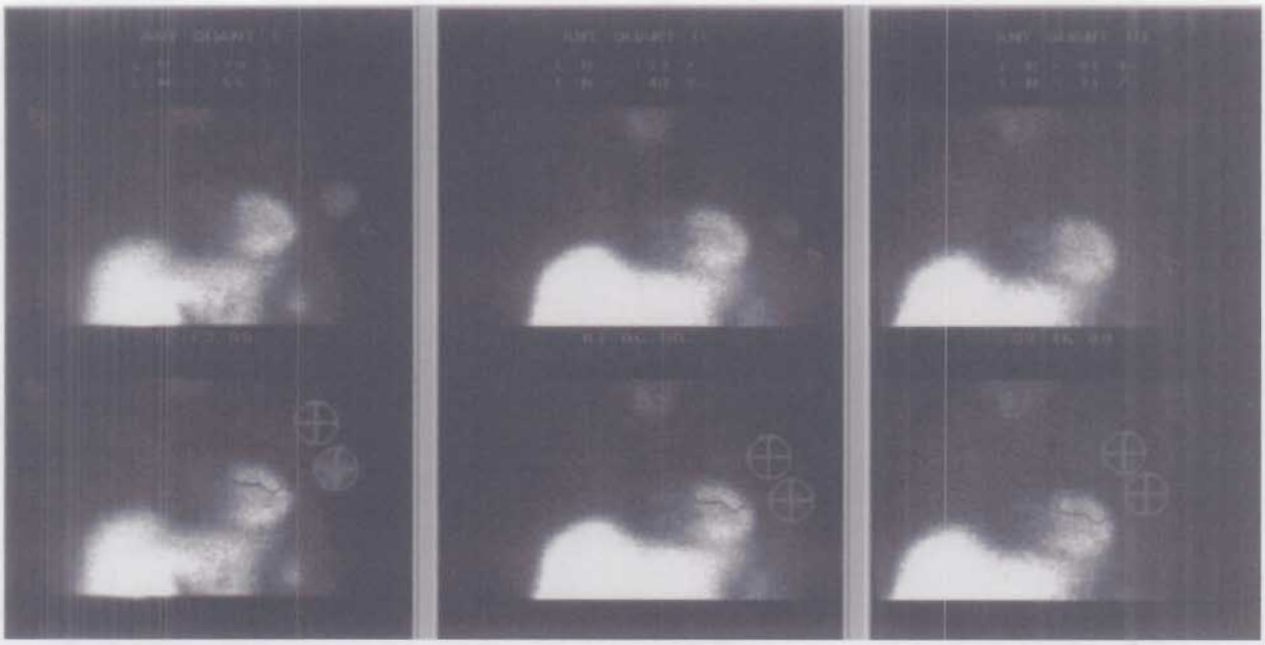

Figure 1. Anterior (*ANT*) planar projection images from a woman with a mass of TET uptake in her left breast (*arrowhead*). The pathology was consistent with a poorly differentiated breast carcinoma positive for HER2/*neu* receptors. Baseline images are shown on the *left*, with comparison images obtained 1 month (*center*) and 3 months (*right*) after chemotherapy with trastuzumab (Herceptin, Genentech, San Francisco, Calif.). Regions of interest placed on the breast lesion, left lung background, and myocardium were used to quantitate (*QUANT*, in counts per pixel) lesion-to-background (*L/B*) and lesion-to-myocardium (*L/M*) ratios, which decreased significantly over the time of therapy. At 3 months, no mass is evident, as indicated by the L/B ratio of less than 1.

prognoses,[7] as well as to improve detection of esophageal cancer with TET compared with MIBI or magnetic resonance imaging.[39] No specific cellular pathway for Tl-201 uptake in malignancies has been demonstrated, but uptake is often noted in inflammatory conditions as well as neoplastic conditions.

MIBI has received Food and Drug Administration approval for detection of breast cancer as an adjunct to mammography. However, TET may also be used for this purpose, with studies suggesting that dedicated scintimammography with TET may be more accurate than evaluation with magnetic resonance imaging, mammography, or ultrasonography of the breast.[30,35,36] In addition, these agents localize within tumor masses of several other varieties, including lung cancer, thymoma, thyroid cancer, lymphoma, and sarcoma.[16-36] Although the mechanism for localization of these agents is uncertain, they are cationic and lipophilic and fractionate with mitochondrial anions in the cytosol.[33] Tumors, such as breast carcinoma, have numerous round to elongated mitochondria, often in a perinuclear distribution.[25,40] The ability of mitochondria to accumulate calcium without becoming uncoupled may be essential in the maintenance of tumor cell viability.[41] On the basis of preliminary data obtained in tumor models, the intensity of TET or MIBI tracer activity should correlate positively with the amount of mitochondrial activity and viable tumor mass.[23,25] In addition, these tracers are also substrates for P-glycoprotein, a mediator of multidrug resistance to chemotherapy.[24,26,28] Thus these agents are scintigraphic markers for drug sensitivity of the neoplasm, as well as indicators of potential blockers of the P-glycoprotein pump.[24]

Initially, it was suggested that scintimammography with MIBI or TET should be useful in the evaluation of patients with indeterminate mammographic study results, rendering complementary data that might enable unnecessary surgery and/or biopsy to be avoided. However, MIBI and TET have proved reliable also for diagnosis of primary cancers, local recurrence, or axillary lymph node or distant metastases.[42] MIBI and TET studies have shown high positive predictive value (>90%) in pilot trials, exceeding the sensitivity and specificity rates of mammography.[31,35,36] One recent study suggested that TET scintimammography was also superior to magnetic resonance imaging of the breast.[36] These tracers are

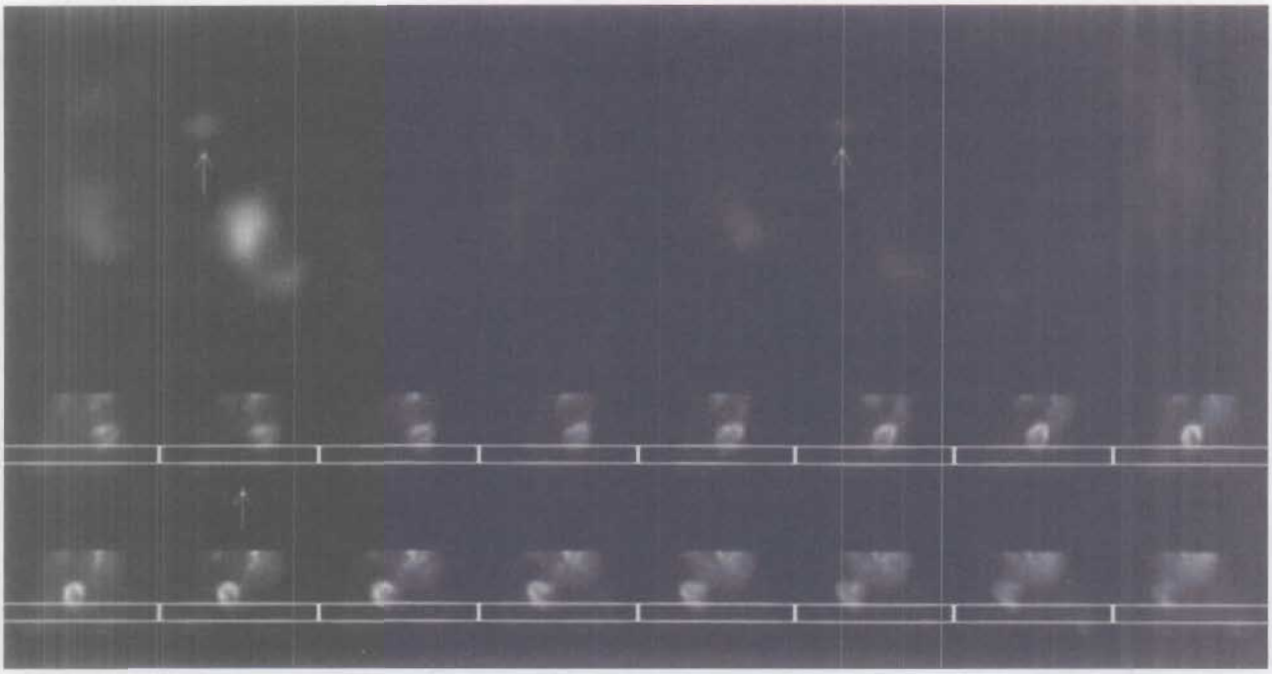

Figure 2. Planar projection images (*top*) and transaxial slices (*bottom*) are from a man with a focal region of intrapulmonary TET uptake in his left lung (*arrowhead*). The patient had no evidence of lung cancer on follow-up for 3 years. This case and 8 other similar appearing lesions on TET (4 included in this study and 4 later cases) without evidence of lung cancer or nodules on clinical follow-up, chest radiography, or computed tomography scanning of the thorax all underwent injection by the same technologist. After the technologist's technique was observed, it was concluded that this might be related to not clearing (flushing) the back-flow of blood occurring during exercise stress from the indwelling catheter before administration of TET. This suggests that the small clinically insignificant thrombi that are routinely flushed into the intravenous line can be "tagged" with TET. No further incidence of this phenomenon occurred after flushing the catheter before tracer injection became the standard technique for all technologists.

especially useful in the evaluation of the tumor response to chemotherapy,[42] patients with dense breast tissue,[35] patients with post-treatment breast cancer,[36] patients with nondiagnostic or difficult mammography results, and high-risk patients.

Conclusions

In patients referred for evaluation of dual-isotope SPECT myocardial perfusion imaging, NCFs are not uncommon. Some are incidental or consistent with known clinical problems. However, because of the potential for Tl-201, TET, and MIBI uptake in neoplastic processes, observation of abnormal noncardiac foci of activity may result in life-saving early cancer identification, especially if uptake of both Tl-201 and a Tc-99m–labeled agent is present in the lesion. Detection and reporting of such abnormalities will most often require careful and informed inspection of raw projection images.

Acknowledgment

Dr. Williams is a researcher and lecturer for Amersham Healthcare, Inc (manufacturer of thallium 201 and technetium 99m tetrofosmin) and a researcher for Bristol Meyers Squibb, Inc (manufacturer of Tc-99m sestamibi).

References

1. Berman DS, Kiat H, Friedman JD, et al. Separate acquisition rest thallium-201/stress technetium-99m sestamibi dual-isotope myocardial perfusion single-photon emission computed tomography: a clinical validation study. J Am Coll Cardiol 1993;22: 1455-64.
2. Hachamovitch R, Berman DS, Kiat H, et al. Incremental prognostic value of adenosine stress myocardial perfusion single-photon emission computed tomography and impact on subsequent management in patients with or suspected of having myocardial ischemia. Am J Cardiol 1997;80:426-33.
3. Kang X, Berman DS, Lewin H, et al. Comparative ability of myocardial perfusion single-photon emission computed tomogra-

phy to detect coronary artery disease in patients with and without diabetes mellitus. Am Heart J 1999;137:949-57.
4. Hachamovitch R, Berman DS, Kiat H, et al. Effective risk stratification using exercise myocardial perfusion SPECT in women: gender-related differences in prognostic nuclear testing. J Am Coll Cardiol 1996;28:34-44.
5. Germano G, Erel J, Kiat H, Kavanagh PB, Berman DS. Quantitative LVEF and qualitative regional function from gated thallium-201 perfusion SPECT. J Nucl Med 1997;38:749-54.
6. Zaret BL, Rigo P, Wackers FJT, et al. Myocardial perfusion imaging with 99m-Tc-tetrofosmin: comparison to ^{201}Tl imaging and coronary angiography in a phase III multicenter trial. The Tetrofosmin International Trial Study Group. Circulation 1995;91: 313-9.
7. Nakada K, Katoh C, Morita K, et al. Relationship among ^{201}Tl uptake, nuclear DNA content and clinical behavior in metastatic thyroid carcinoma. J Nucl Med 1999;40:963-7.
8. Valdes Olmos RA, Koops W, Loftus BM, et al. Correlative ^{201}Tl SPECT, MRI and ex vivo ^{201}Tl uptake in detecting and characterizing cervical lymphadenopathy in head and neck squamous cell carcinoma. J Nucl Med 1999;40:1414-9.
9. Kunisada T, Ozaki T, Kawai A, et al. Imaging assessment of the responses of osteosarcoma patients to preoperative chemotherapy: angiography compared with thallium-201 scintigraphy. Cancer 1999;86:949-56.
10. Suga K, Kume N, Nishigauchi K, et al. ^{201}Tl SPECT as an indicator for early prediction of therapeutic effects in patients with non-small cell lung cancer. Ann Nucl Med 1998;12:355-62.
11. Yigitbasi OG, Tutus A, Bozdemir K, Nardali M, Guney E. ^{201}Tl imaging for differentiating between malignant and benign neck masses. Nucl Med Comm 1998;19:555-60.
12. Lee VW, Antonacci V, Tilak S, Fuller JD, Cooley TP. Intracranial mass lesions: sequential thallium and gallium scintigraphy in patients with AIDS. Radiology 1999;211:507-12.
13. Abdel-Dayem HM, Naddaf SY, Omar WS, Aziz M, Gillooley J. Delayed positive thallium uptake in large B-cell non-Hodgkin's malignant lymphoma. J Nucl Med 1997;38:1213-5.
14. Ramanna L, Waxman A, Binney G, et al. Thallium-201 scintigraphy in bone sarcoma: comparison with gallium-67 and technetium-MDP in the evaluation of chemotherapeutic response. J Nucl Med 1990;31:567-72.
15. Seabold JE, Gurll N, Schurrer ME, Aktay R, Kirchner PT. Comparison of ^{99m}Tc-methoxyisobutyl isonitrile and ^{201}Tl scintigraphy for detection of residual thyroid cancer after ^{131}I ablative therapy. J Nucl Med 1999;40:1434-40.
16. Aktolun C, Bayhan H, Kir M. Clinical experience with Tc-99m MIBI imaging in patients with malignant tumors. Preliminary results and comparison with Tl-201. Clin Nucl Med 1992;17: 171-6.
17. Caner B, Kitapci M, Unlu M, et al. Technetium-99m-MIBI uptake in benign and malignant bone lesions: a comparative study with technetium-99m-MDP. J Nucl Med 1992;33:319-24.
18. Taillefer R, Roidoux A, Lambert R, et al. Technetium-99m sestamibi prone scintimammography to detect primary breast cancer and axillary lymph node involvement. J Nucl Med 1995; 36:1758-65.
19. Ziegels P, Nocaudie M, Huglo D, et al. Comparison of technetium-99m-methoxy-isobutylisonitrile and gallium-67-citrate scanning in assessment of lymphomas. Eur J Nucl Med 1995; 22:126-31.
20. Aktolun C, Bayhan H, Pabuccu Y, et al. Assessment of tumor necrosis and detection of mediastinal lymph node metastasis in bronchial carcinoma with technetium-99m sestamibi imaging: comparison with CT scan. Eur J Nucl Med 1994;21: 973-9.
21. Yen T, Lin H, Lee C, Chang S, Yeh S. The role of technetium-99m sestamibi whole-body scans in diagnosing metastatic Hurtle cell carcinoma of the thyroid gland after total thyroidectomy: a comparison with iodine-131 and thallium-201 whole-body scans. Eur J Nucl Med 1994;21:980-3.
22. Scopinaro F, Schillaci O, Scarpini M, et al. Technetium-99m sestamibi: an indicator of breast cancer invasiveness. Eur J Nucl Med 1994;21:984-7.
23. Van Kriekinge SD, Germano G, Forscher C, et al. Tumor quantitation and monitoring in whole-body planar technetium-99m-sestamibi imaging. J Nucl Med 1997;38:356-61.
24. Luker GD, Facasso PM, Dobkin J, Piwnica-Worms D. Modulation of the multidrug resistance P-glycoprotein: detection with technetium-99m-sestamibi in vivo. J Nucl Med 1997;38:369-72.
25. Mansi L, Rambaldi PF, Cuccurullo V, et al. Diagnostic and prognostic role of ^{99m}-Tc-tetrofosmin in breast cancer. Q J Nucl Med 1997;41:239-50.
26. Tabuenca MJ, Vargas JA, Varela A, et al. Inverse correlation between ^{99m}Tc-tetrofosmin uptake and P-glycoprotein in non-small cell lung cancer. J Nucl Med 1999;40:1223-5.
27. Lind P, Gallowitsch HJ, Langsteger W, et al. Technetium-99m-tetrofosmin whole body scintigraphy in follow-up differentiated thyroid carcinoma. J Nucl Med 1997;38:348-52.
28. Kao CH, Ho YJ, Shen YY, Lee JK. Evaluation of chemotherapy response in patients with small cell lung cancer using technetium-99m-tetrofosmin. Anticancer Res 1999;19:2311-5.
29. Klain M, Maurea S, Lastoria S, et al. Technetium-99m-tetrofosmin imaging of differentiated mixed thyroid cancer. J Nucl Med 1995;36:2248-51.
30. Lind P, Umschaden HW, Forsthuber E, et al. Scintimammography using Tc-99m tetrofosmin. Acta Med Austriaca 1997;24: 50-4.
31. Berghammer P, Obwegeser R, Mulauer-Ertl S, et al. 99m-Tc-tetrofosmin scintigraphy and breast cancer. Gynecol Oncol 1999; 73:87-90.
32. Takekawa H, Shinano H, Tsukamoto E, et al. Technetium-99m-tetrofosmin imaging of lung cancer: relationship with histopathology. Ann Nucl Med 1999;13:71-5.
33. Platts EA, North TL, Pickert RD, et al. Mechanism of uptake of technetium tetrofosmin. I. Uptake into adult rat ventricular myocytes and subcellular localization. J Nucl Cardiol 1995;2: 317-26.
34. Kinuya S, Yokoyama K, Watanabe N, et al. Early response of tumour to radiotherapy should be assessed by both uptake and retention of single photon tracers: in vitro analysis with ^{201}Tl-chloride, ^{99}Tcm-sestamibi and ^{99}Tcm-tetrofosmin in human bladder cancer cells and human leukocytes. Nucl Med Commun 1999;20:581-8.
35. Bongers V, Borel Rinkes IH, Sie-Go DM, et al. Detection of malignant breast tumours in dense breast tissue: results of ^{99m}Tc-tetrofosmin scintimammography related to surgery. Eur J Surg Oncol 1999;25:152-6.
36. Fenlon HM, Phelan NC, O'Sullivan P, et al. Benign versus malignant breast disease: comparison of contrast-enhanced MR imaging and Tc-99m tetrofosmin scintimammography. Radiology 1997;205:214-20.
37. Hendel RC, Gibbons RJ, Bateman TM. Use of rotating (cine) planar images in the interpretation of a tomographic myocardial perfusion study. J Nucl Cardiol 1999;6:2 ;234-40.

38. Kaiser JS, Helvie MA, Blacklaw RL, Roubidoux MA. Palpable breast thickening: role of mammography and US in cancer detection. Radiology 2002;223:839-44.
39. Watanabe N, Hirano T, Fukushima Y, et al. Esophageal cancer detection with Tc-99m tetrofosmin SPECT. Clin Nucl Med 1997; 22:431-3.
40. Ahmed A. Atlas of ultrastructure of human breast diseases. New York: Churchill Livingstone; 1978.
41. Fiskum G. Mitochondrial physiology and pathology. New York: Van Nostrand Reinhold; 1986.
42. Taillefer R. The role of ^{99m}Tc sestamibi and other conventional radiopharmaceuticals in breast cancer diagnosis. Semin Nucl Med 1999;29:16-40.

Comparison of Hypoxia and Ouabain Effects on the Myocardial Uptake Kinetics of Technetium-99m Hexakis 2-Methoxyisobutyl Isonitrile and Thallium-201

Denis J. Meerdink and Jeffrey A. Leppo

Department of Nuclear Medicine and Department of Medicine, Cardiology, University of Massachusetts Medical Center, Worcester, Massachusetts

Effects of hypoxia and ouabain on transcapillary exchange of [^{99m}Tc]hexakis (2-methoxyisobutylisonitrile) [SESTAMIBI, also known as MIBI or HEXAMIBI] and ^{201}Tl were investigated with indicator-dilution studies using isolated rabbit hearts. Peak myocardial extraction (Emax), permeability-surface area products (PScap), and net myocardial extraction (Enet) were compared among serial injections during constant coronary flows. Overall, measures of transcapillary transport (Emax and PScap) for SESTAMIBI were significantly lower ($p < 0.001$) than those simultaneously determined for thallium, but estimates of tissue retention (Enet) for SESTAMIBI and thallium were not statistically distinguishable. Hypoxia had no significant effect on mean (±s.d.) Emax for SESTAMIBI (0.31 ± 0.13) or thallium (0.59 ± 0.11), nor on mean PScap or Enet values. Ouabain (1.5×10^{-7} *M* and 1.5×10^{-6} *M*) had no effect on SESTAMIBI or thallium Emax (respectively, 0.29 ± 0.08 and 0.60 ± 0.05) or on PScap for SESTAMIBI. Thallium PScap was depressed with higher ouabain dose (control, 1.22 ± 0.40; high ouabain, 1.06 ± 0.41 ml/min/g; $p < 0.01$). Ouabain also caused a significant and progressive increase in average SESTAMIBI Enet (control, 0.23 ± 0.10 to high ouabain, 0.33 ± 0.12; $p < 0.05$), but depressed thallium Enet (control, 0.38 ± 0.14 to high ouabain, 0.32 ± 0.18; $p < 0.01$). These results suggest myocardial metabolic and/or functional status have minor influence on transcapillary transport of SESTAMIBI and thallium, but significantly affects cellular retention.

J Nucl Med 30: 1500–1506, 1989

Technetium-99m- (^{99m}Tc) labeled agents have been proposed as alternatives to thallium-201 (^{201}Tl) for imaging myocardial perfusion imaging because of better photon statistics, Anger camera imaging properties, cost, and clinical availability (*1–4*). Clinical images from [^{99m}Tc]-labeled isonitriles compare favorably to those obtained with thallium (*3,5*). Specifically, [^{99m}Tc] hexakis (t-butylisonitrile) (TBI) and its ether derivate, [^{99m}Tc]hexakis 2-methoxyisobutyl isonitrile (SESTAMIBI, also known as MIBI, HEXAMIBI, or RP-30; DuPont Company, No. Billerica, MA), have suitable kinetic characteristics and have shown good potential in preliminary clinical studies. SESTAMIBI, in particular, may have appeal for cardiac studies because of its low lung extraction compared to TBI (*6*).

The interpretation of perfusion images of cardiac uptake for these agents is facilitated from knowledge of the capillary exchange process. To assume that clinical perfusion images realistically represent myocardial blood flow, it must be known that the imaging agent is deposited in myocardial tissue in proportion to the blood it receives, and that this deposition is unaltered by metabolic or functional abnormalities. No previous studies have determined the effects of metabolic aberrations on the transcapillary transport of both thallium and SESTAMIBI in the same hearts with constant coronary flow. Accordingly, the goal of this report was to determine the flow-independent effects of hypoxia and ouabain on myocardial uptake kinetics of these two perfusion agents.

Received Jan. 30, 1989; revision accepted Apr. 20, 1989.
For reprints contact: D. J. Meerdink, PhD, Dept. of Nuclear Medicine, University of Massachusetts Medical Center, 55 Lake Ave., North, Worcester, MA 01655.

MATERIALS AND METHODS

Experimental Preparation

Surgery and perfusion. An isolated, isovolumetrically-contracting rabbit heart preparation, utilizing methods previously described in detail (*7–9*), was used for all experiments. Briefly, male New Zealand white rabbits (1.5–2.5 kg) were heparinized (600 IU/kg i.v.) and anesthetized (sodium pentobarbital, 40 mg/kg i.v.), and the hearts were quickly removed and mounted on a perfusion apparatus (*9*). For hypoxia experiments, the nonrecirculating perfusate consisted of a modified Krebs-Henseleit bicarbonate buffer, pH 7.4, that contained (m*M*): NaCl, 122; $NaHCO_3$, 22; glucose, 5.5; KCl, 4.7; $MgSO_4$, 1.2; $CaCl_2$, 2; KH_2PO_4, 1.2; lactate (neutralized with NaOH), 1; and Na_2EDTA, 0.4. Normoxic buffer and hypoxic buffer were bubbled with 95% O_2/5% CO_2 and 95% N_2/5% CO_2, respectively, for a minimum of 30 min prior to heart perfusion. For ouabain experiments, the perfusate was blood obtained from a second heparinized, anesthetized rabbit as previously described (*8,9*), which recirculated except when indicator dilution injections were made. The blood passed through a membrane oxygenator that was gassed with a 3% CO_2 and air mixture. During experimentation, blood gas measurements were made every 30–40 min, and appropriate adjustments were made with supplemental O_2 and bicarbonate to maintain blood pH. P_{O2}, and P_{CO2} in the physiologic range. Glucose levels were also monitored and adjusted as needed to maintain approximately 100 mg/dl.

For both hypoxia and ouabain protocols, mean coronary perfusion pressure was maintained at 100–125 mmHg by a constant flow pump. A thermistor and pacing catheter were placed in the right ventricle via the right atrium to monitor tissue temperature (37 ± 1°C) and maintain a heart rate of at least 180 bpm. A plastic cannula was also placed in the right ventricle via the pulmonary artery for collecting coronary sinus drainage samples and measuring coronary flow. A latex rubber balloon was inserted and secured into the left ventricle, and filled with saline until an end-diastolic pressure of 5–10 mmHg was recorded. A plastic cannula, placed in the left ventricle at its apex, drained aortic valve leakage, and Thebesian vein flow. Mean aortic pressure, left ventricle (LV) pressure, and the first derivative of LV pressure were continuously recorded. The experimental protocols (described below) began after temperature, ventricular pressure, contraction rate, coronary flow, and aortic pressure stabilized.

SESTAMIBI preparation. The SESTAMIBI salt [supplied by DuPont Company; (*2*)] and formamidine sulfinic acid (FSA) were prepared as a 4 mg/ml and 0.4 mg/ml solution, respectively, in distilled water. A 0.5-ml aliquot of each of the SESTAMIBI and FSA solutions were combined in a nitrogen-purged vial, and ~0.2–0.4 ml of $^{99m}TcO_4^-$ (370 MBq, 10 mCi) was added. The vial was quickly placed in boiling water for 10–15 min and then allowed to cool to room temperature. Binding efficiency was evaluated by thin layer chromatography (*9*), and was always ≥95%.

Isotope injection and sample collection. The indicator cocktail, consisting of a mixture of 20 μCi (0.74 MBq) of indium-111- (^{111}In) labeled albumin (*10*), 35 μCi (1.3 MBq) of $^{201}TlCl$, and 90 μCi (3.3 MBq) of [^{99m}Tc]SESTAMIBI dissolved in perfusate, was thoroughly mixed and a 0.3-ml bolus was loaded into an injection loop that ran parallel to and joined with the aortic inflow with three-way valves. Isotope injection proceeded by rapidly turning the three-way valves so that the bolus was as homogeneously distributed as possible to both coronary arteries. Coronary venous effluent was collected into preweighed plastic tubes at 1.2- to 5-sec intervals (depending on flow rate) over a 0.5–4 min collection time. Coronary flow was measured before and after injections; results were discarded if flows changed more than 10%. Full sample weights were measured, and isotope activities were determined in each sample along with a 0.1-ml aliquot of each injectate by a gamma well counter with corrections for energy crossover, time, background, and physical decay during the counting process. When multiple injections (at constant flow) were made in an individual heart, isotope backgrounds were <1% of peak activity in all instances. In addition, the wet weight of a portion of the left ventricular free wall was determined for subsequent estimation of the tissue water fraction (*7*).

Myocardial transport analysis. For each injection, transcapillary exchange estimates were determined using standard indicator dilution techniques and equations (*9,11,12*). Briefly, normalized transport function curves for albumin [reference, $h_R(t)$] and for SESTAMIBI and thallium [diffusible tracers, $h_D(t)$] were calculated from the general equation, $h(t) = F_s \cdot C(t)/q_o$, where Fs is plasma flow (ml/min/g), t is time (sec), C(t) is isotope activity, and q_o is injected dose. The instantaneous fractional extraction [E(t)] for SESTAMIBI and thallium was calculated for each sample with the equation, $E(t) = 1 - h_D(t)/h_R(t)$, and the capillary permeability-surface area product (PScap, ml/min/g) was calculated with the equation, $PScap = -F_s \cdot \log_e(1-E_{max})$ (*13*). Emax was defined as the maximum E(t) of diffusible tracer observed up to the peak $h_R(t)$, which is the best estimate of average functional extraction (*11,14*). Net tissue extraction (Enet), an estimate of tissue retention, was calculated from normalized time integrals of transport function differences between reference and diffusible tracers with the equation (*14*): $Enet = \int_0^t[h_R(t)-h_D(t)]d\tau / \int_0^t h_R(t)d\tau$, where t was defined as the time (sec) when 99.99% of the albumin reference had emerged in the venous effluent, and τ was the dummy variable for integration.

Results were analyzed with paired t-tests and repeated-measures analysis of variance routines (*15*) and comparisons made among treatments within the hypoxia or ouabain experimental series (*16*).

Experimental Protocols

Hypoxia. To study the effects of hypoxia, eight hearts were initially perfused with buffer gassed with 95% oxygen/5% carbon dioxide and allowed to stabilize for ~10 min, after which the control injection of tracer cocktail was made. The perfusion buffer was then changed to one made hypoxic by gassing with 95% nitrogen/5% carbon dioxide; after 2 and 5 min of hypoxic perfusion, the first and second experimental injections were made while coronary flow remained constant.

Ouabain. Ouabain effects were evaluated in 11 hearts perfused with recirculating blood at constant flow. Following a stabilization period of ~15 min, a control injection was made, after which a ouabain solution was infused into the system over 5 min so that a concentration of 1.5×10^{-7} *M* (LOW dose) was achieved in the recirculating blood. This typically resulted in a transient rise in +dP/dt, but as LV end diastolic pressure began to increase, positive inotropic response could

not be sustained. After the first ouabain dose circulated at least 15 min, the first experimental injection of indicator cocktail was made. A second dose of ouabain was given over 5 min, increasing the ouabain concentration to 1.5×10^{-6} *M* (HIGH dose). The second experimental dilution study was made after the HIGH dose circulated at least 15 min. These ouabain concentrations were based on therapeutic (LOW) and toxic (HIGH) concentrations (*17,18*). Ventricular ectopy increased greatly during these infusions, strongly implying that the ouabain infusions produced pharmacologic concentrations.

Results were reported as mean (±s.d.), and considered significantly different with a probability of 0.05 or less. Statistical analysis included the paired Student's t-test and analysis of variance (uni- and multi-variant, and repeated measures) (*16*), and was performed using the Statistical Analysis System (*15*).

RESULTS

Average (±s.d.) results for the hypoxia and ouabain studies (respectively) include: body weight, 2.22 (±0.18) and 1.67 (±0.11) kg; wet heart weights, 6.03 (±0.55) and 5.41 (±0.36) g; and tissue water fraction, 0.85 (±0.01) and 0.73 (±0.01). Significant differences ($p < 0.02$) existed between hypoxia and ouabain experiments for only body weight and tissue water fraction.

Hemodynamics

Average (±s.d.) results for hemodynamic measurements appear in Table 1. These parameters were not affected by the injection of isotope cocktail during hypoxia or ouabain experiments (data not shown). Repeated-measures analysis of variance of control, 2-, and 5-min hypoxia injections indicate no significant change in coronary perfusion rates, but significant decreases ($p < 0.001$) existed in aortic pressure, peak systolic pressure, +dP/dt, and −dP/dt. The 30% decline in aortic pressure (i.e., perfusion pressure) after 2 min of hypoxic perfusion was not further depressed at 5 min of hypoxia, which indicates a prompt and maximal reduction in vascular resistance. The progressive decline in developed systolic pressure, +dP/dt, and −dP/dt as well as an increase of end diastolic pressure after 2 and 5 min of hypoxia, reflects the severe functional compromise induced by hypoxia. In ouabain experiments, no significant change was noted in perfusion rate, but a small increase in end diastolic pressure reached statistical significance ($p < 0.05$).

Indicator Dilution Analysis

Examples of the indicator transport functions [h(t)] and instantaneous extraction [E(t)] appear in Figure 1 for a control injection. Differences in the height and shape of the h(t) and E(t) curves between thallium and SESTAMIBI suggest fundamental differences in their mechanisms of transcapillary transport. The h(t) curve for thallium is much lower than the SESTAMIBI h(t), which indicates a higher peak extraction (Emax) for thallium.

The tail portion of the h(t) curves also reveal fundamental differences in the extravascular distribution of thallium and SESTAMIBI. The transport function curve [h(t)] for thallium crosses and remains above the reference albumin, which indicates a net flux of initially extracted thallium from the myocardial tissue back into the vascular space. In contrast, SESTAMIBI h(t) remains below the albumin reference h(t) throughout the observation period, indicating relatively little back diffusion of SESTAMIBI.

The E(t) curves for thallium and SESTAMIBI are also quite different, which also reveals their different

TABLE 1
Hemodynamic Results*

	Coronary Flow (ml/min/g)	Aortic Pressure (mm Hg)	Peak Systolic Pressure (mm Hg)	End Diastolic Pressure (mm Hg)	+dP/dt (mm Hg/s)	−dP/dt (mm Hg/s)
Hypoxia						
Control	5.52 (1.47)	47.0 (10.3)	77.9 (12.6)	6.5 (0.9)	1630 (284)	1362 (327)
2 min.	5.49 (1.51)	39.6 (15.4)	50.8 (28.4)	9.3 (6.4)	1176 (564)	877 (493)
5 min.	5.48 (1.56)	32.3 (11.6)	32.9 (12.9)	12.3 (10.1)	586 (234)	418 (146)
p**	NS	<0.001	<0.001	<0.001	<0.001	<0.001
Ouabain						
Control	1.96 (0.63)	120.4 (25.3)	63.3 (18.0)	12.1 (5.4)	1261 (546)	658 (424)
LOW Dose	1.96 (0.62)	131.1 (27.8)	62.8 (21.9)	18.4 (10.6)	1196 (812)	658 (563)
HIGH Dose	1.89 (0.69)	154.0 (37.8)	68.0 (29.4)	19.9 (15.0)	1602 (1292)	800 (676)
p**	NS	<0.01	<0.03	NS	NS	NS

* Mean ± s.d.
** Probability of equality as determined by repeated-measures analysis of variance (15).
NS = not significant.

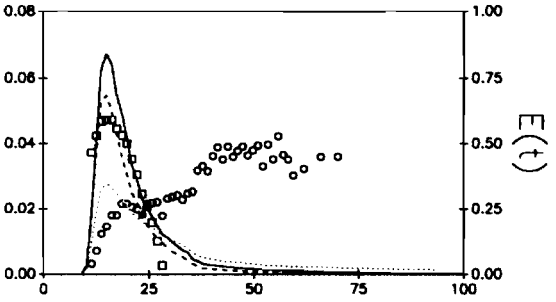

FIGURE 1
Representative plot of the transport function [h(t)] and instantaneous fractional extraction [E(t)] versus sampling time. The left ordinate are the h(t) values for [^{111}In]albumin (solid line), [^{99m}Tc]SESTAMIBI (dashed line), and ^{201}Tl (dotted line). The right ordinate are the E(t) values for [^{99m}Tc]SESTAMIBI (open circles) and ^{201}Tl (open squares).

transport mechanisms. Thallium E(t) has an early maximal plateau phase followed by rapid fall, which is typical for cations, while SESTAMIBI E(t) displays an early rise and sustained, slowly rising plateau throughout the h(t) curve.

Extraction. Average (±s.d.) maximal instantaneous extractions (Emax) of thallium and SESTAMIBI appear in Figure 2. For all injections in both hypoxia and ouabain experiments, SESTAMIBI Emax determinations were significantly lower ($p < 0.001$) than concurrently-measured thallium values, averaging 48% and 43% lower ($p < 0.001$) in hypoxia and ouabain experiments, respectively. In hypoxia experiments, analysis of variance (repeated measures) and paired t-tests revealed no significant Emax differences for thallium or SESTAMIBI in either experimental injection from their respective control determinations (Fig. 2A). In ouabain experiments (Fig. 2B), Emax for SESTAMIBI tended to increase and thallium tended to decrease, although no statistically significant differences were revealed between experimental injections and their respective controls.

Permeability. Figure 3 illustrates the mean (±s.d.) PScap determinations for thallium and SESTAMIBI for hypoxia and ouabain experiments. PScap for SESTAMIBI averaged 58% of those for thallium for hypoxia experiments and 48% lower in ouabain experiments. In hypoxia experiments (Fig. 3A), PScap values for SESTAMIBI were significantly less ($p < 0.001$) than simultaneously-determined thallium estimates in each of the three injections. Hypoxia treatment also did not significantly change SESTAMIBI or thallium values from their respective controls. In contrast, PScap averages for SESTAMIBI in ouabain experiments (Fig. 3B) were significantly less ($p < 0.02$) than thallium only for control and LOW dose injections, but not for HIGH dose injections. In addition, thallium PScap declined

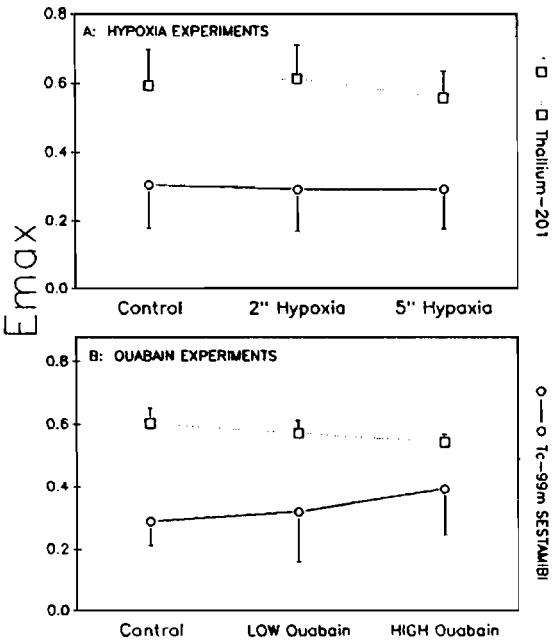

FIGURE 2
Average (±s.d.) Emax estimates for [^{99m}Tc]SESTAMIBI (open circles) and ^{201}Tl (open squares) for hypoxia (panel A) and ouabain (panel B) experiments. See text for treatment descriptions.

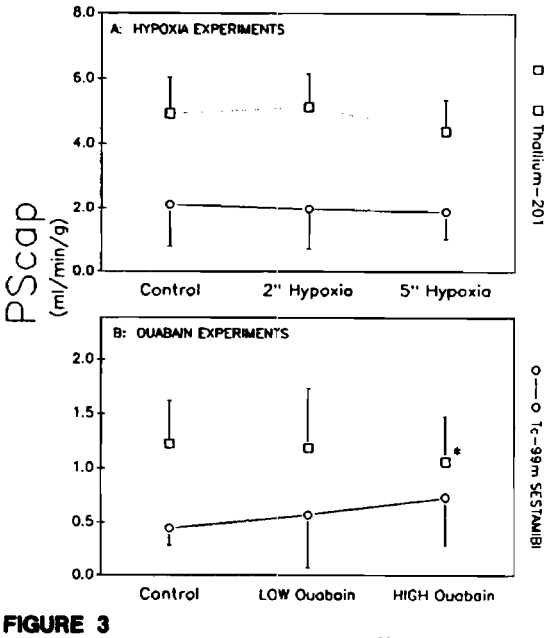

FIGURE 3
Average (±s.d.) PScap estimates for [^{99m}Tc]SESTAMIBI (open circles) and ^{201}Tl (open squares) for hypoxia (panel A) and ouabain (panel B) experiments. See text for treatment descriptions. (* indicates paired difference ($p < 0.015$) from control.)

significantly ($p < 0.02$) from control during the HIGH ouabain dose. PScap values for SESTAMIBI tended to increase with ouabain dose level, but this rise did not achieve significance.

Retention. Average (±s.d.) Enet values for hypoxia and ouabain experiments appear in Figure 4. Unlike Emax and PScap computations, SESTAMIBI Enet estimates were greater than or approximately equal to those for thallium. Paired analysis revealed no significant differences in Enet estimates between SESTAMIBI and thallium for any hypoxia or ouabain injection, except for the ouabain control (SESTAMIBI < thallium; $p < 0.01$). Although the average Enet for SESTAMIBI tended to increase with hypoxia (Fig. 4A), a difference from control reached statistical significance only for 2-min hypoxia determinations ($p < 0.05$) because of the relatively large variation in 5-min hypoxia estimates. SESTAMIBI Enet in ouabain experiments (Fig. 4B) also increased and reached statistical significance with HIGH ouabain dose (<0.01). In contrast, a significant and progressive decline in thallium Enet was noted for both LOW and HIGH ouabain doses ($p < 0.01$).

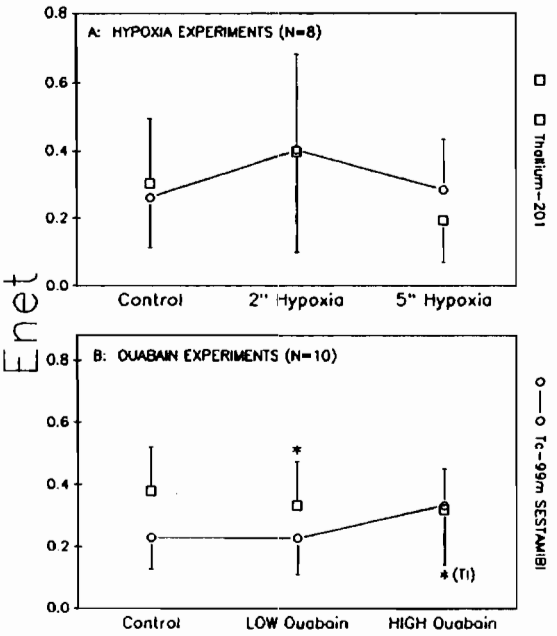

FIGURE 4
Average (±s.d.) Enet estimates for [^{99m}Tc]SESTAMIBI (open circles) and ^{201}Tl (open squares) for hypoxia (panel A) and ouabain (panel B) experiments. See text for treatment descriptions. (* indicates paired difference ($p < 0.015$) from control.)

DISCUSSION

The present study demonstrates that hypoxia and ouabain have small but significant effects on the myocardial transcapillary transport of SESTAMIBI and thallium in the perfused rabbit heart model. However, net cellular retention of these two tracers is more sensitive to hypoxia and ATPase inhibition than peak extraction or permeability.

Isolated Heart Model: Critiques

Using hemoglobin-free buffer in hypoxia experiments necessitates a two- to three-fold increase in the normal (2-4 ml/min/g) coronary perfusion rate of a normal rabbit heart (*19*) so that the tissue receives adequate oxygen supplies. Using protein-free buffer in hypoxia experiments also caused an average 16% higher tissue water fraction than what was observed using blood perfusate (ouabain studies). Both increased perfusion rate and tissue edema would affect kinetic estimates (*9*). Specifically, during high flows and increased interstitial space, peak extraction (Emax) and permeability (PScap) could be underestimated. These alterations in buffer-perfused hearts makes the comparison of absolute transport rates with studies using blood perfusates difficult and therefore was not attempted nor implied.

Measures of Treatment Effect

Hypoxia. Previous reports of hearts perfused with hypoxic buffer (*20*) have shown flow-independent hemodynamic alterations similar to those observed in the present study (Table 1), which demonstrate the severe cellular functional compromise induced by hypoxic perfusion. Although function deteriorated rapidly with hypoxic treatment, flow rate remained constant. Therefore, observed changes in transcapillary transport in this study cannot be explained by fluctuations in flow.

Ouabain. Ouabain produced a significant change in aortic pressure and peak systolic pressure (Table 1), but no significant increase in +dP/dt was observed. As previously noted, an increase in positive or negative dP/dt was not sustained, which might indicate insufficient drug levels. However, the ouabain doses are in the therapeutic and toxic ranges (*17,18*). In other unpublished studies, further increases in ouabain dose produced ventricular fibrillation and rapid heart failure. Although the drug concentration in the perfusate was not measured directly, the doses appear to have achieved a pharmacologic effect. With these considerations, we assumed the hearts received adequate ouabain to achieve functional inhibition of Na^+/K^+ ATPase.

Indicator Dilution Analysis

Transcapillary exchange. These experiments confirm previous results (*9,20*) by demonstrating that SESTAMIBI transcapillary exchange is significantly less than that of thallium. In the present studies, peak extractions (Emax) and capillary permeability-surface

area products (PScap) for SESTAMIBI averaged ~40% and 30%, respectively, of thallium. These relationships in Emax and PScap were unaffected by either hypoxia or ouabain. However, in ouabain experiments, opposing effects are noted for SESTAMIBI Emax (increase) and thallium (decrease). This trend becomes statistically apparent in the Enet analysis (below).

The control Emax estimates for thallium of about 0.60 (Fig. 2) compare to maximum extractions of above 0.70 in previous reports (*7*). The lower thallium extraction observed in the present studies is probably a result of higher myocardial flow since rabbit hearts have intrinsic perfusion rates of two to three times that of other species (*19*), which appreciably reduces peak thallium extraction.

In a previous study with cultured heart cells (*21*), ouabain or other metabolic inhibitors had little effect on SESTAMIBI or thallium uptake. Thallium extraction has been reported to be insensitive to hypoxia in perfused rabbit hearts (*20*) and open-chest dogs (*22*). Weich et al. (*23*) observed a drop of 11% in thallium extraction fraction during hypoxia in open-chest dogs, but coronary flow was not constant and could increase enough during hypoxia to account for the calculated decrease in extraction. Therefore, it seems reasonable to conclude that peak SESTAMIBI and thallium extraction fraction is relatively insensitive to normal tissue oxygenation.

PScap is a measure of unidirectional tracer flux across the capillary endothelium to the myocardial tissue (*11*, *13*,*24*). PScap estimates were unaltered by hypoxia, indicating that tracer movement from the vascular compartment is not influenced by the level of myocyte oxygenation or function. However, in ouabain experiments, a significant decrease in the PScap estimate for thallium implies that capillary surface area available for exchange is reduced or that thallium extraction (Emax) at the capillary level is impeded. Regarding the former possibility, ouabain might reduce exchanging capillary area by increasing coronary resistance (*18*). However, as thallium PScap decreased with ouabain, SESTAMIBI PScap tended to increase (statistically insignificant), which would not support the premise that ouabain induced an overall decrease in exchangeable surface area. Therefore, Na^+/K^+ ATPase inhibition is the most likely cause for the observed decrease in thallium PScap. It is generally accepted that myocardial thallium uptake is mediated in part by the Na^+/K^+ ATPase system (*23*, *25*), but this is not the only mechanism (*26*). The small decrease in thallium PScap may relate to the incomplete inhibition of the ATPase transport mechanism or to the relative insignificance of ATPase transport in thallium exchange compared to other transport mechanisms.

Retention. As an estimate of tracer retention, the Enet function (*27*) measures the net result of tracer influx and backflux between capillary (vascular) and tissue. Enet estimates for SESTAMIBI and thallium are similar despite a lower influx (i.e., PScap) for SESTAMIBI because SESTAMIBI has a lower backflux than thallium during the tail portion of the h(t) curves (Fig. 1). Enet values for SESTAMIBI increased with hypoxia and ouabain, probably from an enlarged extravascular volume of distribution rather than increased uptake since Emax and PScap were not significantly changed for SESTAMIBI by either experimental treatment. For thallium, Enet was unchanged by hypoxia, but a relatively large and progressive decline was noted with ouabain. This decline for thallium probably results from depressed capillary influx (PScap reduced with ouabain, not hypoxia) and from accelerated cellular back diffusion (decreased cellular volume of distribution). More rigorous modeling efforts (*9*) would be helpful in further substantiating these present results.

Clinical Implications

It is important to note that indicator-dilution results and model estimates are not inherently comparable to in vivo clinical studies where recirculation and redistribution effects of tracer play a prominent role. However, these in-vivo experiments permit independent manipulation of factors that would be expected to affect myocardial transport of SESTAMIBI and thallium.

We have observed that transcapillary exchange of thallium is greater than that of SESTAMIBI, but Enet values at control determinations show less disparity. This suggests that the relative high first-pass extraction of thallium compared to SESTAMIBI is somewhat offset by a shorter tissue residence time, resulting in net retention for thallium only slightly greater than for SESTAMIBI. Although hypoxia and ouabain did not induce much change in Emax or PScap for SESTAMIBI or thallium, significant differences were noted in Enet calculations. Therefore, alterations in myocardial cellular function from tissue hypoxia and ATPase inhibition, independent of coronary flow, can affect myocardial transport of these tracers. Specifically, these observations imply that Enet for SESTAMIBI would tend to increase despite a constant coronary perfusion during acute tissue hypoxia and membrane ATPase inhibition. In contrast, hypoxia and ouabain appears to have the opposite effect on net myocardial retention of thallium. Although myocardial transport of SESTAMIBI and thallium are dominated by flow, interpretation of clinical scintigraphic studies should also consider these contributing effects of cellular dysfunction and membrane inhibition.

ACKNOWLEDGMENT

The authors acknowledge the technical support, suggestions, and encouragement of Dr. James B. Bassingthwaighte of the University of Washington (NIH Grant RR1243). In

addition, the assistance for product support by Dr. Stephen J. Williams (E.I. duPont de Nemours and Co., Biomedical Products Department), and technical contributions of Ms. Michele A. Thurber are gratefully acknowledged.

These studies were supported in part by U.S. Public Health grant HL34199 of the National Heart, Lung, and Blood Institute.

REFERENCES

1. Jones AG, Davison A, Abrams MJ, et al. Investigations of a new class of technetium cations [Abstract]. *J Nucl Med* 1982; 23:P16.
2. Abrams MJ, Davison A, Jones AG, Costello CE, Pang H. Synthesis and characterization of hexakis (9-alkylisocyanide) and hexakis (arylisocyanide) complexes of technetium (I). *Inorg Chem* 1983; 22:2798–2800.
3. Holman BL, Jones AG, Lister-James J, et al. A new ^{99m}Tc-labeled myocardial imaging agent, hexakis (t-butyl-isonitrile)-technetium (I) (^{99m}TcTBI): initial experience in the human. *J Nucl Med* 1984; 25:1350–1355.
4. McKusick K, Holman BL, Jones AG, Rigo P, Sporn V, Vosberg H. Comparison of three Tc-99m isonitriles for detection of ischemic heart disease in humans [Abstract]. *J Nucl Med* 1986; 27:878.
5. McKusick K, Beller GA, Berman D. Initial clinical results with Tc-99m methoxyisobutyl isonitrile [Abstract]. *J Am Coll Cardiol* 1987; 9:28A.
6. Williams SJ, Mousa SA, Morgan RA, Carroll TR, Maheu LJ. Pharmacology of Tc-99m-isonitriles: agents with favorable characteristics for heart imaging [Abstract]. *J Nucl Med* 1986; 27:877–878.
7. Leppo JA. Myocardial uptake of thallium and rubidium during alterations in perfusion and oxygenation in isolated rabbit hearts. *J Nucl Med* 1987; 28:878–885.
8. Grice WN, Konishi T, Apstein CS. Resistance of neonatal myocardium to injury during normothermic and hypothermic ischemic arrest and reperfusion. *Circulation* 1988; 75(suppl. V):V150–V155.
9. Leppo JA, Meerdink DJ. A comparison of the myocardial uptake of a technetium-labeled isonitrile analogue and thallium. *Circ Res* 1989: in press.
10. Hnatowich DJ, Layne WW, Childs RL. The preparation and labeling of DTPA-coupled albumin. *Int J Appl Radiat Isot* 1982; 33:327–331.
11. Bassingthwaighte JB, Goresky CA. Modeling in the analysis of solute and water exchange in the microvasculature. In: Handbook of physiology. sect. 2, the cardiovascular system. Vol. IV. Bethesda, MD: American Physiological Society, 1984:549–626.
12. Bassingthwaighte JB, Kuikka JT, Chan IS, Arts T, Reneman RS. A comparison of ascorbate and glucose transport in the heart. *Am J Physiol* 1985; 249:H141–H149.
13. Crone C. The permeability of capillaries in various organs as determined by use of the 'indicator diffusion' method. *Acta Physiol Scand* 1963; 58:292–305.
14. Bassingthwaighte JB, Chinard FP, Crone C, et al. Terminology for mass transport and exchange. *Am J Physiol* 1986; 250:H539–H545.
15. SAS Institute Inc. Statistical analysis system. Carey, NC: SAS Institute, Inc., 1985.
16. Snedecor GW, Cochran WG. 6th ed. Ames, Iowa: Iowa State University Press, 1967:593.
17. Caprio A, Farah A. The effect of the ionic milieu on the response of rabbit cardiac muscle to ouabain. *J Pharmacol Exp Ther* 1967; 155:403–414.
18. Tanz RD, Russell NJ. Mechanism of cardiac glycoside-induced toxicity: physiology, biochemistry and electron microscopy. *Federation Proc* 1983; 42:2470–2474.
19. Bartum RJ Jr, Berkowitz DM, Hollenberg NK. A simple radioactive microsphere method for measuring flow and cardiac output. *Invest Radiol* 1974; 9:126–132.
20. Leppo JA, Macneil PB, Moring AF, Apstein CS. Separate effects of ischemia, hypoxia, and contractility on thallium-201 kinetics in rabbit myocardium. *J Nucl Med* 1986; 27:66–74.
21. Maublant JC, Gachon P, Moins N. Hexakis (2-methoxy isobutylisonitrile) technetium-99m and thallium-201 chloride: uptake and release in cultured myocardial cells. *J Nucl Med* 1988; 29:48–54.
22. Forman R, Kirk ES. Thallium-201 accumulation during reperfusion of ischemic myocardium: dependence on regional blood flow rather than viability. *Am J Cardiol* 1984; 54:659–663.
23. Weich HF, Strauss HW, Pitt B. The extraction of thallium-201 by the myocardium. *Circulation* 1977; 56:188–191.
24. Renkin EM. Transport of potassium-42 from blood to tissue in isolated mammalian skeletal muscles. *Am J Physiol* 1959; 197:1205–1210.
25. Pohost GM, Alpert NM, Ingwall JS, Strauss HW. Thallium redistribution: mechanisms and clinical utility. *Semin Nucl Med* 1980; 10:70–93.
26. Gehring PJ, Hammond PB. The interrelationship between thallium and potassium in animals. *J Pharmacol Exp Ther* 1967; 155:187–201.
27. Lassen NA, Crone C. The extraction fraction of a capillary bed to hydrophilic molecules: theoretical considerations regarding the single injection technique with a discussion of the role of diffusion between laminar streams (Taylor's effect). In: Crone C, Lassen NA, eds. *Capillary permeability*. Copenhagen: Munksgaard, 1970:48–59.

Absolute Quantification of Regional Myocardial Uptake of ^{99m}Tc-Sestamibi with SPECT: Experimental Validation in a Porcine Model

Angela J. Da Silva, H. Roger Tang, Kenneth H. Wong, Max C. Wu, Michael W. Dae, and Bruce H. Hasegawa

Department of Radiology and Cardiovascular Research Institute, University of California at San Francisco, San Francisco; and Joint Bioengineering Graduate Group, University of California at San Francisco and Berkeley, San Francisco and Berkeley, California

We have evaluated a method for absolute in vivo quantification of ^{99m}Tc-sestamibi uptake in a porcine model of myocardial perfusion. **Methods:** Correlated CT and radionuclide images were obtained from eight adult pigs using a combined CT–SPECT imaging system. In each case, the CT image is used to generate an object-specific attenuation map that is incorporated into an iterative algorithm for reconstruction and attenuation correction of the radionuclide image. Anatomic information available from the correlated CT image is used to correct the radionuclide image for partial-volume errors by mathematically modeling the radionuclide imaging process. A volume of interest, or template, that approximates the geometric extent of the myocardium is defined from the CT image. Once defined, the template is assigned unit activity and is mathematically projected using a realistic physical model of the radionuclide imaging process including nonideal collimation and object-specific attenuation. The template is then reconstructed from these projections to obtain a pixel-by-pixel partial-volume correction for the myocardium in the radionuclide image. The CT image is also used to delimit the anatomic boundaries of the myocardium for quantification of the radionuclide images. The pixel intensities in the corrected radionuclide image are calibrated in units of activity concentration (MBq/g) and compared with the ex vivo activity concentration measured directly from the excised myocardium. **Results:** Without corrections, the measured in vivo activity concentration in the porcine myocardium was only 10% of the true value. Correcting for object-specific attenuation improved the accuracy of this measurement but resulted in values that were still only 42% of the true value. By correcting for both attenuation and partial-volume errors, we were able to achieve absolute quantification with an accuracy error near 10%. **Conclusion:** We have shown that, by applying object-specific attenuation corrections and suitable partial-volume corrections, absolute regional activity concentration can be measured accurately in the porcine myocardium.

Key Words: SPECT; quantification; partial-volume effects; image coregistration; myocardial perfusion

J Nucl Med 2001; 42:772–779

Since the 1980s, SPECT imaging has been used to study myocardial perfusion noninvasively. Current techniques for assessing myocardial perfusion studies generally rely on visual interpretation and on analysis of relative tracer activity within the myocardial regions defined by an individual SPECT study. Most of these techniques rely on maximal counts derived from radial sectors of reconstructed short-axis slices (maximum count circumferential profiles) normalized by count values in regions of peak intensity assumed to represent normally perfused regions (*1*) to determine relative tracer activity at rest and after stress. One serious limitation of these relative quantification techniques is that there is no guarantee that there will be a normally perfused myocardial segment. Consider patients with multivessel disease. Although qualitative and relative quantitative analysis may identify the most severely stenosed coronary artery, less severely stenosed arteries may not be identified without an absolute measure of the radionuclide uptake in the myocardium. In the extreme case of balanced triple-vessel disease (*2*), an overall reduction in activity may be completely overlooked if the data are examined on a relative scale but may be quite evident when evaluated on an absolute scale.

Making only a relative measurement of the radionuclide distribution has further limitations. It does not allow one to compare the amount of tracer uptake at rest with the amount of tracer uptake after stress, which could provide an estimate of coronary artery flow reserve capacity (*3*). Furthermore, it does not allow for quantitative longitudinal measurements that would show absolute changes in coronary reserve capacity resulting from therapeutic intervention (*3*).

The ultimate goal is to achieve absolute quantification—that is, to make an absolute measurement of becquerels of tracer per gram of tissue in a specified region of the left ventricular myocardium. Unfortunately, photon attenuation, scatter radiation, partial-volume errors, and other perturbations compromise absolute quantification of radionuclide uptake from SPECT (*4–6*). Despite the advent of patient-specific attenuation correction, the relatively poor spatial resolution of SPECT remains a major limiting factor for the

Received Apr. 27, 2000; revision accepted Sep. 14, 2000.
For correspondence or reprints contact: Bruce H. Hasegawa, PhD, Physics Research Laboratory, University of California at San Francisco, 389 Oyster Point Blvd., Ste. 1, South San Francisco, CA 94080.

accuracy of quantitative studies. Once attenuation corrections have been applied, partial-volume effects become a major source of error for absolute quantification of the activity concentration in myocardial SPECT, resulting in underestimation of the true radionuclide content by approximately 50% (*7–9*). These partial-volume effects severely limit the ability of SPECT to account for structurally dependent variations in reconstructed myocardial activity between individuals (*10*) and can cause artifactual regional variations in activity around the myocardium within a given individual (*11*) because of variations in wall thickness (*12*).

To achieve absolute quantification of single-photon radiopharmaceuticals using a noninvasive technique, we must compensate for physical errors such as photon attenuation, scatter radiation, and partial-volume errors. Traditionally, radionuclide quantification has focused on methods that compensate the radionuclide image for these effects. However, methods that correct the radionuclide image for partial-volume errors using collimator response models cannot recover spatial frequencies that are lost during image acquisition. Similarly, the use of recovery coefficients (*13,14*) requires a priori information about size and shape and generally is used only for simple target geometries (e.g., spheres or circular annuli (*15*)). We have departed from this paradigm by developing a method that incorporates a physical model of the image acquisition process into the quantification process itself (*9,16*) rather than compensating for these effects in the reconstruction of the radionuclide image. In this study we show absolute quantification of radiolabeled tracers in a porcine model of myocardial perfusion by comparing in vivo tracer uptake measurements obtained with a combined CT–SPECT imaging system with ex vivo tracer uptake measurements obtained directly from excised tissue.

MATERIALS AND METHODS

System Description

Our studies were performed using a dual-mode imaging system that combines a commercial CT scanner (GE 9800 Quick; General Electric Medical Systems, Milwaukee, WI) with a single-head scintillation camera (model 600 XR/T; General Electric) into a single imaging system capable of recording coregistered anatomic information from CT and function information from SPECT (*17*). Because the CT–SPECT system uses a common patient table, no repositioning (other than table translation) is required between the CT and SPECT data acquisitions, which minimizes shifts in internal anatomy and allows accurate image registration. The two datasets are coregistered in software using a rigid-body transformation matrix derived from the images of fiducial markers scanned in the CT–SPECT system (*7*). Volumes of interest defined in one space can then be easily transferred to the other image space using this transformation matrix. Furthermore, the coregistered CT image can be used to generate an object-specific attenuation map that is incorporated into an iterative maximum-likelihood expectation maximization (MLEM) reconstruction algorithm for attenuation compensation of the radionuclide image (*7,8,18,19*). Details of the image registration technique and the attenuation map generation have been published (*7,20*).

Data Acquisition

For all imaging studies, CT data were acquired at 140 kVp, 70 mA, with a 2-s scan time and a 48-cm field of view. The scan region covered the full extent of the myocardium and extended past the dome of the liver. Axial slice collimation and spacing was 3 mm over the entire scan region. The total scan time was approximately 10 min. The CT images were reconstructed with a 512 × 512 format using the filtered backprojection algorithm provided by the scanner manufacturer (General Electric) before being transferred to a workstation for further processing.

The correlated radionuclide images were acquired with 128 angular views over 360° using a 128 × 128 matrix, 15 s per view, a 15% energy window centered at 140 keV, a 23-cm radius of rotation, and a low-energy, high-resolution (LEHR) collimator. With our single-head scintillation camera, the total data acquisition time was approximately 40 min. The radionuclide data were reconstructed as 128 × 128 images using 30 iterations of an MLEM algorithm (*21*) both with and without attenuation compensation using the object-specific attenuation map derived from the CT image. As shown by previous experiments in our laboratory (*18*), 30 iterations are sufficient to reach near-convergence with the MLEM algorithm for objects of the size of the myocardium.

Animal Study Protocol

Animal studies were performed on the combined CT–SPECT imaging system to determine if absolute in vivo quantification of a radiotracer uptake could be measured accurately in a porcine model of myocardial perfusion using ^{99m}Tc-sestamibi (DuPont Pharmaceuticals, Wilmington, DE). In these experiments, in vivo measurements of the radionuclide uptake in the myocardium could be compared directly with ex vivo activity concentration measurements of the excised tissue. All animal studies were performed with the approval of the institutional committee on animal research.

Eight adult pigs, each weighing approximately 30 kg (mean weight, 28.3 ± 1.5 kg; weight range, 26.3–30.6 kg), were anesthetized and mechanically ventilated on a respirator (Harvard Apparatus, Inc., South Natick, MA). At least 60 min before imaging, each animal was injected intravenously with 1.11 GBq (30 mCi) ^{99m}Tc-sestamibi. In two animals, myocardial blood flow was modified by a vasodilator (dipyridamole). Dipyridamole was infused over a 4-min period with ^{99m}Tc-sestamibi administered 7 min after the start of the dipyridamole infusion. In three animals, regional myocardial blood flow was modified by occlusion of the left anterior descending (LAD) coronary artery. A left lateral thoracotomy was performed in the fifth intercostal space and the LAD coronary artery was isolated distal to the first major diagonal branch. A snare occluder was placed around the artery and the ribs were repositioned to approximate a closed-chest configuration. Once the animal was positioned on the imaging table, the occlusion was initiated by tightening the snare occluder surrounding the LAD coronary artery. To allow for blood clearance of the radiopharmaceutical, the occlusion was maintained for a total of 6 min, with the administration of ^{99m}Tc-sestamibi occurring 2 min after the start of the occlusion. After the 6-min occlusion, the snare occluder was released and the LAD coronary artery was reperfused.

All animals were imaged in the supine position. During CT data acquisition, iodinated contrast agent (300 mg I/mL iohexol) was infused continuously through an ear vein catheter at a constant rate

of 5 mL/min to opacify the cardiac blood pool, thus allowing the myocardium to be visualized. To reduce streak artifacts in the CT image caused by respiratory motion, use of the ventilator was suspended during CT image acquisition. After CT data acquisition, the imaging table was extended to the scintillation camera without repositioning the animal on the table in preparation for SPECT scanning. To reduce effects associated with hepatic activity, a minimum of 60 min was allowed to elapse after the ^{99m}Tc-sestamibi was injected before SPECT imaging was initiated. After the desired images were acquired, the animal was killed and a set of CT and SPECT images was acquired free of any respiratory or cardiac motion effects.

Ex Vivo Quantification

To quantify the regional activity concentration in the myocardium, the heart was removed from the dead animal after the imaging study. Starting from the apex, the myocardium was sliced into approximately 1-cm-thick short-axis slices. Then, for each slice, the left ventricle was separated from the right ventricle and, using the junction of the right ventricle as a reference, the left ventricle was further divided into four roughly equal-sized sections corresponding to the septal, anterior, lateral, and inferior walls. For those animals without a surgically induced defect, the apical slice typically was left intact. The individual tissue samples were then weighed and the radionuclide contents were measured by placing the tissue samples directly on the face of the scintillation camera with a vial containing a known activity of ^{99m}Tc as a calibration source. For identification, the myocardial segments were numbered according to the layout shown in Figure 1. For those cases in which the apical slice was left intact, it would be numbered segment 4 and the remaining segments would be numbered as shown (i.e., there would be no segment 1, 2, or 3).

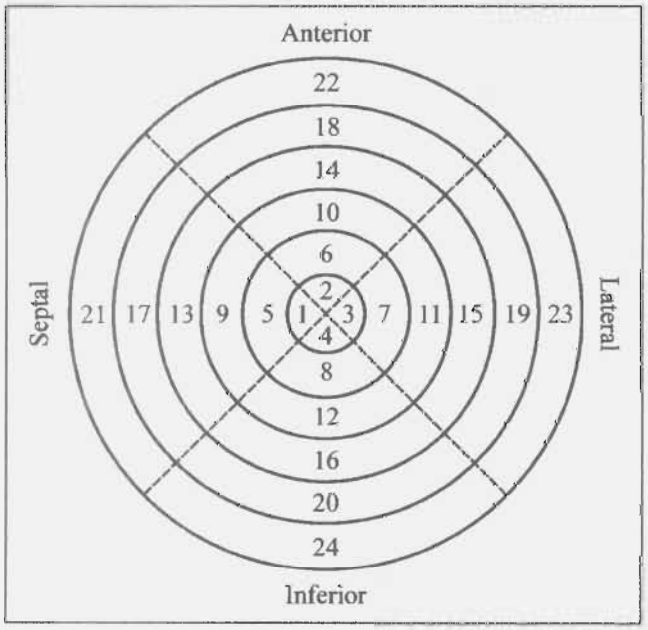

FIGURE 1. Schematic bull's eye plot indicates numbering sequence used to identify various myocardial segments. When apical slice was left intact, it would be numbered segment 4 and remaining segments would be numbered as shown.

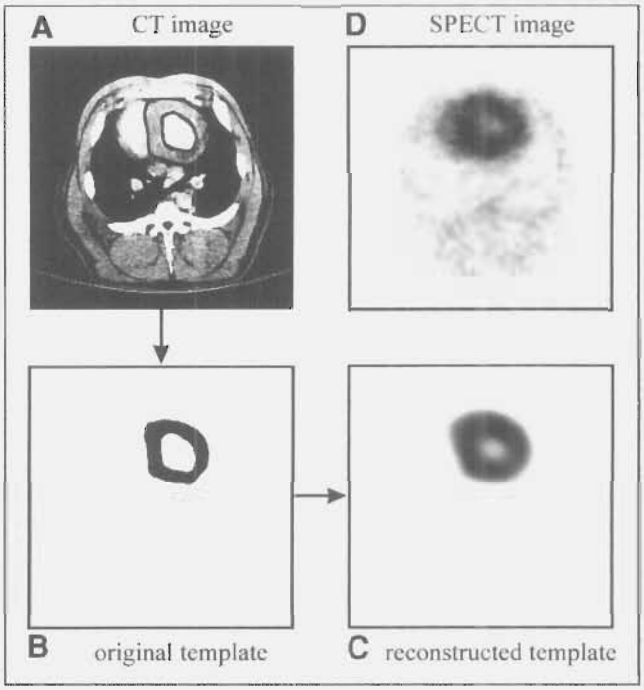

FIGURE 2. (A) Axial slice from one CT image of normal pig shown with endocardial and epicardial borders drawn. (B) Myocardial region of interest, or template, derived from CT image. Each pixel in template is assigned value of 1 to represent uniform activity concentration distribution over extent of myocardium. (C) Reconstructed template image obtained after mathematically modeling SPECT acquisition process. (D) Corresponding ^{99m}Tc-sestamibi image.

SPECT Quantification

To calibrate the reconstructed image values into units of activity concentration (kBq/mL), a 14.3-cm-diameter cylindric water phantom containing a known uniform activity concentration of ^{99m}Tc was also imaged in the CT–SPECT system. To avoid any possible errors caused by changes in camera efficiency or technique, the calibration factor was measured for each animal study. As expected, the measured calibration factor remained relatively constant between experiments, with a mean value of 0.666 ± 0.011 (kBq/mL)/reconstruction counts and a range of 0.655–0.688 (kBq/mL)/reconstruction counts.

To model the partial-volume effects and other distortions resulting from the imaging process, the high-resolution CT images are used to model a perfectly uniform myocardial distribution of activity that accurately reflects the geometry of the myocardial mass. Because iodinated contrast agent is used during the CT data acquisition, the myocardial wall can be visualized on the CT image. Endocardial and epicardial borders are defined manually on each of the transaxial slices of the CT image (Fig. 2A) to delineate the myocardial volume of interest. All pixels in this volume of interest, or template, are assigned a value of 1 to represent a uniform activity distribution over the geometric extent of the myocardium (Fig. 2B). Then, using a realistic physical model of the SPECT imaging process (including photon attenuation and nonideal collimation), the template is mathematically projected into 128 angular views to simulate the SPECT acquisition. In the projection model, photon attenuation is calculated using the attenuation map created from the correlated CT image (*7,16*), and

nonideal collimation is accounted for using a distance-dependent blurring model for the LEHR collimator (*16,22*). Finally, the template image is reconstructed (Fig. 2C) with the same iterative MLEM algorithm and attenuation map used to reconstruct the radionuclide image (Fig. 2D). Whereas the original template, defined on the high-resolution CT image, specifies the geometry for the volume of interest on the radionuclide image, the reconstructed template image is effectively a map of correction factors for the volume of interest on the radionuclide image (*9*). This technique is similar to methods used to correct for partial-volume errors in PET of the brain using registered MR images (*23–25*).

After reconstruction, the radionuclide image and the template are reoriented into short-axis slices. Because the original template defines the geometry of the myocardium, it can be used to specify the region of interest to be quantified in the radionuclide image. This can be particularly useful for quantifying ischemic regions, where it can be difficult to identify the myocardium on the radionuclide image alone (Fig. 3). For all of our studies, the relative activity concentration for the myocardium is determined from the mean pixel value within the myocardial volume of interest as defined by the CT-derived template. The mean myocardial pixel value is then scaled by the calibration factor measured with the uniform water phantom described previously to convert to absolute activity concentration. To correct for partial-volume effects, the reconstructed image is divided by the reconstructed template on a pixel-by-pixel basis before quantification. Note that, unlike conventional image correction techniques, the method we describe focuses on quantification of the image rather than improving image quality. To quantify the activity concentration, the reconstructed image is divided by the reconstructed template. However, outside of the region of interest to be quantified (i.e., the myocardial volume), the reconstructed template contains zero-value pixels, which creates discontinuities. Because the activity concentration is determined from the mean pixel value within the myocardial volume of interest, the resulting discontinuities do not affect the quantification process. However, they do prevent one from using this method to produce a radionuclide image that is corrected for partial-volume effects.

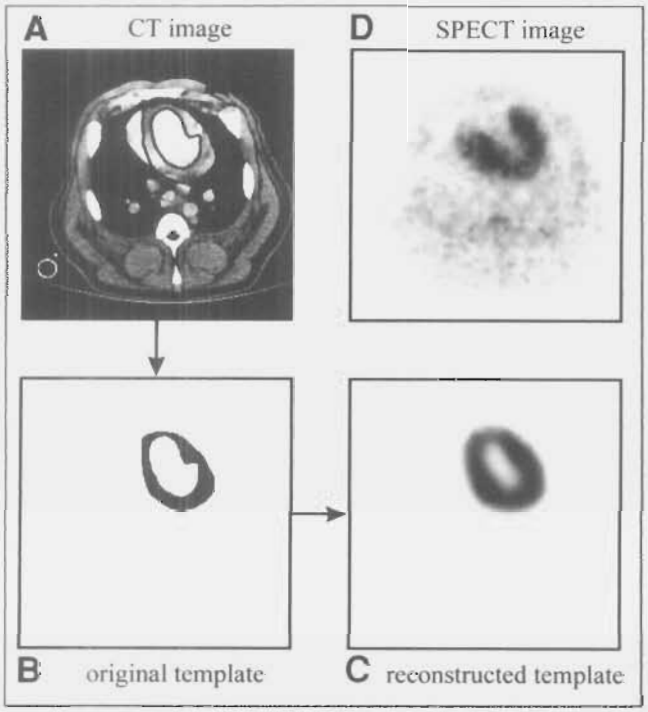

FIGURE 3. (A) Axial slice from one CT image of pig with surgically induced LAD coronary artery occlusion shown with endocardial and epicardial borders drawn. Cross section through ventilation tube is visible in lower left corner of CT image. (B) Myocardial region of interest, or template, derived from CT image. (C) Reconstructed template image obtained after mathematically modeling SPECT acquisition process. (D) Corresponding ^{99m}Tc-sestamibi image shows severe anteroseptal perfusion defect.

The in vivo and ex vivo activity measurements were compared by matching the thickness of excised myocardial tissue slices with those of the reconstructed SPECT images. This was done by determining the activity concentration from the average counts within the CT-derived volume of interest averaged over the five tomographic slices of the radionuclide image corresponding to the 1-cm-thick myocardial tissue slice. Then, using the junction of the right ventricle as a reference, the CT-derived volume of interest is divided into four segments corresponding to the septal, anterior, lateral, and inferior walls to quantify the regional activity concentration of each segment to compare with the ex vivo measurement described earlier.

Because the in vivo and ex vivo measurements were obtained at different times, a correction for the changing activity concentration of ^{99m}Tc-sestamibi within the myocardium was required. This correction must account for the physical decay of the radionuclide and the biologic washout of the radiopharmaceutical from the myocardium. We assume a monoexponential model for the biologic washout. To determine the biologic half-life (t_{biol}) of ^{99m}Tc-sestamibi in the porcine myocardium, we acquired a series of anterior planar images at specific times over the course of one of the imaging studies. A region of interest was drawn around the myocardium on the planar image and the integral counts within this region of interest were determined for each dataset. Then, by plotting the integral counts (n) within the myocardial region of interest as a function of time (t), we can determine t_{biol} by fitting the data to:

$$N = N_0 e^{\{-\ln(2)(t/T_{phys})\}} e^{\{-\ln(2)(t/T_{biol})\}}, \qquad \text{Eq. 1}$$

where N_0 is a normalization factor and t_{phys} is the physical half-life of ^{99m}Tc (i.e., 6 h).

RESULTS

Biologic Washout of ^{99m}Tc-Sestamibi

The biologic washout of ^{99m}Tc-sestamibi is illustrated in Figure 4, where the integral counts in the myocardial region of interest for the planar images from one animal are plotted as a function of measurement time. Before the time at which the animal is killed, the myocardial activity concentration decreases more rapidly than the physical decay of the isotope alone, indicating both physical and biologic decay. These data were fit to Equation 1 to obtain a t_{biol} for ^{99m}Tc-sestamibi in porcine myocardium of 355 ± 24 min. This is approximately half of the t_{biol} of ^{99m}Tc-sestamibi in normal human myocardium (680 ± 45 min) (*26*). After the animal is killed, the myocardial activity concentration de-

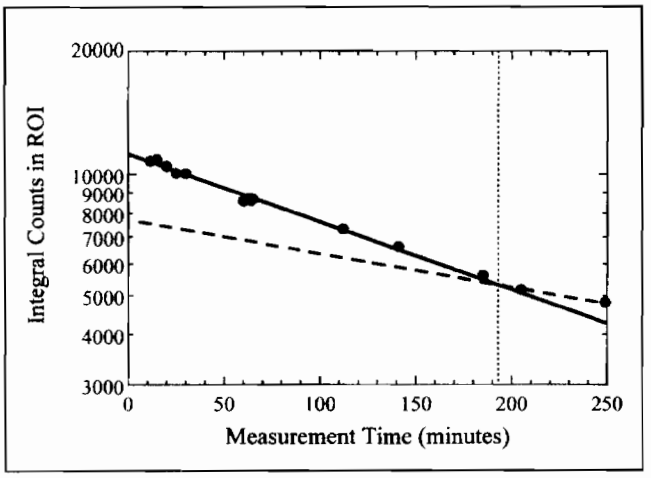

FIGURE 4. Integral counts in myocardial region of interest (ROI) from planar images obtained at various times throughout imaging study. Dotted vertical line represents time of cardiac arrest. Solid curve is fit to data obtained while animal was alive, assuming both physical decay and biologic washout (Eq. 1). Dashed curve represents physical decay only, expected after animal is dead.

creases with the t_{phys} of ^{99m}Tc as indicated in Figure 4. To correct for physical decay and tracer kinetics in all subsequent measurements, we assume both physical decay and biologic washout while the animal is alive (with half-lives of 360 min and 355 min, respectively), but only physical decay after the animal has been killed.

Ex Vivo Quantification

For our control animals (normal myocardial blood flow), the distribution of ^{99m}Tc-sestamibi uptake was not uniform throughout the myocardium. As indicated in Figure 5, the biologic variation in the radionuclide uptake in the normal porcine myocardium is significantly larger than the statistical uncertainty of the regional ex vivo measurements.

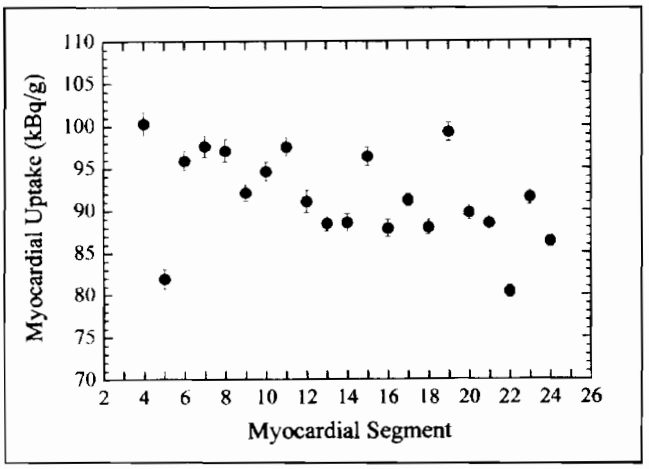

FIGURE 5. Ex vivo activity concentration measured in each myocardial segment of one control animal (normal myocardial blood flow). Refer to Figure 1 for physical location of myocardial segments.

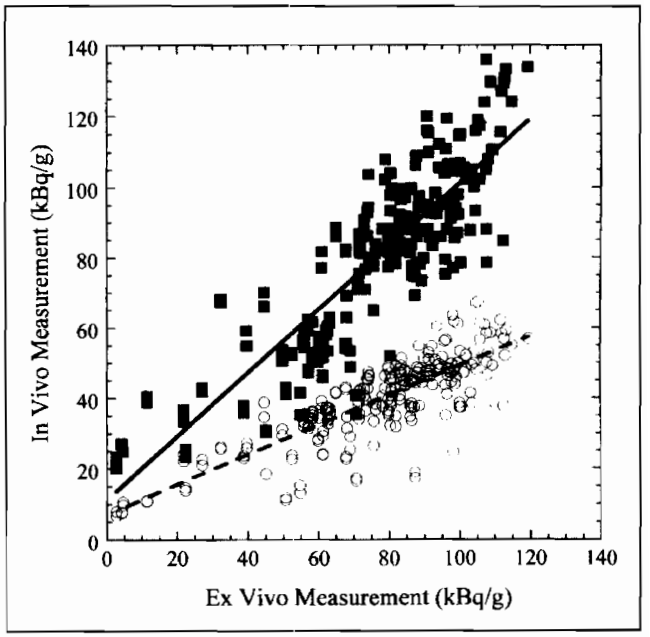

FIGURE 6. In vivo vs. ex vivo activity concentration measurement for eight pigs included in study. ○ = activity concentration measured in every myocardial segment with only attenuation correction applied. Dashed line is least-squares linear fit to data with slope of 0.421 and offset of 7.09 kBq/g (r = 0.821). ■ = activity concentration measured in every myocardial segment with both attenuation and partial-volume corrections applied. Solid line is least-squares linear fit to data with slope of 0.901 and offset of 11.17 kBq/g (r = 0.863).

In Vivo Quantification

Figure 6 shows a scatter plot of the in vivo measurement obtained with attenuation correction only and with both attenuation and partial-volume corrections versus the ex vivo measurement for all pigs included in this study. Linear fits to these two datasets are also shown in Figure 6. In the ideal case, the data would fall along a line with unit slope and zero offset. For the measurement with attenuation correction only, the slope of the line fit is 0.421, indicating that the in vivo activity concentration is approximately 58% too low. However, with both the attenuation and partial-volume corrections applied, the slope of the line fit is 0.901, indicating that the in vivo activity concentration is within 10% of the true value. In both cases, the small offset in the line fit is most probably caused by scatter and background activity.

Although not shown in Figure 6, the in vivo activity concentration was also determined for some animals from images reconstructed with an iterative MLEM algorithm that included attenuation compensation and a distance-dependent blurring model (*16,22*) for the LEHR collimator used for the data acquisition. Using this approach, the quantitative accuracy was better than with attenuation correction alone, but the true activity concentration was still underestimated by approximately 35%.

DISCUSSION

Quantification of myocardial perfusion studies can improve reproducibility, reduce interobserver variability, and lead to more standardized, objective reports. Current quantification techniques used in myocardial perfusion studies provide only relative tracer activity within myocardial regions defined by an individual SPECT acquisition. Absolute quantification (i.e., determining the absolute tracer activity in becquerels per gram of tissue) could provide significant advantages over these relative measurements because it would allow patients to serve as their own controls. Absolute quantification provides the ability to compare two SPECT scans under different conditions (e.g., stress and rest) or at different times (response to therapy) and to quantitatively determine the change in tracer uptake. Unfortunately, achieving absolute quantification is a difficult task because of effects such as photon attenuation, partial-volume errors, and scatter radiation. Nonetheless, the technique we describe appears to overcome these difficulties.

Variations in intensity on the reconstructed template image (Fig. 2C) are caused by resolution effects. Furthermore, the reconstructed image appears to be somewhat distorted because of the interplay between the spatially variant attenuation characteristics and the distance dependence of the collimator resolution. It is clear from these images that a simple three-dimensional blurring of the original template will not reproduce the reconstructed template image. This suggests that these effects cannot be accurately corrected for with a deconvolution technique using the point-spread function measured at the isocenter. However, the template correction technique corrects for the partial-volume effects and the distortions resulting from the imaging process during the course of quantification. For comparison, other attempts were made to compensate for the limited spatial resolution of the SPECT system, including modeling the intrinsic spatial resolution and depth-dependent collimator response in the reconstruction of the radionuclide image (*16,22*). Although this method does improve the quantitative accuracy and image quality, it cannot fully recover the activity concentration because of resolution losses.

Slight distortions occur in the imaging and reconstruction process because of the interplay between the distance-dependent collimator blur and the spatially variant attenuation effects. Because the reconstructed template is also subject to these distortion effects, it may be more appropriate to use a thresholded version of the reconstructed template to define the volume of interest to be quantified as opposed to the original template defined by the CT image. However, quantitatively, the results obtained using the template correction technique were relatively insensitive to which template (i.e., the original CT-defined template or the reconstructed template) was used to define the regions of interest.

Finally, an iterative MLEM reconstruction algorithm was chosen simply so that we could compare the results of including attenuation correction alone directly with the results obtained by including attenuation and partial-volume corrections. Because the template correction technique models the physical effects of the image acquisition process, it is not necessary to use an iterative reconstruction algorithm. In fact, similar quantitative results were obtained using filtered backprojection to reconstruct the radionuclide and template images, which significantly reduced computation time. For this quantification technique, the particular choice of reconstruction algorithm itself is relatively unimportant, provided that the same algorithm is used to reconstruct both the radionuclide and the template images.

A potential limitation of our analysis is that we do not explicitly account for scatter radiation. However, because the calibration factor was determined from a water phantom measurement that contains scatter, some of the effects of scatter radiation are accounted for indirectly. To ensure that we were not overlooking a potential problem, we did acquire some datasets with secondary energy windows and analyzed these datasets with two of the scatter correction techniques described in the literature (*27,28*). The results obtained with these scatter correction methods were quantitatively comparable with the results obtained without an explicit scatter correction. This was not entirely unexpected because simulation studies performed by our group suggest that, for the pig anatomy, large regional variations caused by scatter from hepatic activity are not expected across the myocardium (*29*). Therefore, by including the effects of scatter only indirectly (i.e., by using the water tank calibration factor) we are still able to determine the regional myocardial activity concentration relatively accurately.

A second potential limitation of our analysis is that we do not account for cardiac and respiratory motions. Although gated acquisitions could be used in conjunction with the methodology we present to account for motion, we have tried to assess both cardiac and respiratory motion effects.

To assess cardiac motion effects, we performed one gated SPECT study; unfortunately, we are unable to do gated CT imaging with our system. In the gated SPECT study, the values obtained at diastole were approximately 15% different than those obtained at systole, with the values obtained by including data for the entire cardiac cycle falling midway in-between. Because the CT image is ungated, we do introduce a motion blur into the template process. Comparison of the CT image acquired while the animal is alive with a comparable CT image acquired after the animal has been killed, we see that the myocardial wall, as defined by CT, is generally thicker when the animal is alive because of motion blur. Effectively, the point-spread function of the system is increased because of the motion effects.

To assess respiratory motion (in the absence of cardiac motion) we also performed one imaging study in which the animal was mechanically ventilated after it had been killed. The animal was also imaged without being ventilated, and the values obtained in the two cases varied, on average, by about 10%.

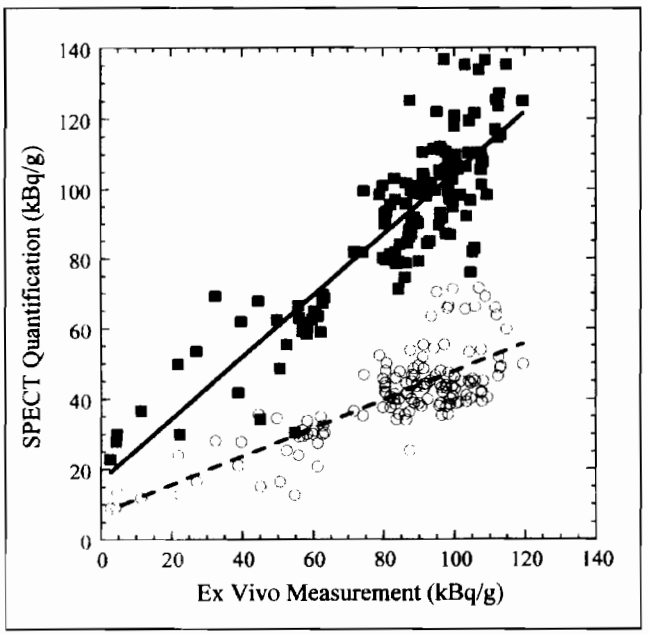

FIGURE 7. SPECT quantification obtained from postmortem images vs. ex vivo activity concentration for eight pigs included in study. ○ = activity concentration measured in every myocardial segment with only attenuation correction applied. Dashed line is least-squares linear fit to data with slope of 0.402 and offset of 7.53 kBq/g (r = 0.776). ■ = activity concentration measured in every myocardial segment with both attenuation and partial-volume corrections applied. Solid line is least-squares linear fit to data with slope of 0.877 and offset of 16.72 kBq/g (r = 0.876).

Both of these studies seem to suggest that cardiac and respiratory motion effects lead to quantitative errors on the order of 10%. Nevertheless, motion effects do not appear to be the dominant source of remaining error. For the animal studies reported here, we also acquired CT and SPECT images after the animal had been killed to allow evaluation of our methods without the added complications of cardiac and respiratory motion. Even in these cases, we obtained results that were quantitatively similar to those obtained with animals that were alive: SPECT quantification of the absolute activity concentration within about 10%–15% of the true values, as shown in Figure 7. This suggests that motion effects may not be the dominant limitation of this methodology.

We have shown that absolute regional quantification is possible in a porcine model of myocardial perfusion; further work will be necessary to indicate the clinical usefulness of such a measurement. One obvious direction is to determine how this information could be used to ascertain coronary artery flow reserve capacity.

CONCLUSION

Absolute rather than relative quantification of myocardial perfusion studies would be a significant advance (*3*). We describe a new technique for quantifying myocardial SPECT images that accounts for attenuation and partial-volume errors using coregistered CT images. The CT image provides both an object-specific attenuation map for SPECT reconstruction and an anatomic template to define regions of interest for quantification of the SPECT image. The effectiveness of this technique has been shown in animal experiments in which we have been able to measure the absolute regional radionuclide content in porcine myocardium in vivo.

ACKNOWLEDGMENTS

The authors acknowledge the expertise in animal care and handling provided by Carol Stillson and the surgical skill provided by Dr. Dong Wei Gao. This work is supported in part by National Institutes of Health grant 2R01-CA50539-09, the American Heart Association, and U.S. Army Breast Cancer Research Program Postdoctoral Fellowship DAMD17-98-1-8192. The authors also acknowledge a significant equipment grant from General Electric Medical Systems.

REFERENCES

1. Garcia EV, Van Train K, Maddahi J, et al. Quantification of rotational thallium-201 myocardial tomography. *J Nucl Med.* 1985;26:17–26.
2. Martin W, Tweddel AC, Hutton I. Balanced triple-vessel disease: enhanced detection by estimated myocardial thallium uptake. *Nucl Med Commun.* 1992; 13:149–153.
3. Watson DD. Quantitative SPECT. *Semin Nucl Med.* 1999;29:192–203.
4. Jaszczak RJ, Coleman RE, Whitehead FR. Physical factors affecting quantitative measurements using camera-based single photon emission computed tomography (SPECT). *IEEE Trans Nucl Sci.* 1981;28:69–80.
5. Tsui BMW, Frey EC, Zhao X, Lalush DS, Johnston RE, McCartney WH. The importance and implementation of accurate three-dimensional compensation methods for quantitative SPECT. *Phys Med Biol.* 1994;39:509–530.
6. Rosenthal MS, Cullom J, Hawkins W, Moore SC, Tsui BMW, Yester M. Quantitative SPECT imaging: a review and recommendations by the focus committee of the Society of Nuclear Medicine Computer and Instrumentation Council. *J Nucl Med.* 1995;36:1489–1513.
7. Blankespoor SC, Wu X, Kalki K, et al. Attenuation correction of SPECT using x-ray CT on an emission-transmission CT system: myocardial perfusion assessment. *IEEE Trans Nucl Sci.* 1996;43:2263–2274.
8. Kalki K, Blankespoor SC, Brown JK, et al. Myocardial perfusion imaging with a combined x-ray CT and SPECT system. *J Nucl Med.* 1997;38:1535–1540.
9. Da Silva AJ, Tang HR, Wu MC, Hasegawa BH. Absolute quantitation of myocardial activity in phantoms. *IEEE Trans Nucl Sci.* 1999;46:659–666.
10. Galt JR, Garcia EV, Robbins WL. Effects of myocardial wall thickness on SPECT quantification. *IEEE Trans Med Imaging.* 1990;9:144–150.
11. Bartlett ML, Bacharach SL, Voipio-Pulkki LM, Dilsizian V. Artifactual inhomogeneities in myocardial PET and SPECT scans in normal subjects. *J Nucl Med.* 1995;36:188–195.
12. Clausen M, Bice AN, Civelek AC, Hutchins GM, Wagner HNJ. Circumferential wall thickness measurements of the human left ventricle: reference data for thallium-201 single-photon emission computed tomography. *Am J Cardiol.* 1986; 58:827–831.
13. Hoffman EJ, Huang SC, Phelps ME. Quantitation in positron emission computed tomography. 1. Effect of object size. *J Comput Assist Tomogr.* 1979;3:299–308.
14. Kessler RM, Ellis JR, Eden M. Analysis of emission tomographic scan data: limitations imposed by resolution and background. *J Comput Assist Tomogr.* 1984;8:514–522.
15. Henze E, Huang SC, Ratib O, Hoffman E, Phelps ME, Schelbert HR. Measurements of regional tissue and blood-pool radiotracer concentrations from serial tomographic images of the heart. *J Nucl Med.* 1983;24:987–996.
16. Tang HR. *A Combined X-Ray CT Scintillation Camera System for Measuring Radionuclide Uptake in Tumors* [dissertation]. San Francisco and Berkeley, CA: Joint Bioengineering Graduate Group, University of California; 1998.
17. Blankespoor SC, Hasegawa BH, Brown JK, Heanue JA, Gould RG, Cann CE. Development of an emission-transmission CT system combining x-ray CT and SPECT. *Conf Rec IEEE Nucl Sci Symp Med Imaging Conf.* 1995;4:1758–1761.

18. Hasegawa BH, Lang TF, Brown JK, et al. Object-specific attenuation correction of SPECT with correlated dual-energy x-ray CT. *IEEE Trans Nucl Sci.* 1993;40: 1242–1252.
19. LaCroix KJ, Tsui BMW, Hasegawa BH, Brown JK. Investigation of the use of x-ray CT images for attenuation in SPECT. *IEEE Trans Nucl Sci.* 1994;41:2793–2799.
20. Tang HR, Brown JK, Da Silva AJ, et al. Implementation of a combined x-ray CT-scintillation camera imaging system for localizing and measuring radionuclide uptake: experiments in phantoms and patients. *IEEE Trans Nucl Sci.* 1999;46:551–557.
21. Shepp LA, Vardi Y. Maximum likelihood reconstruction for emission tomography. *IEEE Trans Med Imaging.* 1982;1:113–122.
22. Zeng GL, Gullberg GT. Frequency domain implementation of the three-dimensional geometric point response correction in SPECT imaging. *IEEE Trans Nucl Sci.* 1992;39:1444–1453.
23. Müller-Gärtner HW, Links JM, Prince JL, et al. Measurement of radiotracer concentration in brain gray matter using positron emission tomography: MRI-based correction for partial volume effects. *J Cereb Blood Flow Metab.* 1992; 12:571–583.
24. Meltzer CC, Zubieta JK, Links JM, Brakeman P, Stumpf MJ, Frost JJ. MR-based correction of brain PET measurements for heterogeneous gray matter radioactivity distribution. *J Cereb Blood Flow Metab.* 1996;16:650–658.
25. Rousset OG, Ma Y, Evans AC. Correction for partial volume effects in PET: principle and validation. *J Nucl Med.* 1998;39:904–911.
26. Munch G, Neverve J, Matsunari I, Schroter G, Schwaiger M. Myocardial technetium-99m-tetrofosmin and technetium-99m-sestamibi kinetics in normal subjects and patients with coronary artery disease. *J Nucl Med.* 1997;38: 428–432.
27. Jaszczak RJ, Greer KL, Floyd CE, Harris CC, Coleman RE. Improved SPECT quantification using compensation for scattered photons. *J Nucl Med.* 1984;25: 893–900.
28. Ogawa K, Chugo A, Ichihara T, Kubo A, Hashimoto S. Quantitative image reconstruction using position-dependent scatter correction in single photon emission CT. *Conf Rec IEEE Nucl Sci Symp Med Imaging Conf.* 1992;2: 1011–1013.
29. Tang HR, Da Silva AJ, Hasegawa BH. The relative impact of scatter on absolute myocardial perfusion quantitation: an EGS4 Monte Carlo study. *Conf Rec IEEE Nucl Sci Symp Med Imaging Conf.* 1999;3:1224–1228.

Myocardial Viability Index in Chronic Coronary Artery Disease: Technetium-99m-Methoxy Isobutyl Isonitrile Redistribution

Simone Maurea, Alberto Cuocolo, Andrea Soricelli, Luisa Castelli, Fiorenzo Squame, Massimo Imbriaco, Nicola De Luca, Bruno Trimarco and Marco Salvatore

Nuclear Medicine Department, CNR Nuclear Medicine Center and Medical Clinic, University Federico II; and National Cancer Institute, Naples, Italy

The purpose of this study was to evaluate whether an additional redistribution image after a rest ^{99m}Tc-MIBI injection enhances detection of viable myocardium and predicts functional recovery after coronary revascularization in patients with chronic coronary artery disease (CAD). **Methods:** Thirty-one patients (29 men, mean age 55 ± 10 yr) with proven CAD and left ventricular (LV) dysfunction (ejection fraction 39% ± 9%) underwent resting ^{99m}Tc-MIBI tomography with initial (1 hr) and delayed (5 hr) images. Within 1 wk of MIBI imaging, all patients underwent rest-redistribution ^{201}Tl imaging. Eight patients also underwent two-dimensional echocardiography before and 5 ± 3 mo after coronary revascularization. **Results:** On the initial ^{99m}Tc-MIBI images, 302 myocardial segments were normal, 183 showed moderate and 197 severe reduction of tracer uptake. Of these 197 segments, 47 (24%) demonstrated increased tracer uptake (≥10% versus initial) on delayed images (from 43% ± 8% to 60% ± 8%, $p<0.001$) and were considered as showing ^{99m}Tc-MIBI redistribution. These 47 segments were observed in 20 (65%) patients in whom ^{201}Tl images detected viable myocardium in the same segments. In the eight patients studied before and after revascularization, 83% of segments with ^{99m}Tc-MIBI redistribution and abnormal LV function showed functional recovery after revascularization, while 96% of segments without ^{99m}Tc-MIBI redistribution did not show functional recovery. **Conclusion:** Resting ^{99m}Tc-MIBI redistribution frequently occurs in patients with chronic CAD. Acquisition of ^{99m}Tc-MIBI redistribution images enhances detection of viable myocardium and predicts functional recovery after revascularization.

Key Words: technetium-99m-sestamibi; left ventricular dysfunction; functional recovery; thallium-201

J Nucl Med 1995; 36:1953–1960

Technetium-99m-methoxy isobutyl isonitrile (MIBI) is a cardiac perfusion agent that initially distributes in the myocardium proportional to coronary blood flow, similar to ^{201}Tl (*1,2*). It has been suggested that ^{99m}Tc-MIBI does not show significant redistribution (*1*). Recent studies, however, demonstrated that delayed ^{99m}Tc-MIBI redistribution may be observed in a model of transient myocardial ischemia (*3*) or under conditions of sustained low coronary flow (*4*). Furthermore, it has also been reported that myocardial uptake and retention of ^{99m}Tc-MIBI are dependent on both cell viability and regional blood flow and that tissue viability is required for ^{99m}Tc-MIBI redistribution (*5–9*).

Clinical studies evaluated the phenomenon of ^{99m}Tc-MIBI redistribution after stress injection in patients with CAD (*10,11*). The occurrence of ^{99m}Tc-MIBI redistribution after rest injection and its clinical implications have not yet been widely evaluated. Preliminary results reported by Dilsizian et al. recently suggested that ^{99m}Tc-MIBI redistribution imaging following tracer injection at rest can detect viable myocardium using standard imaging protocols (*12*). Furthermore, these authors suggest that detection of viable myocardium may be enhanced with ^{99m}Tc-MIBI cardiac imaging if an additional redistribution image is acquired after tracer injection at rest (*12*). It is still uncertain, however, whether ^{99m}Tc-MIBI redistribution after rest injection is predictive of improved ventricular function after coronary revascularization.

The purpose of this study was to evaluate whether an additional redistribution image after rest ^{99m}Tc-MIBI injection enhances detection of viable myocardium and predicts functional recovery after coronary revascularization in patients with chronic coronary artery disease (CAD).

MATERIALS AND METHODS

Patients

We prospectively studied 31 patients (29 men, 2 women; mean age 55 ± 10 yr) with angiographically documented CAD and with left ventricular dysfunction (Tables 1 and 2). Seven patients had significant stenosis of all three major coronary vessels, 11 had significant stenosis of two major coronary vessels and 13 had significant stenosis of only one major coronary vessel. The mean left ventricular ejection fraction (LVEF) by resting equilibrium radionuclide angiography was 39% ± 9%. All patients had a previous myocardial infarction that was documented clinically and by electrocardiography. No patient, however, had an acute myocardial infarction within 6 mo of the study. The majority of patients

Received Jan. 1, 1995; revision accepted Jul. 14, 1995
For correspondence or reprints contact: Simone Maurea, MD, via Raffaele De Cesare 7, 80132 Napoli, Italy.

TABLE 1
Patient Characteristics

Patient no.	Sex	Age (yr)	LVEF (%)	Site of myocardial infarction	Stable angina
1	M	62	42	Posterolateral	Yes
2	M	62	24	Inferior, anterior	Yes
3	M	44	49	Anteroseptal	Yes
4	M	63	38	Anterior	Yes
5	M	57	44	Inferior	Yes
6	M	67	42	Inferior	Yes
7	M	60	39	Inferolateral	Yes
8	M	49	35	Anteroseptal, inferoapical	No
9	M	69	39	Inferolateral	Yes
10	M	46	34	Anterior	Yes
11	M	63	48	Inferolateral	Yes
12	M	48	28	Anterior	Yes
13	M	43	41	Anteroseptal	Yes
14	M	61	42	Inferior, anterior	Yes
15	M	40	48	Anteroseptal	Yes
16	M	63	31	Anteroseptal, inferior	Yes
17	M	54	30	Inferolateral	Yes
18	M	66	47	Anteroapical	Yes
19	M	58	49	Inferior	Yes
20	M	65	48	Anterior	Yes
21	M	61	30	Anterior	Yes
22	M	68	49	Anterior	Yes
23	M	50	36	Anteroseptal	Yes
24	M	57	48	Anteroseptal, apical	Yes
25	M	38	23	Anterior	No
26	M	32	26	Anterior, inferior	No
27	M	42	20	Anterior	Yes
28	M	53	49	Anterior	Yes
29	M	47	44	Anterolateral	Yes
30	F	57	46	Inferior	Yes
31	F	65	44	Anterior	Yes

LVEF = left ventricular ejection fraction.

(n = 28) were symptomatic with episodes of stable angina requiring antianginal treatment, while three patients were asymptomatic. All patients, however, underwent radionuclide studies after withdrawal of all medications. Eight of the 31 patients were also studied after coronary revascularization, coronary artery bypass graft in six and percutaneous transluminal coronary angioplasty in two. In these patients, none had clinical evidence of perioperative or postangioplasty myocardial infarction or restenosis. Informed consent, as part of the protocol approved by the Institutional Clinical Research Subpanel on Human Studies at our University, was obtained from all patients.

Technetium-99m-MIBI Imaging

After an overnight fast, all patients underwent rest-redistribution ^{99m}Tc-MIBI myocardial tomography. Patients were ambulatory and remained in the resting condition for 30 min before intravenous injection of ^{99m}Tc-MIBI (740 MBq). Initial images were acquired 1 hr after tracer administration. Delayed images were then taken 5 hr later.

SPECT was performed as previously described (*13*) using a rotating large field of view gamma camera equipped with a low-energy, all-purpose, parallel-hole collimator and connected with a dedicated computer system. Briefly, 32 projections (40 sec/projection) were obtained over a semicircular 180° arch, which extended from the 30° right anterior oblique to the left posterior oblique position. A 20% symmetric energy window centered on the 140-keV peak was used. All projection images were stored on magnetic disk in a 64 × 64 word matrix. Each projection image was corrected for nonuniformity, with a 120-million count image obtained weekly from a uniform ^{57}C flood source. The mechanical center of rotation was determined from the projection data to align the detector data with respect to the reconstruction matrix (*14*). The raw data were initially smoothed with a nine-point weighted average algorithm. Filtered backprojection was then performed with a low-resolution Butterworth filter with a cutoff frequency of 0.5 cycles/pixel, order 5.0, to reconstruct transverse axial tomograms of 6.2-mm thickness per slice, which encompassed the entire heart. Sagittal and oblique tomograms parallel to the long-axis and short-axis of the left ventricle were then extracted from the filtered transaxial tomograms by performing coordinate transformation with the appropriate interpolation (*14*). No attenuation or scatter correction was applied.

Thallium-201 Imaging

All patients underwent rest-redistribution ^{201}Tl myocardial tomography. Patients were ambulatory and remained in the resting condition for 30 min before thallium administration. After an overnight fast, ^{201}Tl (111 MBq) was intravenously injected at rest. Initial and delayed images were acquired 15 min and 4 hr after injection. During the time between the initial and delayed images, all patients were ambulatory and remained in the fasting state. A 3-day interval separated the thallium from ^{99m}Tc-MIBI study. SPECT acquisition was performed with the same gamma camera, matrix and computer system used for the ^{99m}Tc-MIBI studies. The photopeak was centered on the 68-keV with a 20% window.

Echocardiography

During the same week of ^{99m}Tc-MIBI and ^{201}Tl imaging, all patients underwent echocardiographic studies. A phased-array sector scanner with a 2.5 MHz transducer was used. Two-dimensional images of the left ventricle were obtained at rest with the patient lying in the left lateral decubitus position using multiple imaging sections, including the parasternal long- and short-axes and apical two- and four-chamber views. Images were recorded on videotape for analysis. In the eight patients studied before and after coronary revascularization, two sequential echocardiographic studies were performed. The first evaluation (baseline) was performed during the same week of ^{99m}Tc-MIBI and ^{201}Tl studies. The second evaluation (follow-up) was performed an average of 5 ± 3 mo after coronary revascularization. No patient received beta-blockers or inotropic drugs during the follow-up evaluation.

Data Analysis

In each patient, corresponding initial and delayed ^{99m}Tc-MIBI and rest-redistribution ^{201}Tl tomographic images were evaluated for direct comparison, as previously described (*13*). For each study, tomograms were divided into 22 myocardial segments (Fig. 1). Regional ^{99m}Tc-MIBI and ^{201}Tl uptake were quantitatively analyzed. In each tomogram, the myocardial region with the maximum counts was considered as the normal reference region. Technetium-99m-MIBI and ^{201}Tl uptake in all other segments were then expressed as the percentage of the activity measured in the reference region.

To assess the normal range for quantitative data analysis, a group of 14 age-matched normal volunteers (13 men, 1 woman) with no evidence of cardiovascular or pulmonary disease was also studied. In these subjects, clinical examination, echocardiograms and stress electrocardiograms were normal. A myocardial segment

TABLE 2
Angiographic Data, Site of Left Ventricular Dysfunction and Technetium-99m-MIBI Redistribution on Delayed Imaging

Patient no.	Coronary artery stenosis (≥50%)	Site of wall motion abnormalities	Site of Segments with ^{99m}Tc-MIBI redistribution
1	LAD, LCx, PDA	Lateral	Lateral, inferoseptal, apical (n = 4)
2	LAD, PDA	Inferior, apical	Inferoseptal, anteroseptal (n = 2)
3	LAD, LCx	Septal, apical	Anteroseptal, apical, inferior (n = 8)
4	LAD, LCx, PDA	Septal, lateral, apical	Inferoseptal, inferolateral, apical (n = 3)
5	PDA	Inferolateral	Inferolateral, septal (n = 5)
6	LAD, PDA	Inferior	None
7	LAD, LCx	Septal, inferoapical, lateral	Apical (n = 1)
8	LAD	Inferoapical	Apical (n = 1)
9	LAD, LCx, PDA	Septal, posterolateral	Inferoseptal (n = 1)
10	LAD, PDA	Anteroapical	Inferolateral, anterior (n = 2)
11	LAD, PDA	Septal, inferolateral	Lateral (n = 1)
12	LCx	Anteroseptal, apical	Anteroseptal, inferolateral (n = 5)
13	LAD, LCx	Septal	None
14	LAD, LCx, PDA	Inferoapical	Inferolateral (n = 1)
15	LAD	Septal	None
16	LAD, LCx, PDA	Anteroseptal, apical	Apical (n = 1)
17	LAD, PDA	Inferoapical	None
18	LAD	Anterior, apical	None
19	PDA	Inferoapical	None
20	LAD, LCx	Anteroseptal	None
21	LAD	Anteroapical, inferior	Anteroseptal, apical (n = 4)
22	LAD, LCx, PDA	Septal	None
23	LAD	Septal	None
24	LAD	Apical	None
25	LAD	Anterior, inferoapical	Inferoseptal (n = 1)
26	LAD, LCx	Anterior, inferior, apical	None
27	LAD	Anterior, apical	Septal (n = 1)
28	LCx, PDA	Septal	Inferoseptal (n = 1)
29	LAD	Anteroseptal	Inferoseptal, inferolateral (n = 3)
30	LAD, LCx, PDA	Inferoapical, septal	Inferolateral (n = 1)
31	LAD	Anteroseptal, apical	Apical (n = 1)

LAD = left anterior descending artery; LCx = left circumflex artery; PDA = posterior descending artery.

was considered abnormal if initial ^{99m}Tc-MIBI or ^{201}Tl uptake was >2 s.d. below the mean observed in the same region for age- and sex-matched normal volunteers. On initial ^{99m}Tc-MIBI images, segments with abnormal uptake were subgrouped on the basis of severity of reduction in tracer activity: moderate (≥50% of peak activity) and severe (<50% of peak) defects, as previously reported (*12,15,16*). On the basis of previous reproducibility measurements performed by other authors and in our laboratory (*12,17*), a segment with reduced activity on initial ^{99m}Tc-MIBI or ^{201}Tl images was considered reversible if the activity increased ≥10% on delayed ^{99m}Tc-MIBI or ^{201}Tl images, respectively. Alternatively, a segment with reduced activity on initial ^{99m}Tc-MIBI or ^{201}Tl images was considered irreversible if the activity did not increase ≥10% or increased ≥10% but remained <50% on delayed ^{99m}Tc-MIBI or ^{201}Tl images, respectively. Thallium-201 irreversible defects were divided on the basis of severity of reduction in tracer activity: moderate (≥50% of peak activity) and severe (<50% of peak) defects, as previously reported (*12,17*).

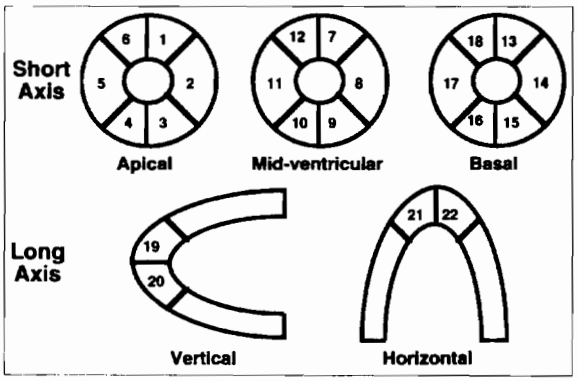

FIGURE 1. Diagram of standard segmentation scheme used for regional quantitative analysis of ^{99m}Tc-MIBI and ^{201}Tl uptake.

Echocardiographic images were interpreted by two experienced observers who were unaware of clinical, radionuclide and angiographic findings. A third investigator blindly reviewed the echocardiograms when the first two observers did not agree. Regional left ventricular function was assessed according to the recommendations of the American Society of Echocardiography (*18,19*). Segmental left ventricular wall motion was graded as: 1, normal; 2, hypokinetic; 3, akinetic; and 4, dyskinetic. The echocardiographic

results were directly compared with those of ^{99m}Tc-MIBI and ^{201}Tl, as previously described (*20*). In the eight patients studied before and after coronary revascularization, a myocardial segment was considered as showing functional recovery when the regional wall motion score was abnormal at baseline and improved at least one echocardiographic grade during the follow-up study, as previously reported (*21*). Conversely, a myocardial segment was considered as showing no functional recovery when regional wall motion score was severely impaired at baseline (grade 3 or 4) and did not change during follow-up (*21*).

Statistical Analysis

Data are expressed as mean ± 1 s.d. Differences in the mean values were assessed by Student's t-test for unpaired data with Bonferroni correction for multiple groups comparison, or Student's t test for paired data, as appropriate. Bonferroni correction establishes that the p value for each comparison should be multiplied by the total number of comparisons undertaken (*22*). The Spearman correlation coefficient (ρ) was used to assess the relationships between wall motion score and tracer uptake. Linear regression was used to evaluate the relationship between LVEF and the number of myocardial segments showing reversible ^{99m}Tc-MIBI defects. Chi square analysis was used to assess differences between proportions. Probability values <0.05 were considered significant.

RESULTS

Technetium-99m-MIBI

A total of 682 myocardial segments were analyzed. On initial ^{99m}Tc-MIBI images, 302 (44%) segments had normal tracer uptake, 183 (27%) showed moderate and 197 (29%) severe reduction of tracer uptake.

Myocardial segments with moderate reduction of ^{99m}Tc-MIBI uptake on the initial images were observed in all 31 patients (range 3–10 segments/patient, mean 5.9 ± 1.9). Of the 183 segments with moderate reduction of ^{99m}Tc-MIBI uptake on initial images, 51 (28%) were reversible on delayed images, showing significant increased tracer uptake (from 61% ± 7% to 78% ± 10% of peak activity, $p<0.001$). Moderate reversible ^{99m}Tc-MIBI defects on delayed images were observed in 23 (74%) patients (range 1–5 segments/patient, mean 2.2 ± 1.2). The remaining 132 (72%) segments with moderate reduction of ^{99m}Tc-MIBI uptake on initial images were irreversible on delayed images, showing no significant change in tracer uptake (from 63% ± 6% to 58% ± 9% of peak activity).

Myocardial segments with severe reduction of ^{99m}Tc-MIBI uptake on initial images were observed in all 31 patients (range 1–14 segments/patient, mean 6.4 ± 3.6). Of the 197 segments with severe reduction of ^{99m}Tc-MIBI uptake on initial images, 47 (24%) were reversible on delayed images, showing significant increased tracer uptake (from 43% ± 8% to 60% ± 8% of peak activity, $p<0.001$) (Fig. 2). Severe reversible ^{99m}Tc-MIBI defects on delayed images were observed in 20 (65%) patients (range 1–8 segments/patient, mean 2.3 ± 1.9) (Table 2). The remaining 150 (76%) segments with severe reduction of ^{99m}Tc-MIBI uptake on the initial images were irreversible on delayed images, showing no significant change in tracer uptake (from 33% ± 12% to 32% ± 12% of peak activity) (Fig. 3). In particular, reversible severe ^{99m}Tc-MIBI defects showed significantly higher tracer uptake on initial images compared to irreversible ^{99m}Tc-MIBI defects (43% ± 8% versus 33% ± 12%, $p<0.001$).

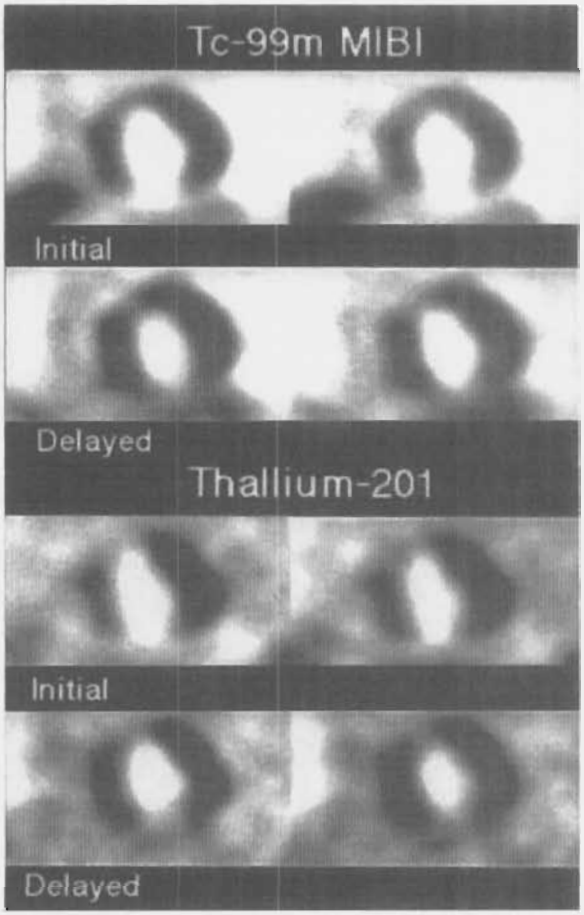

FIGURE 2. Technetium-99m-MIBI cardiac imaging under resting conditions: short-axis slices show a reversible defect involving the septal region (top). Corresponding rest-redistribution ^{201}Tl cardiac tomography: short-axis slices show a reversible defect involving the septal region (bottom).

Thallium-201

Of the 51 myocardial segments with moderate reversible ^{99m}Tc-MIBI defects, 17 had normal thallium uptake, 19 showed reversible and 15 moderate irreversible thallium defects. None of the 132 segments with moderate irreversible ^{99m}Tc-MIBI defects showed severe irreversible thallium defects. In particular, 28 had normal thallium uptake, 31 showed reversible and 73 moderate irreversible thallium defects.

None of the 47 myocardial segments with severe reversible ^{99m}Tc-MIBI defects showed severe irreversible ^{201}Tl defects. In particular, 3 of these segments had normal thallium uptake, 22 showed reversible and 22 moderate

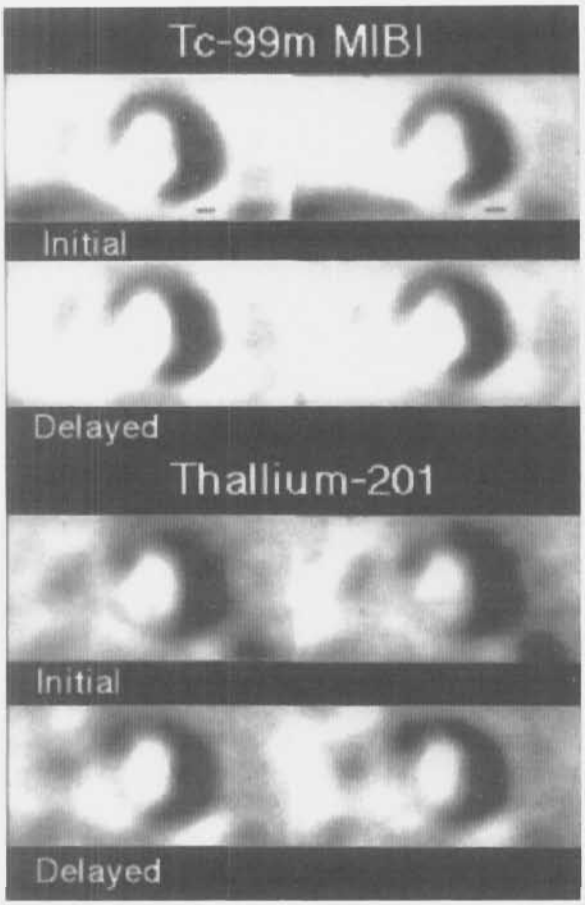

FIGURE 3. Technetium-99m-MIBI cardiac tomography under resting conditions: short-axis slices show a large irreversible defect involving the septal and inferior regions (top). Corresponding rest-redistribution ^{201}Tl cardiac tomography: short-axis slices show a large irreversible defect involving the septal and inferior regions (bottom).

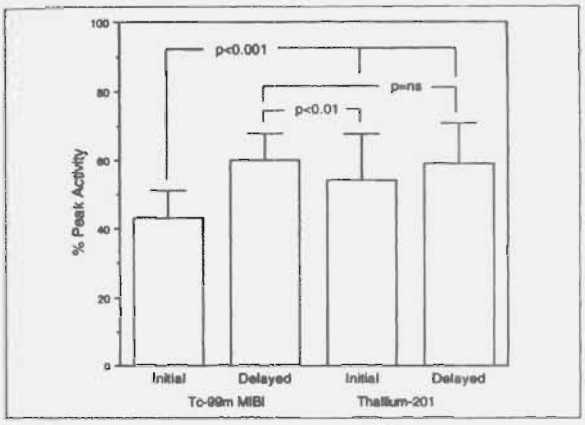

FIGURE 4. Technetium-99m-MIBI and ^{201}Tl uptake (expressed as percentage of peak activity) in myocardial segments with severe reduction of initial ^{99m}Tc-MIBI uptake and increased tracer uptake on delayed images. ns = nonsignificant.

irreversible thallium defects (Fig. 2). On the other hand, the majority (80%) of myocardial segments with severe irreversible ^{99m}Tc-MIBI defects showed severe irreversible ^{201}Tl defects (Fig. 3).

In the 47 myocardial segments with severe reversible ^{99m}Tc-MIBI defects, initial ^{99m}Tc-MIBI uptake was significantly lower ($p<0.001$) compared to both initial and delayed thallium uptake (Fig. 4). On the other hand, in these segments delayed ^{99m}Tc-MIBI uptake was significantly higher ($p<0.01$) compared to initial thallium uptake, but not different from delayed thallium uptake (Fig. 4).

Relation with Left Ventricular Function

Of the total 682 myocardial segments, 332 (49%) showed normal wall motion (Group 1) on echocardiographic images, 160 (23%) were hypokinetic (Group 2) and 190 (28%) were akinetic or dyskinetic (Group 3). Initial and delayed thallium uptake were significantly higher ($p<0.001$) for Group 1 in segments compared with those of Groups 2 and 3 and in Group 2 segments compared to those of Group 3 (Table 3). Similarly, initial and delayed ^{99m}Tc-MIBI uptake were significantly higher ($p<0.001$) in Group 1 segments compared with those of Groups 2 and 3 and in Group 2 segments compared to those of Group 3 (Table 3). A significant relationship ($p<0.001$) between wall motion score and initial ($\rho = -0.45$) and delayed ($\rho = -0.41$) thallium uptake was observed. Similarly, a significant relationship ($p<0.001$) between wall motion score and initial ($\rho = -0.50$) and delayed ($\rho = -0.47$) ^{99m}Tc-MIBI uptake was found. No significant relationship was observed between LVEF and the number of myocardial segments showing moderate and/or severe reversible ^{99m}Tc-MIBI defects.

Follow-up after Coronary Revascularization

In the eight patients studied before and after coronary revascularization, 33 (19%) myocardial segments with wall motion abnormalities showed moderate reduction of ^{99m}Tc-MIBI uptake on initial images. Of these 33 segments, 13 were reversible and 20 did not change on delayed ^{99m}Tc-MIBI images. Moderate reversible ^{99m}Tc-MIBI defects on

TABLE 3.
Initial and Delayed Technetium-99m-MIBI and Thallium-201 Uptake in Myocardial Segments*

	Group 1	Group 2	Group 3
Myocardial segments (no.)	332	160	190
Initial ^{99m}Tc-MIBI uptake (%)	89 ± 13	60 ± 11†	38 ± 16‡
Delayed ^{99m}Tc-MIBI uptake (%)	87 ± 14	62 ± 14†	39 ± 18‡
Initial ^{201}Tl uptake (%)	88 ± 14	65 ± 14†	42 ± 20‡
Delayed ^{201}Tl uptake (%)	87 ± 15	67 ± 14†	45 ± 21‡

*Group 1 = normal wall motion; Group 2 = hypokinetic segments; Group 3 = segments with akinesia or dyskinesia.
†$p < 0.001$ versus Group 1; ‡$p < 0.001$ versus Groups 1 and 2.

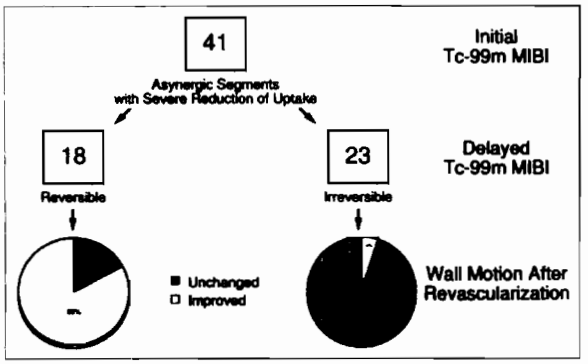

FIGURE 5. Flow diagram shows wall motion after coronary revascularization in asynergic segments with severe reduction of ^{99m}Tc-MIBI uptake on initial images and reversible or irreversible defects on delayed images.

delayed images were observed in seven of these patients (range 0–4 segments/patient, mean 2.1 ± 1.4). The majority of segments with moderate reversible ^{99m}Tc-MIBI defects (85%) showed functional recovery after revascularization. Furthermore, 41 (23%) segments with wall motion abnormalities showed severe reduction of ^{99m}Tc-MIBI uptake on initial images. Of these 41 segments, 18 were reversible and 23 did not change on delayed ^{99m}Tc-MIBI images. Severe reversible ^{99m}Tc-MIBI defects on delayed images were observed in all these patients (range 1–8 segments/patient, mean 3.1 ± 2.6). The majority (83%) of segments with severe reversible ^{99m}Tc-MIBI defects showed functional recovery after revascularization (Fig. 5). Conversely, the majority (96%) of segments with severe irreversible ^{99m}Tc-MIBI defects did not show improved wall motion after revascularization ($p<0.001$ versus severe reversible defects) (Fig. 5). In these patients, LVEF significantly ($p<0.01$) improved after revascularization (from 42% ± 7% at baseline to 47% ± 7% after revascularization).

DISCUSSION

Our results agree with those of Dilsizian et al. (*12*) and demonstrate that in patients with chronic CAD and left ventricular dysfunction ^{99m}Tc-MIBI redistribution on delayed images occurs in 24% to 38% of myocardial segments with severe reduction of tracer uptake at rest. Delayed ^{99m}Tc-MIBI imaging improves the differentiation between ischemic but still viable myocardium from fibrotic tissue in regions with severe reduction of resting ^{99m}Tc-MIBI uptake. Furthermore, ^{99m}Tc-MIBI redistribution is predictive of functional recovery following coronary revascularization.

Technetium-99m-MIBI Identification of Myocardial Viability

Previous clinical studies demonstrated that severe reduction of ^{99m}Tc-MIBI uptake underestimates the presence of viable myocardium in patients with chronic CAD and left ventricular dysfunction (*12,15,16,23–31*). In particular, comparative studies between ^{99m}Tc-MIBI scintigraphy and metabolic imaging with [^{18}F] fluorodeoxyglucose showed that ^{99m}Tc-MIBI myocardial uptake on conventional 1-hr imaging is mainly related to regional coronary blood flow rather than tissue viability (*15,31*). Experimental studies, however, have shown that myocardial retention of ^{99m}Tc-MIBI depends not only on coronary blood flow but also on cellular viability (*5,6*). Furthermore, recent clinical reports suggest that quantitative analysis of resting ^{99m}Tc-MIBI may enhance differentiation between viable myocardium from necrotic tissue in patients with chronic ischemic left ventricular dysfunction (*12,32*).

Technetium-99m-MIBI Redistribution

The occurrence of ^{99m}Tc-MIBI redistribution has been previously demonstrated in a model of transient ischemia or under conditions of sustained reduced coronary blood flow (*3,4*). In particular, Li et al. showed that normalization of ^{99m}Tc-MIBI defects in ischemic regions is progressive over time and that such redistribution is detectable on tomographic images and also confirmed by serial myocardial biopsies (*3*). Sinusas et al. recently demonstrated that ^{99m}Tc-MIBI redistributes in the presence of severe coronary artery stenosis, as documented by gamma well counting techniques and by high-resolution postmortem gamma camera imaging of myocardial slices (*4*). In clinical studies, there are conflicting data on ^{99m}Tc-MIBI redistribution after stress imaging. Taillefer et al. (*10*) described a decrease in ^{99m}Tc-MIBI defect size after exercise with serial planar imaging between 1 hr and 3 hr following stress injection. On the other hand, Villanueva-Meyer et al. (*11*) recently reported no change in defect size between 1 and 4 hr after stress ^{99m}Tc-MIBI injection using quantitative tomographic imaging. Dilsizian et al. recently described redistribution of ^{99m}Tc-MIBI after rest injection in a small number of patients with chronic CAD and severe left ventricular dysfunction (*12*). Its clinical utility, however, has not yet gained wide application.

The results of the present study show the occurrence of ^{99m}Tc-MIBI redistribution after rest injection in patients with chronic ischemic left ventricular dysfunction, suggesting that acquisition of delayed images after resting ^{99m}Tc-MIBI injection may enhance the detection of severely hypoperfused but still viable myocardium. We focused our analysis on the clinical significance of ^{99m}Tc-MIBI redistribution in myocardial segments with severe reduction of tracer uptake on initial images, in whom the presence of viable tissue is in question. In particular, 24% of segments with severe reduction of ^{99m}Tc-MIBI uptake on initial images showed a significant increase in tracer uptake on delayed images. Our results with earlier data of Dilsizian et al. in a group of patients with chronic CAD (*12*). These authors described ^{99m}Tc-MIBI redistribution in 38% of myocardial segments with irreversible defects on stress-rest ^{99m}Tc-MIBI imaging (*12*). Furthermore, our results confirm the experimental evidence of resting ^{99m}Tc-MIBI redistribution in a model of sustained coronary low flow (*4*).

In our study, the occurrence of ^{99m}Tc-MIBI redistribution on delayed images in myocardial segments with severe reduction of ^{99m}Tc-MIBI uptake on initial images was observed in 65% of the patients. This finding may be clinically relevant since it demonstrates that ^{99m}Tc-MIBI redistribution may occur in a substantial number of patients with chronic ischemic left ventricular dysfunction.

Comparison with Thallium-201 Imaging

The results of rest-redistribution ^{201}Tl cardiac imaging in myocardial segments with ^{99m}Tc-MIBI redistribution support the hypothesis that these regions may contain hypoperfused but viable myocardium. In particular, each segment showed evidence of myocardial viability according to thallium imaging criteria. In myocardial segments with severe reversible ^{99m}Tc-MIBI defects, initial ^{99m}Tc-MIBI uptake was significantly lower compared to both initial and delayed thallium uptake. A possible explanation for this finding could be that only segments with severe reduction of initial ^{99m}Tc-MIBI uptake and increased tracer activity on delayed images were included in the analysis. Moreover, none of these segments showed severe irreversible thallium defects. On the other hand, delayed ^{99m}Tc-MIBI uptake was significantly higher compared to initial thallium uptake but not different compared to delayed thallium uptake. These data correlate with previous comparative studies between ^{201}Tl and ^{99m}Tc-MIBI cardiac imaging (*26–29*). Furthermore, Dilsizian et al. recently reported concordant results between resting ^{99m}Tc-MIBI redistribution and ^{201}Tl reinjection imaging studies (*12*). These findings suggest that resting ^{99m}Tc-MIBI redistribution imaging identifies the presence of hypoperfused but viable myocardium in patients with chronic ischemic left ventricular dysfunction. Thus, it may have important clinical implications.

Follow-up after Coronary Revascularization

Although thallium uptake is usually considered an accurate marker of myocardial viability in patients with chronic CAD (*33–40*), the definite gold standard for the presence of viable tissue in such patients is functional recovery after coronary revascularization (*41*). In the present study, we evaluated whether resting ^{99m}Tc-MIBI redistribution is predictive of improved left ventricular function after coronary revascularization and, thus, of myocardial viability. Our results obtained after revascularization support the hypothesis that ^{99m}Tc-MIBI redistribution reflects the presence of viable myocardium. In fact, the majority of segments with severely impaired ventricular function and increased ^{99m}Tc-MIBI uptake on delayed images showed improved wall motion after revascularization. Conversely, the majority of akinetic segments with no change on delayed ^{99m}Tc-MIBI images did not show functional recovery after coronary revascularization. Furthermore, a significant improvement of global LVEF was observed after coronary revascularization. Therefore, these findings demonstrate that delayed redistribution cardiac imaging after resting ^{99m}Tc-MIBI injection can detect severely hypoperfused but still viable myocardium as well as predict reversibility of severe regional wall motion abnormalities after coronary revascularization in patients with chronic ischemic left ventricular dysfunction.

Study Limitations

Two potential limitations of this study deserve comment. First, follow-up evaluation after coronary revascularization was obtained in a limited number of the patients in whom resting ^{99m}Tc-MIBI redistribution was observed. Although our data need confirmation in larger series of patients, the follow-up results of the present study confirm and may be considered representative of the enhanced detection of viable myocardium by resting ^{99m}Tc-MIBI cardiac imaging using delayed acquisition. Second, since there are no established criteria in the literature to assess the severity of ^{99m}Tc-MIBI defects, the selection of the threshold value for severely reduced ^{99m}Tc-MIBI uptake was chosen arbitrarily. The same threshold, however, has been used in previous studies (*12,15,16*).

CONCLUSION

Resting ^{99m}Tc-MIBI redistribution frequently occurs in patients with chronic CAD and left ventricular dysfunction. Acquisition of delayed ^{99m}Tc-MIBI images enhances the differentiation between severely hypoperfused, but still viable myocardium from fibrotic tissue in such patients. The presence of ^{99m}Tc-MIBI redistribution may be predictive of functional recovery after coronary revascularization. Therefore, our results suggest that resting ^{99m}Tc-MIBI cardiac imaging should be delayed when assessing myocardial viability in patients with chronic CAD.

REFERENCES

1. Okada RD, Glover D, Gaffney T, Williams S. Myocardial kinetics of technetium-99m-hexakis-2-methoxy-2-methylpropyl-isonitrile. *Circulation* 1988; 77:491–498.
2. Canby RC, Silber S, Pohost GM. Relations of the myocardial imaging agents Tc-99m MIBI and Tl-201 to myocardial blood flow in a canine model of myocardial ischemic insult. *Circulation* 1990;81:289–296.
3. Li QS, Solot A, Frank TL, Wagner HN, Becker LC. Myocardial redistribution of technetium-99m methoxy isobutyl isonitrile (sestamibi). *J Nucl Med* 1990;31:1069–1076.
4. Sinusas AJ, Bergin JD, Edwards NC, et al. Redistribution of Tc-99m sestamibi and Tl-201 in the presence of a severe coronary artery stenosis. *Circulation* 1994;89:2332–2341.
5. Beanlands RSB, Dawood F, Wen WH, et al. Are the kinetics of technetium-99m-methoxyisobutyl isonitrile affected by cell metabolism and viability? *Circulation* 1990;82:1802–1814.
6. Freeman I, Grunwald AM, Hoory S, Bodenheimer MM. Effect of coronary occlusion and myocardial viability on myocardial activity of technetium-99m-sestamibi. *J Nucl Med* 1991;32:292–299.
7. Glover DK, Okada RD. Myocardial technetium-99m sestamibi kinetics after reperfusion in a canine model. *Am Heart J* 1993;125:657–666.
8. Beller GA, Glover DK, Edwards NC, Ruiz M, Simanis JP, Watson DD. Technetium-99m-sestamibi uptake and retention during myocardial ischemia and reperfusion. *Circulation* 1993;87:2033–2042.
9. Merhi J, Arsenault A, Latour JG. Time course of technetium-99m-sestamibi myocardial distribution in dogs with a permanent or transient coronary occlusion. *Eur J Nucl Med* 1994;21:481–487.
10. Taillefer R, Primeau M, Costi P, Lambert R, Leveille J, Latour Y. Technetium-99m-sestamibi myocardial perfusion imaging in detection of coronary artery disease: comparison between initial (1-hour) and delayed (3-hour) postexercise. *J Nucl Med* 1991;32:1961–1965.
11. Villanueva-Meyer J, Mena I, Diggles L, Narahara KA. Assessment of myocardial perfusion defect size after early and delayed SPECT imaging with

technetium-99m-hexakis 2-methoxyisobutyl isonitrile after stress. *J Nucl Med* 1993;34:187–192.
12. Dilsizian V, Arrighi JA, Diodati JG, et al. Myocardial viability in patients with chronic coronary artery disease. Comparison of ^{99m}Tc-sestamibi with thallium reinjection and [^{18}F]fluorodeoxyglucose. *Circulation* 1994;89:578–587.
13. Cuocolo A, Soricelli A, Pace L, et al. Adenosine technetium-99m methoxy isobutyl isonitrile myocardial tomography in patients with coronary artery disease: comparison with exercise. *J Nucl Med* 1994;35:1110–1115.
14. Borrello JA, Clinthorne NH, Rogers WL, Thrall JH, Keyes JW. Oblique-angle tomography: a reconstructing algorithm for transaxial tomographic data. *J Nucl Med* 1981;22:471–473.
15. Sawada SG, Allman KC, Muzik O, et al. Positron emission tomography detects evidence of viability in rest technetium-99m sestamibi defects. *J Am Coll Cardiol* 1994;23:92–98.
16. Rocco TP, Dilsizian V, Strauss HW, Boucher CA. Technetium-99m isonitrile myocardial uptake at rest. II. Relation to clinical markers of potential viability. *J Am Coll Cardiol* 1989;14:1678–1684.
17. Maurea S, Cuocolo A, Soricelli A, et al. Enhanced detection of viable myocardium by technetium-99m methoxy isobutyl isonitrile tomography after nitrates administration in patients with chronic coronary artery disease. *J Nucl Med* 1945;36:1945–1952.
18. Henry WL, De Maria A, Feigenbaum H, et al. Report of the American Society of Echocardiography Committee on nomenclature and standards: Identification of Myocardial Wall Segments. American Society of Echocardiography, November 1982, North Carolina: Duke University Medical Center.
19. Shiller NB, Shah PM, Crawford M, et al. American Society of Echocardiography Committee on Standards, Subcommittee on Quantitation of Two-dimensional Echocardiograms: recommendations for quantitation of the left ventricle by two-dimensional echocardiography. *J Am Soc Echo* 1989;2:358–367.
20. Pozzoli MMA, Fioretti PM, Salustri A, Reijis AEM, Roelandt JRTC. Exercise echocardiography and technetium-99m MIBI single-photon emission computed tomography in the detection of coronary artery disease. *Am J Cardiol* 1991;67:350–355.
21. Marzullo P, Parodi O, Reisenhofer B, et al. Value of rest thallium-201/technetium-99m sestamibi scans and dobutamine echocardiography for detecting myocardial viability. *Am J Cardiol* 1993;71:166–172.
22. Matthews DE, Farewell V. Data analysis. A formal discussion of multiple comparisons. In: *Using and understanding medical statistics*. Basel: Karger S; 1985:169–172.
23. Cuocolo A, Pace L, Ricciardelli B, Chiariello M, Trimarco B, Salvatore M. Identification of viable myocardium in patients with chronic coronary artery disease: comparison of thallium-201 scintigraphy with reinjection and technetium-99m-methoxyisobutyl isonitrile. *J Nucl Med* 1992;33:505–511.
24. Marzullo P, Sambuceti G, Parodi O. The role of sestamibi scintigraphy in the radioisotopic assessment of myocardial viability. *J Nucl Med* 1992;33:1925–1930.
25. Altehoefer C, Kaiser HJ, Dorr R, et al. Fluorine-18-deoxyglucose PET for assessment of viable myocardium in perfusion defects in Tc-99m-MIBI SPECT: a comparative study in patients with coronary artery disease. *Eur J Nucl Med* 1992;19:334–342.
26. Dondi M, Tartagni F, Fallani F, et al. A comparison of rest sestamibi and rest-redistribution thallium single photon emission tomography: possible implications for myocardial viability detection in infarcted patients. *Eur J Nucl Med* 1993;20:26–31.
27. Maurea S, Cuocolo A, Pace L, et al. Rest-injected thallium-201 redistribution and resting technetium-99m methoxy isobutyl isonitrile uptake in coronary artery disease: relation to the severity of coronary artery stenosis. *Eur J Nucl Med* 1993;20:502–510.
28. Cuocolo A, Maurea S, Pace L, et al. Resting technetium-99m-methoxy isobutyl isonitrile cardiac imaging in chronic coronary artery disease: comparison with rest-redistribution thallium-201 scintigraphy. *Eur J Nucl Med* 1993;20:1186–1192.
29. Maurea S, Cuocolo A, Pace L, et al. Left ventricular dysfunction in coronary artery disease: comparison between rest-redistribution thallium-201 and resting technetium-99m-methoxy isobutyl isonitrile cardiac imaging. *J Nucl Cardiol* 1994;1:65–71.
30. Maurea S, Cuocolo A, Nicolai E, Salvatore M. Improved detection of viable myocardium by thallium-201 reinjection in chronic coronary artery disease: comparison with technetium-99m-MIBI imaging *J Nucl Med* 1994;35:621–624.
31. Altehoefer C, vom Dahl J, Biedermann M, et al. Significance of defect severity in technetium-99m-MIBI SPECT at rest to assess myocardial viability: comparison with fluorine-18-FDG PET. *J Nucl Med* 1994;35:569–574.
32. Udelson JE, Coleman PS, Metherall J, et al. Predicting recovery of severe regional ventricular dysfunction. Comparison of resting scintigraphy with Tl-201 and Tc-99m sestamibi. *Circulation* 1994;89:2552–2561.
33. Bonow RO, Dilsizian V, Cuocolo A, Bacharach SL. Identification of viable myocardium in patients with chronic coronary artery disease and left ventricular dysfunction. Comparison of thallium scintigraphy with reinjection and PET imaging with ^{18}F-fluorodeoxyglucose. *Circulation* 1991;83:26–37.
34. Dilsizian V, Perrone-Filardi P, Arrighi JA, et al. Concordance and discordance between stress-redistribution-reinjection and rest-redistribution thallium imaging for assessing viable myocardium. Comparison with metabolic activity by positron emission tomography. *Circulation* 1993;88:941–952.
35. Kiat H, Berman DS, Maddahi J, et al. Late reversibility of tomographic myocardial thallium-201 defects. An accurate marker of myocardial viability. *J Am Coll Cardiol* 1988;12:1456–1463.
36. Kayden DS, Sigal S, Soufer R, Mattera J, Zaret BL, Wackers FJ. Thallium-201 for assessment of myocardial viability: quantitative comparison of 24-hour redistribution imaging with imaging after reinjection at rest. *J Am Coll Cardiol* 1991;18:1480–1486.
37. Dilsizian V, Smeltzer WR, Freedman NMT, Dextras R, Bonow RO. Thallium reinjection after stress-redistribution imaging. Does 24-hour delayed imaging after reinjection enhance detection of viable myocardium? *Circulation* 1991;83:1247–1255.
38. Mori T, Minamiji K, Kurogane H, Ogawa K, Yoshida Y. Rest-injected thallium-201 imaging for assessing viability of severe asynergic regions. *J Nucl Med* 1991;32:1718–1724.
39. Ragosta M, Beller GA, Watson DD, Kaul S, Gimple LW. Quantitative planar rest-redistribution Tl-201 imaging in detection of myocardial viability and prediction of improvement in left ventricular function after coronary bypass surgery in patients with severely depressed left ventricular function. *Circulation* 1993;87:1630–1641.
40. Altehoefer C, vom Dahl J, Buell U, Uebis R, Kleinhans E, Hanrath P. Comparison of thallium-201 single-photon emission tomography after rest injection and fluorodeoxyglucose positron emission tomography for assessment of myocardial viability in patients with chronic coronary artery disease. *Eur J Nucl Med* 1994;21:37–45.
41. Braunwald E, Rutherford JD. Reversible ischemic left ventricular dysfunction: evidence for "hibernating" myocardium. *J Am Coll Cardiol* 1986;8:1467–1470.

Reverse Redistribution of Technetium-99m-Sestamibi Following Direct PTCA in Acute Myocardial Infarction

Yasuchika Takeishi, Hiroyasu Sukekawa, Satomi Fujiwara, Eichiro Ikeno, Yasuhiko Sasaki and Hitonobu Tomoike
First Department of Internal Medicine, Yamagata University School of Medicine and Division of Cardiology, Ishinomaki Red Cross Hospital, Yamagata, Japan

A pattern of reverse redistribution (RR) has not been documented in myocardial ^{99m}Tc-sestamibi imaging. The purpose of the study was to clarify the time-related changes in myocardial distribution of ^{99m}Tc-sestamibi in patients with acute myocardial infarction. **Methods:** Myocardial SPECT with ^{99m}Tc-sestamibi was performed in 27 patients with acute myocardial infarction within 1 wk after the onset. Twenty-three patients received direct percutaneous transluminal coronary angioplasty (PTCA) and 4 patients did not. Myocardial images were obtained 1 hr (early) and 3 hr (delayed) after the injection of ^{99m}Tc-sestamibi. Regional myocardial uptake of ^{99m}Tc-sestamibi was scored from 4 (normal) to 0 (no activity), and the RR pattern was defined as a decrease of more than 1 in the regional score at the 3-hr delayed images. Regional myocardial uptake and clearance of ^{99m}Tc-sestamibi was also assessed quantitatively. Coronary arteriography and left ventriculography were performed 1 mo later. **Results:** Out of 22 patients with successful PTCA, RR of ^{99m}Tc-sestamibi was observed in 15 patients (68%). Persistent defects (PD) were seen in 12 patients (7 patients with successful PTCA, 1 patient with unsuccessful PTCA, and 4 patients who did not receive angioplasty). In patients with RR, regional uptake of ^{99m}Tc-sestamibi in the area of myocardial infarction decreased from 54% ± 10% in the early images to 43% ± 8% in the delayed images ($p < 0.01$). Technetium-99m-sestamibi clearance from the myocardium was faster in the infarct area than in the normal area (26% ± 7% versus 9% ± 6%, $p < 0.01$). Coronary arteriography performed 1 mo later revealed that the patency of the infarct related artery was 100% (15/15) in patients with RR and 50% (6/12) in those with PD ($p < 0.01$). The extent and severity of a wall motion abnormality were less in patients with RR than in those with PD (extent: 24 ± 10 versus 36 ± 9 chord, $p < 0.01$; severity: −2.7 ± 0.4 versus −3.4 ± 0.6 s.d./chord, $p < 0.01$). **Conclusion:** The RR of ^{99m}Tc-sestamibi was observed in 68% of patients after successful direct PTCA and was associated with the accelerated clearance of ^{99m}Tc-sestamibi from the myocardium. The presence of RR in ^{99m}Tc-sestamibi imaging indicates the patency of the infarct-related artery and predicts the preserved left ventricular function.

Key Words: technetium-99m-sestamibi; acute myocardial infarction; percutaneous transluminal coronary angioplasty

J Nucl Med 1996; 37:1289–1294

A pattern of reverse redistribution is defined as the worsening of a perfusion defect during the redistribution phase of ^{201}Tl scintigraphy (*1,2*). This phenomenon includes either the worsening of a perfusion defect apparent on the initial images or the appearance of a new perfusion defect on the redistribution images. Reverse redistribution of ^{201}Tl on the redistribution images has been shown after exercise (*1,2*), pharmacologic vasodilation with dipyridamole (*3*), and resting ^{201}Tl scintigraphy (*4*). Reverse redistribution has been found to be associated with acute myocardial infarction following thrombolytic therapy (*5,6*) and chronic coronary artery disease of varying severity (*1–4,7*). It has also been reported in patients after bypass surgery with a patent graft (*8*). Although the reverse redistribution phenomenon on ^{201}Tl images has been extensively investigated, its pathophysiological meanings, including etiology, mechanism and clinical significance, have not been completely settled (*9*).

Technetium-99m-methoxyisobutyl isonitrile (^{99m}Tc-sestamibi) has been used as a myocardial perfusion tracer (*10,11*). Unlike ^{201}Tl, an apparent lack of redistribution of ^{99m}Tc-sestamibi has been shown in experimental and clinical studies (*12,13*). Therefore, ^{99m}Tc-sestamibi permits the delayed imaging after the injection, because the late images still represent the myocardial perfusion at the time of injection (*14*). However, it has recently been reported that redistribution of ^{99m}Tc-sestamibi is detectable in patients with chronic coronary artery disease (*15,16*). Although reverse redistribution of ^{201}Tl has been most commonly observed following coronary thrombolysis in patients with acute myocardial infarction (*5*), time-related changes in myocardial ^{99m}Tc-sestamibi distribution have not been examined in these patients.

Technetium-99m-sestamibi distribution could be serialy changed in the reperfused myocardium, where there is a mixture of scarring with stunned or hibernating myocardium. The purpose of the present study was to: (a) assess the prevalence of ^{99m}Tc-sestamibi reverse redistribution pattern after direct percutaneous transluminal coronary angioplasty (PTCA) in patients with acute myocardial infarction and (b) evaluate the clinical implications of this phenomenon.

METHODS

Subjects and Study Protocol

We examined 27 consecutive patients with acute myocardial infarction. Acute myocardial infarction was defined as nitroglycerin-resistant chest pain persisting for more than 30 min accompanied by an ECG with more than 0.1-mV ST-segment elevation in two or more contiguous leads (*17*). Twenty-three patients admitted within 6 hr after the onset of symptoms received direct PTCA. The remaining 4 patients did not receive PTCA or thrombolytic therapy because they were admitted late after the onset of pain. Intravenous heparin and lidocaine were given to all patients. Patients receiving PTCA were immediately transported to the catheterization laboratory and underwent coronary arteriography followed by direct PTCA if indicated. The angioplasty was considered to be technically successful when there was a residual stenosis of less than 50% and an angiographic TIMI grade was 2 or 3 at the end of angioplasty procedure.

Myocardial perfusion imaging with ^{99m}Tc-sestamibi was performed within 1 wk (average 3 days after the onset). Coronary arteriography and left ventriculography were performed after 1 mo

Received June 6, 1995; revision accepted Sept. 7, 1995.
For correspondence or reprints contact: Yasuchika Takeishi, MD, First Department of Internal Medicine, Yamagata University School of Medicine, 2-2-2 Iida-Nishi, Yamagata, 990-23 Japan.

to evaluate patency of the infarct-related artery and left ventricular wall motion. Informed written consent was obtained from all patients.

Myocardial Perfusion Imaging with Technetium-99m-Sestamibi

Data Acquisition and Processing. Myocardial SPECT was performed in all patients as previously described (*18–20*). Briefly, after an overnight fast, a 740-MBq dose of ^{99m}Tc-sestamibi was injected intravenously in the resting supine position. The patients ate a meal after the ^{99m}Tc-sestamibi injection to hasten the excretion of the isotope through the gallbladder into the bowel. Data acquisition was carried out 1 hr and 3 hr after the ^{99m}Tc-sestamibi administration. All images were obtained on a large field of view rotating gamma camera equipped with a parallel-hole, high-resolution collimator. Energy discrimination was provided by a 20% window centered at 140 keV. An anterior projection planar image was accumulated for 5 min. Then 32 images were obtained over a 180° arc from the 30° right anterior oblique to the 60° left posterior oblique positions. Each image was accumulated for 30 sec. The data were stored on a 64 × 64 matrix. Data processing was performed on a nuclear medicine computer system. A series of 6-mm thick contiguous transaxial images was reconstructed with a filtered back-projection algorithm without attenuation correction. These transaxial images were then reoriented in the short-axis, vertical long-axis and horizontal long-axis of the left ventricle.

Image Interpretation. The myocardial distribution of ^{99m}Tc-sestamibi was analyzed in the three standard orthogonal tomographic imaging planes as follows: the anterior, septal, inferior and lateral regions in the short-axis view; the anterior, apical and inferior regions in the vertical long-axis view; and the septal, apical and lateral regions in the horizontal long-axis view. The left ventricle was divided into 9 segments by splitting the anterior, septal, inferior and lateral wall into basal and apical segments, including an extra segment for the apex (*21*). The image was interpreted by two independent observers (Y.T. and S.F.) who were unaware of the clinical histories and angiographic findings of the patients. A five-point scoring system was used for evaluating the regional myocardial uptake of the tracer as described previously (*21*): 4 = normal, 3 = slightly reduced, 2 = moderately reduced, 1 = severely reduced and 0 = no activity. Reverse redistribution was defined as a decrease of more than 1 in the segmental score at the 3-hr delayed images. The grading was settled by consensus between the two observers. When they disagreed on the results, the third observer reviewed the images and made the final judgment.

Quantification of Myocardial Images. Myocardial accumulation of the tracer was assessed quantitatively by previously described methods (*22*). Six regions of interest (ROIs), 4 × 4 pixels in size (6 × 6 mm), were determined over the myocardium on the short-axis images. The mean counts in each ROI was measured and normalized to the maximal value in the myocardium. The clearance of ^{99m}Tc-sestamibi from the myocardium was calculated from the absolute counts in early (Ce) and delayed (Cd) images as follows:

$$\text{Clearance} = (Ce - Cd \times Cf) \times 100/Ce$$

$$Cf = 1/(1/2)^x,\ x = (Td - Te)/6$$

where Td = time for delayed image and Te = time for early image.

Circumferential profile analysis was applied to each of the short-axis slices from apex to base as previously described (*23*). These circumferential profiles were plotted in polar coordinates and arranged into a bull's eye map. Male and female normal files had been separately constructed from 17 men and 15 women normal subjects. In the present study, each pixel was compared with the corresponding pixel in the gender-matched profile. Pixels that were more than 2 s.d.s below the normal mean value were defined as abnormal and displayed on a color-coded standard deviation map. The ratio of the numbers of abnormal pixels to those of total pixels was defined as an extent score.

Heart-to-Background Count Ratio. On the anterior planar image, square ROIs were defined for areas of the left upper lung field (6 × 6 pixels in size), the left ventricular myocardium (4 × 4 pixels), and the liver (6 × 6 pixels) (*24*). The myocardial ROI was placed over the myocardium with the peak count density. The lung ROI and liver ROI were placed over the most intense activity in the lung and liver areas, respectively. Heart-to-lung and heart-to-liver count ratios were calculated as a fraction of the mean counts per pixel in the myocardium divided by those in the lung and liver, respectively.

Coronary Arteriography and Left Ventriculography

Coronary arteriography was performed after 1 mo in multiple projections with the standard Judkins' technique for assessing patency of the infarct-related artery. The biplane left ventriculograms were obtained for the assessment of left ventricular function. Regional wall motion was analyzed by the centerline method using 100 chords (*25*). Each shortening fraction was normalized to the end-diastolic perimeter of the left ventricle. This normalized motion was converted into units of normal standard deviations from the normal mean at each chord, previously determined in 13 normal subjects (*26*). The circumferential extent of a wall motion abnormality was assessed as the number of contiguous chords with motion of less than 2 s.d.s below the normal mean value. The degree of a wall motion abnormality was expressed as the sum of the standard deviations for all abnormal chords divided by the number of abnormal chords.

Statistical Analysis

Data were reported in mean ± 1 s.d. Continuous variables were compared by a Student's t-test, and the differences in proportion (categorical variables) were examined by a chi square test. A p value of <0.05 was considered significant.

RESULTS

Of the 23 patients who received direct PTCA, successful coronary reflow was achieved in 22 patients (Table 1). In one patient, the infarct-related artery could not be opened.

Interpretation of Technetium-99m-Sestamibi Images

Myocardial perfusion images with ^{99m}Tc-sestamibi of a patient with acute anterior myocardial infarction are shown in Figure 1. In this case, a direct PTCA was successfully performed to the left anterior descending artery. In the early images, there are perfusion defects in the anterior and septal regions of the left ventricle. The worsening of these defects is seen on the delayed images (reverse redistribution).

Figure 2 shows myocardial short-axis images with ^{99m}Tc-sestamibi of a patient with acute inferior myocardial infarction. Successful coronary reperfusion was obtained by a direct PTCA to the right coronary artery. The reverse redistribution of ^{99m}Tc-sestamibi is also observed in the inferior region of the left ventricle.

Such reverse redistribution of ^{99m}Tc-sestamibi was observed in 15 of 22 patients (68%) with successful direct PTCA. The remaining 7 of 22 patients showed persistent defects of ^{99m}Tc-sestamibi. Persistent defects were also observed in a patient who failed to achieve coronary reflow and in 4 patients who did not receive PTCA. There were no differences between the patients with reverse redistribution and persistent defects regarding the age, sex, the site of myocardial infarction and the location of the infarct-related artery (Table 1). Out of 5 patients

TABLE 1
Patient Characteristics and Angiographic and Scintigraphic Results

Patient No.	Sex	Age (yr)	Site of infarction	IRA	CAG	PTCA	RR	Uptake (%) Early	Uptake (%) Delay	Clearance (%)
1	M	68	POST	RCA	100	Successful	+	53	44	22
2	F	68	INF	RCA	99	Successful	−	47	43	−1
3	F	78	LAT	LCX	100	Successful	+	51	42	17
4	M	67	ANT, SEP	LAD	100	Unsuccessful	−	35	31	14
5	M	60	LAT	LMT	100 *	Successful	+	63	50	30
6	F	77	POST, LAT	RCA	100	Successful	−	51	50	15
7	M	56	ANT	LAD	99	Successful	+	51	38	37
8	M	86	INF	RCA	100	Successful	−	46	43	21
9	M	66	ANT, SEP	LAD	100	Not performed	−	39	42	−3
10	M	56	INF	RCA	100	Successful	+	50	41	15
11	M	57	ANT	LAD	100	Successful	−	55	51	15
12	M	52	ANT	LAD	100 *	Successful	+	52	37	32
13	F	59	INF	RCA	99	Successful	−	58	55	14
14	M	56	LAT	LCX	99	Successful	+	51	43	30
15	M	48	ANT, SEP	LAD	100	Successful	+	52	41	25
16	M	70	ANT	LAD	100	Successful	−	59	57	16
17	M	49	ANT, SEP	LAD	99 *	Successful	+	84	67	33
18	M	52	INF	RCA	100	Successful	+	48	40	21
19	M	69	INF, POST	LCX	100	Not performed	−	53	50	20
20	M	73	ANT, SEP	LAD	100 *	Not performed	−	40	42	5
21	F	77	POST, LAT	LCX	99	Successful	+	44	36	20
22	M	75	INF	RCA	90	Not performed	−	61	57	17
23	F	63	ANT, SEP	LAD	100	Successful	+	56	43	32
24	M	67	ANT, SEP	LAD	100	Successful	+	49	39	28
25	M	62	INF	RCA	99	Successful	−	48	49	−4
26	F	69	INF	RCA	100 *	Successful	+	59	46	30
27	M	71	ANT, SEP	LAD	99	Successful	+	47	39	20

*Patients with collateral vessels filling of epicardial coronary artery.
ANT = anterior; SEP = septal; INF = inferior; POST = posterior; LAT = lateral; IRA = infarct-related artery; LAD = left anterior descending artery; RCA = right coronary artery; LCX = left circumflex artery; CAG = coronary arteriography; PTCA = percutaneous transluminal coronary angioplasty; RR = reverse redistribution. + = positive; − = negative.

with collateral vessels before PTCA, 4 patients showed reverse redistribution of ^{99m}Tc-sestamibi.

Quantitative Analysis of Technetium-99m-Sestamibi Images

In patients with reverse redistribution, regional uptake of ^{99m}Tc-sestamibi in the area of myocardial infarction decreased significantly from 54% ± 10% in the early images to 43% ± 8% in the delayed images ($p < 0.01$, Fig. 3). In patients with persistent defects, ^{99m}Tc-sestamibi uptake in the infarct area was unchanged between the early and delayed images (49% ± 8% versus 48% ± 8%). Technetium-99m-sestamibi uptake in the normal area was not different between the early and delayed images in patients with reverse redistribution (82% ± 9% versus 80% ± 10%) and persistent defects (83% ± 8% versus 84% ± 11%). In patients with reverse redistribution, extent scores of ^{99m}Tc-sestamibi defects were larger in the delayed images than in the early images (0.46 ± 0.15 versus 0.38 ± 0.13, $p < 0.01$). In patients with persistent defects, the extent scores were unchanged between the early and delayed images (0.40 ± 0.15 versus 0.42 ± 0.13).

In patients with reverse redistribution, ^{99m}Tc-sestamibi clearance from the myocardium was higher in the infarct area than in

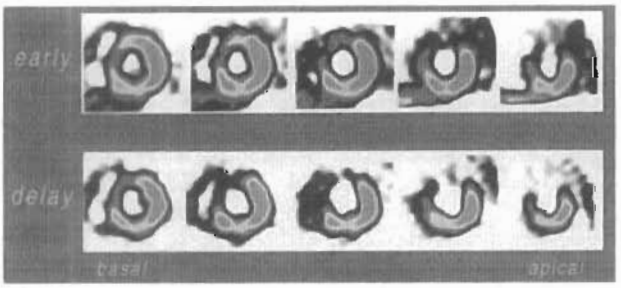

FIGURE 1. Short-axis images of myocardial ^{99m}Tc-sestamibi imaging in a patient (No. 24 in Table 1) with acute anterior myocardial infarction. Upper panels are early images and the lower panels are delayed images. Left anterior descending artery was occluded, and successful coronary reflow was achieved by direct PTCA. Perfusion defects are seen in the anterior and septal regions of the left ventricle, and these defects are more extensive in the delayed images (reverse redistribution).

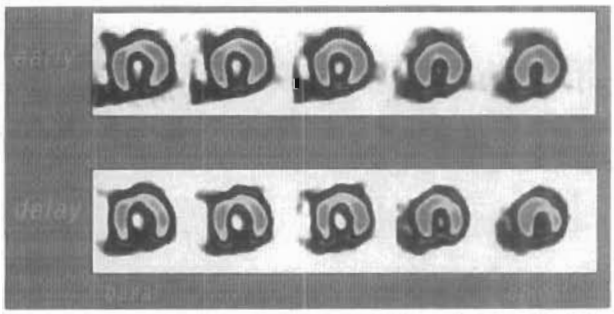

FIGURE 2. Short-axis images of ^{99m}Tc-sestamibi in a patient (No. 10 in Table 1) with acute inferior myocardial infarction. Right coronary artery was successfully reperfused by direct PTCA. Reverse redistribution of ^{99m}Tc-sestamibi is evident in the inferior region of the left ventricle.

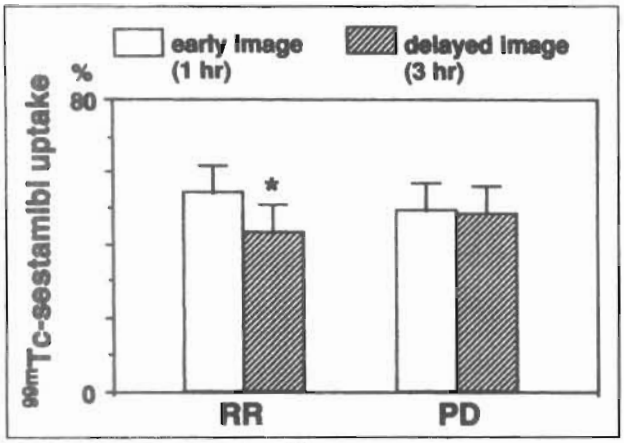

FIGURE 3. Changes in regional ^{99m}Tc-sestamibi uptake in the area of myocardial infarction from the early to the delayed images. RR = reverse redistribution; PD = persistent defects. *p < 0.01.

the normal area (26% ± 7% versus 9% ± 6%, p < 0.01, Fig. 4). Technetium-99m-sestamibi clearance from the infarct area was higher in patients with reverse redistribution than in those with persistent defects (26% ± 7% versus 11% ± 9%, p < 0.01).

Heart-to-background count ratios were obtained from the anterior planar images. A heart-to-lung ratio in the early (2.6 ± 0.6 versus 2.5 ± 0.5) and delayed (2.9 ± 1.1 versus 3.1 ± 1.3) images was not different between the patients with reverse redistribution and persistent defects. A heart-to-liver ratio was also comparable between the patients with reverse redistribution and persistent defects (early: 0.8 ± 0.3 versus 0.6 ± 0.3, delayed: 1.8 ± 0.5 versus 1.7 ± 0.6).

Relation of Reverse Redistribution of Technetium-99m-Sestamibi with the Patency of the Infarct-Related Artery and Left Ventricular Function

Coronary arteriography performed 1 mo later revealed that the infarct-related artery was patent in all patients with reverse redistribution (15/15, 100%). However, in patients with persistent defects the patency of the infarct-related artery was confirmed in 6 of 12 patients (50%, p < 0.01). In 2 of 7 patients with persistent defects after successful PTCA, the infarct-related coronary artery was occluded.

Left ventriculography was also performed after 1 mo to evaluate a left ventricular wall motion abnormality. As shown

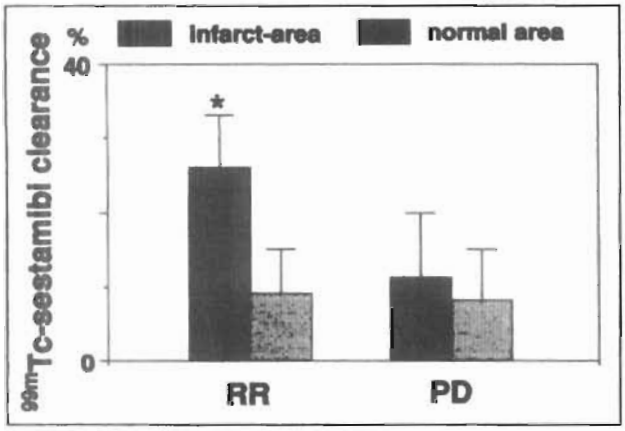

FIGURE 4. Comparison of ^{99m}Tc-sestamibi clearance from the myocardium. RR = reverse redistribution; PD = persistent defects. *p < 0.01.

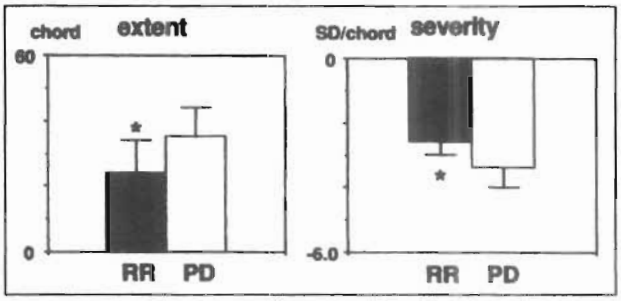

FIGURE 5. Comparison of the extent and severity of a wall motion abnormality between patients with reverse redistribution (RR) and those with persistent defects (PD). *p < 0.01.

in Figure 5, the circumferential extent of segments with decreased wall motion was less in patients with reverse redistribution than in those with persistent defects (24 ± 10 versus 35 ± 9 chord, p < 0.01). The degree of regional wall motion abnormality was also less in patients with reverse redistribution than in those with persistent defects (−2.6 ± 0.4 versus −3.4 ± 0.6 SD/chord, p < 0.01).

DISCUSSION

We demonstrated that reverse redistribution of ^{99m}Tc-sestamibi was evident after direct PTCA in patients with acute myocardial infarction. The presence of reverse redistribution of ^{99m}Tc-sestamibi was associated with the patent infarct-related artery and the preserved left ventricular function.

Redistribution of Technetium-99m-Sestamibi

Technetium-99m-sestamibi has a very slow washout from the myocardium with minimal redistribution. Okada et al. (*12*) found that clearance of ^{99m}Tc-sestamibi was similar from the normal and ischemic myocardial regions in dogs, and that redistribution was not evident. Therefore, ^{99m}Tc-sestamibi imaging can be delayed after the injection, because myocardial perfusion at the time of injection can be frozen by ^{99m}Tc-sestamibi. Thus, ^{99m}Tc-sestamibi has been used for assessing the amount of myocardium at risk in acute myocardial infarction without any delay in initiating the revascularization therapy (*14*).

Li et al. (*27*) examined time-related changes in myocardial distribution of ^{99m}Tc-sestamibi in reperfused dog hearts. They reported that following transient ischemia and reperfusion, ^{99m}Tc-sestamibi underwent myocardial redistribution, although the process was slower and less complete than ^{201}Tl. Sinusas et al. (*28*) reported that there was detectable redistribution of ^{99m}Tc-sestamibi in the presence of a severe coronary stenosis in open-chest dogs. It has been recently reported that redistribution of ^{99m}Tc-sestamibi is detectable in patients with chronic coronary artery disease (*15,16*). In the present study, 2 patients showed slight redistribution on the delayed images by visual inspection. They were categorized in a persistent defects group, because the increase of ^{99m}Tc-sestamibi uptake on the delayed images was not evident by quantitative analysis. It may require further examination to clarify the clinical significance of redistribution of ^{99m}Tc-sestamibi in patients with acute myocardial infarction.

Reverse Redistribution of Thallium-201

Reverse redistribution of ^{201}Tl was commonly observed following thrombolytic therapy in acute myocardial infarction (*5,6*). Weiss et al. (*5*) reported that this phenomenon was a sign of nontransmural myocardial infarction with a patent infarct-related coronary artery. Reverse redistribution of ^{201}Tl has also

been noted soon after coronary artery bypass surgery in the presence of a patent graft (*8*). It has been described after exercise (*1,2,7*), pharmacologic vasodilation with dipyridamole (*3*) and resting ^{201}Tl scintigraphy (*4*) in patients with chronic coronary artery disease of varying severity. Although the reverse redistribution phenomenon on ^{201}Tl images has been extensively investigated, its pathophysiological meaning has not been completely settled (*9*).

A pattern of reverse redistribution includes either the worsening of a perfusion defect apparent on the initial images or the appearance of a new perfusion defect on the delayed images. Pace et al. (*4*) reported that, out of the total 375 segments analyzed, the former pattern was noted in 6 segments and the latter pattern of ^{201}Tl reverse redistribution was in 26 segments. They showed that myocardial segments with the latter pattern of ^{201}Tl reverse redistribution were supplied by severely stenosed coronary arteries, although ^{201}Tl uptake was normal on the early images. In the present study, 1 of 15 patients with reverse redistribution of ^{99m}Tc-sestamibi showed the latter pattern. This patient had a 99% stenosis at the proximal left anterior descending artery along with the presence of well-developed collateral vessels from the right coronary artery. In this patient, left ventriculography performed 1 mo later showed near-normal wall motion in myocardial segments with reverse redistribution.

Technical Considerations

In the present study, patients ate after the ^{99m}Tc-sestamibi injection to decrease gallbladder activity. However, activity excreted from the biliary tract into the bowel might interfere with the image interpretation in the inferior wall of the heart in some patients. Taking a meal would influence ^{99m}Tc-sestamibi clearance and redistribution as noted in ^{201}Tl. However, there was no difference in the location of myocardial infarction between the patients with reverse redistribution and persistent defects.

An increase of background activity might possibly impair precise assessment of myocardial distribution and clearance of ^{99m}Tc-sestamibi. In the present study, heart-to-lung and heart-to-liver count ratios were not different between the patients with reverse redistribution and persistent defects. Thus, the background activity did not modify the present results.

Possible Mechanism of Reverse Redistribution of Technetium-99m-Sestamibi

A pattern of reverse redistribution of ^{99m}Tc-sestamibi has not been previously documented in either experimental or clinical studies. Because reverse redistribution of ^{201}Tl has been most commonly observed in patients with acute myocardial infarction following thrombolytic therapy (*5*), such a phenomenon could be detected in the case of administering ^{99m}Tc-sestamibi after direct PTCA.

The following possible mechanism for reverse redistribution of ^{99m}Tc-sestamibi might be suggested. The infarct-myocardium can receive the initially delivered ^{99m}Tc-sestamibi after the revascularization procedure, but cannot hold ^{99m}Tc-sestamibi in the myocardium with time. A mixture of viable but stunned myocardium with nonviable myocardium exists in the reperfused myocardium following direct PTCA. The ability of myocytes to retain the tracer may be impaired in this stunned myocardium (*9*). In the present study, four of five patients with collateral opacification before coronary angioplasty showed reverse redistribution of ^{99m}Tc-sestamibi. All myocardial regions with reverse redistribution of ^{99m}Tc-sestamibi were subtended by a patent infarct-related artery. Left ventriculography performed 1 mo later showed that reverse redistribution of ^{99m}Tc-sestamibi was associated with the preserved left ventricular wall motion. The viable but stunned myocardium might recover their function after 1 mo (*29*).

Beller et al. (*30*) have recently reported that in the reperfused dog hearts, sestamibi uptake and retention are dependent on myocardial viability as well as regional flow. They show that necrotic cells can neither extract nor retain sestamibi, and sestamibi may be a valid viability agent in the setting of reperfusion. Udelson et al. (*29*) have recently showed that ^{99m}Tc-sestamibi uptake is higher in the viable myocardium than in the nonviable myocardium. In the present study, ^{99m}Tc-sestamibi uptake on the early images tended to be higher in patients with reverse redistribution than in those with persistent defects (54% ± 10% versus 49% ± 8%, p = ns).

Clinical Implications

The development of noninvasive methods to assess the patency status of the infarct-related artery is urgent, because silent reocclusion of the infarct-related artery is occasionally documented following successful reperfusion (*17,31*). From our observation, the presence of reverse redistribution of ^{99m}Tc-sestamibi indicates that the patency of the infarct-related artery has been maintained and predicts the reversibility of regional wall motion abnormality after reperfusion. Reverse redistribution of ^{99m}Tc-sestamibi after direct PTCA will provide a clue for successful revascularization and, thus, myocardial viability.

ACKNOWLEDGMENTS

This study was supported in part by grants-in-aid for scientific research numbers 06213209, 06454284, 07266202 and 07557052 from the Ministry of Education, Science and Culture, Japan.

REFERENCES

1. Hecht H, Hopkins J, Rose J, et al. Reverse redistribution: worsening of thallium-201 myocardial images from exercise to redistribution. *Radiology* 1981;140:177–181.
2. Silberstein E, DeVries D. Reverse redistribution phenomenon in thallium-201 stress tests: angiographic correlation and clinical significance. *J Nucl Med* 1985;26:707–710.
3. Popma J, Smitherman T, Walker B, et al. Reverse redistribution of thallium-201 detected by SPECT imaging after dipyridamole in angina pectoris. *Am J Cardiol* 1990;65:1176–1180.
4. Pace L, Cuocolo A, Maurea S, et al. Reverse redistribution in resting thallium-201 myocardial scintigraphy in patients with coronary artery disease: relation to coronary anatomy and ventricular function. *J Nucl Med* 1993;34:1688–1692.
5. Weiss A, Maddahi J, Lew A, et al. Reverse redistribution of thallium-201: a sign of nontransmural myocardial infarction with patency of the infarct-related coronary artery. *J Am Coll Cardiol* 1986;7:51–57.
6. Biggi A, Parinelli M, Bruna C, et al. Thallium-201 reverse redistribution at rest: a pattern of myocardial infarction. *J Nucl Med Allied Sci* 1987;31:331–336.
7. Marin-Neto J, Dilsizian V, Arrighi J, et al. Thallium reinjection demonstrates viable myocardium in regions with reverse redistribution. *Circulation* 1993;88:1736–1745.
8. Nishimura T, Uehara T, Hayashida K, Kozuka T. Clinical significance of ^{201}Tl reverse redistribution in patients with aorto-coronary bypass surgery. *Eur J Nucl Med* 1987;13:139–142.
9. Lin P, Burns R. Easy come, easy go: time to pause and put thallium reverse redistribution in perspective. *J Nucl Med* 1993;34:1692–1694.
10. Wackers F, Berman D, Maddahi J, et al. Technetium-99m hexakis 2-methoxyisobutyl isonitrile: human biodistribution, dosimetry, safety and preliminary comparison to thallium-201 for myocardial perfusion imaging. *J Nucl Med* 1989;30:301–311.
11. Berman D, Kiat H, Train K, et al. Technetium-99m-sestamibi in the assessment of chronic coronary artery disease. *Semin Nucl Med* 1991;21:190–212.
12. Okada R, Glover D, Gaffney T, Williams S. Myocardial kinetics of technetium-99m-hexakis-2-methoxy-2-methylpropyl-isonitrile. *Circulation* 1988;77:491–498.
13. Beller G, Watson D. Physiological basis of myocardial perfusion imaging with the technetium-99m agents. *Semin Nucl Med* 1991;21:173–181.
14. Gibbons R, Verani M, Behrenbeck T, et al. Feasibility of tomographic ^{99m}Tc-hexakis-2-methoxy-2-methylpropyl-isonitrile imaging for the assessment of myocardial area at risk and the effect of treatment in acute myocardial infarction. *Circulation* 1989;80:1277–1286.
15. Dilsizian V, Arrighi J, Diodati J, et al. Myocardial viability in patients with chronic coronary artery disease. Comparison of ^{99m}Tc-sestamibi with thallium reinjection and [^{18}F] fluorodeoxyglucose. *Circulation* 1994;89:578–587.
16. Maurea S, Cuocolo A, Soricelli A, et al. Resting technetium-99m MIBI redistribution in patients with chronic coronary artery disease [Abstract]. *J Nucl Med* 1994;35 (suppl):114P.
17. TIMI Study Group. Comparison of invasive and conservative strategies after treatment with intravenous tissue plasminogen activator in acute myocardial infarction. Results

of the thrombolisis in myocardial infarction (TIMI) phase II trial. *N Engl J Med* 1989;320:618–627.
18. Takeishi Y, Tonooka I, Ikeda K, et al. Dilatation of the left ventricular cavity on dipyridamole thallium-201 imaging: a new maker of triple-vessel disease. *Am Heart J* 1991;121:466–475.
19. Takeishi Y, Tonooka I, Chiba J, et al. Simultaneous assessment of left ventricular wall motion and myocardial perfusion at rest and during exercise by technetium-99m methoxy isobutyl isonitrile. *Jpn Circ J* 1991;55:1192–1199.
20. Takeishi Y, Sukekawa H, Saito H, et al. Left ventricular function and myocardial perfusion during dipyridamole infusion assessed by a single injection of ^{99m}Tc-sestamibi in patients unable to exercise. *Nucl Med Commun* 1994;15:697–703.
21. Takeishi Y, Chiba J, Abe S, et al. Adenosine-induced heterogeneous perfusion accompanies myocardial ischemia in the presence of advanced coronary artery disease. *Am Heart J* 1994;127:1262–1268.
22. Takeishi Y, Chiba J, Abe S, et al. Heterogeneous myocardial distribution of iodine-123 15-(p-iodophenyl)-3-R,S-methylpentadecanoic acid (BMIPP) in patients with hypertrophic cardiomyopathy. *Eur J Nucl Med* 1992;19:775–782.
23. Takeishi Y, Tonooka I, Meguro M, et al. The relationship between chest pain during thallium-201 scintigraphy with dipyridamole and myocardial ischemia. *Jpn Circ J* 1991;55:465–472.
24. Takeishi Y, Chiba J, Abe S, Tomoike H. Ratio of lung-to-heart thallium-201 uptake on exercise and dipyridamole stress imaging in coronary artery disease. Implication of SPECT. *Jpn Circ J* 1993;57:379–383.
25. Sheehan F, Bolson E, Dodge H, et al. Advantages and applications of the centerline method for characterizing regional ventricular function. *Circulation* 1986;74:293–305.
26. Miyawaki H, Tsuiki K, Yamaguchi S, et al. The response of left ventricular regional function to afterload stress in patients with old myocardial infarction and ventricular aneurysm. *Jpn Circ J* 1991;55:1211–1223.
27. Li Q, Solot G, Frank T, et al. Myocardial redistribution of technetium-99m-methoxyisobutyl isonitrile (sestamibi). *J Nucl Med* 1990;31:1069–1076.
28. Sinusas A, Bergin J, Edwards N, et al. Redistribution of ^{99m}Tc-sestamibi and ^{201}Tl in the presence of a severe coronary artery stenosis. *Circulation* 1994;89:2332–2341.
29. Udelson J, Coleman P, Metherall J, et al. Predicting recovery of severe regional ventricular dysfunction. Comparison of resting scintigraphy with ^{201}Tl and ^{99m}Tc-sestamibi. *Circulation* 1994;89:2552–2561.
30. Beller G, Glover D, Edwards N, et al. ^{99m}Tc-sestamibi uptake and retention during myocardial ischemia and reperfusion. *Circulation* 1993;87:2033–2042.
31. Gibson W, Christian T, Pellikka P, et al. Serial tomographic imaging with technetium-99m-sestamibi for the assessment of infarct-related arterial patency following reperfusion therapy. *J Nucl Med* 1992;33:2080–2085.

Regional Myocardial Perfusion Assessed with Generator-Produced Copper-62-PTSM and PET

Pilar Herrero, Judy J. Hartman, Mark A. Green, Carolyn J. Anderson, Michael J. Welch, Joanne Markham and Steven R. Bergmann

Cardiovascular Division, Division of Radiation Sciences and Biomedical Computer Laboratory, Washington University School of Medicine, St. Louis, Missouri and School of Pharmacy and Pharmacal Sciences, Purdue University, West Lafayette, Indiana

We have previously demonstrated that myocardial perfusion can be estimated accurately in experimental animals with the generator-produced positron-emitting tracer, ^{62}Cu-pyruvaldehyde bis (N^4-methylthio-semicarbazone)(^{62}Cu-PTSM) and PET. This study evaluated the feasibility of quantifying regional myocardial blood flow using ^{62}Cu-PTSM and PET in human subjects. **Methods:** Regional perfusion was estimated using a previously described and validated two-compartment model from dynamic PET scans obtained after an intravenous bolus of ^{62}Cu-PTSM in 10 healthy volunteers and in 6 patients with coronary artery disease at rest; and in 9 of the volunteers and 4 of the patients after administration of dipyridamole intravenously. Flow estimates were compared with those obtained using $H_2{}^{15}O$. **Results:** Contrast was high between myocardium and blood or lung with ^{62}Cu-PTSM, resulting in high-quality myocardial images. Liver uptake was also high. At flows of up to 1.5 ml/g/min, flow estimated with ^{62}Cu-PTSM correlated closely with estimates obtained with $H_2{}^{15}O$ ($y = 0.71x + 0.21$, $n = 169$ regional comparisons, $r = 0.66$, $p < 0.05$), but this relationship was not maintained at higher flows. **Conclusion:** The results demonstrate that quantification of myocardial perfusion with ^{62}Cu-PTSM is feasible in human subjects but cannot be used to estimate hyperemic flows due most likely to the strong binding of the tracer to human serum albumin. Copper-62-PTSM congeners with less avidity for human albumin may prove more suitable for evaluation of hyperemic flows.

Key Words: PET; myocardial blood flow; copper-62-PTSM

J Nucl Med 1996; 37:1294–1300

Delineation of myocardial perfusion and perfusion reserve is paramount for the diagnosis of coronary artery disease and for the evaluation of therapies designed to enhance nutritive myocardial perfusion. PET has been shown to be excellent for quantification of regional myocardial blood flow because of its ability to accurately delineate the distribution of positron emitting radionuclides within the myocardium. PET has been shown to be highly sensitive and specific for the delineation of coronary artery disease with the cyclotron-produced flow tracers ^{13}N-ammonia (*1,2*) or ^{15}O-water (*3–8*) as well as with generator-produced ^{82}Rb-chloride (*9–13*). Generator-produced PET radiopharmaceuticals free operations from the necessity of a hospital-based cyclotron and add flexibility and convenience to patient studies.

Our group has shown, in experimental studies, that accurate quantitative flow measurements can be obtained with ^{82}Rb-chloride over a wide range of physiological flows with a two-compartment kinetic model (*14*). Nonetheless, the short physical half-life of this tracer (1.3 min) makes ^{82}Rb-chloride less than ideal for the quantification of myocardial perfusion and there has been interest in the development of alternative generator-produced PET flow tracers. The lipophilic compound copper(II) pyruvaldehyde bis (N^4-methylthiosemicarbazone) (Cu-PTSM), is one candidate. Copper-PTSM can be labeled with several single-photon radionuclides as well as with generator-produced, positron-emitting ^{62}Cu ($t_{1/2}$ = 9.7 min). Although the parent, ^{62}Zn, only possesses a 9.3-hr half-life, it and ^{62}Cu-PTSM are easily produced in the quantities that would be required for regional or nationwide delivery (*15,16*). Copper-62-PTSM is highly extracted and retained in organs for prolonged periods of time due to intracellular reductive decomposition of the lipophilic Cu-PTSM complex to liberate the ^{62}Cu ion which cannot rapidly escape the cell (*17,18*) facilitating imaging of heart, kidney and brain, and making this tracer an attractive one for multi-organ flow imaging (*19–21*).

In studies on intact dogs, myocardial extraction of Cu-PTSM

Received June 14, 1995; revision accepted Nov. 13, 1995.
For correspondence or reprints contact: Steven R. Bergmann, MD, PhD, Cardiovascular Division, Washington University School of Medicine, Box 8086, 660 S. Euclid Ave., St. Louis, MO 63110.

Cardiac scintigraphic findings of mitochondrial myopathy, encephalopathy, lactic acidosis and stroke-like episodes: A case report

Shinro Matsuo MD PhD[1], Kenichi Nakajima MD PhD[1], Seigo Kinuya MD PhD[1], Yuichi Sato MD PhD[2], Naoya Matsumoto MD PhD[2], Minoru Horie MD PhD[3]

S Matsuo, K Nakajima, S Kinuya, Y Sato, N Matsumoto, M Horie. Cardiac scintigraphic findings of mitochondrial myopathy, encephalopathy, lactic acidosis and stroke-like episodes: A case report. Exp Clin Cardiol 2008;13(2):93-95.

A 49-year-old woman was admitted to hospital because of heart failure. She was diagnosed as having mitochondrial cardiomyopathy and diabetes mellitus. Echocardiography revealed a hypertrophic and poorly contracting left ventricle. A diagnosis of mitochondrial myopathy, encephalopathy, lactic acidosis and stroke-like episodes was established by muscle biopsy. She underwent technetium-99m-sestamibi (^{99m}Tc-MIBI) and beta-methyl-p-^{123}I-iodophenyl-pentadecanoic acid (^{123}I-BMIPP) scintigraphic examinations. ^{99m}Tc-MIBI single-photon emission computed tomography revealed reduced tracer uptake in the hypertrophic left ventricular inferior wall. In contrast, there was an increase in ^{123}I-BMIPP uptake in the in the region of reduced ^{99m}Tc-MIBI uptake (^{99m}Tc-MIBI/^{123}I-BMIPP mismatch). There was rapid washout of ^{99m}Tc-MIBI from the myocardium (washout rate increased by 30%). Decreased ^{99m}Tc-MIBI and increased ^{123}I-BMIPP uptake (^{99m}Tc-MIBI/^{123}I-BMIPP mismatch) were the characteristics of cardiac involvement in mitochondrial myopathy, encephalopathy, lactic acidosis and stroke-like episodes.

Key Words: *^{99m}Tc-MIBI/^{123}I-BMIPP mismatch; ^{99m}Tc-MIBI washout; MELAS*

Mitochondrial disorders are a heterogeneous group of diseases resulting from abnormalities in mitochondrial DNA and function. In mitochondrial myopathy, encephalopathy, lactic acidosis and stroke-like episodes (MELAS), cardiac involvement manifesting as hypertrophic (symmetrical or asymmetrical) or dilated cardiomyopathy is frequently observed (1-6). We describe cardiac scintigraphic findings in a patient with MELAS and reviewed previous reports in the literature.

CASE PRESENTATION

A 49-year-old woman was admitted to hospital with dyspnea accompanied by orthopnea. She had been treated for insulin-dependent diabetes mellitus for four years. Three years before admission, she had undergone coronary angiography, which revealed normal coronary arteries. One year before admission, she had had pacemaker implantation because of a third-degree atrioventricular block. She had symptoms of a common cold eight days before admission. One day before admission, she had diarrhea and vomiting, as well as dyspnea, leading to hospital admission. On admission, her blood pressure was 80/46 mmHg, and her heart rate was 120 beats/min when 6 μg/kg/min infusions of dopamine and dobutamine were administered. Physical examination revealed a third heart sound, moist rales in the bilateral lung fields and pretibial edema. She was 145 cm tall and her weight was 40 kg. Her two daughters were also of short stature. She had difficulty hearing and muscle weakness. Her mother had difficulty hearing and died of a stroke. Echocardiography revealed biphasic P waves on the right precordial leads, left ventricular hypertrophy and decreased amplitude of R waves. Chest x-ray showed pulmonary congestion and cardiomegaly (cardiothoracic ratio was 62%). Laboratory tests found increased levels of brain natriuretic peptide (6.8×10^5 ng/L), glutamic-pyruvic transaminase (13,102 U/L) and glutamate oxaloacetate transaminase (5167 U/L). Her fasting blood glucose level was 1.44 mmol/L and hemoglobin A1c was 6.7%. Echocardiography (Figure 1) showed a markedly dilated, as well as diffusely hypertrophic and hypocontractile, left ventricle (end-diastolic septal thickness was 11 mm, posterior end-diastolic dimension was 77 mm, end-systolic dimension was 67 mm and ejection fraction was 16%). In addition, there was a small amount of pericardial effusion. She underwent plasma exchange, continuous hemodiafiltration, volume expansion and infusion of inotropic agents for heart failure. Arterial blood gas data on the third day showed worsening of metabolic acidosis. Incubation and arterial ventilation were performed. She was given a large dose of coenzyme Q10 (210 mg/day).

On the ninth day in hospital, muscle biopsy (taken from musculus sternocleidomastoideus) was performed. Mitochondrial DNA sequence analysis by polymerase chain reaction revealed an A-to-G mutation in the mitochondrial transfer RNA(Leu[UUR]) gene at nucleotide position 3243 (Figure 2), a finding consistent with MELAS (7). Myocardial biopsy was not carried out because a pacemaker had been implanted.

On the 55th day in hospital, the patient underwent rest technetium-99m-sestamibi (^{99m}Tc-MIBI) cardiac scintigraphy (740 MBq). The planar and single-photon emission computed tomography (SPECT) views were obtained approximately 30 min after injection as previously reported (8). Analysis by

[1]*Department of Nuclear Medicine, Kanazawa University Hospital, Kanazawa;* [2]*Department of Cardiology, Nihon University School of Medicine, Tokyo;* [3]*Department of Cardiovascular and Respiratory Medicine, Shiga University of Medical Science, Otsu, Japan*
Correspondence: Dr Shinro Matsuo, Department of Nuclear Medicine, Kanazawa University Hospital, 13-1 Takara-machi, Kanazawa, Ishikawa, 920-8641, Japan. Telephone +81-76-265-2333, fax +81-76-234-4257, e-mail: smatsuo@mmd.m.kanazawa-u.ac.jp
Received October 24, 2007. Accepted February 26, 2008

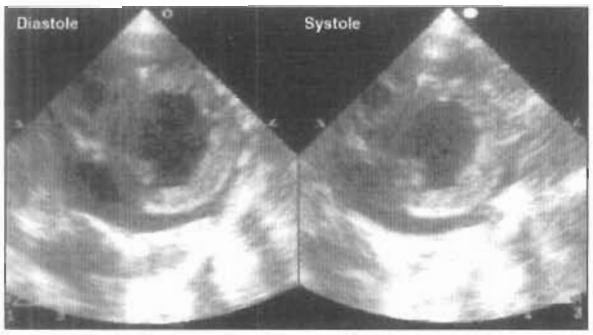

Figure 1) *Echocardiogram in the short-axis view showing left ventricular hypertrophy and left ventricular dilation with decreased contraction. A small amount of pericardial effusion is also noted*

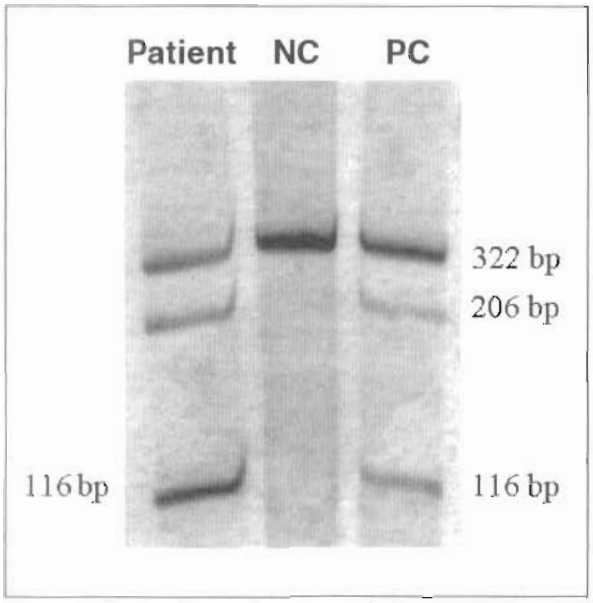

Figure 2) *Southern blot analysis of mitochondrial DNA in the mitochondrial transfer RNA (Leu[UUR]) gene showing, in the presence of A3243G point mutation, the 322 bp polymerase chain reaction product is cut into a 206 bp and a 116 bp fragment. NC Negative control; PC Positive control*

the electrocardiograph-gated quantitative gated SPECT software revealed decreased left ventricular systolic function with an end-diastolic volume of 83 mL, end-systolic volume of 60 mL and ejection fraction of 29%. Heart to mediastinum count ratio (H/M) of ^{99m}Tc-MIBI on the initial and delayed images were 2.4 and 2.5, respectively. There was an increase of 30% in the ^{99m}Tc-MIBI washout rate (normal washout rate is 15% or lower). SPECT images showed mild hypoperfusion in the inferior segments (Figure 3, upper panel).

On the 58th hospital day, beta-methyl-p-^{123}I-iodophenyl-pentadecanoic acid (^{123}I-BMIPP, Nihon Medi-Physics, Japan) scintigraphy was performed. Under fasting and resting conditions, 111 MBq of ^{123}I-BMIPP was administered intravenously and immediately flushed with 10 mL of saline. ^{123}I-BMIPP SPECT images were obtained as previously reported (9), and it

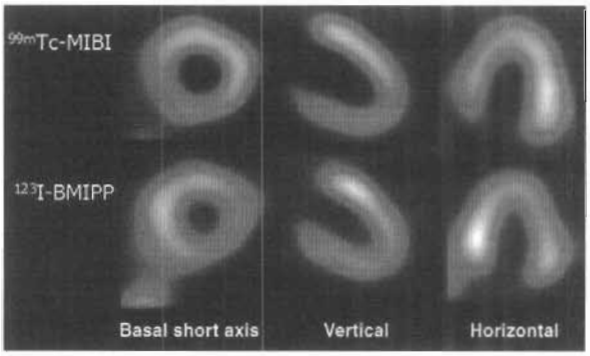

Figure 3) *^{99m}Tc-sestamibi (^{99m}Tc-MIBI) (upper panel) and beta-methyl-p-^{123}I-iodophenyl-pentadecanoic acid (^{123}I-BMIPP) (lower panel) single-photon emission computed tomography images showing decreased ^{99m}Tc-MIBI uptake in the inferoseptal segments and increased ^{123}I-BMIPP uptake in the inferoseptal and septal segments (^{99m}Tc-MIBI/^{123}I-BMIPP mismatch)*

showed increased uptake in the inferoseptal segment (Figure 3, lower panel).

DISCUSSION

Lactic acidosis is one of the common biochemical hallmarks of mitochondrial disorders. However, it also occurs in healthy subjects as nonspecific laboratory abnormalities after episodes of anoxic events, shock, hypoperfusion or CO intoxication. Because the brain and nervous system, in addition to muscle, are greatly dependent on energy production by mitochondrial oxidation, these tissues are more vulnerable to mitochondrial defects. The majority of patients with MELAS have malignant clinical outcomes, and it is frequently associated with heart failure (1-6) and arrhythmias, including advanced atrioventricular block (10), as observed in our patient.

Echocardiography demonstrated left ventricular hypertrophy, which is believed to be one of the morphological features of cardiac involvement in MELAS (4). A reduced uptake of ^{99m}Tc-MIBI was observed in the inferior myocardial segments. Also, there was a rapid washout of ^{99m}Tc-MIBI from the myocardium. ^{99m}Tc-MIBI circulates as a monovalent positive ion and distributes specifically in the myocardium after intravenous administration. Although ^{99m}Tc-MIBI was initially developed as a tracer for the evaluation of myocardial blood flow, recent studies (11-14) indicate that it is selectively incorporated (over 90%) into mitochondria in a membrane potential-dependent manner after passive diffusion into the myocardium. Thus, ^{99m}Tc-MIBI is a potentially useful agent for evaluating mitochondrial function. It has been suggested that mitochondrial DNA mutation in patients with dilated cardiomyopathy may also be associated with mitochondrial dysfunction. Mitochondrial dysfunction may be indicated by increased ^{99m}Tc-MIBI washout from the myocardium, presumably because of an inability of mitochondria to retain the tracer (15). Several studies (16,17) have reported mitochondrial DNA mutation along with mitochondrial abnormalities. Arbustini et al (16) identified a small subgroup of patients with pathological mutations in mitochondrial DNA in idiopathic dilated cardiomyopathy. The mutations may be a sign of increasing stress to the myocardium, promoting additional damage to mitochondrial DNA (17). The kinetics of ^{99m}Tc-MIBI in

MELAS is not well documented, but a recent report by Ikawa et al (18) described increased ^{99m}Tc-MIBI washout in five patients with MELAS. In their study, patients had decreased ^{99m}Tc-MIBI uptake and an increased ^{99m}Tc-MIBI washout rate, which correlated inversely with left ventricular ejection fraction. In addition, they found increased uptake of ^{123}I-BMIPP in the region of decreased ^{99m}Tc-MIBI uptake (^{99m}Tc-MIBI/^{123}I-BMIPP mismatch) in two patients with severe left ventricular dysfunction, which was consistent with our patient. ^{123}I-BMIPP is an analogue of free fatty acid, which enters the intracellular triglyceride pool. In mitochondrial respiratory chain failure, energy production shifts from the aerobic to the anaerobic pathway (glycolytic pathway), resulting in increased lactic acid formation and increased uptake of ^{123}I-BMIPP (19). Thus, ^{99m}Tc-MIBI/^{123}I-BMIPP mismatch, together with the increased ^{99m}Tc-MIBI washout rate, appears to reflect alterations in energy state due to mitochondrial respiratory failure, and this association may be useful to evaluate the severity of cardiac involvement in MELAS.

REFERENCES

1. Sato W, Tanaka M, Sugiyama S, et al. Cardiomyopathy and angiopathy in patients with mitochondrial myopathy, encephalopathy, lactic acidosis, and strokelike episodes. Am Heart J 1994;128:733-41.
2. Hiruta Y, Chin K, Shitomi K, et al. Mitochondrial encephalomyopathy with A to G transition of mitochondrial transfer RNA(Leu(UUR)) 3,243 presenting hypertrophic cardiomyopathy. Intern Med 1995;34:670-3.
3. Shinomiya H, Fukuda N, Takeichi N, et al. [Evaluation of cardiac function by various cardiac imaging techniques in mitochondrial cardiomyopathy: A case report.] J Cardiol 1998;31:109-14.
4. Okajima Y, Tanabe M, Takayanagi M, Aotsuka H. A follow up study of myocardial involvement in patients with mitochondrial encephalomyopathy, lactic acidosis, and stroke-like episodes (MELAS). Heart 1998;80:292-95.
5. Ueno H, Shiotani H. Cardiac abnormalities in diabetic patients with mutation in the mitochondrial tRNA(Leu(UUR)) gene. Jpn Circ J 1999;63:877-80.
6. Higashikata T, Koyama J, Shimada H, Yazaki M, Owa M, Ikeda S. An 80-year-old mitochondrial disease patient with A3243G tRNA(Leu(UUR)) gene presenting cardiac dysfunction as the main symptom. Intern Med 2001;40:405-8.
7. Goto Y, Nonaka I, Horai S. A mutation in the tRNA(Leu)(UUR) gene associated with the MELAS subgroup of mitochondrial encephalomyopathies. Nature 1990;348:651-3.
8. Matsuo S, Nakae I, Matsumoto T, Horie M. Impact of endothelial dysfunction on left ventricular remodeling after successful primary coronary angioplasty for acute myocardial infarction – analysis by quantitative ECG-gated SPECT. Ann Nucl Med 2006;20:57-62.
9. Matsuo S, Nakamura Y, Takahashi M, Mitsunami K, Kinoshita M. Myocardial metabolic abnormalities in hypertrophic cardiomyopathy assessed by iodine-123-labeled beta-methyl-branched fatty acid myocardial scintigraphy and its relation to exercise-induced ischemia. Jpn Circ J 1998;62:167-72.
10. Lev D, Nissenkorn A, Leshinsky-Silver E, et al. Clinical presentations of mitochondrial cardiomyopathies. Pediatr Cardiol 2004;25:443-50.
11. Okada RD, Glover D, Gaffney T, Williams S. Myocardial kinetics of technetium-99m-hexakis-2-methoxy-2-methylpropyl-isonitrile. Circulation 1988;77:491-8.
12. Piwnica-Worms D, Kronauge JF, Chiu ML. Uptake and retention of hexakis (2-methoxyisobutyl isonitrile) technetium (I) in cultured chick myocardial cells: mitochondrial and plasma membrane potential dependence. Circulation 1990;82:1826-38.
13. Carvalho PA, Chiu ML, Kronauge JF, et al. Subcellular distribution and analysis of technetium-99m-MIBI in isolated perfused rat hearts. J Nucl Med 1992;33:1516-22.
14. Crane P, Laliberté R, Heminway S, Thoolen M, Orlandi C. Effect of mitochondrial viability and metabolism on technetium-99m-sestamibi myocardial retention. Eur J Nucl Med 1993;20:20-5.
15. Matsuo S, Nakae I, Tsutamoto T, Okamoto N, Horie M. A novel clinical indicator using Tc-99m sestamibi for evaluating cardiac mitochondrial function in patients with cardiomyopathies. J Nucl Cardiol 2007;14:215-20.
16. Arbustini E, Diegoli M, Fasani R, et al. Mitochondrial DNA mutations and mitochondrial abnormalities in dilated cardiomyopathy. Am J Pathol 1998;153:1501-10.
17. Ruppert V, Maisch B. Mitochondrial DNA deletions in cardiomyopathies. Herz 2000;25:161-7.
18. Ikawa M, Kawai Y, Arakawa K, et al. Evaluation of respiratory chain failure in mitochondrial cardiomyopathy by assessments of 99mTc-MIBI washout and 123I-BMIPP/99mTc-MIBI mismatch. Mitochondrion 2007;7:164-70.

Myocardial Viability Index in Chronic Coronary Artery Disease: Technetium-99m-Methoxy Isobutyl Isonitrile Redistribution

Simone Maurea, Alberto Cuocolo, Andrea Soricelli, Luisa Castelli, Fiorenzo Squame, Massimo Imbriaco, Nicola De Luca, Bruno Trimarco and Marco Salvatore

Nuclear Medicine Department, CNR Nuclear Medicine Center and Medical Clinic, University Federico II; and National Cancer Institute, Naples, Italy

The purpose of this study was to evaluate whether an additional redistribution image after a rest ^{99m}Tc-MIBI injection enhances detection of viable myocardium and predicts functional recovery after coronary revascularization in patients with chronic coronary artery disease (CAD). **Methods:** Thirty-one patients (29 men, mean age 55 ± 10 yr) with proven CAD and left ventricular (LV) dysfunction (ejection fraction 39% ± 9%) underwent resting ^{99m}Tc-MIBI tomography with initial (1 hr) and delayed (5 hr) images. Within 1 wk of MIBI imaging, all patients underwent rest-redistribution ^{201}Tl imaging. Eight patients also underwent two-dimensional echocardiography before and 5 ± 3 mo after coronary revascularization. **Results:** On the initial ^{99m}Tc-MIBI images, 302 myocardial segments were normal, 183 showed moderate and 197 severe reduction of tracer uptake. Of these 197 segments, 47 (24%) demonstrated increased tracer uptake (≥10% versus initial) on delayed images (from 43% ± 8% to 60% ± 8%, $p<0.001$) and were considered as showing ^{99m}Tc-MIBI redistribution. These 47 segments were observed in 20 (65%) patients in whom ^{201}Tl images detected viable myocardium in the same segments. In the eight patients studied before and after revascularization, 83% of segments with ^{99m}Tc-MIBI redistribution and abnormal LV function showed functional recovery after revascularization, while 96% of segments without ^{99m}Tc-MIBI redistribution did not show functional recovery. **Conclusion:** Resting ^{99m}Tc-MIBI redistribution frequently occurs in patients with chronic CAD. Acquisition of ^{99m}Tc-MIBI redistribution images enhances detection of viable myocardium and predicts functional recovery after revascularization.

Key Words: technetium-99m-sestamibi; left ventricular dysfunction; functional recovery; thallium-201

J Nucl Med 1995; 36:1953–1960

Technetium-99m-methoxy isobutyl isonitrile (MIBI) is a cardiac perfusion agent that initially distributes in the myocardium proportional to coronary blood flow, similar to ^{201}Tl (*1,2*). It has been suggested that ^{99m}Tc-MIBI does not show significant redistribution (*1*). Recent studies, however, demonstrated that delayed ^{99m}Tc-MIBI redistribution may be observed in a model of transient myocardial ischemia (*3*) or under conditions of sustained low coronary flow (*4*). Furthermore, it has also been reported that myocardial uptake and retention of ^{99m}Tc-MIBI are dependent on both cell viability and regional blood flow and that tissue viability is required for ^{99m}Tc-MIBI redistribution (*5–9*).

Clinical studies evaluated the phenomenon of ^{99m}Tc-MIBI redistribution after stress injection in patients with CAD (*10,11*). The occurrence of ^{99m}Tc-MIBI redistribution after rest injection and its clinical implications have not yet been widely evaluated. Preliminary results reported by Dilsizian et al. recently suggested that ^{99m}Tc-MIBI redistribution imaging following tracer injection at rest can detect viable myocardium using standard imaging protocols (*12*). Furthermore, these authors suggest that detection of viable myocardium may be enhanced with ^{99m}Tc-MIBI cardiac imaging if an additional redistribution image is acquired after tracer injection at rest (*12*). It is still uncertain, however, whether ^{99m}Tc-MIBI redistribution after rest injection is predictive of improved ventricular function after coronary revascularization.

The purpose of this study was to evaluate whether an additional redistribution image after rest ^{99m}Tc-MIBI injection enhances detection of viable myocardium and predicts functional recovery after coronary revascularization in patients with chronic coronary artery disease (CAD).

MATERIALS AND METHODS

Patients

We prospectively studied 31 patients (29 men, 2 women; mean age 55 ± 10 yr) with angiographically documented CAD and with left ventricular dysfunction (Tables 1 and 2). Seven patients had significant stenosis of all three major coronary vessels, 11 had significant stenosis of two major coronary vessels and 13 had significant stenosis of only one major coronary vessel. The mean left ventricular ejection fraction (LVEF) by resting equilibrium radionuclide angiography was 39% ± 9%. All patients had a previous myocardial infarction that was documented clinically and by electrocardiography. No patient, however, had an acute myocardial infarction within 6 mo of the study. The majority of patients

Received Jan. 1, 1995; revision accepted Jul. 14, 1995
For correspondence or reprints contact: Simone Maurea, MD, via Raffaele De Cesare 7, 80132 Napoli, Italy.

TABLE 1
Patient Characteristics

Patient no.	Sex	Age (yr)	LVEF (%)	Site of myocardial infarction	Stable angina
1	M	62	42	Posterolateral	Yes
2	M	62	24	Inferior, anterior	Yes
3	M	44	49	Anteroseptal	Yes
4	M	63	38	Anterior	Yes
5	M	57	44	Inferior	Yes
6	M	67	42	Inferior	Yes
7	M	60	39	Inferolateral	Yes
8	M	49	35	Anteroseptal, inferoapical	No
9	M	69	39	Inferolateral	Yes
10	M	46	34	Anterior	Yes
11	M	63	48	Inferolateral	Yes
12	M	48	28	Anterior	Yes
13	M	43	41	Anteroseptal	Yes
14	M	61	42	Inferior, anterior	Yes
15	M	40	48	Anteroseptal	Yes
16	M	63	31	Anteroseptal, inferior	Yes
17	M	54	30	Inferolateral	Yes
18	M	66	47	Anteroapical	Yes
19	M	58	49	Inferior	Yes
20	M	65	48	Anterior	Yes
21	M	61	30	Anterior	Yes
22	M	68	49	Anterior	Yes
23	M	50	36	Anteroseptal	Yes
24	M	57	48	Anteroseptal, apical	Yes
25	M	38	23	Anterior	No
26	M	32	26	Anterior, inferior	No
27	M	42	20	Anterior	Yes
28	M	53	49	Anterior	Yes
29	M	47	44	Anterolateral	Yes
30	F	57	46	Inferior	Yes
31	F	65	44	Anterior	Yes

LVEF = left ventricular ejection fraction.

(n = 28) were symptomatic with episodes of stable angina requiring antianginal treatment, while three patients were asymptomatic. All patients, however, underwent radionuclide studies after withdrawal of all medications. Eight of the 31 patients were also studied after coronary revascularization, coronary artery bypass graft in six and percutaneous transluminal coronary angioplasty in two. In these patients, none had clinical evidence of perioperative or postangioplasty myocardial infarction or restenosis. Informed consent, as part of the protocol approved by the Institutional Clinical Research Subpanel on Human Studies at our University, was obtained from all patients.

Technetium-99m-MIBI Imaging

After an overnight fast, all patients underwent rest-redistribution ^{99m}Tc-MIBI myocardial tomography. Patients were ambulatory and remained in the resting condition for 30 min before intravenous injection of ^{99m}Tc-MIBI (740 MBq). Initial images were acquired 1 hr after tracer administration. Delayed images were then taken 5 hr later.

SPECT was performed as previously described (*13*) using a rotating large field of view gamma camera equipped with a low-energy, all-purpose, parallel-hole collimator and connected with a dedicated computer system. Briefly, 32 projections (40 sec/projection) were obtained over a semicircular 180° arch, which extended from the 30° right anterior oblique to the left posterior oblique position. A 20% symmetric energy window centered on the 140-keV peak was used. All projection images were stored on magnetic disk in a 64 × 64 word matrix. Each projection image was corrected for nonuniformity, with a 120-million count image obtained weekly from a uniform ^{57}C flood source. The mechanical center of rotation was determined from the projection data to align the detector data with respect to the reconstruction matrix (*14*). The raw data were initially smoothed with a nine-point weighted average algorithm. Filtered backprojection was then performed with a low-resolution Butterworth filter with a cutoff frequency of 0.5 cycles/pixel, order 5.0, to reconstruct transverse axial tomograms of 6.2-mm thickness per slice, which encompassed the entire heart. Sagittal and oblique tomograms parallel to the long-axis and short-axis of the left ventricle were then extracted from the filtered transaxial tomograms by performing coordinate transformation with the appropriate interpolation (*14*). No attenuation or scatter correction was applied.

Thallium-201 Imaging

All patients underwent rest-redistribution ^{201}Tl myocardial tomography. Patients were ambulatory and remained in the resting condition for 30 min before thallium administration. After an overnight fast, ^{201}Tl (111 MBq) was intravenously injected at rest. Initial and delayed images were acquired 15 min and 4 hr after injection. During the time between the initial and delayed images, all patients were ambulatory and remained in the fasting state. A 3-day interval separated the thallium from ^{99m}Tc-MIBI study. SPECT acquisition was performed with the same gamma camera, matrix and computer system used for the ^{99m}Tc-MIBI studies. The photopeak was centered on the 68-keV with a 20% window.

Echocardiography

During the same week of ^{99m}Tc-MIBI and ^{201}Tl imaging, all patients underwent echocardiographic studies. A phased-array sector scanner with a 2.5 MHz transducer was used. Two-dimensional images of the left ventricle were obtained at rest with the patient lying in the left lateral decubitus position using multiple imaging sections, including the parasternal long- and short-axes and apical two- and four-chamber views. Images were recorded on videotape for analysis. In the eight patients studied before and after coronary revascularization, two sequential echocardiographic studies were performed. The first evaluation (baseline) was performed during the same week of ^{99m}Tc-MIBI and ^{201}Tl studies. The second evaluation (follow-up) was performed an average of 5 ± 3 mo after coronary revascularization. No patient received beta-blockers or inotropic drugs during the follow-up evaluation.

Data Analysis

In each patient, corresponding initial and delayed ^{99m}Tc-MIBI and rest-redistribution ^{201}Tl tomographic images were evaluated for direct comparison, as previously described (*13*). For each study, tomograms were divided into 22 myocardial segments (Fig. 1). Regional ^{99m}Tc-MIBI and ^{201}Tl uptake were quantitatively analyzed. In each tomogram, the myocardial region with the maximum counts was considered as the normal reference region. Technetium-99m-MIBI and ^{201}Tl uptake in all other segments were then expressed as the percentage of the activity measured in the reference region.

To assess the normal range for quantitative data analysis, a group of 14 age-matched normal volunteers (13 men, 1 woman) with no evidence of cardiovascular or pulmonary disease was also studied. In these subjects, clinical examination, echocardiograms and stress electrocardiograms were normal. A myocardial segment

TABLE 2
Angiographic Data, Site of Left Ventricular Dysfunction and Technetium-99m-MIBI Redistribution on Delayed Imaging

Patient no.	Coronary artery stenosis (≥50%)	Site of wall motion abnormalities	Site of Segments with ^{99m}Tc-MIBI redistribution
1	LAD, LCx, PDA	Lateral	Lateral, inferoseptal, apical (n = 4)
2	LAD, PDA	Inferior, apical	Inferoseptal, anteroseptal (n = 2)
3	LAD, LCx	Septal, apical	Anteroseptal, apical, inferior (n = 8)
4	LAD, LCx, PDA	Septal, lateral, apical	Inferoseptal, inferolateral, apical (n = 3)
5	PDA	Inferolateral	Inferolateral, septal (n = 5)
6	LAD, PDA	Inferior	None
7	LAD, LCx	Septal, inferoapical, lateral	Apical (n = 1)
8	LAD	Inferoapical	Apical (n = 1)
9	LAD, LCx, PDA	Septal, posterolateral	Inferoseptal (n = 1)
10	LAD, PDA	Anteroapical	Inferolateral, anterior (n = 2)
11	LAD, PDA	Septal, inferolateral	Lateral (n = 1)
12	LCx	Anteroseptal, apical	Anteroseptal, inferolateral (n = 5)
13	LAD, LCx	Septal	None
14	LAD, LCx, PDA	Inferoapical	Inferolateral (n = 1)
15	LAD	Septal	None
16	LAD, LCx, PDA	Anteroseptal, apical	Apical (n = 1)
17	LAD, PDA	Inferoapical	None
18	LAD	Anterior, apical	None
19	PDA	Inferoapical	None
20	LAD, LCx	Anteroseptal	None
21	LAD	Anteroapical, inferior	Anteroseptal, apical (n = 4)
22	LAD, LCx, PDA	Septal	None
23	LAD	Septal	None
24	LAD	Apical	None
25	LAD	Anterior, inferoapical	Inferoseptal (n = 1)
26	LAD, LCx	Anterior, inferior, apical	None
27	LAD	Anterior, apical	Septal (n = 1)
28	LCx, PDA	Septal	Inferoseptal (n = 1)
29	LAD	Anteroseptal	Inferoseptal, inferolateral (n = 3)
30	LAD, LCx, PDA	Inferoapical, septal	Inferolateral (n = 1)
31	LAD	Anteroseptal, apical	Apical (n = 1)

LAD = left anterior descending artery; LCx = left circumflex artery; PDA = posterior descending artery.

was considered abnormal if initial ^{99m}Tc-MIBI or ^{201}Tl uptake was >2 s.d. below the mean observed in the same region for age- and sex-matched normal volunteers. On initial ^{99m}Tc-MIBI images, segments with abnormal uptake were subgrouped on the basis of severity of reduction in tracer activity: moderate (≥50% of peak activity) and severe (<50% of peak) defects, as previously reported (*12,15,16*). On the basis of previous reproducibility measurements performed by other authors and in our laboratory (*12,17*), a segment with reduced activity on initial ^{99m}Tc-MIBI or ^{201}Tl images was considered reversible if the activity increased ≥10% on delayed ^{99m}Tc-MIBI or ^{201}Tl images, respectively. Alternatively, a segment with reduced activity on initial ^{99m}Tc-MIBI or ^{201}Tl images was considered irreversible if the activity did not increase ≥10% or increased ≥10% but remained <50% on delayed ^{99m}Tc-MIBI or ^{201}Tl images, respectively. Thallium-201 irreversible defects were divided on the basis of severity of reduction in tracer activity: moderate (≥50% of peak activity) and severe (<50% of peak) defects, as previously reported (*12,17*).

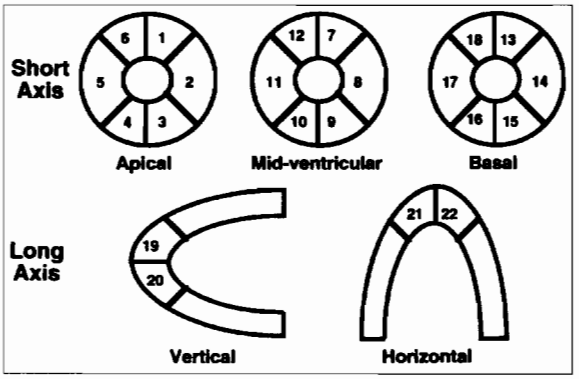

FIGURE 1. Diagram of standard segmentation scheme used for regional quantitative analysis of ^{99m}Tc-MIBI and ^{201}Tl uptake.

Echocardiographic images were interpreted by two experienced observers who were unaware of clinical, radionuclide and angiographic findings. A third investigator blindly reviewed the echocardiograms when the first two observers did not agree. Regional left ventricular function was assessed according to the recommendations of the American Society of Echocardiography (*18,19*). Segmental left ventricular wall motion was graded as: 1, normal; 2, hypokinetic; 3, akinetic; and 4, dyskinetic. The echocardiographic

results were directly compared with those of ^{99m}Tc-MIBI and ^{201}Tl, as previously described (*20*). In the eight patients studied before and after coronary revascularization, a myocardial segment was considered as showing functional recovery when the regional wall motion score was abnormal at baseline and improved at least one echocardiographic grade during the follow-up study, as previously reported (*21*). Conversely, a myocardial segment was considered as showing no functional recovery when regional wall motion score was severely impaired at baseline (grade 3 or 4) and did not change during follow-up (*21*).

Statistical Analysis

Data are expressed as mean ± 1 s.d. Differences in the mean values were assessed by Student's t-test for unpaired data with Bonferroni correction for multiple groups comparison, or Student's t test for paired data, as appropriate. Bonferroni correction establishes that the p value for each comparison should be multiplied by the total number of comparisons undertaken (*22*). The Spearman correlation coefficient (ρ) was used to assess the relationships between wall motion score and tracer uptake. Linear regression was used to evaluate the relationship between LVEF and the number of myocardial segments showing reversible ^{99m}Tc-MIBI defects. Chi square analysis was used to assess differences between proportions. Probability values <0.05 were considered significant.

RESULTS

Technetium-99m-MIBI

A total of 682 myocardial segments were analyzed. On initial ^{99m}Tc-MIBI images, 302 (44%) segments had normal tracer uptake, 183 (27%) showed moderate and 197 (29%) severe reduction of tracer uptake.

Myocardial segments with moderate reduction of ^{99m}Tc-MIBI uptake on the initial images were observed in all 31 patients (range 3–10 segments/patient, mean 5.9 ± 1.9). Of the 183 segments with moderate reduction of ^{99m}Tc-MIBI uptake on initial images, 51 (28%) were reversible on delayed images, showing significant increased tracer uptake (from 61% ± 7% to 78% ± 10% of peak activity, $p<0.001$). Moderate reversible ^{99m}Tc-MIBI defects on delayed images were observed in 23 (74%) patients (range 1–5 segments/patient, mean 2.2 ± 1.2). The remaining 132 (72%) segments with moderate reduction of ^{99m}Tc-MIBI uptake on initial images were irreversible on delayed images, showing no significant change in tracer uptake (from 63% ± 6% to 58% ± 9% of peak activity).

Myocardial segments with severe reduction of ^{99m}Tc-MIBI uptake on initial images were observed in all 31 patients (range 1–14 segments/patient, mean 6.4 ± 3.6). Of the 197 segments with severe reduction of ^{99m}Tc-MIBI uptake on initial images, 47 (24%) were reversible on delayed images, showing significant increased tracer uptake (from 43% ± 8% to 60% ± 8% of peak activity, $p<0.001$) (Fig. 2). Severe reversible ^{99m}Tc-MIBI defects on delayed images were observed in 20 (65%) patients (range 1–8 segments/patient, mean 2.3 ± 1.9) (Table 2). The remaining 150 (76%) segments with severe reduction of ^{99m}Tc-MIBI uptake on the initial images were irreversible on delayed images, showing no significant change in tracer uptake (from 33% ± 12% to 32% ± 12% of peak activity) (Fig. 3). In particular, reversible severe ^{99m}Tc-MIBI defects showed significantly higher tracer uptake on initial images compared to irreversible ^{99m}Tc-MIBI defects (43% ± 8% versus 33% ± 12%, $p<0.001$).

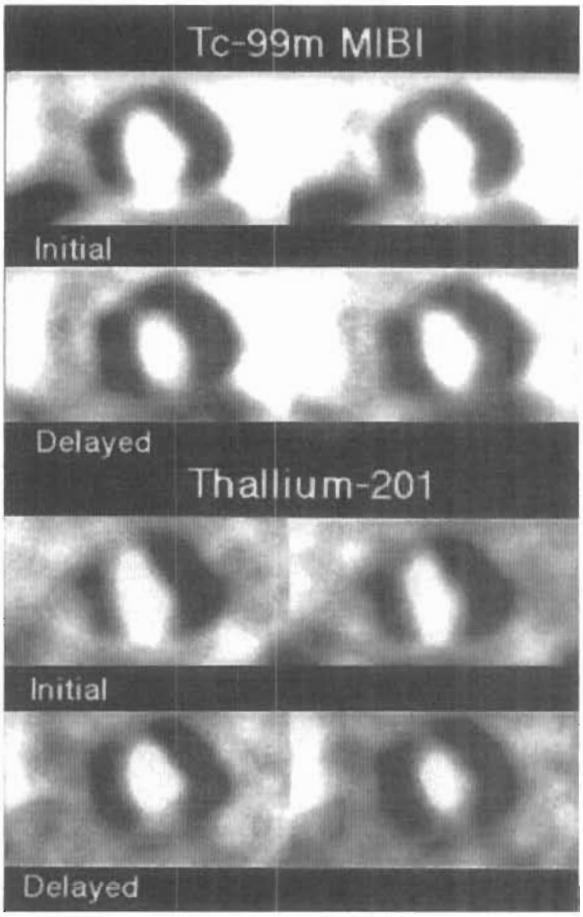

FIGURE 2. Technetium-99m-MIBI cardiac imaging under resting conditions: short-axis slices show a reversible defect involving the septal region (top). Corresponding rest-redistribution ^{201}Tl cardiac tomography: short-axis slices show a reversible defect involving the septal region (bottom).

Thallium-201

Of the 51 myocardial segments with moderate reversible ^{99m}Tc-MIBI defects, 17 had normal thallium uptake, 19 showed reversible and 15 moderate irreversible thallium defects. None of the 132 segments with moderate irreversible ^{99m}Tc-MIBI defects showed severe irreversible thallium defects. In particular, 28 had normal thallium uptake, 31 showed reversible and 73 moderate irreversible thallium defects.

None of the 47 myocardial segments with severe reversible ^{99m}Tc-MIBI defects showed severe irreversible ^{201}Tl defects. In particular, 3 of these segments had normal thallium uptake, 22 showed reversible and 22 moderate

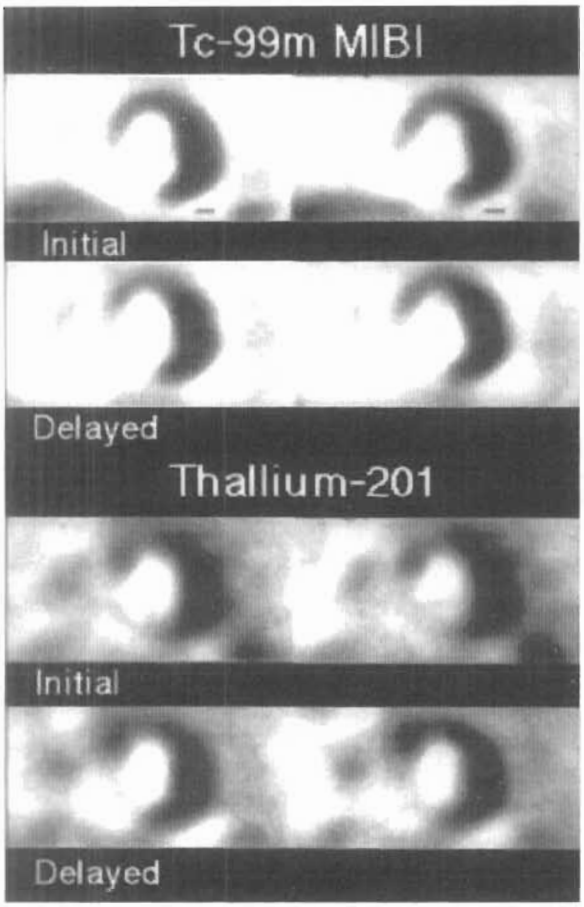

FIGURE 3. Technetium-99m-MIBI cardiac tomography under resting conditions: short-axis slices show a large irreversible defect involving the septal and inferior regions (top). Corresponding rest-redistribution ^{201}Tl cardiac tomography: short-axis slices show a large irreversible defect involving the septal and inferior regions (bottom).

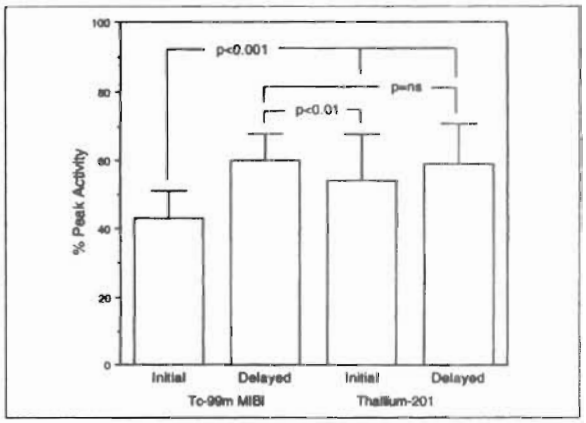

FIGURE 4. Technetium-99m-MIBI and ^{201}Tl uptake (expressed as percentage of peak activity) in myocardial segments with severe reduction of initial ^{99m}Tc-MIBI uptake and increased tracer uptake on delayed images. ns = nonsignificant.

irreversible thallium defects (Fig. 2). On the other hand, the majority (80%) of myocardial segments with severe irreversible ^{99m}Tc-MIBI defects showed severe irreversible ^{201}Tl defects (Fig. 3).

In the 47 myocardial segments with severe reversible ^{99m}Tc-MIBI defects, initial ^{99m}Tc-MIBI uptake was significantly lower ($p<0.001$) compared to both initial and delayed thallium uptake (Fig. 4). On the other hand, in these segments delayed ^{99m}Tc-MIBI uptake was significantly higher ($p<0.01$) compared to initial thallium uptake, but not different from delayed thallium uptake (Fig. 4).

Relation with Left Ventricular Function

Of the total 682 myocardial segments, 332 (49%) showed normal wall motion (Group 1) on echocardiographic images, 160 (23%) were hypokinetic (Group 2) and 190 (28%) were akinetic or dyskinetic (Group 3). Initial and delayed thallium uptake were significantly higher ($p<0.001$) for Group 1 in segments compared with those of Groups 2 and 3 and in Group 2 segments compared to those of Group 3 (Table 3). Similarly, initial and delayed ^{99m}Tc-MIBI uptake were significantly higher ($p<0.001$) in Group 1 segments compared with those of Groups 2 and 3 and in Group 2 segments compared to those of Group 3 (Table 3). A significant relationship ($p<0.001$) between wall motion score and initial ($\rho = -0.45$) and delayed ($\rho = -0.41$) thallium uptake was observed. Similarly, a significant relationship ($p<0.001$) between wall motion score and initial ($\rho = -0.50$) and delayed ($\rho = -0.47$) ^{99m}Tc-MIBI uptake was found. No significant relationship was observed between LVEF and the number of myocardial segments showing moderate and/or severe reversible ^{99m}Tc-MIBI defects.

Follow-up after Coronary Revascularization

In the eight patients studied before and after coronary revascularization, 33 (19%) myocardial segments with wall motion abnormalities showed moderate reduction of ^{99m}Tc-MIBI uptake on initial images. Of these 33 segments, 13 were reversible and 20 did not change on delayed ^{99m}Tc-MIBI images. Moderate reversible ^{99m}Tc-MIBI defects on

TABLE 3.
Initial and Delayed Technetium-99m-MIBI and Thallium-201 Uptake in Myocardial Segments*

	Group 1	Group 2	Group 3
Myocardial segments (no.)	332	160	190
Initial ^{99m}Tc-MIBI uptake (%)	89 ± 13	60 ± 11†	38 ± 16‡
Delayed ^{99m}Tc-MIBI uptake (%)	87 ± 14	62 ± 14†	39 ± 18‡
Initial ^{201}Tl uptake (%)	88 ± 14	65 ± 14†	42 ± 20‡
Delayed ^{201}Tl uptake (%)	87 ± 15	67 ± 14†	45 ± 21‡

*Group 1 = normal wall motion; Group 2 = hypokinetic segments; Group 3 = segments with akinesia or dyskinesia.
†$p < 0.001$ versus Group 1; ‡$p < 0.001$ versus Groups 1 and 2.

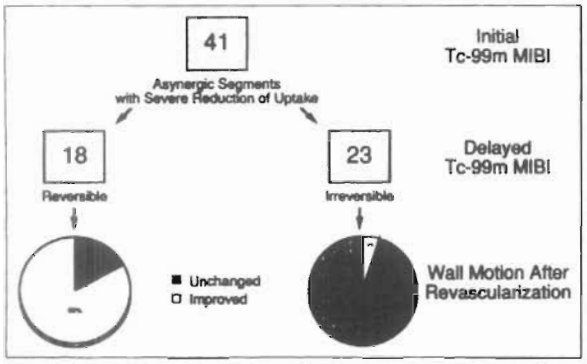

FIGURE 5. Flow diagram shows wall motion after coronary revascularization in asynergic segments with severe reduction of ^{99m}Tc-MIBI uptake on initial images and reversible or irreversible defects on delayed images.

delayed images were observed in seven of these patients (range 0–4 segments/patient, mean 2.1 ± 1.4). The majority of segments with moderate reversible ^{99m}Tc-MIBI defects (85%) showed functional recovery after revascularization. Furthermore, 41 (23%) segments with wall motion abnormalities showed severe reduction of ^{99m}Tc-MIBI uptake on initial images. Of these 41 segments, 18 were reversible and 23 did not change on delayed ^{99m}Tc-MIBI images. Severe reversible ^{99m}Tc-MIBI defects on delayed images were observed in all these patients (range 1–8 segments/patient, mean 3.1 ± 2.6). The majority (83%) of segments with severe reversible ^{99m}Tc-MIBI defects showed functional recovery after revascularization (Fig. 5). Conversely, the majority (96%) of segments with severe irreversible ^{99m}Tc-MIBI defects did not show improved wall motion after revascularization ($p<0.001$ versus severe reversible defects) (Fig. 5). In these patients, LVEF significantly ($p<0.01$) improved after revascularization (from 42% ± 7% at baseline to 47% ± 7% after revascularization).

DISCUSSION

Our results agree with those of Dilsizian et al. (*12*) and demonstrate that in patients with chronic CAD and left ventricular dysfunction ^{99m}Tc-MIBI redistribution on delayed images occurs in 24% to 38% of myocardial segments with severe reduction of tracer uptake at rest. Delayed ^{99m}Tc-MIBI imaging improves the differentiation between ischemic but still viable myocardium from fibrotic tissue in regions with severe reduction of resting ^{99m}Tc-MIBI uptake. Furthermore, ^{99m}Tc-MIBI redistribution is predictive of functional recovery following coronary revascularization.

Technetium-99m-MIBI Identification of Myocardial Viability

Previous clinical studies demonstrated that severe reduction of ^{99m}Tc-MIBI uptake underestimates the presence of viable myocardium in patients with chronic CAD and left ventricular dysfunction (*12,15,16,23–31*). In particular, comparative studies between ^{99m}Tc-MIBI scintigraphy and metabolic imaging with [^{18}F] fluorodeoxyglucose showed that ^{99m}Tc-MIBI myocardial uptake on conventional 1-hr imaging is mainly related to regional coronary blood flow rather than tissue viability (*15,31*). Experimental studies, however, have shown that myocardial retention of ^{99m}Tc-MIBI depends not only on coronary blood flow but also on cellular viability (*5,6*). Furthermore, recent clinical reports suggest that quantitative analysis of resting ^{99m}Tc-MIBI may enhance differentiation between viable myocardium from necrotic tissue in patients with chronic ischemic left ventricular dysfunction (*12,32*).

Technetium-99m-MIBI Redistribution

The occurrence of ^{99m}Tc-MIBI redistribution has been previously demonstrated in a model of transient ischemia or under conditions of sustained reduced coronary blood flow (*3,4*). In particular, Li et al. showed that normalization of ^{99m}Tc-MIBI defects in ischemic regions is progressive over time and that such redistribution is detectable on tomographic images and also confirmed by serial myocardial biopsies (*3*). Sinusas et al. recently demonstrated that ^{99m}Tc-MIBI redistributes in the presence of severe coronary artery stenosis, as documented by gamma well counting techniques and by high-resolution postmortem gamma camera imaging of myocardial slices (*4*). In clinical studies, there are conflicting data on ^{99m}Tc-MIBI redistribution after stress imaging. Taillefer et al. (*10*) described a decrease in ^{99m}Tc-MIBI defect size after exercise with serial planar imaging between 1 hr and 3 hr following stress injection. On the other hand, Villanueva-Meyer et al. (*11*) recently reported no change in defect size between 1 and 4 hr after stress ^{99m}Tc-MIBI injection using quantitative tomographic imaging. Dilsizian et al. recently described redistribution of ^{99m}Tc-MIBI after rest injection in a small number of patients with chronic CAD and severe left ventricular dysfunction (*12*). Its clinical utility, however, has not yet gained wide application.

The results of the present study show the occurrence of ^{99m}Tc-MIBI redistribution after rest injection in patients with chronic ischemic left ventricular dysfunction, suggesting that acquisition of delayed images after resting ^{99m}Tc-MIBI injection may enhance the detection of severely hypoperfused but still viable myocardium. We focused our analysis on the clinical significance of ^{99m}Tc-MIBI redistribution in myocardial segments with severe reduction of tracer uptake on initial images, in whom the presence of viable tissue is in question. In particular, 24% of segments with severe reduction of ^{99m}Tc-MIBI uptake on initial images showed a significant increase in tracer uptake on delayed images. Our results with earlier data of Dilsizian et al. in a group of patients with chronic CAD (*12*). These authors described ^{99m}Tc-MIBI redistribution in 38% of myocardial segments with irreversible defects on stress-rest ^{99m}Tc-MIBI imaging (*12*). Furthermore, our results confirm the experimental evidence of resting ^{99m}Tc-MIBI redistribution in a model of sustained coronary low flow (*4*).

In our study, the occurrence of ^{99m}Tc-MIBI redistribution on delayed images in myocardial segments with severe reduction of ^{99m}Tc-MIBI uptake on initial images was observed in 65% of the patients. This finding may be clinically relevant since it demonstrates that ^{99m}Tc-MIBI redistribution may occur in a substantial number of patients with chronic ischemic left ventricular dysfunction.

Comparison with Thallium-201 Imaging

The results of rest-redistribution ^{201}Tl cardiac imaging in myocardial segments with ^{99m}Tc-MIBI redistribution support the hypothesis that these regions may contain hypoperfused but viable myocardium. In particular, each segment showed evidence of myocardial viability according to thallium imaging criteria. In myocardial segments with severe reversible ^{99m}Tc-MIBI defects, initial ^{99m}Tc-MIBI uptake was significantly lower compared to both initial and delayed thallium uptake. A possible explanation for this finding could be that only segments with severe reduction of initial ^{99m}Tc-MIBI uptake and increased tracer activity on delayed images were included in the analysis. Moreover, none of these segments showed severe irreversible thallium defects. On the other hand, delayed ^{99m}Tc-MIBI uptake was significantly higher compared to initial thallium uptake but not different compared to delayed thallium uptake. These data correlate with previous comparative studies between ^{201}Tl and ^{99m}Tc-MIBI cardiac imaging (*26–29*). Furthermore, Dilsizian et al. recently reported concordant results between resting ^{99m}Tc-MIBI redistribution and ^{201}Tl reinjection imaging studies (*12*). These findings suggest that resting ^{99m}Tc-MIBI redistribution imaging identifies the presence of hypoperfused but viable myocardium in patients with chronic ischemic left ventricular dysfunction. Thus, it may have important clinical implications.

Follow-up after Coronary Revascularization

Although thallium uptake is usually considered an accurate marker of myocardial viability in patients with chronic CAD (*33–40*), the definite gold standard for the presence of viable tissue in such patients is functional recovery after coronary revascularization (*41*). In the present study, we evaluated whether resting ^{99m}Tc-MIBI redistribution is predictive of improved left ventricular function after coronary revascularization and, thus, of myocardial viability. Our results obtained after revascularization support the hypothesis that ^{99m}Tc-MIBI redistribution reflects the presence of viable myocardium. In fact, the majority of segments with severely impaired ventricular function and increased ^{99m}Tc-MIBI uptake on delayed images showed improved wall motion after revascularization. Conversely, the majority of akinetic segments with no change on delayed ^{99m}Tc-MIBI images did not show functional recovery after coronary revascularization. Furthermore, a significant improvement of global LVEF was observed after coronary revascularization. Therefore, these findings demonstrate that delayed redistribution cardiac imaging after resting ^{99m}Tc-MIBI injection can detect severely hypoperfused but still viable myocardium as well as predict reversibility of severe regional wall motion abnormalities after coronary revascularization in patients with chronic ischemic left ventricular dysfunction.

Study Limitations

Two potential limitations of this study deserve comment. First, follow-up evaluation after coronary revascularization was obtained in a limited number of the patients in whom resting ^{99m}Tc-MIBI redistribution was observed. Although our data need confirmation in larger series of patients, the follow-up results of the present study confirm and may be considered representative of the enhanced detection of viable myocardium by resting ^{99m}Tc-MIBI cardiac imaging using delayed acquisition. Second, since there are no established criteria in the literature to assess the severity of ^{99m}Tc-MIBI defects, the selection of the threshold value for severely reduced ^{99m}Tc-MIBI uptake was chosen arbitrarily. The same threshold, however, has been used in previous studies (*12,15,16*).

CONCLUSION

Resting ^{99m}Tc-MIBI redistribution frequently occurs in patients with chronic CAD and left ventricular dysfunction. Acquisition of delayed ^{99m}Tc-MIBI images enhances the differentiation between severely hypoperfused, but still viable myocardium from fibrotic tissue in such patients. The presence of ^{99m}Tc-MIBI redistribution may be predictive of functional recovery after coronary revascularization. Therefore, our results suggest that resting ^{99m}Tc-MIBI cardiac imaging should be delayed when assessing myocardial viability in patients with chronic CAD.

REFERENCES

1. Okada RD, Glover D, Gaffney T, Williams S. Myocardial kinetics of technetium-99m-hexakis-2-methoxy-2-methylpropyl-isonitrile. *Circulation* 1988; 77:491–498.
2. Canby RC, Silber S, Pohost GM. Relations of the myocardial imaging agents Tc-99m MIBI and Tl-201 to myocardial blood flow in a canine model of myocardial ischemic insult. *Circulation* 1990;81:289–296.
3. Li QS, Solot A, Frank TL, Wagner HN, Becker LC. Myocardial redistribution of technetium-99m methoxy isobutyl isonitrile (sestamibi). *J Nucl Med* 1990;31:1069–1076.
4. Sinusas AJ, Bergin JD, Edwards NC, et al. Redistribution of Tc-99m sestamibi and Tl-201 in the presence of a severe coronary artery stenosis. *Circulation* 1994;89:2332–2341.
5. Beanlands RSB, Dawood F, Wen WH, et al. Are the kinetics of technetium-99m-methoxyisobutyl isonitrile affected by cell metabolism and viability? *Circulation* 1990;82:1802–1814.
6. Freeman I, Grunwald AM, Hoory S, Bodenheimer MM. Effect of coronary occlusion and myocardial viability on myocardial activity of technetium-99m-sestamibi. *J Nucl Med* 1991;32:292–299.
7. Glover DK, Okada RD. Myocardial technetium-99m sestamibi kinetics after reperfusion in a canine model. *Am Heart J* 1993;125:657–666.
8. Beller GA, Glover DK, Edwards NC, Ruiz M, Simanis JP, Watson DD. Technetium-99m-sestamibi uptake and retention during myocardial ischemia and reperfusion. *Circulation* 1993;87:2033–2042.
9. Merhi J, Arsenault A, Latour JG. Time course of technetium-99m-sestamibi myocardial distribution in dogs with a permanent or transient coronary occlusion. *Eur J Nucl Med* 1994;21:481–487.
10. Taillefer R, Primeau M, Costi P, Lambert R, Leveille J, Latour Y. Technetium-99m-sestamibi myocardial perfusion imaging in detection of coronary artery disease: comparison between initial (1-hour) and delayed (3-hour) postexercise. *J Nucl Med* 1991;32:1961–1965.
11. Villanueva-Meyer J, Mena I, Diggles L, Narahara KA. Assessment of myocardial perfusion defect size after early and delayed SPECT imaging with

technetium-99m-hexakis 2-methoxyisobutyl isonitrile after stress. *J Nucl Med* 1993;34:187–192.
12. Dilsizian V, Arrighi JA, Diodati JG, et al. Myocardial viability in patients with chronic coronary artery disease. Comparison of ^{99m}Tc-sestamibi with thallium reinjection and [^{18}F]fluorodeoxyglucose. *Circulation* 1994;89:578–587.
13. Cuocolo A, Soricelli A, Pace L, et al. Adenosine technetium-99m methoxy isobutyl isonitrile myocardial tomography in patients with coronary artery disease: comparison with exercise. *J Nucl Med* 1994;35:1110–1115.
14. Borrello JA, Clinthorne NH, Rogers WL, Thrall JH, Keyes JW. Oblique-angle tomography: a reconstructing algorithm for transaxial tomographic data. *J Nucl Med* 1981;22:471–473.
15. Sawada SG, Allman KC, Muzik O, et al. Positron emission tomography detects evidence of viability in rest technetium-99m sestamibi defects. *J Am Coll Cardiol* 1994;23:92–98.
16. Rocco TP, Dilsizian V, Strauss HW, Boucher CA. Technetium-99m isonitrile myocardial uptake at rest. II. Relation to clinical markers of potential viability. *J Am Coll Cardiol* 1989;14:1678–1684.
17. Maurea S, Cuocolo A, Soricelli A, et al. Enhanced detection of viable myocardium by technetium-99m methoxy isobutyl isonitrile tomography after nitrates administration in patients with chronic coronary artery disease. *J Nucl Med* 1945;36:1945–1952.
18. Henry WL, De Maria A, Feigenbaum H, et al. Report of the American Society of Echocardiography Committee on nomenclature and standards: Identification of Myocardial Wall Segments. American Society of Echocardiography, November 1982, North Carolina: Duke University Medical Center.
19. Shiller NB, Shah PM, Crawford M, et al. American Society of Echocardiography Committee on Standards, Subcommittee on Quantitation of Two-dimensional Echocardiograms: recommendations for quantitation of the left ventricle by two-dimensional echocardiography. *J Am Soc Echo* 1989;2:358–367.
20. Pozzoli MMA, Fioretti PM, Salustri A, Reijis AEM, Roelandt JRTC. Exercise echocardiography and technetium-99m MIBI single-photon emission computed tomography in the detection of coronary artery disease. *Am J Cardiol* 1991;67:350–355.
21. Marzullo P, Parodi O, Reisenhofer B, et al. Value of rest thallium-201/technetium-99m sestamibi scans and dobutamine echocardiography for detecting myocardial viability. *Am J Cardiol* 1993;71:166–172.
22. Matthews DE, Farewell V. Data analysis. A formal discussion of multiple comparisons. In: *Using and understanding medical statistics*. Basel: Karger S; 1985:169–172.
23. Cuocolo A, Pace L, Ricciardelli B, Chiariello M, Trimarco B, Salvatore M. Identification of viable myocardium in patients with chronic coronary artery disease: comparison of thallium-201 scintigraphy with reinjection and technetium-99m-methoxyisobutyl isonitrile. *J Nucl Med* 1992;33:505–511.
24. Marzullo P, Sambuceti G, Parodi O. The role of sestamibi scintigraphy in the radioisotopic assessment of myocardial viability. *J Nucl Med* 1992;33:1925–1930.
25. Altehoefer C, Kaiser HJ, Dorr R, et al. Fluorine-18-deoxyglucose PET for assessment of viable myocardium in perfusion defects in Tc-99m-MIBI SPECT: a comparative study in patients with coronary artery disease. *Eur J Nucl Med* 1992;19:334–342.
26. Dondi M, Tartagni F, Fallani F, et al. A comparison of rest sestamibi and rest-redistribution thallium single photon emission tomography: possible implications for myocardial viability detection in infarcted patients. *Eur J Nucl Med* 1993;20:26–31.
27. Maurea S, Cuocolo A, Pace L, et al. Rest-injected thallium-201 redistribution and resting technetium-99m methoxy isobutyl isonitrile uptake in coronary artery disease: relation to the severity of coronary artery stenosis. *Eur J Nucl Med* 1993;20:502–510.
28. Cuocolo A, Maurea S, Pace L, et al. Resting technetium-99m-methoxy isobutyl isonitrile cardiac imaging in chronic coronary artery disease: comparison with rest-redistribution thallium-201 scintigraphy. *Eur J Nucl Med* 1993;20:1186–1192.
29. Maurea S, Cuocolo A, Pace L, et al. Left ventricular dysfunction in coronary artery disease: comparison between rest-redistribution thallium-201 and resting technetium-99m-methoxy isobutyl isonitrile cardiac imaging. *J Nucl Cardiol* 1994;1:65–71.
30. Maurea S, Cuocolo A, Nicolai E, Salvatore M. Improved detection of viable myocardium by thallium-201 reinjection in chronic coronary artery disease: comparison with technetium-99m-MIBI imaging *J Nucl Med* 1994;35:621–624.
31. Altehoefer C, vom Dahl J, Biedermann M, et al. Significance of defect severity in technetium-99m-MIBI SPECT at rest to assess myocardial viability: comparison with fluorine-18-FDG PET. *J Nucl Med* 1994;35:569–574.
32. Udelson JE, Coleman PS, Metherall J, et al. Predicting recovery of severe regional ventricular dysfunction. Comparison of resting scintigraphy with Tl-201 and Tc-99m sestamibi. *Circulation* 1994;89:2552–2561.
33. Bonow RO, Dilsizian V, Cuocolo A, Bacharach SL. Identification of viable myocardium in patients with chronic coronary artery disease and left ventricular dysfunction. Comparison of thallium scintigraphy with reinjection and PET imaging with ^{18}F-fluorodeoxyglucose. *Circulation* 1991;83:26–37.
34. Dilsizian V, Perrone-Filardi P, Arrighi JA, et al. Concordance and discordance between stress-redistribution-reinjection and rest-redistribution thallium imaging for assessing viable myocardium. Comparison with metabolic activity by positron emission tomography. *Circulation* 1993;88:941–952.
35. Kiat H, Berman DS, Maddahi J, et al. Late reversibility of tomographic myocardial thallium-201 defects. An accurate marker of myocardial viability. *J Am Coll Cardiol* 1988;12:1456–1463.
36. Kayden DS, Sigal S, Soufer R, Mattera J, Zaret BL, Wackers FJ. Thallium-201 for assessment of myocardial viability: quantitative comparison of 24-hour redistribution imaging with imaging after reinjection at rest. *J Am Coll Cardiol* 1991;18:1480–1486.
37. Dilsizian V, Smeltzer WR, Freedman NMT, Dextras R, Bonow RO. Thallium reinjection after stress-redistribution imaging. Does 24-hour delayed imaging after reinjection enhance detection of viable myocardium? *Circulation* 1991;83:1247–1255.
38. Mori T, Minamiji K, Kurogane H, Ogawa K, Yoshida Y. Rest-injected thallium-201 imaging for assessing viability of severe asynergic regions. *J Nucl Med* 1991;32:1718–1724.
39. Ragosta M, Beller GA, Watson DD, Kaul S, Gimple LW. Quantitative planar rest-redistribution Tl-201 imaging in detection of myocardial viability and prediction of improvement in left ventricular function after coronary bypass surgery in patients with severely depressed left ventricular function. *Circulation* 1993;87:1630–1641.
40. Altehoefer C, vom Dahl J, Buell U, Uebis R, Kleinhans E, Hanrath P. Comparison of thallium-201 single-photon emission tomography after rest injection and fluorodeoxyglucose positron emission tomography for assessment of myocardial viability in patients with chronic coronary artery disease. *Eur J Nucl Med* 1994;21:37–45.
41. Braunwald E, Rutherford JD. Reversible ischemic left ventricular dysfunction: evidence for "hibernating" myocardium. *J Am Coll Cardiol* 1986;8:1467–1470.

Comparison of Hypoxia and Ouabain Effects on the Myocardial Uptake Kinetics of Technetium-99m Hexakis 2-Methoxyisobutyl Isonitrile and Thallium-201

Denis J. Meerdink and Jeffrey A. Leppo

Department of Nuclear Medicine and Department of Medicine, Cardiology, University of Massachusetts Medical Center, Worcester, Massachusetts

Effects of hypoxia and ouabain on transcapillary exchange of [^{99m}Tc]hexakis (2-methoxyisobutylisonitrile) [SESTAMIBI, also known as MIBI or HEXAMIBI] and ^{201}Tl were investigated with indicator-dilution studies using isolated rabbit hearts. Peak myocardial extraction (Emax), permeability-surface area products (PScap), and net myocardial extraction (Enet) were compared among serial injections during constant coronary flows. Overall, measures of transcapillary transport (Emax and PScap) for SESTAMIBI were significantly lower ($p < 0.001$) than those simultaneously determined for thallium, but estimates of tissue retention (Enet) for SESTAMIBI and thallium were not statistically distinguishable. Hypoxia had no significant effect on mean (±s.d.) Emax for SESTAMIBI (0.31 ± 0.13) or thallium (0.59 ± 0.11), nor on mean PScap or Enet values. Ouabain (1.5×10^{-7} *M* and 1.5×10^{-6} *M*) had no effect on SESTAMIBI or thallium Emax (respectively, 0.29 ± 0.08 and 0.60 ± 0.05) or on PScap for SESTAMIBI. Thallium PScap was depressed with higher ouabain dose (control, 1.22 ± 0.40; high ouabain, 1.06 ± 0.41 ml/min/g; $p < 0.01$). Ouabain also caused a significant and progressive increase in average SESTAMIBI Enet (control, 0.23 ± 0.10 to high ouabain, 0.33 ± 0.12; $p < 0.05$), but depressed thallium Enet (control, 0.38 ± 0.14 to high ouabain, 0.32 ± 0.18; $p < 0.01$). These results suggest myocardial metabolic and/or functional status have minor influence on transcapillary transport of SESTAMIBI and thallium, but significantly affects cellular retention.

J Nucl Med 30: 1500–1506, 1989

Technetium-99m- (^{99m}Tc) labeled agents have been proposed as alternatives to thallium-201 (^{201}Tl) for imaging myocardial perfusion imaging because of better photon statistics, Anger camera imaging properties, cost, and clinical availability (*1–4*). Clinical images from [^{99m}Tc]-labeled isonitriles compare favorably to those obtained with thallium (*3,5*). Specifically, [^{99m}Tc] hexakis (t-butylisonitrile) (TBI) and its ether derivate, [^{99m}Tc]hexakis 2-methoxyisobutyl isonitrile (SESTAMIBI, also known as MIBI, HEXAMIBI, or RP-30; DuPont Company, No. Billerica, MA), have suitable kinetic characteristics and have shown good potential in preliminary clinical studies. SESTAMIBI, in particular, may have appeal for cardiac studies because of its low lung extraction compared to TBI (*6*).

The interpretation of perfusion images of cardiac uptake for these agents is facilitated from knowledge of the capillary exchange process. To assume that clinical perfusion images realistically represent myocardial blood flow, it must be known that the imaging agent is deposited in myocardial tissue in proportion to the blood it receives, and that this deposition is unaltered by metabolic or functional abnormalities. No previous studies have determined the effects of metabolic aberrations on the transcapillary transport of both thallium and SESTAMIBI in the same hearts with constant coronary flow. Accordingly, the goal of this report was to determine the flow-independent effects of hypoxia and ouabain on myocardial uptake kinetics of these two perfusion agents.

Received Jan. 30, 1989; revision accepted Apr. 20, 1989.

For reprints contact: D. J. Meerdink, PhD, Dept. of Nuclear Medicine, University of Massachusetts Medical Center, 55 Lake Ave., North, Worcester, MA 01655.

MATERIALS AND METHODS

Experimental Preparation

Surgery and perfusion. An isolated, isovolumetrically-contracting rabbit heart preparation, utilizing methods previously described in detail (*7–9*), was used for all experiments. Briefly, male New Zealand white rabbits (1.5–2.5 kg) were heparinized (600 IU/kg i.v.) and anesthetized (sodium pentobarbital, 40 mg/kg i.v.), and the hearts were quickly removed and mounted on a perfusion apparatus (*9*). For hypoxia experiments, the nonrecirculating perfusate consisted of a modified Krebs-Henseleit bicarbonate buffer, pH 7.4, that contained (m*M*): NaCl, 122; $NaHCO_3$, 22; glucose, 5.5; KCl, 4.7; $MgSO_4$, 1.2; $CaCl_2$, 2; KH_2PO_4, 1.2; lactate (neutralized with NaOH), 1; and Na_2EDTA, 0.4. Normoxic buffer and hypoxic buffer were bubbled with 95% O_2/5% CO_2 and 95% N_2/5% CO_2, respectively, for a minimum of 30 min prior to heart perfusion. For ouabain experiments, the perfusate was blood obtained from a second heparinized, anesthetized rabbit as previously described (*8,9*), which recirculated except when indicator dilution injections were made. The blood passed through a membrane oxygenator that was gassed with a 3% CO_2 and air mixture. During experimentation, blood gas measurements were made every 30–40 min, and appropriate adjustments were made with supplemental O_2 and bicarbonate to maintain blood pH. P_{O2}, and P_{CO2} in the physiologic range. Glucose levels were also monitored and adjusted as needed to maintain approximately 100 mg/dl.

For both hypoxia and ouabain protocols, mean coronary perfusion pressure was maintained at 100–125 mmHg by a constant flow pump. A thermistor and pacing catheter were placed in the right ventricle via the right atrium to monitor tissue temperature (37 ± 1°C) and maintain a heart rate of at least 180 bpm. A plastic cannula was also placed in the right ventricle via the pulmonary artery for collecting coronary sinus drainage samples and measuring coronary flow. A latex rubber balloon was inserted and secured into the left ventricle, and filled with saline until an end-diastolic pressure of 5–10 mmHg was recorded. A plastic cannula, placed in the left ventricle at its apex, drained aortic valve leakage, and Thebesian vein flow. Mean aortic pressure, left ventricle (LV) pressure, and the first derivative of LV pressure were continuously recorded. The experimental protocols (described below) began after temperature, ventricular pressure, contraction rate, coronary flow, and aortic pressure stabilized.

SESTAMIBI preparation. The SESTAMIBI salt [supplied by DuPont Company; (*2*)] and formamidine sulfinic acid (FSA) were prepared as a 4 mg/ml and 0.4 mg/ml solution, respectively, in distilled water. A 0.5-ml aliquot of each of the SESTAMIBI and FSA solutions were combined in a nitrogen-purged vial, and ~0.2–0.4 ml of $^{99m}TcO_4^-$ (370 MBq, 10 mCi) was added. The vial was quickly placed in boiling water for 10–15 min and then allowed to cool to room temperature. Binding efficiency was evaluated by thin layer chromatography (*9*), and was always ≥95%.

Isotope injection and sample collection. The indicator cocktail, consisting of a mixture of 20 μCi (0.74 MBq) of indium-111- (^{111}In) labeled albumin (*10*), 35 μCi (1.3 MBq) of $^{201}TlCl$, and 90 μCi (3.3 MBq) of [^{99m}Tc]SESTAMIBI dissolved in perfusate, was thoroughly mixed and a 0.3-ml bolus was loaded into an injection loop that ran parallel to and joined with the aortic inflow with three-way valves. Isotope injection proceeded by rapidly turning the three-way valves so that the bolus was as homogeneously distributed as possible to both coronary arteries. Coronary venous effluent was collected into preweighed plastic tubes at 1.2- to 5-sec intervals (depending on flow rate) over a 0.5–4 min collection time. Coronary flow was measured before and after injections; results were discarded if flows changed more than 10%. Full sample weights were measured, and isotope activities were determined in each sample along with a 0.1-ml aliquot of each injectate by a gamma well counter with corrections for energy crossover, time, background, and physical decay during the counting process. When multiple injections (at constant flow) were made in an individual heart, isotope backgrounds were <1% of peak activity in all instances. In addition, the wet weight of a portion of the left ventricular free wall was determined for subsequent estimation of the tissue water fraction (*7*).

Myocardial transport analysis. For each injection, transcapillary exchange estimates were determined using standard indicator dilution techniques and equations (*9,11,12*). Briefly, normalized transport function curves for albumin [reference, $h_R(t)$] and for SESTAMIBI and thallium [diffusible tracers, $h_D(t)$] were calculated from the general equation, $h(t) = F_s \cdot C(t)/q_o$, where Fs is plasma flow (ml/min/g), t is time (sec), C(t) is isotope activity, and q_o is injected dose. The instantaneous fractional extraction [E(t)] for SESTAMIBI and thallium was calculated for each sample with the equation, $E(t) = 1 - h_D(t)/h_R(t)$, and the capillary permeability-surface area product (PScap, ml/min/g) was calculated with the equation, $PScap = -F_s \cdot \log_e(1-E_{max})$ (*13*). Emax was defined as the maximum E(t) of diffusible tracer observed up to the peak $h_R(t)$, which is the best estimate of average functional extraction (*11,14*). Net tissue extraction (Enet), an estimate of tissue retention, was calculated from normalized time integrals of transport function differences between reference and diffusible tracers with the equation (*14*): $Enet = \int_0^t[h_R(t)-h_D(t)]d\tau / \int_0^t h_R(t)d\tau$, where t was defined as the time (sec) when 99.99% of the albumin reference had emerged in the venous effluent, and τ was the dummy variable for integration.

Results were analyzed with paired t-tests and repeated-measures analysis of variance routines (*15*) and comparisons made among treatments within the hypoxia or ouabain experimental series (*16*).

Experimental Protocols

Hypoxia. To study the effects of hypoxia, eight hearts were initially perfused with buffer gassed with 95% oxygen/5% carbon dioxide and allowed to stabilize for ~10 min, after which the control injection of tracer cocktail was made. The perfusion buffer was then changed to one made hypoxic by gassing with 95% nitrogen/5% carbon dioxide; after 2 and 5 min of hypoxic perfusion, the first and second experimental injections were made while coronary flow remained constant.

Ouabain. Ouabain effects were evaluated in 11 hearts perfused with recirculating blood at constant flow. Following a stabilization period of ~15 min, a control injection was made, after which a ouabain solution was infused into the system over 5 min so that a concentration of 1.5×10^{-7} *M* (LOW dose) was achieved in the recirculating blood. This typically resulted in a transient rise in +dP/dt, but as LV end diastolic pressure began to increase, positive inotropic response could

not be sustained. After the first ouabain dose circulated at least 15 min, the first experimental injection of indicator cocktail was made. A second dose of ouabain was given over 5 min, increasing the ouabain concentration to 1.5×10^{-6} *M* (HIGH dose). The second experimental dilution study was made after the HIGH dose circulated at least 15 min. These ouabain concentrations were based on therapeutic (LOW) and toxic (HIGH) concentrations (*17,18*). Ventricular ectopy increased greatly during these infusions, strongly implying that the ouabain infusions produced pharmacologic concentrations.

Results were reported as mean (±s.d.), and considered significantly different with a probability of 0.05 or less. Statistical analysis included the paired Student's t-test and analysis of variance (uni- and multi-variant, and repeated measures) (*16*), and was performed using the Statistical Analysis System (*15*).

RESULTS

Average (±s.d.) results for the hypoxia and ouabain studies (respectively) include: body weight, 2.22 (±0.18) and 1.67 (±0.11) kg; wet heart weights, 6.03 (±0.55) and 5.41 (±0.36) g; and tissue water fraction, 0.85 (±0.01) and 0.73 (±0.01). Significant differences ($p < 0.02$) existed between hypoxia and ouabain experiments for only body weight and tissue water fraction.

Hemodynamics

Average (±s.d.) results for hemodynamic measurements appear in Table 1. These parameters were not affected by the injection of isotope cocktail during hypoxia or ouabain experiments (data not shown). Repeated-measures analysis of variance of control, 2-, and 5-min hypoxia injections indicate no significant change in coronary perfusion rates, but significant decreases ($p < 0.001$) existed in aortic pressure, peak systolic pressure, +dP/dt, and −dP/dt. The 30% decline in aortic pressure (i.e., perfusion pressure) after 2 min of hypoxic perfusion was not further depressed at 5 min of hypoxia, which indicates a prompt and maximal reduction in vascular resistance. The progressive decline in developed systolic pressure, +dP/dt, and −dP/dt as well as an increase of end diastolic pressure after 2 and 5 min of hypoxia, reflects the severe functional compromise induced by hypoxia. In ouabain experiments, no significant change was noted in perfusion rate, but a small increase in end diastolic pressure reached statistical significance ($p < 0.05$).

Indicator Dilution Analysis

Examples of the indicator transport functions [h(t)] and instantaneous extraction [E(t)] appear in Figure 1 for a control injection. Differences in the height and shape of the h(t) and E(t) curves between thallium and SESTAMIBI suggest fundamental differences in their mechanisms of transcapillary transport. The h(t) curve for thallium is much lower than the SESTAMIBI h(t), which indicates a higher peak extraction (Emax) for thallium.

The tail portion of the h(t) curves also reveal fundamental differences in the extravascular distribution of thallium and SESTAMIBI. The transport function curve [h(t)] for thallium crosses and remains above the reference albumin, which indicates a net flux of initially extracted thallium from the myocardial tissue back into the vascular space. In contrast, SESTAMIBI h(t) remains below the albumin reference h(t) throughout the observation period, indicating relatively little back diffusion of SESTAMIBI.

The E(t) curves for thallium and SESTAMIBI are also quite different, which also reveals their different

TABLE 1
Hemodynamic Results*

	Coronary Flow (ml/min/g)	Aortic Pressure (mm Hg)	Peak Systolic Pressure (mm Hg)	End Diastolic Pressure (mm Hg)	+dP/dt (mm Hg/s)	−dP/dt (mm Hg/s)
Hypoxia						
Control	5.52 (1.47)	47.0 (10.3)	77.9 (12.6)	6.5 (0.9)	1630 (284)	1362 (327)
2 min.	5.49 (1.51)	39.6 (15.4)	50.8 (28.4)	9.3 (6.4)	1176 (564)	877 (493)
5 min.	5.48 (1.56)	32.3 (11.6)	32.9 (12.9)	12.3 (10.1)	586 (234)	418 (146)
p**	NS	<0.001	<0.001	<0.001	<0.001	<0.001
Ouabain						
Control	1.96 (0.63)	120.4 (25.3)	63.3 (18.0)	12.1 (5.4)	1261 (546)	658 (424)
LOW Dose	1.96 (0.62)	131.1 (27.8)	62.8 (21.9)	18.4 (10.6)	1196 (812)	658 (563)
HIGH Dose	1.89 (0.69)	154.0 (37.8)	68.0 (29.4)	19.9 (15.0)	1602 (1292)	800 (676)
p**	NS	<0.01	<0.03	NS	NS	NS

* Mean ± s.d.
** Probability of equality as determined by repeated-measures analysis of variance (15).
NS = not significant.

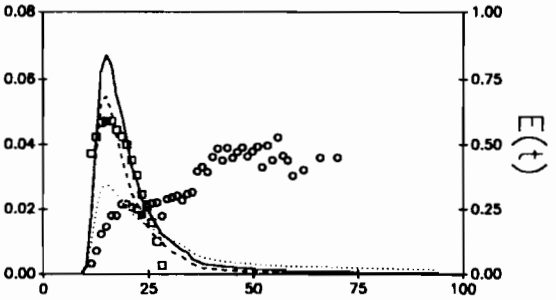

FIGURE 1
Representative plot of the transport function [h(t)] and instantaneous fractional extraction [E(t)] versus sampling time. The left ordinate are the h(t) values for [^{111}In]albumin (solid line), [^{99m}Tc]SESTAMIBI (dashed line), and ^{201}Tl (dotted line). The right ordinate are the E(t) values for [^{99m}Tc]SESTAMIBI (open circles) and ^{201}Tl (open squares).

transport mechanisms. Thallium E(t) has an early maximal plateau phase followed by rapid fall, which is typical for cations, while SESTAMIBI E(t) displays an early rise and sustained, slowly rising plateau throughout the h(t) curve.

Extraction. Average (±s.d.) maximal instantaneous extractions (Emax) of thallium and SESTAMIBI appear in Figure 2. For all injections in both hypoxia and ouabain experiments, SESTAMIBI Emax determinations were significantly lower ($p < 0.001$) than concurrently-measured thallium values, averaging 48% and 43% lower ($p < 0.001$) in hypoxia and ouabain experiments, respectively. In hypoxia experiments, analysis of variance (repeated measures) and paired t-tests revealed no significant Emax differences for thallium or SESTAMIBI in either experimental injection from their respective control determinations (Fig. 2A). In ouabain experiments (Fig. 2B), Emax for SESTAMIBI tended to increase and thallium tended to decrease, although no statistically significant differences were revealed between experimental injections and their respective controls.

Permeability. Figure 3 illustrates the mean (±s.d.) PScap determinations for thallium and SESTAMIBI for hypoxia and ouabain experiments. PScap for SESTAMIBI averaged 58% of those for thallium for hypoxia experiments and 48% lower in ouabain experiments. In hypoxia experiments (Fig. 3A), PScap values for SESTAMIBI were significantly less ($p < 0.001$) than simultaneously-determined thallium estimates in each of the three injections. Hypoxia treatment also did not significantly change SESTAMIBI or thallium values from their respective controls. In contrast, PScap averages for SESTAMIBI in ouabain experiments (Fig. 3B) were significantly less ($p < 0.02$) than thallium only for control and LOW dose injections, but not for HIGH dose injections. In addition, thallium PScap declined

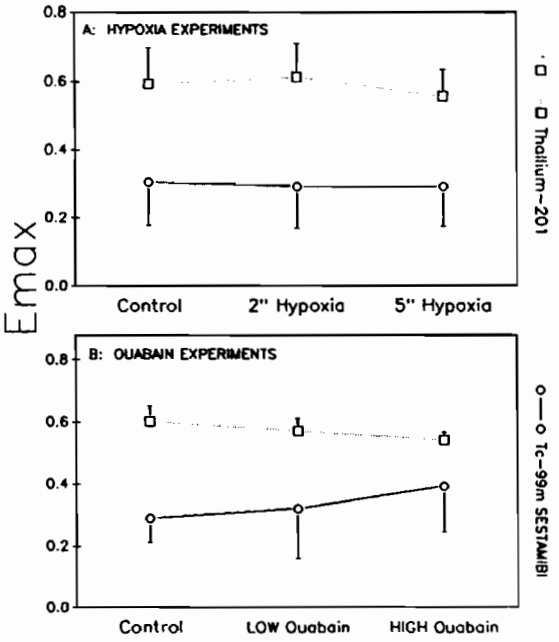

FIGURE 2
Average (±s.d.) Emax estimates for [^{99m}Tc]SESTAMIBI (open circles) and ^{201}Tl (open squares) for hypoxia (panel A) and ouabain (panel B) experiments. See text for treatment descriptions.

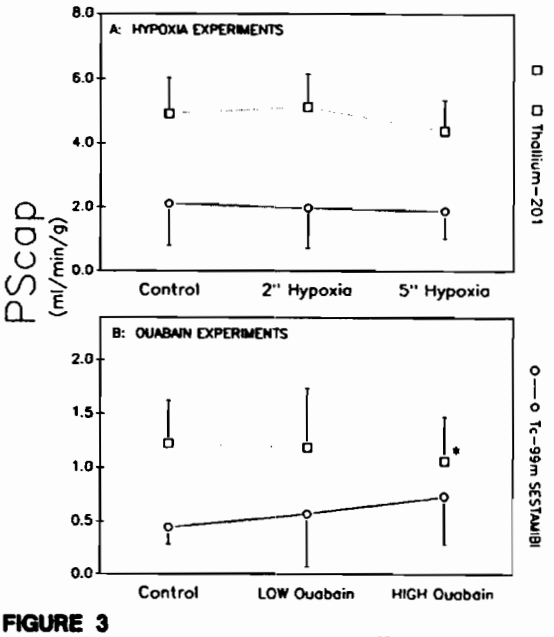

FIGURE 3
Average (±s.d.) PScap estimates for [^{99m}Tc]SESTAMIBI (open circles) and ^{201}Tl (open squares) for hypoxia (panel A) and ouabain (panel B) experiments. See text for treatment descriptions. (* indicates paired difference ($p < 0.015$) from control.)

significantly ($p < 0.02$) from control during the HIGH ouabain dose. PScap values for SESTAMIBI tended to increase with ouabain dose level, but this rise did not achieve significance.

Retention. Average (±s.d.) Enet values for hypoxia and ouabain experiments appear in Figure 4. Unlike Emax and PScap computations, SESTAMIBI Enet estimates were greater than or approximately equal to those for thallium. Paired analysis revealed no significant differences in Enet estimates between SESTAMIBI and thallium for any hypoxia or ouabain injection, except for the ouabain control (SESTAMIBI < thallium; $p < 0.01$). Although the average Enet for SESTAMIBI tended to increase with hypoxia (Fig. 4A), a difference from control reached statistical significance only for 2-min hypoxia determinations ($p < 0.05$) because of the relatively large variation in 5-min hypoxia estimates. SESTAMIBI Enet in ouabain experiments (Fig. 4B) also increased and reached statistical significance with HIGH ouabain dose (<0.01). In contrast, a significant and progressive decline in thallium Enet was noted for both LOW and HIGH ouabain doses ($p < 0.01$).

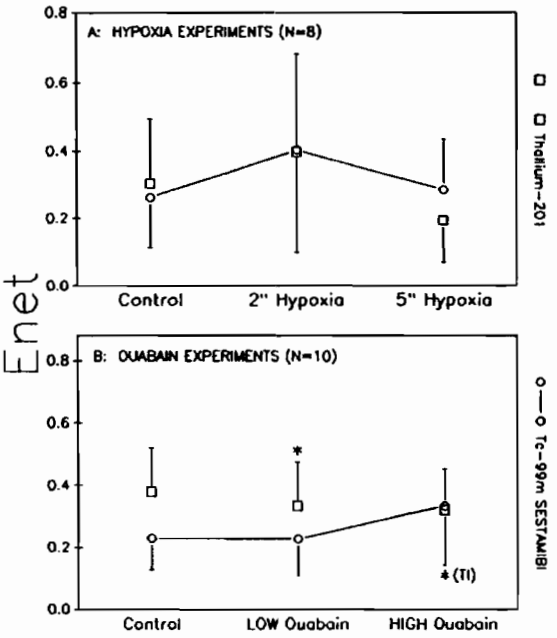

FIGURE 4
Average (±s.d.) Enet estimates for [^{99m}Tc]SESTAMIBI (open circles) and ^{201}Tl (open squares) for hypoxia (panel A) and ouabain (panel B) experiments. See text for treatment descriptions. (* indicates paired difference ($p < 0.015$) from control.)

DISCUSSION

The present study demonstrates that hypoxia and ouabain have small but significant effects on the myocardial transcapillary transport of SESTAMIBI and thallium in the perfused rabbit heart model. However, net cellular retention of these two tracers is more sensitive to hypoxia and ATPase inhibition than peak extraction or permeability.

Isolated Heart Model: Critiques

Using hemoglobin-free buffer in hypoxia experiments necessitates a two- to three-fold increase in the normal (2-4 ml/min/g) coronary perfusion rate of a normal rabbit heart (*19*) so that the tissue receives adequate oxygen supplies. Using protein-free buffer in hypoxia experiments also caused an average 16% higher tissue water fraction than what was observed using blood perfusate (ouabain studies). Both increased perfusion rate and tissue edema would affect kinetic estimates (*9*). Specifically, during high flows and increased interstitial space, peak extraction (Emax) and permeability (PScap) could be underestimated. These alterations in buffer-perfused hearts makes the comparison of absolute transport rates with studies using blood perfusates difficult and therefore was not attempted nor implied.

Measures of Treatment Effect

Hypoxia. Previous reports of hearts perfused with hypoxic buffer (*20*) have shown flow-independent hemodynamic alterations similar to those observed in the present study (Table 1), which demonstrate the severe cellular functional compromise induced by hypoxic perfusion. Although function deteriorated rapidly with hypoxic treatment, flow rate remained constant. Therefore, observed changes in transcapillary transport in this study cannot be explained by fluctuations in flow.

Ouabain. Ouabain produced a significant change in aortic pressure and peak systolic pressure (Table 1), but no significant increase in +dP/dt was observed. As previously noted, an increase in positive or negative dP/dt was not sustained, which might indicate insufficient drug levels. However, the ouabain doses are in the therapeutic and toxic ranges (*17,18*). In other unpublished studies, further increases in ouabain dose produced ventricular fibrillation and rapid heart failure. Although the drug concentration in the perfusate was not measured directly, the doses appear to have achieved a pharmacologic effect. With these considerations, we assumed the hearts received adequate ouabain to achieve functional inhibition of Na^+/K^+ ATPase.

Indicator Dilution Analysis

Transcapillary exchange. These experiments confirm previous results (*9,20*) by demonstrating that SESTAMIBI transcapillary exchange is significantly less than that of thallium. In the present studies, peak extractions (Emax) and capillary permeability-surface

area products (PScap) for SESTAMIBI averaged ~40% and 30%, respectively, of thallium. These relationships in Emax and PScap were unaffected by either hypoxia or ouabain. However, in ouabain experiments, opposing effects are noted for SESTAMIBI Emax (increase) and thallium (decrease). This trend becomes statistically apparent in the Enet analysis (below).

The control Emax estimates for thallium of about 0.60 (Fig. 2) compare to maximum extractions of above 0.70 in previous reports (*7*). The lower thallium extraction observed in the present studies is probably a result of higher myocardial flow since rabbit hearts have intrinsic perfusion rates of two to three times that of other species (*19*), which appreciably reduces peak thallium extraction.

In a previous study with cultured heart cells (*21*), ouabain or other metabolic inhibitors had little effect on SESTAMIBI or thallium uptake. Thallium extraction has been reported to be insensitive to hypoxia in perfused rabbit hearts (*20*) and open-chest dogs (*22*). Weich et al. (*23*) observed a drop of 11% in thallium extraction fraction during hypoxia in open-chest dogs, but coronary flow was not constant and could increase enough during hypoxia to account for the calculated decrease in extraction. Therefore, it seems reasonable to conclude that peak SESTAMIBI and thallium extraction fraction is relatively insensitive to normal tissue oxygenation.

PScap is a measure of unidirectional tracer flux across the capillary endothelium to the myocardial tissue (*11*, *13*,*24*). PScap estimates were unaltered by hypoxia, indicating that tracer movement from the vascular compartment is not influenced by the level of myocyte oxygenation or function. However, in ouabain experiments, a significant decrease in the PScap estimate for thallium implies that capillary surface area available for exchange is reduced or that thallium extraction (Emax) at the capillary level is impeded. Regarding the former possibility, ouabain might reduce exchanging capillary area by increasing coronary resistance (*18*). However, as thallium PScap decreased with ouabain, SESTAMIBI PScap tended to increase (statistically insignificant), which would not support the premise that ouabain induced an overall decrease in exchangeable surface area. Therefore, Na^+/K^+ ATPase inhibition is the most likely cause for the observed decrease in thallium PScap. It is generally accepted that myocardial thallium uptake is mediated in part by the Na^+/K^+ ATPase system (*23*, *25*), but this is not the only mechanism (*26*). The small decrease in thallium PScap may relate to the incomplete inhibition of the ATPase transport mechanism or to the relative insignificance of ATPase transport in thallium exchange compared to other transport mechanisms.

Retention. As an estimate of tracer retention, the Enet function (*27*) measures the net result of tracer influx and backflux between capillary (vascular) and tissue. Enet estimates for SESTAMIBI and thallium are similar despite a lower influx (i.e., PScap) for SESTAMIBI because SESTAMIBI has a lower backflux than thallium during the tail portion of the h(t) curves (Fig. 1). Enet values for SESTAMIBI increased with hypoxia and ouabain, probably from an enlarged extravascular volume of distribution rather than increased uptake since Emax and PScap were not significantly changed for SESTAMIBI by either experimental treatment. For thallium, Enet was unchanged by hypoxia, but a relatively large and progressive decline was noted with ouabain. This decline for thallium probably results from depressed capillary influx (PScap reduced with ouabain, not hypoxia) and from accelerated cellular back diffusion (decreased cellular volume of distribution). More rigorous modeling efforts (*9*) would be helpful in further substantiating these present results.

Clinical Implications

It is important to note that indicator-dilution results and model estimates are not inherently comparable to in vivo clinical studies where recirculation and redistribution effects of tracer play a prominent role. However, these in-vivo experiments permit independent manipulation of factors that would be expected to affect myocardial transport of SESTAMIBI and thallium.

We have observed that transcapillary exchange of thallium is greater than that of SESTAMIBI, but Enet values at control determinations show less disparity. This suggests that the relative high first-pass extraction of thallium compared to SESTAMIBI is somewhat offset by a shorter tissue residence time, resulting in net retention for thallium only slightly greater than for SESTAMIBI. Although hypoxia and ouabain did not induce much change in Emax or PScap for SESTAMIBI or thallium, significant differences were noted in Enet calculations. Therefore, alterations in myocardial cellular function from tissue hypoxia and ATPase inhibition, independent of coronary flow, can affect myocardial transport of these tracers. Specifically, these observations imply that Enet for SESTAMIBI would tend to increase despite a constant coronary perfusion during acute tissue hypoxia and membrane ATPase inhibition. In contrast, hypoxia and ouabain appears to have the opposite effect on net myocardial retention of thallium. Although myocardial transport of SESTAMIBI and thallium are dominated by flow, interpretation of clinical scintigraphic studies should also consider these contributing effects of cellular dysfunction and membrane inhibition.

ACKNOWLEDGMENT

The authors acknowledge the technical support, suggestions, and encouragement of Dr. James B. Bassingthwaighte of the University of Washington (NIH Grant RR1243). In

addition, the assistance for product support by Dr. Stephen J. Williams (E.I. duPont de Nemours and Co., Biomedical Products Department), and technical contributions of Ms. Michele A. Thurber are gratefully acknowledged.

These studies were supported in part by U.S. Public Health grant HL34199 of the National Heart, Lung, and Blood Institute.

REFERENCES

1. Jones AG, Davison A, Abrams MJ, et al. Investigations of a new class of technetium cations [Abstract]. *J Nucl Med* 1982; 23:P16.
2. Abrams MJ, Davison A, Jones AG, Costello CE, Pang H. Synthesis and characterization of hexakis (9-alkylisocyanide) and hexakis (arylisocyanide) complexes of technetium (I). *Inorg Chem* 1983; 22:2798–2800.
3. Holman BL, Jones AG, Lister-James J, et al. A new ^{99m}Tc-labeled myocardial imaging agent, hexakis (t-butyl-isonitrile)-technetium (I) (^{99m}TcTBI): initial experience in the human. *J Nucl Med* 1984; 25:1350–1355.
4. McKusick K, Holman BL, Jones AG, Rigo P, Sporn V, Vosberg H. Comparison of three Tc-99m isonitriles for detection of ischemic heart disease in humans [Abstract]. *J Nucl Med* 1986; 27:878.
5. McKusick K, Beller GA, Berman D. Initial clinical results with Tc-99m methoxyisobutyl isonitrile [Abstract]. *J Am Coll Cardiol* 1987; 9:28A.
6. Williams SJ, Mousa SA, Morgan RA, Carroll TR, Maheu LJ. Pharmacology of Tc-99m-isonitriles: agents with favorable characteristics for heart imaging [Abstract]. *J Nucl Med* 1986; 27:877–878.
7. Leppo JA. Myocardial uptake of thallium and rubidium during alterations in perfusion and oxygenation in isolated rabbit hearts. *J Nucl Med* 1987; 28:878–885.
8. Grice WN, Konishi T, Apstein CS. Resistance of neonatal myocardium to injury during normothermic and hypothermic ischemic arrest and reperfusion. *Circulation* 1988; 75(suppl. V):V150–V155.
9. Leppo JA, Meerdink DJ. A comparison of the myocardial uptake of a technetium-labeled isonitrile analogue and thallium. *Circ Res* 1989: in press.
10. Hnatowich DJ, Layne WW, Childs RL. The preparation and labeling of DTPA-coupled albumin. *Int J Appl Radiat Isot* 1982; 33:327–331.
11. Bassingthwaighte JB, Goresky CA. Modeling in the analysis of solute and water exchange in the microvasculature. In: Handbook of physiology. sect. 2, the cardiovascular system. Vol. IV. Bethesda, MD: American Physiological Society, 1984:549–626.
12. Bassingthwaighte JB, Kuikka JT, Chan IS, Arts T, Reneman RS. A comparison of ascorbate and glucose transport in the heart. *Am J Physiol* 1985; 249:H141–H149.
13. Crone C. The permeability of capillaries in various organs as determined by use of the 'indicator diffusion' method. *Acta Physiol Scand* 1963; 58:292–305.
14. Bassingthwaighte JB, Chinard FP, Crone C, et al. Terminology for mass transport and exchange. *Am J Physiol* 1986; 250:H539–H545.
15. SAS Institute Inc. Statistical analysis system. Carey, NC: SAS Institute, Inc., 1985.
16. Snedecor GW, Cochran WG. 6th ed. Ames, Iowa: Iowa State University Press, 1967:593.
17. Caprio A, Farah A. The effect of the ionic milieu on the response of rabbit cardiac muscle to ouabain. *J Pharmacol Exp Ther* 1967; 155:403–414.
18. Tanz RD, Russell NJ. Mechanism of cardiac glycoside-induced toxicity: physiology, biochemistry and electron microscopy. *Federation Proc* 1983; 42:2470–2474.
19. Bartum RJ Jr, Berkowitz DM, Hollenberg NK. A simple radioactive microsphere method for measuring flow and cardiac output. *Invest Radiol* 1974; 9:126–132.
20. Leppo JA, Macneil PB, Moring AF, Apstein CS. Separate effects of ischemia, hypoxia, and contractility on thallium-201 kinetics in rabbit myocardium. *J Nucl Med* 1986; 27:66–74.
21. Maublant JC, Gachon P, Moins N. Hexakis (2-methoxy isobutylisonitrile) technetium-99m and thallium-201 chloride: uptake and release in cultured myocardial cells. *J Nucl Med* 1988; 29:48–54.
22. Forman R, Kirk ES. Thallium-201 accumulation during reperfusion of ischemic myocardium: dependence on regional blood flow rather than viability. *Am J Cardiol* 1984; 54:659–663.
23. Weich HF, Strauss HW, Pitt B. The extraction of thallium-201 by the myocardium. *Circulation* 1977; 56:188–191.
24. Renkin EM. Transport of potassium-42 from blood to tissue in isolated mammalian skeletal muscles. *Am J Physiol* 1959; 197:1205–1210.
25. Pohost GM, Alpert NM, Ingwall JS, Strauss HW. Thallium redistribution: mechanisms and clinical utility. *Semin Nucl Med* 1980; 10:70–93.
26. Gehring PJ, Hammond PB. The interrelationship between thallium and potassium in animals. *J Pharmacol Exp Ther* 1967; 155:187–201.
27. Lassen NA, Crone C. The extraction fraction of a capillary bed to hydrophilic molecules: theoretical considerations regarding the single injection technique with a discussion of the role of diffusion between laminar streams (Taylor's effect). In: Crone C, Lassen NA, eds. *Capillary permeability*. Copenhagen: Munksgaard, 1970:48–59.

Ann Nucl Med (2007) 21:267–273
DOI 10.1007/s12149-007-0019-x

ORIGINAL ARTICLE

Myocardial kinetics of ^{201}Thallium, ^{99m}Tc-tetrofosmin, and ^{99m}Tc-sestamibi in an acute ischemia–reperfusion model using isolated rat heart

Kenji Fukushima · Mitsuru Momose · Chisato Kondo
Kiyoko Kusakabe · Hiroshi Kasanuki

Received: 12 December 2006 / Accepted: 26 February 2007

Abstract
Objective ^{201}Thallium (TL), ^{99m}Tc-tetrofosmin (TF), and ^{99m}Tc-sestamibi (MIBI) are extensively used as myocardial perfusion agents. The objective of the present study was to evaluate their kinetics under acute ischemia–reperfusion.
Methods Isolated rat hearts, perfused by the Langendorff method at a constant flow rate of 10 ml/min, were allotted to normal control, mild ischemia, and severe ischemia groups, in which 20-min tracer wash-in was conducted followed by a 25-min tracer washout. No-flow ischemia (15 min for mild ischemia groups; 30 min for severe ischemia groups) was induced before conducting wash-in and washout in the ischemia groups. Whole-heart radioactivity was determined with an external gamma detector. Myocardial flow rate (K_1, ml/min) and clearance rate (k_2, min^{-1}) were calculated.
Results K_{1TL}, K_{1TF}, and K_{1MIBI} decreased according to the severity of ischemia (K_{1TL} 5.32 ± 0.53, 4.76 ± 0.70, and 1.44 ± 0.59; K_{1TF} 3.80 ± 0.70, 2.73 ± 0.99, and 1.09 ± 0.45; and K_{1MIBI} 3.45 ± 1.10, 2.15 ± 0.82, and 1.05 ± 0.13, in the normal control, mild, and severe ischemia groups, respectively). K_1 was significantly higher for TL than for the ^{99m}Tc tracers ($P < 0.05$), but the ^{99m}Tc tracers had equivalent K_1 values. k_{2TL} increased significantly ($P < 0.05$) in the ischemia groups (k_{2TL} 0.062 ± 0.013, 0.11 ± 0.045, and 0.12 ± 0.035), but showed no significant difference between the ischemia groups. k_{2MIBI} and k_{2TF} were significantly ($P < 0.05$) lower than k_{2TL} and increased significantly ($P < 0.05$) in the severe ischemia group (k_{2TF} 0.0056 ± 0.0022, 0.0037 ± 0.0015, and 0.024 ± 0.015; and k_{2MIBI} 0.00072 ± 0.0011, 0.00038 ± 0.00076, and 0.042 ± 0.034). k_{2MIBI} was significantly ($P < 0.05$) lower than k_{2TF} in the normal control and mild ischemia groups.
Conclusions Tracer extraction was higher for TL than for the ^{99m}Tc tracers and all tracers decreased according to the severity of ischemia–reperfusion in the three tracer groups. The clearance kinetics of not only MIBI but also TF is possibly useful for the evaluation of the severity of ischemia, and the Langendorff method and a methodological approach by continuous determinations of radioactivity may serve for the quantitative analysis of tracer kinetic profiles.

Keywords ^{201}Thallium · ^{99m}Tc-tetrofosmin · Sestamibi · Myocardial kinetics · Isolated rat heart

K. Fukushima · H. Kasanuki
Department of Cardiology, Tokyo Women's Medical University, Tokyo, Japan

M. Momose (✉) · C. Kondo · K. Kusakabe
Department of Radiology, Tokyo Women's Medical University, 8-1 Kawada-cho, Shinjuku-ku, Tokyo 162-8666, Japan
e-mail: mmomose@rad.twmu.ac.jp

Introduction

Myocardial perfusion imaging evaluates myocardial blood flow and viability in coronary artery disease. ^{201}Thallium (TL) is a K^+ analog that is related to the cell membrane potential, Na^+ K^+-ATPase activity. TL, available since the 1970s, provides useful information to devise clinical strategies [1]. ^{99m}Tc-tetrofosmin ([^{99m}Tc(1,2-bis[(2-ethoxyethyl)phosphino]ethane)$_2$)O_2]; TF) and ^{99m}Tc-sestamibi (^{99m}Tc-hexakis-2-methoxy-2-methylpropyl isonitrile; MIBI), both commercially available since the 1990s, have been used extensively as myocardial perfusion agents for the scintigraphic evaluation of cardiac

disease. These ^{99m}Tc agents are characterized by rapid myocardial uptake and stable retention [2, 3].

^{201}Thallium, TF, and MIBI have shown marked ability to diagnose myocardial ischemia and infarction. Many previous studies have reported that the extraction and washout kinetics of these agents vary depending on various conditions of the myocardium such as ischemia, stunning, and infarction. Therefore, knowledge of the myocardial kinetics of the perfusion agents would be important to interpret images in a clinical study. Nevertheless, only a limited number of kinetic studies that have simultaneously examined the retention and washout kinetics of the three tracers, like the present study, are available. The objective of the present study was to dynamically (continuous determinations of radioactivity on a count/s basis) clarify the kinetic profiles of TL, TF, and MIBI in isolated rat hearts.

Materials and methods

Preparation of radiopharmaceuticals

The following three radiopharmaceuticals were used in the present study: MIBI, TF, and TL. MIBI and TL were supplied by Daiichi Radiopharmaceuticals (Tokyo, Japan) as lyophilized kit formulations. Each vial contained 1 mg of MIBI and TL. TF was supplied by Medi-Physics Healthcare (Tokyo, Japan) in freeze-dried vials.

The purity of all the agents was determined by thin-layer chromatography.

Perfusion of isolated rat hearts and perfusion protocol

Male Wistar rats ($n = 54$; body weight 250–350 g; aged 3–5 weeks; Saitama Jikken Animals, Saitama, Japan) were assigned to the following study groups in order to receive the test tracers: TL (five for control group, five for mild ischemia group, and seven for severe ischemia group); TF (five for control group, seven for mild ischemia group, and seven for severe ischemia group); and MIBI (six for control group, five for mild ischemia group, and seven for severe ischemia group). The animals were anesthetized by an intraperitoneal injection of barbiturate (0.03 mg/g of body weight) and were also given 100 units of heparin sodium intravenously. Subsequently, the heart was quickly isolated, and the aorta was cannulated to initiate retrograde perfusion according to the Langendorff method (LE 05.200; Panlab, Barcelona, Spain). A thermometer inserted in the left ventricle of the isolated heart was connected with a thermostat (LE 13206 Thermostat Letica, Barcelona, Spain) to measure the temperature of the chamber and maintain it at 37°C. The circulation pressure and ECG were monitored continuously with an amplifier (Bio Amp; Power Lab System AD Instruments, Barcelona, Spain). The isolated heart was perfused with a Krebs–Henseleit bicarbonate buffer [components (g/l): D-glucose (2.0), magnesium sulfate (0.141), potassium phosphate monobasic (0.16), potassium chloride (0.35), and sodium chloride (6.9); SIGMA Chemical, St. Louis, MO, USA] into which $NaHCO_3$ 2.1 mg/l and $CaCl_2$ 0.175 mg/l were added. The buffer was continuously supplied with 95% O_2/5% CO_2 throughout the study. The heart, isolated and wrapped with Parafilm to maintain moisture content throughout the study, was perfused with the buffer using a pump system (Miniplus3 Peristaltic Pump and STH Pump Controller; AD Instruments) at a constant flow rate of 10 ml/min. Throughout the present study, a Parafilm-covered external gamma probe (ALOKA, Tokyo, Japan) connected with an analyzer (Gamma-Chaser, ALOKA) was applied onto the whole heart to determine its radioactivity on a count/s basis (Fig. 1).

Figure 2 shows the protocol of the present study. The isolated hearts were allocated to the following three groups per tracer: the normal control, mild ischemia, and severe ischemia groups. The present study followed the same protocol, except for the duration of ischemia between the ischemia groups. A 15-min stabilization, namely, each tracer in the buffer was perfused at the above constant rate for 20 min, was followed by a 25-min tracer-free washout. Regarding the ischemia model preparation, no-flow ischemia lasted for 15 min and 30 min in the mild and severe ischemia groups, respectively.

The radioactivity in the buffer was determined with a gamma well counter (ALOKA). Radioactivity in

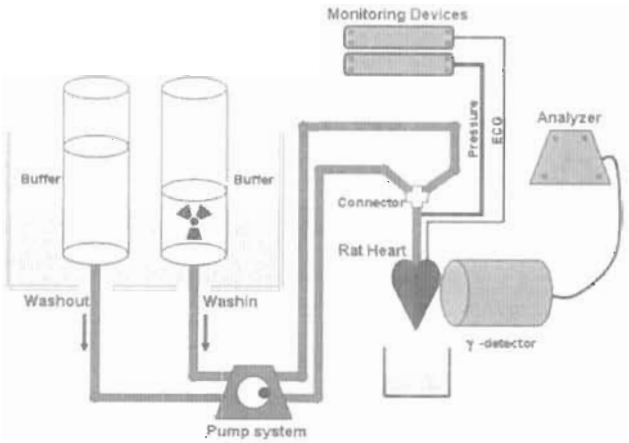

Fig. 1 The schema of Langendorff method and the external gamma detector system

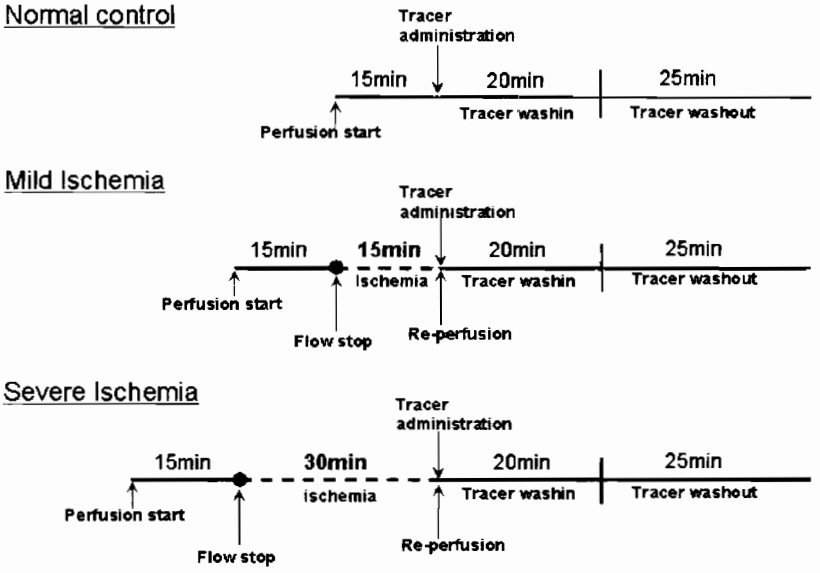

Fig. 2 Protocol of the study. Tracers were washed in for 20 min, followed by a 25-min washout in the normal control, mild ischemia, and severe ischemia groups. No-flow ischemia was induced before conducting wash-in and washout in the ischemia groups. *TL*, thallium; *TF*, tetrofosmin; *MIBI*, sestamibi

count/s, as determined with the gamma detector, was calibrated against that in count/min, as determined with a gamma well counter, to adjust determination units by using 1 ml of radioactive water containing ^{99m}Tc or ^{201}TL in five test tubes at a range of 100–2000 cps.

Time–activity curves and data analysis

Sampling energy windows were set to 70–120 keV and 140–180 keV for ^{201}TL and ^{99m}Tc tracers, respectively. A personal computer was used to record sampling data every second in the Excel format, from which time–activity curves were generated by Excel. All the curves were corrected for radioactive decay.

Tracer kinetics in the present study was formulated as the simplest model possible. As the perfusion rate is always constant, tracer density in the vascular space is presumed to reach its plateau shortly after perfusion. Therefore, we used the one-compartment tracer kinetics model (Fig. 3). When defining radioactivity in myocardial cells as $C_{1(t)}$ at a constant flow rate, the kinetics is formulated as follows:

$$\frac{dC_1}{dt} = K_1 C_{inf} - k_2 C_1 \quad (1)$$

where C_{inf} is the tracer concentration in the buffer for infusion into the vascular space, K_1 is the myocardial flow rate from the vascular space, and K_2 is the clearance rate constant from the myocardial cell. The differential equation was converted to the following formulas:

$$C_1(t) = \frac{K_1 C_{inf}}{k_2}(1 - e^{-k_2 t}) + B \quad (2)$$

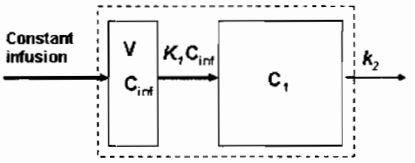

Fig. 3 One-compartment model describing the kinetics of perfusion tracers. The area bounded by the *dotted line* indicates gamma-detector sampling activity in the whole heart. *V*, vascular system; C_{inf}, radioactive concentration in the vascular system

$$C_1(t) = Ae^{-k_2(t-t_1)} \quad (3)$$

where A and B are constant values. Equations 2 and 3 are equations for myocardial flow and clearance kinetics, respectively; t_1 is the starting time of the washout phase.

The time–activity curves were analyzed by a curve-fitting software, Graph Pad Prism, to calculate K_1 (unit expressed as ml/min) and k_2 (min^{-1}).

Statistical analysis

Values are expressed as mean ± SD and are compared with nonparametric data. A Windows software, StatView (version 5.0, SAS Institute, NC, USA), was used to conduct the Kruskal–Wallis test and Mann–Whitney test in an attempt to compare the generated data. A value of $P < 0.05$ was considered statistically significant.

Table 1 Hemodynamic data of isolated rat hearts under study conditions

	Stabilization	No flow	Wash-in	Washout
Control ($n = 16$)				
Circulation pressure (mmHg)	63 ± 22	ND	57 ± 34	79 ± 31
Heart rate (bpm)	248 ± 87	ND	265 ± 92	277 ± 73
Mild ischemia ($n = 17$)				
Circulation pressure (mmHg)	72 ± 33	1.8 ± 0.29	93 ± 42*	99 ± 44*
Heart rate (bpm)	273 ± 103	34 ± 16	226 ± 56	261 ± 87
Severe ischemia ($n = 20$)				
Circulation pressure (mmHg)	60 ± 29	2.5 ± 0.13	124 ± 29†	136 ± 70†
Heart rate (bpm)	252 ± 69	15 ± 10	70 ± 40*§	25 ± 34*§

ND not done
* $P < 0.05$ versus normal, † $P < 0.05$ versus mild ischemia, § $P < 0.01$ versus normal control and mild ischemia

Table 2 Mean values of the kinetic data of tracers examined

	TL	TF	MIBI
K_1 (ml/min)			
Normal control	5.32 ± 0.53§ ($n = 5$)	3.80 ± 0.70 ($n = 5$)	3.45 ± 1.10 ($N = 6$)
Mild ischemia	4.76 ± 0.70§ ($n = 5$)	2.73 ± 0.99* ($n = 7$)	2.15 ± 0.82* ($N = 5$)
Severe ischemia	1.44 ± 0.59*†§ ($n = 6$)	1.09 ± 0.45*† ($n = 7$)	1.05 ± 0.13*† ($n = 7$)
k_2 (min^{-1})			
Normal control	0.062 ± 0.013§ ($n = 5$)	0.0056 ± 0.0022 ($n = 5$)	0.00072 ± 0.0011‡ ($n = 6$)
Mild ischemia	0.11 ± 0.045*§ ($n = 5$)	0.0037 ± 0.0015 ($n = 7$)	0.00038 ± 0.00076*‡ ($n = 5$)
Severe ischemia	0.12 ± 0.035*§ ($n = 6$)	0.024 ± 0.0015*† ($n = 7$)	0.042 ± 0.034*† ($n = 7$)

* $P < 0.05$ versus normal control, † $P < 0.05$ versus mild ischemia, ‡ $P < 0.05$ versus TF, § $P < 0.05$ versus TF and MIBI

Postmortem analysis

After the protocol was completed, isolated hearts were cut into blocks and fixed in paraformaldehyde; the thin sections of the apex and mid-ventricle were stained with hematoxylin and eosin before examination under a microscope.

Results

Hemodynamic data

The temperature of the left ventricle did not change significantly (36.8 ± 2.1°C, $n = 54$) in the three groups of each tracer. As shown in Table 1, the circulation pressure increased according to the severity of ischemia (normal vs. mild ischemia, $P < 0.05$; mild ischemia vs. severe ischemia, $P < 0.05$). Heart rate did not change in the mild ischemia group against the normal control group, but decreased significantly ($P < 0.01$) in the severe ischemia group even when the heart was mechanically paced at 240 bpm.

Tracer kinetics

The mean values of the kinetic data of the tracers examined are shown in Table 2. Figure 4 shows the typical time–activity curves in the three groups of each tracer. K_1 of TL, TF, and MIBI decreased significantly in the mild ischemia group ($P < 0.05$) against the normal control group and in the severe ischemia group ($P < 0.05$) against the mild ischemia group. Tracer extraction (=K_1/constant flow rate, 10 ml/min) was significantly higher for TL than for the ^{99m}Tc tracers, but the latter had equivalent extraction values.

The myocardial clearance k_{2TL} was significantly ($P < 0.05$) higher for TL than for TF and MIBI. Furthermore, k_{2TL} accelerated significantly ($P < 0.05$) in the ischemia groups compared with the normal control group, but showed no significant difference between the ischemia groups.

k_{2MIBI} was significantly ($P < 0.05$) lower than k_{2TF} in the normal control group. k_{2MIBI} and k_{2TF} remained unchanged in the mild ischemia group, but increased significantly ($P < 0.05$) in the severe ischemia group.

Findings in specimens

There was no significant difference in tracers among the three groups, and no myocardial necrosis was apparent in the ischemia groups.

Discussion

In the present study, we dynamically assessed and compared the kinetic profiles of TL, TF, and MIBI in a no-

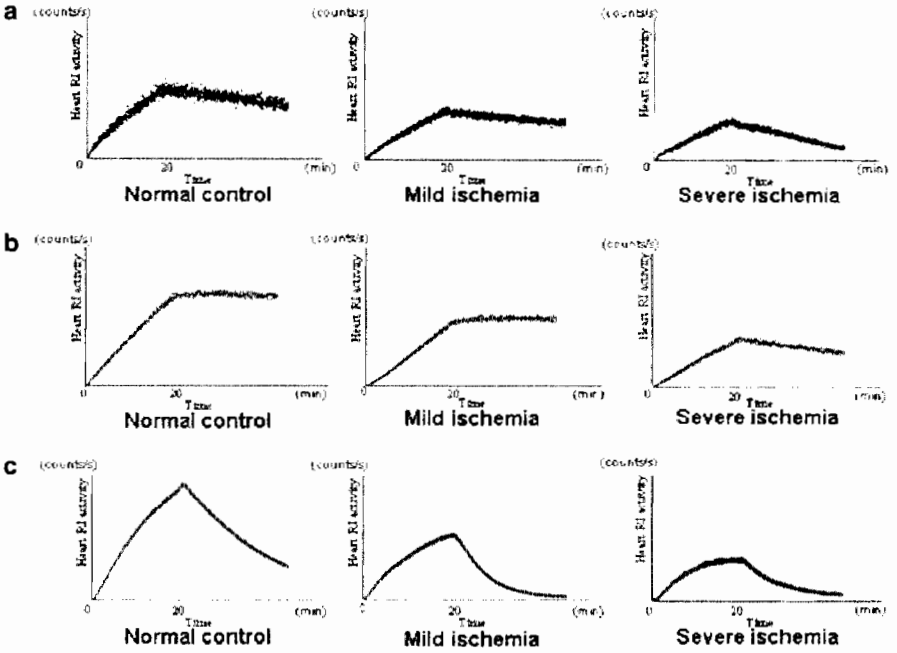

Fig. 4 Typical diagrams of three tracers (**a** Tl wash-in–washout curves; **b** MIBI wash-in–washout curves; and **c** TL wash-in–washout curves)

flow ischemia–reperfusion model. Myocardial flow constant, K_1, of all the three tracers decreased according to the severity of ischemia induced by no-flow ischemia–reperfusion, which indicated decreased tracer retention followed by a transient ischemic condition in each tracer. Myocardial microvessels may be collapsed by interstitial edema, shrinkage, or spasm after an ischemia–reperfusion injury, thus resulting in an increase in circulation pressure. Several studies have reported that increased circulation pressure was observed in ischemic conditions according to Langendorff's method [4, 5]. Microembolism in vessels was considered quite unlikely to occur in the perfusion system because the main components of the perfusion medium were the K–H buffer containing no blood plasma, blood cells, or platelets. Several studies have examined the ischemia–reperfusion injury provoked by no-flow ischemia in isolated rat heart models with different durations of ischemia. Consequently, no-flow ischemia of <30 min duration provoked no myocardial necrosis; however, changes were induced by ischemic injury, e.g., increased myocardial levels of lactate and LDH, as well as mitochondrial damage, certainly developed [6–8]. Liu remarked that irreversible mitochondrial damage caused by 60 min of no-flow ischemia induced accelerated MIBI clearance. Beanlands reported that mitochondrial damage caused by toxic cell injury, detected with electron microscopy, in the rat heart in turn accelerated MIBI clearance [9, 10]. Our data on histochemical staining showed no evidence indicative of myocardial necrosis, suggesting that isolated hearts were in a stunning or hibernation state induced by the ischemia–reperfusion injury.

The clearance of TL was much higher than that of ^{99m}Tc agents in the normal control group and accelerated significantly in the ischemia groups. TL has been reported to have both active and passive transport systems involving the Na–K ATPase channel. Ischemic injury would induce the loss of Na^+, K^+-ATPase activity [11, 12]. Moore [13] reported that the myocardium injured by reperfusion accelerated the TL clearance more extensively than did the non-ischemic myocardium. Ayalew [14] described that the TL kinetics in the interstitial compartment was negligible in an isolated rabbit heart study.

We also gave no consideration to the interstitial compartment when analyzing the model because our results revealed that the kinetics of TL was considered to be more rapid in the interstitial compartment than in myocardial cells. Actually, the TL washout curves were not biphasic, but monoexponential, suggesting that washout depended on slow kinetics, i.e., kinetics of myocardial cells.

^{201}Thallium washout accelerated in the mild ischemia group, but did not further accelerate in the severe ischemia group even at lower K_1 in the presence of severe hemodynamic changes. In the mild ischemia group, we conjecture that the sufficiently intense washout of TL occurred so that myocardial cells might have no capability to accelerate the washout even if ischemia lasted for a longer duration.

^{99m}Tc-tetrofosmin showed relatively stable retention in the normal control and mild ischemia groups compared to TL. However, TF showed a significant increase in washout in the severe ischemia group.

^{201}Thallium and ^{99m}Tc agents showed different kinetics in clearance patterns. Namely, ^{99m}Tc agents showed no change in clearance in the mild ischemia group compared to the normal control group, but exhibited significantly higher clearance ($P < 0.05$) in the severe ischemia group. This finding was noted with both TF and MIBI. Kurokawa [15] reported the reverse redistribution of TF in the infarcted myocardium after reperfusion therapy, implying that TF might be washed out from the severely damaged myocardium after acute reperfusion–ischemia. The reverse redistribution may be explained by the present results. Namely, K_{1Tl} decreased in parallel with ischemia severity, whereas k_{2Tl} showed no change in kinetic profiles in the mild ischemia group, but exhibited accelerated washout only in the severe ischemia group. TF indicates accelerated washout in severe ischemia–reperfusion injury.

These two ^{99m}Tc agents have been reported to present similar kinetics in the myocardium. However, some previous studies have reported that there was some difference in the myocardial kinesis between the two tracers because the intracellular distribution of TF and MIBI may be different. (The intracellular distribution of MIBI mainly depends on mitochondrial membrane potential, and that of TF is related to cytosolic and mitochondrial accumulation.) [16–20]. In the present study, the k_2 values of TF and MIBI differed in the normal control group, and the k_{2Tl} value was nearly tenfold greater than that of k_{2MIBI}. MIBI showed more stable retention in the normal and mild ischemia groups than TF.

The present study suggested that MIBI is scarcely washed out from the slightly damaged myocardium. Okada et al. reported that the MIBI clearance accelerated in the severely damaged myocardium [21, 22]. The present study indicated that the greater loss of the reperfused area resulted in the acceleration of MIBI clearance. When severe ischemia–reperfusion injury occurs, mitochondrial dysfunction probably becomes irreversible. Consequently, MIBI may be washed out rapidly, and the myocardium would lose its viability.

Limitations of the study

Our perfusion system was not truly equivalent to coronary perfusion, because the system performed retrograde constant perfusion throughout the study and did not provide a physiologic, systemic recirculation environment. Despite these limitations, our study was successful in providing the dynamic data of the three tracers and in comparing their kinetic profiles.

Conclusions

The present study led to the following conclusions: (1) the clearance kinetics of not only MIBI but also TF is possibly useful in the evaluation of ischemia–reperfusion severity, and the clearance kinetics of TF is applicable to routine clinical settings; and (2) the Langendorff method and a methodological approach with continuous determinations of radioactivity may serve for the quantitative analysis of tracer kinetic profiles.

References

1. Strauss HW, Harrison K, Langan JK, Lebowitz E, Pitt B. Thallium-201 for myocardial imaging. Relation of thallium-201 to regional myocardial perfusion. Circulation 1975;51:641–5.
2. Berman DS. Introduction—technetium-99m myocardial perfusion imaging agents and their relation to thallium-201. Am J Cardiol 1990;66:1E–4E.
3. Reyes E, Loong CY, Harbinson M. A comparison of Tl-201, Tc-99m sestamibi, and Tc-99m tetrofosmin myocardial perfusion scintigraphy in patients with mild to moderate coronary stenosis. J Nucl Cardiol 2006;13:488–4.
4. Young BC, Phillips MI, Ambuehl PEJ. Increase in angiotensin II type 1 receptor expression immediately after ischemia-reperfusion in isolated rat hearts. Circulation 1997;96:922–6.
5. Young BC, Virmami R, Nichols WW, Mehta JL. Platelets protect against myocardial dysfunction and injury induced by ischemia and reperfusion in isolated rat hearts. Circ Res 1993;72:1181–90.
6. van Bilsen M, van der Vusse GJ, Willemsen PH, Coumans WA, Roemen TH, Reneman RS. Lipid alterations in isolated, working rat hearts during ischemia and reperfusion: its relation to myocardial damage. Circ Res 1989;64:304–14.
7. Ooie T, Takahashi N, Saikawa T, Nawata T, Arikawa M, Yamanaka K, et al. Single oral dose of geranylgeranylacetone induces heat-shock protein 72 and renders protection against ischemia/reperfusion injury in rat heart. Circulation 2001;104:1837–43.
8. Asimakis GK, Sandhu GS, Conti VR, Sordahl LA, Zwischenberger JB. Intermittent ischemia produces a cumulative depletion of mitochondrial adenine nucleotides in the isolated perfused rat heart. Circ Res 1990;66:302–10.
9. Liu Z, Johnson G, Beju D, Okada RD. Detection of myocardial viability in ischemic-reperfused rat hearts by Tc-99m sestamibi kinetics. J Nucl Cardiol 2001;8:677–86.
10. Beanlands RS, Dawood F, Wen WH, Maclaughlin PR. Are the kinetics of technetium-99m methoxyisobutyl isonitrile affected by cell metabolism and viability? Circulation 1990;82:1802–14.
11. Skulskii IA, Manninen V, Jarnefelt J. Thallium inhibition of ouabain-sensitive sodium transport and of the (Na^+ plus K^+)-ATPase in human erythrocytes. Biochim Biophys Acta 1975;394:569–76.

12. Kim MS, Akera T. O_2 free radicals: cause of ischemia-reperfusion injury to cardiac Na^+–K^+-ATPase. Am J Physiol 1987;252:H252–57.
13. Moore CA, Cannon J, Watson DD, Kaul S, Beller GA. Thallium 201 kinetics in stunned myocardium characterized by severe postischemic systolic dysfunction. Circulation 1990; 81:1622–32.
14. Ayalew A, Marie PY, Menu P, Mertes PM, Audonnet S, Bertrand A, et al. (201)Tl and (99m)Tc-MIBI retention in an isolated heart model of low-flow ischemia and stunning: evidence of negligible impact of myocyte metabolism on tracer kinetics. J Nucl Med 2002;43:566–74.
15. Kurokawa K, Ohte N, Miyabe H, Akita S, Yajima K, Hayano J, et al. Reverse redistribution phenomenon on rest (99m)Tc-tetrofosmin myocardial single photon emission computed tomography involves impaired left ventricular contraction in patients with acute myocardial infarction. Circ J 2003;67: 830–34.
16. Schaefer WM, Moka D, Brockmann HA, Schomaecker K, Schicha H. 201Tl, 99mTc-MIBI, 99mTc-tetrofosmin and 99mTc-furifosmin: relative retention and clearance kinetics in retrogradely perfused guinea pig hearts. Nucl Med Biol 2002;29:243–54.
17. Carvalho PA, Chiu ML, Kronauge JF, Kawamura M, Jones AG, Holman BL, et al. Subcellular distribution and analysis of technetium-99m-MIBI in isolated perfused rat hearts. J Nucl Med 1992;33:1516–22.
18. Arbab S, Koizumi K, Toyama K, Arai T. Thechnetium-99m-tetrofosmin, thechnetium-99m-MIBI and thallium-201 uptake in rat myocardial cells. J Nucl Med 1998;39:266–71.
19. Dahlberg T, Meerdink D, Gilmore P, Leppo A. Myocardial extraction of technetium-99m-[2-(1-methoxybutyl) isonitrile] in the isolated rabbit heart: a myocardial perfusion agent with high extraction and stable retention. J Nucl Med 1993;34: 927–31.
20. Piwnica-Worms D, Kronauge JF, Chiu ML. Uptake and retention of hexakis (2-methoxyisobtyl isonitrile) technetium (I) in cultured chick myocardial cells. Mitochondrial and plasma membrane potential dependence. Circulation 1990;82: 1826–38.
21. Beller GA, Glover DK, Edwards NC, Ruiz M. 99mTc-sestamibi uptake and retention during myocardial ischemia and reperfusion. Circulation 1993;87:2033–42.
22. Okada RD, Glover DK, Nguyen KN, Johnson G, 3rd. Technetium-99m sestamibi kinetics in reperfused canine myocardium. Eur J Nucl Med 1995;22:600–7.

FW: mibi 5min and 2hr

From: **RM Fleming** (rmfmd7@hotmail.com)
Sent: Thu 8/23/07 6:30 PM
To: Mike Hansen PD corrected (mike_hansen@fd.org)

Dear Mike,

Search on "sestamibi heart uptake rate" yields no abstract references to "uptake rate". References all refer to "uptake" as an amount and apply "rate" to "clearance" or "washout". Many references see that rate as diagnostic. Whether uptake increases after 5-10min seems unaddressed in abstracts. What is concluded is that levels can be lower after an hour or more and that differences (clearance or washout rate) are diagnostic. I think the answer is to list a number of such references with their conclusions quoted. I am sending the first of many such abstracts.

In examining the witnesses we can then present the abstracts with those conclusions high-lighted. That can probably be done in depositions. We may need full text backup for legal purposes.
It really doesn't matter what the uptake rate is if the tracer does not "stick around" for the full 6 hours of the tracers radioactive half-life. Clearly articles showing changes in the first few hours, show the tracer does not "stick" around. Its relevance will have little meaning or understanding for a jury. We simply need to show that the medical literature supports changes in the two images over time, whether it is due to uptake or washout or something completely unknown to mankind. No one will doubt that gravity exists, yet none of the jurors can define it. The first person who does will get the Nobel Prize, yet no one doubts its existence. The medical literature supports having information provided by two images, since the papers to follow show changes over serial images.

> 29: Eur J Nucl Med. 1995 Jan;22(1):49-55. Related Articles, Links
>
> Washout and redistribution between immediate and two-hour myocardial
> images using technetium-99m sestamibi.
>
> Richter WS, Cordes M, Calder D, Eichstaedt H, Felix R.
>
> Universitätsklinikum Rudolf Virchow, Freie Universität Berlin, Germany.
>
> The aim of this study was to assess whether a clinically relevant
> change in myocardial sestamibi activity could be documented within the
> first 120 min following injection (p.i.). In 17 patients planar anterior
> imaging of the heart was performed 5 min and 120 min p.i. During this
> time interval, mean decay-corrected myocardial activity declined to
> 77.9% +/- 9.7% after stress and to 85.7% +/- 7.9% after injection at
> rest (P < 0.05). In 19 patients with angiographically documented
> coronary artery disease, single-photon emission tomography was performed
> 5 min and 120 min after injection at maximum stress. For analysis,
> sestamibi activity was scored semiquantitatively in six left ventricular
> segments. Furthermore, sestamibi uptake was assessed quantitatively
> using a circumferential profile method. In 35 of 114 segments the score
> improved within 120 min p.i. (early fill-in); in these segments relative
> sestamibi activity rose from 69.9% +/- 22.5% to 74.5% +/- 20.8% (P <
> 0.01). In five patients this early fill-in was the only sign of
> exercise-induced hypoperfusion. In 7 of 114 segments the score

> deteriorated 120 min p.i. (early tracer washout); in these segments
> relative sestamibi activity declined from 85.6% +/- 9.9% to 80.1% +/-
> 10.7% (P < 0.02). In three of four patients with early tracer washout
> the corresponding coronary artery was significantly narrowed. In
> conclusion, a global myocardial sestamibi washout was registered within
> the first 120 min after injection. A fill-in of initial defects as well
> as an early tracer loss could be detected in a relevant number of
> patients with chronic coronary artery disease during the first 2 h
> p.i.(ABSTRACT TRUNCATED AT 250 WORDS)
>
> Publication Types:
>
> * Comparative Study
>
>
> PMID: 7698155 [PubMed - indexed for MEDLINE]

I will be forwarding a number of abstracts to you without additional intro or closure.
>
Yours,

Dr. Fleming

FW: clearance rate thallium mibi

From: **RM Fleming** (rmfmd7@hotmail.com)
Sent: Thu 8/23/07 6:33 PM
To: Mike Hansen PD corrected (mike_hansen@fd.org)

> 20: Eur J Nucl Med. 2000 Nov;27(11):1632-40. Related Articles, Links
> Click here to read
> A comparison of the overall first-pass kinetics of thallium-201 and
> technetium-99m MIBI in normoxic and low-flow ischaemic myocardium.
>
> Ayalew A, Marie PY, Menu P, Mertes PM, Hassan N, Danchin N, Olivier
> P, Karcher G, Bertrand A.
>
> Department of Nuclear Medicine, UPRES EA 2403, CHU-Nancy, France.
>
> The specific impact of ischaemia on the myocardial kinetics of
> thallium-201 and technetium-99m 2-methoxy-2-isobutylisonitrile (MIBI)
> remains a matter of debate. Using an isolated heart model perfused with
> red blood cell-enhanced perfusate, we compared the overall first-pass
> kinetics of 201Tl and MIBI under haemodynamically stable conditions of
> low-flow ischaemia (> 50% reduction in normal coronary flow and a > or =
> 20 mmHg fall in systolic contraction pressure, n = 10) and normoxia (n =
> 11). For both 201Tl and MIBI, we found that under ischaemic conditions
> (as compared with normoxia) there was a higher initial net extraction
> fraction (201Tl: 0.78 +/- 0.03 vs 0.72 +/- 0.06, P = 0.006; MIBI: 0.49
> +/- 0.10 vs 0.39 +/- 0.11, P = 0.03), a lower clearance rate in the 30
> min following extraction (% decrease in cardiac uptake: 201Tl: 30 +/- 12
> vs 47 +/- 14, P = 0.02; MIBI: 5 +/- 5 vs 13 +/- 11, P = 0.02) and a
> higher retention fraction at 30 min (201Tl: 0.54 +/- 0.10 vs 0.39 +/-
> 0.12, P = 0.004; MIBI: 0.46 +/- 0.08 vs 0.33 +/- 0.12, P = 0.01).
> Multivariate analyses, however, revealed that all myocardial kinetic
> parameters of both tracers were dependent only on coronary flow rates,
> without any additional significant impact of the presence of ischaemia
> or states of contractility or oxidative metabolism. **We conclude that the**
> myocardial fractional retention of both 201Tl and MIBI is strongly
> correlated with the decrease in coronary flow during ischaemia. This
> inverse relationship with coronary flow derives from both the
> flow-dependent increase in the initial myocardial extraction and the
> decrease in the subsequent myocardial washout of the tracers.
>
> Publication Types:
>
> * Comparative Study
> * Research Support, Non-U.S. Gov't
>
>
> PMID: 11105819 [PubMed - indexed for MEDLINE]

FW: mibi 60min clearance

From: **RM Fleming** (rmfmd7@hotmail.com)
Sent: Thu 8/23/07 6:35 PM
To: Mike Hansen PD corrected (mike_hansen@fd.org)

> *26: *J Nucl Cardiol. <javascript:AL_get(this, 'jour', 'J Nucl
> Cardiol.');> 2001 Nov-Dec;8(6):677-86. Related Articles
>
<http://www.ncbi.nlm.nih.gov/sites/entrez?Db=pubmed&DbFrom=pubmed&Cmd=Link&LinkName=pubmed_pubmed&LinkReadableName=Related%20Articles&IdsFromResult=11725264&ordinalpos=26&itool=EntrezSystem2.PEntrez.Pubmed.Pubmed_ResultsPanel.Pubmed_RVAbstract>,
> Links <javascript:PopUpMenu2_Set(Menu11725264);>
>
> Click here to read
> <http://www.ncbi.nlm.nih.gov/entrez/utils/fref.fcgi?PrId=3048&itool=Abstract-def&uid=11725264&db=pubmed&url=http://linkinghub.elsevier.com/retrieve/pii/S1071-3581%2801%2954260-9>
>
> *Detection of myocardial viability in ischemic-reperfused rat hearts
> by Tc-99m sestamibi kinetics.*
>
> *Liu Z*
>
<http://www.ncbi.nlm.nih.gov/sites/entrez?Db=pubmed&Cmd=Search&Term=%22Liu%20Z%22%5BAuthor%5D&itool=EntrezSystem2.PEntrez.Pubmed.Pubmed_ResultsPanel.Pubmed_RVAbstract>,
> *Johnson G 3rd*
>
<http://www.ncbi.nlm.nih.gov/sites/entrez?Db=pubmed&Cmd=Search&Term=%22Johnson%20G%203rd%22%5BAuthor%5D&itool=EntrezSystem2.PEntrez.Pubmed.Pubmed_ResultsPanel.Pubmed_RVAbstract>,
> *Beju D*
>
<http://www.ncbi.nlm.nih.gov/sites/entrez?Db=pubmed&Cmd=Search&Term=%22Beju%20D%22%5BAuthor%5D&itool=EntrezSystem2.PEntrez.Pubmed.Pubmed_ResultsPanel.Pubmed_RVAbstract>,
> *Okada RD*
>
<http://www.ncbi.nlm.nih.gov/sites/entrez?Db=pubmed&Cmd=Search&Term=%22Okada%20RD%22%5BAuthor%5D&itool=EntrezSystem2.PEntrez.Pubmed.Pubmed_ResultsPanel.Pubmed_RVAbstract>.
>
> William K. Warren Medical Research Institute of the University of
> Oklahoma Health Sciences Center, Tulsa , USA. zliu@u.arizona.edu
>
> BACKGROUND: The purpose of this study was to evaluate technetium 99m
> sestamibi (MIBI) kinetics in assessing myocardial viability in
> hearts subjected to different ischemia-reperfusion treatments,
> resulting in graded severity of injury. METHODS AND RESULTS: Sixteen
> isolated Krebs-Henseleit-perfused rat hearts were divided into 3
> groups: control (flow, 12 mL/min; n = 5), ischemic-reperfused with
> glucose (IR+G, n = 6), and ischemic-reperfused without glucose
> (IR-G, n = 5). MIBI (11.1 mBq [300 microCi]) was infused for 60
> minutes (uptake), followed by a 60-minute clearance. MIBI uptake
> (percent injected dose per gram) was significantly decreased in the
> IR+G (2.07 +/- 0.31) and IR-G groups (2.03 +/- 0.23; P = not
> significant with IR+G) compared with the control group (3.06 +/-
> 0.25, P <.05). Fractional washout of MIBI was more rapid in the IR-G
> group (72.7% +/- 3.9%, P <.05) than in the control (21.9% +/- 1.9%)

> and IR+G groups (20.3% +/- 1.7%). End retention (percent injected
> dose per gram) of MIBI in the IR-G (0.60 +/- 0.12) and IR+G groups
> (1.60 +/- 0.18) was significantly less than in the control group
> (2.30 +/- 0.11, P <.05), respectively. The retention in the IR-G
> group was less than in the IR+G group (P <.05). Creatine kinase
> assay, triphenyltetrazolium chloride staining, and transmission
> electron microscopy analysis demonstrated more serious myocardial
> damage in the IR-G group than in the IR+G group. End MIBI activity
> was highly correlated with myocardial viability determined by
> triphenyltetrazolium chloride staining (r = 0.94; P <.05) and
> creatine kinase assay (r = -0.86; P <.05). CONCLUSIONS: **Clearance of**
> **Tc-99m sestamibi is sensitive to metabolic states and may be used**
> **for assessment of ongoing myocardial damage.**
>
> PMID: 11725264 [PubMed - indexed for MEDLINE]
>
>

FW: tracer comparison rabbits graphics attached

From: **RM Fleming** (rmfmd7@hotmail.com)
Sent: Thu 8/23/07 11:38 AM
To: Mike Hansen PD corrected (mike_hansen@fd.org)

1 attachment

272.pdf (139.5 KB)

>
> 19: J Nucl Med. 2001 Feb;42(2):272-81. Related Articles, Links
> Click here to read
> Comment in:
>
> * J Nucl Med. 2001 Feb;42(2):282-4.
>
>
> Kinetic analysis of 125I-iodorotenone as a deposited myocardial flow
> tracer: comparison with 99mTc-sestamibi.
>
> Marshall RC, Powers-Risius P, Reutter BW, Taylor SE, VanBrocklin HF,
> Huesman RH, Budinger TF.
>
> Center for Functional Imaging, E.O. Lawrence Berkeley National
> Laboratory, University of California, Berkeley 94720, USA.
>
> The goal of this investigation was to assess the accuracy of
> 7'-Z-[125I]iodorotenone (125I-iodorotenone) as a new deposited
> myocardial flow tracer and compare the results with those for
> 99mTc-sestamibi. METHODS: The kinetics of these two flow tracers were
> evaluated in 25 isolated, erythrocyte- and albumin-perfused rabbit
> hearts over a flow range relevant to patients. The two flow tracers and
> a vascular reference tracer (131I-albumin) were introduced
> simultaneously as a compact bolus through a port just above the aortic
> cannula in the absence of tracer recirculation. Myocardial extraction,
> retention, washout, and uptake parameters were computed from the venous
> outflow curves using the multiple-indicator dilution technique and
> spectral analysis. RESULTS: The extraction of 125I-iodorotenone was much
> higher than the extraction of 99mTc-sestamibi (0.84 +/- 0.05 vs. 0.48
> +/- 0.10, respectively, P < 0.001). 125I-iodorotenone extraction was
> also less affected by flow than was 99mTc-sestamibi (P < 0.001). Net
> retention of 125I-iodorotenone was significantly greater than
> 99mTc-sestamibi net retention at 1 min (0.77 +/- 0.08 vs. 0.41 +/- 0.11,
> respectively, P < 0.001) and 26 min (0.46 +/- 0.13 vs. 0.27 +/- 0.11,
> respectively, P < 0.001) after tracer injection. Flow had less effect on
> 125I-iodorotenone net retention than on 99mTc-sestamibi net retention 1
> min after tracer injection (P < 0.04). However, at 26 min, flow had an
> equivalent effect on the retention of both flow tracers (P < 0.4). The
> relationship between 125I-iodorotenone and 99mTc-sestamibi washout was
> complex and depended on elapsed time after isotope introduction and
> perfusion rate. Reflecting the favorable extraction and retention
> characteristics of 125I-iodorotenone, both its maximum myocardial uptake
> and its 26-min uptake were more closely related to flow than were those
> of 99mTc-sestamibi (P < 0.001 for both comparisons). CONCLUSION: **The**
> extraction and retention of 125I-iodorotenone were greater than those of

> 99mTc-sestamibi, making 125I-iodorotenone the superior flow tracer in
> the isolated rabbit heart.
>
> Publication Types:
>
> * Comparative Study
> * In Vitro
> * Research Support, U.S. Gov't, Non-P.H.S.
> * Research Support, U.S. Gov't, P.H.S.
>
>
> PMID: 11216526 [PubMed - indexed for MEDLINE]
>
Note attached pdf.

FW: mibi clearance rats

From: **RM Fleming** (rmfmd7@hotmail.com)
Sent: Thu 8/23/07 6:39 PM
To: Mike Hansen PD corrected (mike_hansen@fd.org)

> 18: J Nucl Cardiol. 2001 Nov-Dec;8(6):677-86. Related Articles, Links
> Click here to read
> Detection of myocardial viability in ischemic-reperfused rat hearts
> by Tc-99m sestamibi kinetics.
>
> Liu Z, Johnson G 3rd, Beju D, Okada RD.
>
> William K. Warren Medical Research Institute of the University of
> Oklahoma Health Sciences Center, Tulsa , USA. zliu@u.arizona.edu
>
> BACKGROUND: The purpose of this study was to evaluate technetium 99m
> sestamibi (MIBI) kinetics in assessing myocardial viability in hearts
> subjected to different ischemia-reperfusion treatments, resulting in
> graded severity of injury. METHODS AND RESULTS: Sixteen isolated
> Krebs-Henseleit-perfused rat hearts were divided into 3 groups: control
> (flow, 12 mL/min; n = 5), ischemic-reperfused with glucose (IR+G, n =
> 6), and ischemic-reperfused without glucose (IR-G, n = 5). MIBI (11.1
> mBq [300 microCi]) was infused for 60 minutes (uptake), followed by a
> 60-minute clearance. MIBI uptake (percent injected dose per gram) was
> significantly decreased in the IR+G (2.07 +/- 0.31) and IR-G groups
> (2.03 +/- 0.23; P = not significant with IR+G) compared with the control
> group (3.06 +/- 0.25, P <.05). Fractional washout of MIBI was more rapid
> in the IR-G group (72.7% +/- 3.9%, P <.05) than in the control (21.9%
> +/- 1.9%) and IR+G groups (20.3% +/- 1.7%). End retention (percent
> injected dose per gram) of MIBI in the IR-G (0.60 +/- 0.12) and IR+G
> groups (1.60 +/- 0.18) was significantly less than in the control group
> (2.30 +/- 0.11, P <.05), respectively. The retention in the IR-G group
> was less than in the IR+G group (P <.05). Creatine kinase assay,
> triphenyltetrazolium chloride staining, and transmission electron
> microscopy analysis demonstrated more serious myocardial damage in the
> IR-G group than in the IR+G group. End MIBI activity was highly
> correlated with myocardial viability determined by triphenyltetrazolium
> chloride staining (r = 0.94; P <.05) and creatine kinase assay (r =
> -0.86; P <.05). CONCLUSIONS: **Clearance of Tc-99m sestamibi is sensitive
> to metabolic states and may be used for assessment of ongoing myocardial
> damage.**
>
> PMID: 11725264 [PubMed - indexed for MEDLINE]r
>

FW: Delayed image mibi text unavilable

From: **RM Fleming** (rmfmd7@hotmail.com)
Sent: Thu 8/23/07 6:40 PM
To: Mike Hansen PD corrected (mike_hansen@fd.org)

> 15: Kaku Igaku. 2002 May;39(2):117-24. Related Articles, Links
>
> [Rest delayed images on 99mTc-MIBI myocardial SPECT as a noninvasive
> screen for the diagnosis of vasospastic angina pectoris]
>
> [Article in Japanese]
>
> Ono S, Yamaguchi H, Takayama S, Kurabe A, Heito T.
>
> Department of Radiology, Yamagata Prefectural Shinjo Hospital.
>
> Diagnostic usefulness of 99mTc-MIBI myocardial SPECT at rest was
> examined in 39 cases of coronary vasospastic angina pectoris who were
> diagnosed by a positive reaction to ergonovine provocation. SPECT was
> performed 45 minutes (early image) and 3 hours (delayed image) after the
> intravenous injection of approximately 600 MBq of MIBI. Decrease in
> accumulation was ranked by four defect scores (0: normal; 1: slight
> decrease; 2: moderate decrease; 3: severe decrease) and the total defect
> score was evaluated semiquantitatively. The washout rate between the
> normal area and the spasm area was also evaluated quantitatively using
> bull's eye. As a result, 15 cases (15/39; 38.4%) showed decreased
> accumulation in the early image and 27 cases (27/39; 69.2%) showed
> decreased accumulation in the delayed image. All of the cases which
> showed decreased accumulation in the early image had decreased
> accumulation in the delayed image as well. In 6 cases (6/34; 17.6%)
> showed ST wave changes during exercise ECG and 16 cases (16/34: 47%)
> showed decreased accumulation in the exercise myocardial SPECT. The
> washout rate of MIBI in the decreased accumulation area was
> significantly higher than that of the normal area. Of 32 ergonovine
> induced vasospastic area, 23 areas (72%) exhibited decreased
> accumulation in the delayed image for the same area. **Decreased**
> **accumulation in the delayed image in MIBI was due to the enhanced**
> **washout, which, in turn, indicated declined retention of MIBI by**
> **mitochondrial membrane. In coronary vasospastic angina pectoris, spasm**
> **induced ischemia was thought to have an effect on the mitochondria. This**
> **study suggested that even with a normal exercise ECG and exercise**
> **myocardial SPECT, there's a strong possibility of coronary vasospastic**
> **angina pectoris if a decreased accumulation was found in the delayed**
> **image in the MIBI myocardial SPECT at rest. Hence, in diagnosing**
> **coronary vasospastic angina pectoris, the delayed image in the MIBI**
> **myocardial SPECT at rest was believed to be useful.**
>
> Publication Types:
>
> * English Abstract
>
>
> PMID: 12058420 [PubMed - indexed for MEDLINE]
>

FW: mibi washout rate

From: **RM Fleming** (rmfmd7@hotmail.com)
Sent: Thu 8/23/07 6:42 PM
To: Mike Hansen PD corrected (mike_hansen@fd.org)

> 13: Ann Nucl Med. 2002 Jun;16(4):237-42. Related Articles, Links
>
> Assessment of myocardial washout of Tc-99m-sestamibi in patients
> with chronic heart failure: comparison with normal control.
>
> Kumita S, Seino Y, Cho K, Nakajo H, Toba M, Fukushima Y, Okamoto N,
> Takano T, Kumazaki T.
>
> Department of Radiology, Nippon Medical School, Tokyo, Japan.
> s-kumita@nms.ac.jp
>
> BACKGROUND: In contrast to 201TlCl, 99mTc-sestamibi shows very slow
> myocardial clearance after its initial myocardial uptake. In the present
> study, myocardial washout of 99mTc-sestamibi was calculated in patients
> with non-ischemic chronic heart failure (CHF) and compared with
> biventricular parameters obtained from first-pass and ECG-gated
> myocardial perfusion SPECT data. METHODS AND RESULTS: After
> administration of 99mTc-sestamibi, 25 patients with CHF and 8 normal
> controls (NC) were examined by ECG-gated myocardial perfusion SPECT and
> planar data acquisition in the early and delayed (interval of 3 hours)
> phase. Left ventricular ejection fraction (LVEF, %), peak filling rate
> (PFR, sec(-1)), end-diastolic volume (LVEDV, ml) and end-systolic volume
> (LVESV, ml) were automatically calculated from the ECG-gated SPECT data.
> **Myocardial washout rates over 3 hours were calculated from the early and**
> **delayed planar images.** Myocardial washout rates in the CHF group
> (39.6+/-5.2%) were significantly higher than those in the NC group
> (31.2+/-5.5%, $p < 0.01$). The myocardial washout rates for the 33
> subjects showed significant correlations with LVEF ($r = -0.61$, $p <$
> 0.001), PFR ($r = -0.47$, $p < 0.01$), LVEDV ($r = 0.45$, $p < 0.01$) and LVESV
> ($r = 0.48$, $p < 0.01$). CONCLUSION: **The myocardial washout rate of**
> **99Tc-sestamibi is considered to be a novel marker for the diagnosis of**
> **myocardial damage in patients with chronic heart failure.**
>
> Publication Types:
>
> * Clinical Trial
> * Comparative Study
> * Controlled Clinical Trial
> * Research Support, Non-U.S. Gov't
>
>
> PMID: 12126092 [PubMed - indexed for MEDLINE]
>

FW: mibi 10min and 60min

From: **RM Fleming** (rmfmd7@hotmail.com)
Sent: Thu 8/23/07 6:43 PM
To: Mike Hansen PD corrected (mike_hansen@fd.org)

> 10: Q J Nucl Med Mol Imaging. 2005 Sep;49(3):281-5. Related Articles,
> Links
> Click here to read
> Washout of [99mTc] sestamibi in predicting response to chemotherapy
> in patients with multiple myeloma.
>
> Pace L, Catalano L, Del Vecchio S, De Renzo A, Fonti R, Salvatore B,
> Andretta C, Di Nuzzo C, Rotoli B, Salvatore M.
>
> Nuclear Medicine Unit, Department of Biomorphological and Functional
> Sciences, Federico II University, Naples, Italy. pace@unina.it
>
> AIM: Technetium-99m 2-methoxy-isobutyl-isonitrile ([99mTc] MIBI) has
> been successfully used to study patients with multiple myeloma (MM).
> This tracer is also a substrate for P-glycoprotein (Pgp). Since Pgp
> overexpression is one of the primary mechanisms of multidrug resistance
> in MM, the aim of this study was to test whether [99mTc] MIBI could be
> an index of Pgp overexpression and function in MM and therefore predicts
> response to chemotherapy. METHODS: Forty patients with MM (12 in stage
> I, 15 in stage II, and 13 in stage III) showing diffuse bone marrow
> [99mTc] MIBI uptake were included in the study. All patients underwent
> whole body scintigraphy **at 10 and 60 minutes** after i.v. injection of 555
> MBq of [99mTc] MIBI. [99mTc] MIBI washout was measured, after decay
> correction, as: (10 minute counts/pixel minus 60 minute counts/pixel)
> divided by 10 minute counts/pixel, computed on a region of interest
> drawn on the thoracic spine (posterior projection), taking care of
> avoiding heart and splanchnic organs. Disease restaging was performed at
> a mean time of 32+/-20 months, and patients were considered to be in
> remission (complete or partial) or to show disease progression on the
> basis of a complete clinical and hematological evaluation. RESULTS:
> Patients showing disease progression at restaging (n=26) had higher
> washout (19.3+/-9.8% vs 12.8+/-6.9%, p<0.05) than patients in remission
> (n=14). Disease free survival was significantly better in patients with
> lower washout of [99mTc] MIBI. No differences in therapeutic regimen and
> stage of disease at admission were found between the 2 groups. When
> patients treated with melphalan were excluded from the analysis, 87.5%
> of patients in remission had low washout. CONCLUSIONS: **The present study**
> suggests a potential role of [99mTc] MIBI washout in predicting response
> to chemotherapy in patients with MM.
>
> Publication Types:
>
> * Clinical Trial
>
> PMID: 16172574 [PubMed - indexed for MEDLINE]

FW: mibi washout useful

From: **RM Fleming** (rmfmd7@hotmail.com)
Sent: Thu 8/23/07 6:45 PM
To: Mike Hansen PD corrected (mike_hansen@fd.org)

> 8: J Nucl Cardiol. 2006 Jan-Feb;13(1):64-8. Related Articles, Links
> Click here to read
> Usefulness of Tc-99m methoxyisobutylisonitrile scintigraphy for
> evaluating congestive heart failure.
>
> Sugiura T, Takase H, Toriyama T, Goto T, Ueda R, Dohi Y.
>
> Department of Internal Medicine, Enshu General Hospital, Hamamatsu,
> and Department of Internal Medicine and Molecular Science, Graduate
> School of Medical Sciences, Nagoya City University, Japan.
>
> BACKGROUND: Evidence is accumulating that technetium 99m
> methoxyisobutylisonitrile (MIBI) is not retained in the impaired
> myocardium. The purpose of this study was to determine whether the
> severity of congestive heart failure (CHF) can be evaluated by use of
> the washout rate (WR) of MIBI. METHODS AND RESULTS: Seventeen patients
> with CHF and ten healthy volunteers were enrolled in this study. MIBI
> and iodine 123 metaiodobenzylguanidine (MIBG) scintigraphy techniques
> were performed, and the WR was calculated. The blood was also sampled
> for the measurement of levels of brain natriuretic peptide, which is a
> powerful predictor of the severity of CHF. The WR of MIBI was higher in
> CHF patients (31.2%+/-6.3%) than in healthy volunteers (25.2%+/-4.7%)
> (P<.05). There were positive correlations between the WR of MIBI and
> brain natriuretic peptide levels (r=0.723, P<.0001) and a negative
> correlation between the WR of MIBI and the left ventricular ejection
> fraction (r=-0.545, P<.01). The WR of MIBI was correlated with that of
> MIBG (r=0.603, P<.01). CONCLUSIONS: **MIBI scintigraphy is useful in**
> evaluating the severity of congestive heart failure.
>
> Publication Types:
>
> * Comparative Study
> * Controlled Clinical Trial
>
>
> PMID: 16464718 [PubMed - indexed for MEDLINE]
>

>

FW: mibi delayed

From: **RM Fleming** (rmfmd7@hotmail.com)
Sent: Thu 8/23/07 6:46 PM
To: Mike Hansen PD corrected (mike_hansen@fd.org)

>
> 7: Ann Nucl Med. 2006 Jun;20(5):349-56. Related Articles, Links
>
> Clinical implication of reverse redistribution on 99mTc-sestamibi
> images for evaluating ischemic heart disease.
>
> Tanaka R, Nakamura T, Chiba S, Ono T, Yoshitani T, Miyamoto A,
> Yamazaki J.
>
> Radiological Department, Kushiro-shi Ishikai Hospital, Hokkaido,
> Japan. r_tanaka@kushiro-ishikai.or.jp
>
> OBJECTIVE: The purpose of this study was to clarify the usefulness
> of 99mTc-sestamibi (MIBI) delayed imaging in the assessment of the
> severity of myocardial ischemia in patients with coronary artery
> stenosis. METHODS: Forty-three angina pectoris with coronary stenosis of
> greater than 75% were enrolled in this study. Myocardial perfusion SPECT
> images were obtained 1 and 6 hours after an intravenous injection of
> MIBI at rest. Stress myocardial perfusion SPECT images were also
> acquired after the injection of MIBI. And myocardial fatty acid
> metabolism images were obtained 30 minutes after the injection of BMIPP
> at rest. Myocardial perfusion SPECT images were divided into 20 segments
> which were semiquantitatively assessed according to a 4-level defect
> score scale: score 0 (normal) to score 3 (severely); then the extent
> score (ES) and severity score (SS) were calculated. RESULTS: The
> sensitivity for myocardial ischemia showed the highest rate at 88.3%
> with MIBI delayed SPECT. According to the coronary angiography findings,
> MIBI stress SPECT and MIBI delayed SPECT detected the severity and
> extent of ischemia with more sensitivity than MIBI early SPECT in 12
> patients (group A) with stenosis of more than 75% but less than 90% (p <
> 0.01). Even though MIBI stress SPECT detected the severity and extent of
> ischemia in 31 patients (group B) with stenosis of more than 90% but
> less than 100%, there was no significant difference between MIBI stress
> SPECT and MIBI delayed SPECT. BMIPP SPECT revealed significant
> differences between group A and group B regarding the severity of
> myocardial ischemia. MIBI reverse redistribution was observed in 33
> patients and no significant difference existed between groups A and B.
> CONCLUSIONS: **Myocardial washout of MIBI was frequently observed in**
> patients with angina pectoris and the detection accuracy for ischemia
> was high. MIBI imaging is considered useful for assessment not only of
> myocardial perfusion but also mitochondrial function. The imagings with
> BMIPP and delayed MIBI could serve to determine the severity of
> myocardial ischemia more accurately.
>
> Publication Types:
>
> * Clinical Trial
>
>

> PMID: 16878707 [PubMed - indexed for MEDLINE]
>
>

FW: mibi slow washout by reference

From: **RM Fleming** (rmfmd7@hotmail.com)
Sent: Thu 8/23/07 6:49 PM
To: Mike Hansen PD corrected (mike_hansen@fd.org)

> J Nucl Cardiol. 2006 Nov;13(6):779-90. Related Articles, Links
> Click here to read
> Organ biodistribution and myocardial uptake, washout, and
> redistribution kinetics of Tc-99m N-DBODC5 when injected during
> vasodilator stress in canine models of coronary stenoses.
>
> Hatada K, Ruiz M, Riou LM, Lima RL, Goode AR, Watson DD, Beller GA,
> Glover DK.
>
> Second Department of Internal Medicine, Cardiovascular Division,
> Kansai Medical University Takii Hospital Moriguchi City, Osaka, Japan.
>
> BACKGROUND: Technetium 99m N-DBODC5 is a new myocardial perfusion
> tracer shown to exhibit high heart uptake and rapid liver clearance in
> normal rats. The objectives of this canine study were (1) to compare the
> organ biodistribution and myocardial uptake, washout, and redistribution
> kinetics of Tc-99m N-DBODC5 with Tc-99m sestamibi over a period of 3
> hours in a more clinically relevant large animal species and (2) to
> compare the myocardial uptake of Tc-99m N-DBODC5 with thallium 201 when
> co-injected during vasodilator stress in dogs with coronary stenoses.
> METHODS AND RESULTS: At peak adenosine-induced hyperemia, 10 dogs with
> critical left anterior descending artery stenoses received either Tc-99m
> N-DBODC5 (n = 6) or Tc-99m sestamibi (n = 4) and microspheres, followed
> by serial imaging and blood sampling over a period of 3 hours. Another
> 14 dogs with either critical (n = 7) or mild (n = 7) left anterior
> descending artery stenoses underwent simultaneous injection of Tc-99m
> N-DBODC5, Tl-201, and microspheres during peak vasodilator stress. Like
> sestamibi, Tc-99m N-DBODC5 showed good myocardial uptake with slow
> washout and minimal redistribution over a period of 3 hours (P = not
> significant); however, Tc-99m N-DBODC5 cleared more rapidly from the
> liver (heart-lung ratio at 30 minutes, 0.92+/-0.11 versus 0.51 +/- 0.05;
> P < .05). When injected during hyperemic flow, the myocardial extraction
> plateau for Tc-99m N-DBODC5 was lower than that for Tl-201 and was
> intermediate between Tc-99m sestamibi and Tc-99m tetrofosmin.
> CONCLUSIONS: Excellent organ biodistribution and myocardial uptake and
> clearance kinetic properties, combined with rapid liver clearance and a
> favorable flow-extraction relationship, make Tc-99m N-DBODC5 a very
> promising new myocardial perfusion imaging agent.
>
> Publication Types:
>
> * Research Support, Non-U.S. Gov't
>
> PMID: 17174809 [PubMed - indexed for MEDLINE]
>

FW: mibi comparison reference

From: **RM Fleming** (rmfmd7@hotmail.com)
Sent: Thu 8/23/07 6:51 PM
To: Mike Hansen PD corrected (mike_hansen@fd.org)
>
Mike,

The uptake of the trace is dependent upon both blood flow and something alive (mitochondria) at the end of the blood flow.

> 5: Nucl Med Biol. 2007 Jan;34(1):109-16. Epub 2006 Nov 28. Related
> Articles, Links
> Click here to read
> Mitochondrial avid radioprobes. Preparation and evaluation of
> 7'(Z)-[125I]iodorotenone and 7'(Z)-[125I]iodorotenol.
>
> VanBrocklin HF, Hanrahan SM, Enas JD, Nandanan E, O'Neil JP.
>
> Department of Functional Imaging, Lawrence Berkeley National
> Laboratory, Berkeley, CA 94720, USA. hfvanbrocklin@lbl.gov
>
> The loss of mitochondrial function has been implicated in a number
> of maladies such as Huntington's disease, Parkinson's disease (PD),
> cancer and cardiovascular disease. The objective of this research was to
> develop a radiolabeled mitochondrial probe. Two tracers,
> 7'-Z-iodorotenol and 7'-Z-iodorotenone, analogs of rotenone a natural
> product that inhibits Complex I of the mitochondrial electron transport
> chain, have been labeled with iodine-125 in 45-85% yield in a single
> step from the corresponding tributylstannyl precursor. In vivo
> distribution in adult male Sprague-Dawley rats for both compounds showed
> high accumulation in the heart (1.7-3.7 %ID/g at 1 h), a tissue with
> high mitochondrial content. Z-Iodorotenol did not washout of most
> tissues between 1 and 2 h postinjection, whereas Z-iodorotenone showed
> moderate washout (7-26%) over the same period. By 24 h, there was
> significant loss of both compounds from most tissues including the
> heart. Heart-to-blood, -lung and -liver ratios for Z-iodorotenone of
> 28.9, 10.7 and 2.4, respectively, were two- to fourfold higher than the
> Z-iodorotenol ratios. Compared to the current clinical perfusion
> tracers, 99mTc-sestamibi and 99mTc-tetrofosmin, Z-iodorotenone
> demonstrates similar 1 h heart accumulation and significantly higher
> heart-to-lung ratio (P<.001). Z-Iodorotenone heart-to-liver ratio is
> equivalent to 99mTc-sestamibi. 7'-Z-Iodorotenone possesses distribution
> characteristics of an improved tracer for SPECT perfusion studies.
>
> Publication Types:
>
> * Evaluation Studies
> * Research Support, N.I.H., Extramural
> * Research Support, U.S. Gov't, Non-P.H.S.
> PMID: 17210467 [PubMed - indexed for MEDLINE]

FW: mibi WOR

From: **RM Fleming** (rmfmd7@hotmail.com)
Sent: Thu 8/23/07 6:53 PM
To: Mike Hansen PD corrected (mike_hansen@fd.org)

> 4: Mitochondrion. 2007 Feb-Apr;7(1-2):164-70. Epub 2006 Dec 5.
> Related Articles, Links
> Click here to read
> Evaluation of respiratory chain failure in mitochondrial
> cardiomyopathy by assessments of 99mTc-MIBI washout and
> 123I-BMIPP/99mTc-MIBI mismatch.
>
> Ikawa M, Kawai Y, Arakawa K, Tsuchida T, Miyamori I, Kuriyama M,
> Tanaka M, Yoneda M.
>
> Second Department of Internal Medicine, Faculty of Medical Sciences,
> University of Fukui, 23-3 Shimoaiduki, Matsuoka, Fukui 910-1193, Japan.
>
> Cardiomyopathy is one of the main features that determines prognosis
> in patients with mitochondrial encephalomyopathy. We investigated
> respiratory chain failure using 99mTc-MIBI- and 123I-BMIPP-SPECT in vivo
> in five patients with mitochondrial cardiomyopathty. With the lowering
> of cardiac function, the 99mTc-MIBI-washout rate (WOR) increased, and
> the 99mTc-MIBI-uptake decreased, conversely. In patients who showed
> severe cardiac involvement, 99mTc-MIBI-uptake was markedly reduced, and
> by contrast, 123I-BMIPP-uptake increased (123I-BMIPP/99mTc-MIBI
> mismatch). There were significant correlations between the WOR on
> 99mTc-MIBI-SPECT and interventricular septal thickness (IVST) on
> echocardiography and between WOR and left ventricular ejection fraction
> (LVEF) on 99mTc-MIBI-SPECT. **The increased WOR and decreased uptake of**
> **99mTc-MIBI were reflected by the lowered mitochondrial membrane**
> **potential created by mitochondrial respiratory chain whereas**
> **123I-BMIPP/99mTc-MIBI mismatch may be created by the enhanced**
> **triglyceride-pool. These nuclear medicine techniques are the potential**
> **tools to evaluate the energy state in mitochondrial cardiomyopathy.**
>
> PMID: 17280875 [PubMed - indexed for MEDLINE]
>

FW: mibi clearance rate

From: **RM Fleming** (rmfmd7@hotmail.com)
Sent: Thu 8/23/07 6:54 PM
To: Mike Hansen PD corrected (mike_hansen@fd.org)

> 1: Ann Nucl Med. 2007 Jul;21(5):267-73. Epub 2007 Jul 25. Related
> Articles, Links
> Click here to read
> Myocardial kinetics of (201)Thallium, (99m)Tc-tetrofosmin, and
> (99m)Tc-sestamibi in an acute ischemia-reperfusion model using isolated
> rat heart.
>
> Fukushima K, Momose M, Kondo C, Kusakabe K, Kasanuki H.
>
> Department of Cardiology, Tokyo Women's Medical University, Tokyo,
> Japan.
>
> OBJECTIVE: (201)Thallium (TL), (99m)Tc-tetrofosmin (TF), and
> (99m)Tc-sestamibi (MIBI) are extensively used as myocardial perfusion
> agents. The objective of the present study was to evaluate their
> kinetics under acute ischemia-reperfusion. METHODS: Isolated rat hearts,
> perfused by the Langendorff method at a constant flow rate of 10 ml/min,
> were allotted to normal control, mild ischemia, and severe ischemia
> groups, in which 20-min tracer wash-in was conducted followed by a
> 25-min tracer washout. No-flow ischemia (15 min for mild ischemia
> groups; 30 min for severe ischemia groups) was induced before conducting
> wash-in and washout in the ischemia groups. Whole-heart radioactivity
> was determined with an external gamma detector. Myocardial flow rate (K
> (1), ml/min) and clearance rate (k (2), min(-1)) were calculated.
> RESULTS: K (1TL), K (1TF), and K (1MIBI) decreased according to the
> severity of ischemia (K (1TL) 5.32 +/- 0.53, 4.76 +/- 0.70, and 1.44 +/-
> 0.59; K (1TF) 3.80 +/- 0.70, 2.73 +/- 0.99, and 1.09 +/- 0.45; and K
> (1MIBI) 3.45 +/- 1.10, 2.15 +/- 0.82, and 1.05 +/- 0.13, in the normal
> control, mild, and severe ischemia groups, respectively). K (1) was
> significantly higher for TL than for the (99m)Tc tracers ($P < 0.05$), but
> the (99m)Tc tracers had equivalent K (1) values. k (2TL) increased
> significantly ($P < 0.05$) in the ischemia groups (k (2TL) 0.062 +/-
> 0.013, 0.11 +/- 0.045, and 0.12 +/- 0.035), but showed no significant
> difference between the ischemia groups. k (2MIBI) and k (2TF) were
> significantly ($P < 0.05$) lower than k (2TL) and increased significantly
> ($P < 0.05$) in the severe ischemia group (k (2TF) 0.0056 +/- 0.0022,
> 0.0037 +/- 0.0015, and 0.024 +/- 0.015; and k (2MIBI) 0.00072 +/-
> 0.0011, 0.00038 +/- 0.00076, and 0.042 +/- 0.034). k (2MIBI) was
> significantly ($P < 0.05$) lower than k (2TF) in the normal control and
> mild ischemia groups. CONCLUSIONS: **Tracer extraction was higher for TL**
> than for the (99m)Tc tracers and all tracers decreased according to the
> severity of ischemia-reperfusion in the three tracer groups. The
> clearance kinetics of not only MIBI but also TF is possibly useful for
> the evaluation of the severity of ischemia, and the Langendorff method
> and a methodological approach by continuous determinations of
> radioactivity may serve for the quantitative analysis of tracer kinetic
> profiles.

>
> PMID: 17634844 [PubMed - in process]

FW: What is reverse distribution? mibi

From: **RM Fleming** (rmfmd7@hotmail.com)
Sent: Thu 8/23/07 6:55 PM
To: Mike Hansen PD corrected (mike_hansen@fd.org)

>
> 17: J Nucl Cardiol. 1998 Mar-Apr;5(2):119-27. Related Articles, Links
> Click here to read
> Comment in:
>
> * J Nucl Cardiol. 1998 Mar-Apr;5(2):202-5.
>
>
> Prediction of functional recovery in acute myocardial infarction:
> comparison between sestamibi reverse redistribution and sestamibi/BMIPP
> mismatch.
>
> Fujiwara S, Takeishi Y, Atsumi H, Yamaki M, Takahashi N, Yamaoka M,
> Tojo T, Tomoike H.
>
> First Department of Internal Medicine, Yamagata University School of
> Medicine, Iida-Nishi, Japan. sfujiwar@med.id.yamagata-u.ac.jp
>
> BACKGROUND: It has been known that Tc 99m sestamibi/iodine 123
> betamethyliodophenylpentadecanoic (123I-BMIPP) (sestamibi/BMIPP)
> mismatch is an indicator of viable myocardium in acute myocardial
> infarction (AMI). We have reported that reverse redistribution of
> sestamibi in AMI indicates the patency of infarct-related artery and a
> preserved left ventricular function in the chronic stage. In this study
> we investigated the relationship between reverse redistribution of
> sestamibi and sestamibi/BMIPP mismatch in patients with AMI. METHODS:
> Twenty-three patients with AMI who received direct percutaneous
> transluminal coronary angioplasty underwent both BMIPP and sestamibi
> SPECT within 2 weeks after onset. Sestamibi images were obtained 1 hour
> (early) and 3 hours (delayed) after injection of sestamibi. BMIPP
> imaging was carried out 30 minutes after injection. The left ventricle
> was divided into 17 segments, and regional myocardial uptakes of the
> tracers in each segment were scored from 0 (normal) to 3 (no activity).
> A reverse redistribution pattern was defined as an increase of > or =1
> in the regional score at the delayed images. More reduced BMIPP uptake
> than sestamibi uptake in each segment was determined as sestamibi/BMIPP
> mismatch. Contrast left ventriculography was performed soon after
> revascularization and repeated 1 month later. RESULTS: Of 15 patients
> with sestamibi reverse redistribution, sestamibi/BMIPP mismatch was
> observed in 14 patients (93%), whereas mismatch was seen in only one of
> seven patients (14%) without reverse redistribution ($p < 0.01$). In
> patients with sestamibi reverse redistribution, regional scores of BMIPP
> agreed with those of early and delayed images of sestamibi in 51
> segments (46%) and in 92 segments (83%), respectively. In the chronic
> stage, both regional wall motion and left ventricular ejection fraction
> improved in patients with sestamibi reverse redistribution (wall motion
> score: 6.7 +/- 2.4 vs 2.7 +/- 2.1, $p < 0.01$; ejection fraction: 56% +/-
> 7% vs 64% +/- 8%, $p < 0.01$), but not in those without reverse

> redistribution. CONCLUSION: **Both reverse redistribution of sestamibi and**
> **sestamibi/BMIPP mismatch reflect the recovery of left ventricular**
> **function and thus imply myocardial viability in AMI. Because the**
> **presence of reverse redistribution of sestamibi agreed with that of**
> **sestamibi/BMIPP mismatch, additional BMIPP images can be replaced by the**
> **delayed images after a single injection of sestamibi.**
>
> Publication Types:
>
> * Comparative Study
> * Research Support, Non-U.S. Gov't
>
>
> PMID: 9588663 [PubMed - indexed for MEDLINE]

FW: tumors mibi

From: **RM Fleming** (rmfmd7@hotmail.com)
Sent: Thu 8/23/07 6:58 PM
To: Mike Hansen PD corrected (mike_hansen@fd.org)

>
> *3: *Ann Nucl Med. <javascript:AL_get(this, 'jour', 'Ann Nucl Med.');>
> 2005 Jul;19(5):387-92. Related Articles
>
<http://www.ncbi.nlm.nih.gov/sites/entrez?Db=pubmed&DbFrom=pubmed&Cmd=Link&LinkName=pubmed_pubmed&LinkReadableName=Related%20Articles&IdsFromResult=16164195&ordinalpos=3&itool=EntrezSystem2.PEntrez.Pubmed.Pubmed_ResultsPanel.Pubmed_RVAbstract>,
> Links <javascript:PopUpMenu2_Set(Menu16164195);>
>
>
> *Relation between Tc-99m sestamibi uptake and biological factors in
> hyperparathyroidism.*
>
> *Cermik TF*
>
<http://www.ncbi.nlm.nih.gov/sites/entrez?Db=pubmed&Cmd=Search&Term=%22Cermik%20TF%22%5BAuthor%5D&itool=EntrezSystem2.PEntrez.Pubmed.Pubmed_ResultsPanel.Pubmed_RVAbstract>,
> *Puyan FO*
>
<http://www.ncbi.nlm.nih.gov/sites/entrez?Db=pubmed&Cmd=Search&Term=%22Puyan%20FO%22%5BAuthor%5D&itool=EntrezSystem2.PEntrez.Pubmed.Pubmed_ResultsPanel.Pubmed_RVAbstract>,
> *Sezer A*
>
<http://www.ncbi.nlm.nih.gov/sites/entrez?Db=pubmed&Cmd=Search&Term=%22Sezer%20A%22%5BAuthor%5D&itool=EntrezSystem2.PEntrez.Pubmed.Pubmed_ResultsPanel.Pubmed_RVAbstract>,
> *Firat MF*
>
<http://www.ncbi.nlm.nih.gov/sites/entrez?Db=pubmed&Cmd=Search&Term=%22Firat%20MF%22%5BAuthor%5D&itool=EntrezSystem2.PEntrez.Pubmed.Pubmed_ResultsPanel.Pubmed_RVAbstract>,
> *Berkarda S*
>
<http://www.ncbi.nlm.nih.gov/sites/entrez?Db=pubmed&Cmd=Search&Term=%22Berkarda%20S%22%5BAuthor%5D&itool=EntrezSystem2.PEntrez.Pubmed.Pubmed_ResultsPanel.Pubmed_RVAbstract>.
>
> Department of Nuclear Medicine, School of Medicine, Trakya
> University, Edirne, Turkey. cermik@trakya.edu.tr
>
> PURPOSE: The aim of this study was to evaluate the relation between
> uptake ratios of Tc-99m sestamibi (MIBI) and tumor volume, serum
> biochemical values (i-PTH, Ca, P) and oxyphil cell content.
> MATERIALS AND METHODS: The study population consisted of 19 patients
> (2 M, 17 F; mean +/- SD: 47 +/- 12 y). Anterior planar images of the
> neck and chest were acquired early (15 min) and triple late phase
> (1, 2 and 3-4 h) after intravenous injections of 740 MBq MIBI. Each
> of the surgical materials was reviewed retrospectively. The
> percentage of cell type (chief, oxyphil and clear cells) in the
> tumors was calculated by light microscopy. RESULTS: The uptake ratio
> obtained from L1 (1 hour) phase was found to be higher than the

> uptake ratio obtained from early phase, and the difference was
> statistically significant (1.57 +/- 0.34 and 1.43 +/- 0.29, p =
> 0.004, respectively). There was no significant correlation between
> uptake ratios that were obtained from 4 different imaging phases and
> lesion volumes, i-PTH levels and calcium levels (p > 0.05). However,
> there was a significant adverse correlation between L2 and L3 uptake
> ratios and serum phosphorus values (r = -0.44, p = 0.04 and r =
> -0.46, p = 0.04, respectively). Additionally, no significant
> correlation between MIBI uptake ratios of each imaging phase and the
> laboratory data, volume of lesion or oxyphil percentage volume was
> found after the multiple regression analysis (E: p = 0.46, r = 0.49;
> L1: p = 0.24, r = 0.58; L2: p = 0.27, r = 0.57; L3: p = 0.32, r =
> 0.55, respectively. There was no correlation between gland oxyphil
> percentage volume and MIBI uptake ratios (p > 0.05). CONCLUSION: **The
> results of our study show that the optimal imaging times after
> intravenous injection of MIBI are 15 minutes and 1 hour because of
> the shorter examination time without loss of diagnostic ability. In
> the present study, there was no significant correlation between MIBI
> uptake ratios and increased gland volume, or serum Ca and i-PTH
> levels. Besides, we think that oxyphil cell content may not have a
> main effect on MIBI uptake and retention. The fact of an adverse
> relation between phosphorus and MIBI retention in our study suggests
> that phosphorus level should be considered prior to MIBI imaging.**
>
> PMID: 16164195 [PubMed - indexed for MEDLINE]
>

FW: heart-to-lung all references on Medline

From: **RM Fleming** (rmfmd7@hotmail.com)
Sent: Thu 8/23/07 7:04 PM
To: Mike Hansen PD corrected (mike_hansen@fd.org)
Mike,

Changes in time have resulted in an understanding that "even though everyone knows sestamibi heart to lung ratios are not important" because Thallium 201 and sestamibi "behave differently." Apparently someone forgot to tell the sestamibi it "shouldn't behave this way."

> Items 1 - 5 of 5
>
> One page.
>
> *1: *Ann Nucl Med. <javascript:AL_get(this, 'jour', 'Ann Nucl Med.');>
> 2006 Dec;20(10):663-70. Related Articles
>
<http://www.ncbi.nlm.nih.gov/sites/entrez?Db=pubmed&DbFrom=pubmed&Cmd=Link&LinkName=pubmed_pubmed&LinkReadableName=Related%20Articles&IdsFromResult=17385304&ordinalpos=1&itool=EntrezSystem2.PEntrez.Pubmed.Pubmed_ResultsPanel.Pubmed_RVAbstract>,
> Links <javascript:PopUpMenu2_Set(Menu17385304);>
>
>
> *Myocardial uptake characteristics of three 99mTc-labeled tracers
> for myocardial perfusion imaging one hour after rest injection.*
>
> *Manka-Waluch A*
> <http://www.ncbi.nlm.nih.gov/sites/entrez?Db=pubmed&Cmd=Search&Term=%22Manka-Waluch%20A%22%5BAuthor%5D&itool=EntrezSystem2.PEntrez.Pubmed.Pubmed_ResultsPanel.Pubmed_RVAbstract>,
> *Palmedo H*
>
<http://www.ncbi.nlm.nih.gov/sites/entrez?Db=pubmed&Cmd=Search&Term=%22Palmedo%20H%22%5BAuthor%5D&itool=EntrezSystem2.PEntrez.Pubmed.Pubmed_ResultsPanel.Pubmed_RVAbstract>,
> *Reinhardt MJ*
>
<http://www.ncbi.nlm.nih.gov/sites/entrez?Db=pubmed&Cmd=Search&Term=%22Reinhardt%20MJ%22%5BAuthor%5D&itool=EntrezSystem2.PEntrez.Pubmed.Pubmed_ResultsPanel.Pubmed_RVAbstract>,
> *Joe AY*
>
<http://www.ncbi.nlm.nih.gov/sites/entrez?Db=pubmed&Cmd=Search&Term=%22Joe%20AY%22%5BAuthor%5D&itool=EntrezSystem2.PEntrez.Pubmed.Pubmed_ResultsPanel.Pubmed_RVAbstract>,
> *Manka C*
>
<http://www.ncbi.nlm.nih.gov/sites/entrez?Db=pubmed&Cmd=Search&Term=%22Manka%20C%22%5BAuthor%5D&itool=EntrezSystem2.PEntrez.Pubmed.Pubmed_ResultsPanel.Pubmed_RVAbstract>,
> *Guhlke S*
>
<http://www.ncbi.nlm.nih.gov/sites/entrez?Db=pubmed&Cmd=Search&Term=%22Guhlke%20S%22%5BAuthor%5D&itool=EntrezSystem2.PEntrez.Pubmed.Pubmed_ResultsPanel.Pubmed_RVAbstract>,
> *Biersack HJ*
>
<http://www.ncbi.nlm.nih.gov/sites/entrez?Db=pubmed&Cmd=Search&Term=%22Biersack%20HJ%22%5BAuthor%5D&itool=EntrezSystem2.PEntrez.Pubmed.Pubmed_ResultsPanel.Pubmed_RVAbstract>,

> *Bucerius J*
>
<http://www.ncbi.nlm.nih.gov/sites/entrez?Db=pubmed&Cmd=Search&Term=%22Bucerius%20J%22%5BAuthor%5D&itool=EntrezSystem2.PEntrez.Pubmed.Pubmed_ResultsPanel.Pubmed_RVAbstract>.
>
> Department of Nuclear Medicine, University of Bonn, Bonn; Germany.
>
> OBJECTIVE: 99mTc-tetrofosmin and 99mTc-sestamibi are approved
> tracers for myocardial perfusion studies. Recently, a 99mTc-MIBI
> preparation from a different manufacturer (99mTc-cardiospect-MIBI)
> has been introduced to the market. Therefore, the aim of this study
> was the evaluation of 99mTc-tetrofosmin as well as of two different
> 99mTc-labeled MIBI tracers with regard to differences in imaging
> quality under resting conditions. METHODS: Sixty patients (mean age
> 63.8 years +/- 1.25) with known or suspected coronary artery disease
> but without evidence of rest-ischemia were included. Twenty patients
> in each group were examined by a two-day-rest-stress protocol using
> the three 99mTc-labeled tracers. Visual analysis of all images was
> performed by two experienced physicians blinded with regard to the
> applied tracer. Regions of interest (ROI) were defined over the
> heart, lung and whole body only in the rest imaging in order to
> calculate heart-to-lung, lung-to-whole body-, and heart-to-whole
> body-ratios. RESULTS: The heart-to-lung ratio was statistically
> significant higher for 99mTc-cardiospect-MIBI as compared to
> 99mTc-sestamibi as well as to 99mTc-tetrofosmin. Furthermore, a
> significantly higher heart-to-lung ratio was found for
> 99mTc-sestamibi as compared to 99mTc-tetrofosmin. The heart-to-whole
> body-ratio and the lung-to-whole body-ratio were equivalent between
> all tracers. Visual analysis revealed only slight differences
> regarding image quality between all tracers. CONCLUSIONS: **ROI**
> analysis surprisingly revealed a significant higher myocardial
> uptake and consequently a higher heart-to-lung ratio for
> 99mTc-cardiospect-MIBI. Whether this leads to a better visual image
> quality has to be evaluated in future studies with larger study
> populations as well as semiquantitative segmental analysis of the
> myocardial perfusion images.
>
> Publication Types:
>
> * Comparative Study <javascript:AL_get(this, 'ptyp',
> 'Comparative Study');>
> * Evaluation Studies <javascript:AL_get(this, 'ptyp',
> 'Evaluation Studies');>
>
>
> PMID: 17385304 [PubMed - indexed for MEDLINE]
>
> ---
>
> *2: *Nucl Med Biol. <javascript:AL_get(this, 'jour', 'Nucl Med Biol.');>
> 2007 Jan;34(1):109-16. Epub 2006 Nov 28. Related Articles
>
<http://www.ncbi.nlm.nih.gov/sites/entrez?Db=pubmed&DbFrom=pubmed&Cmd=Link&LinkName=pubmed_pubmed&LinkReadableName=Related%20Articles&IdsFromResult=17210467&ordinalpos=2&itool=EntrezSystem2.PEntrez.Pubmed.Pubmed_ResultsPanel.Pubmed_RVAbstract>,
> Links <javascript:PopUpMenu2_Set(Menu17210467);>

>
> Click here to read
> <http://www.ncbi.nlm.nih.gov/entrez/utils/fref.fcgi?PrId=3048&itool=Abstract-def&uid=17210467&db=pubmed&url=http://linkinghub.elsevier.com/retrieve/pii/S0969-8051%2806%2900201-0>
>
> *Mitochondrial avid radioprobes. Preparation and evaluation of
> 7'(Z)-[125I]iodorotenone and 7'(Z)-[125I]iodorotenol.*
>
> *VanBrocklin HF*
>
<http://www.ncbi.nlm.nih.gov/sites/entrez?Db=pubmed&Cmd=Search&Term=%22VanBrocklin%20HF%22%5BAuthor%5D&itool=EntrezSystem2.PEntrez.Pubmed.Pubmed_ResultsPanel.Pubmed_RVAbstract>,
> *Hanrahan SM*
>
<http://www.ncbi.nlm.nih.gov/sites/entrez?Db=pubmed&Cmd=Search&Term=%22Hanrahan%20SM%22%5BAuthor%5D&itool=EntrezSystem2.PEntrez.Pubmed.Pubmed_ResultsPanel.Pubmed_RVAbstract>,
> *Enas JD*
>
<http://www.ncbi.nlm.nih.gov/sites/entrez?Db=pubmed&Cmd=Search&Term=%22Enas%20JD%22%5BAuthor%5D&itool=EntrezSystem2.PEntrez.Pubmed.Pubmed_ResultsPanel.Pubmed_RVAbstract>,
> *Nandanan E*
>
<http://www.ncbi.nlm.nih.gov/sites/entrez?Db=pubmed&Cmd=Search&Term=%22Nandanan%20E%22%5BAuthor%5D&itool=EntrezSystem2.PEntrez.Pubmed.Pubmed_ResultsPanel.Pubmed_RVAbstract>,
> *O'Neil JP*
>
<http://www.ncbi.nlm.nih.gov/sites/entrez?Db=pubmed&Cmd=Search&Term=%22O%27Neil%20JP%22%5BAuthor%5D&itool=EntrezSystem2.PEntrez.Pubmed.Pubmed_ResultsPanel.Pubmed_RVAbstract>.
>
> Department of Functional Imaging, Lawrence Berkeley National
> Laboratory, Berkeley, CA 94720, USA. hfvanbrocklin@lbl.gov
>
> **The loss of mitochondrial function has been implicated in a number
> of maladies such as Huntington's disease, Parkinson's disease (PD),
> cancer and cardiovascular disease. The objective of this research
> was to develop a radiolabeled mitochondrial probe. Two** tracers,
> 7'-Z-iodorotenol and 7'-Z-iodorotenone, analogs of rotenone a
> natural product that inhibits Complex I of the mitochondrial
> electron transport chain, have been labeled with iodine-125 in
> 45-85% yield in a single step from the corresponding tributylstannyl
> precursor. In vivo distribution in adult male Sprague-Dawley rats
> for both compounds showed high accumulation in the heart (1.7-3.7
> %ID/g at 1 h), a tissue with high mitochondrial content.
> Z-Iodorotenol did not washout of most tissues between 1 and 2 h
> postinjection, whereas Z-iodorotenone showed moderate washout
> (7-26%) over the same period. By 24 h, there was significant loss of
> both compounds from most tissues including the heart.
> Heart-to-blood, -lung and -liver ratios for Z-iodorotenone of 28.9,
> 10.7 and 2.4, respectively, were two- to fourfold higher than the
> Z-iodorotenol ratios. Compared to the current clinical perfusion
> tracers, 99mTc-sestamibi and 99mTc-tetrofosmin, Z-iodorotenone
> demonstrates similar 1 h heart accumulation and significantly higher
> heart-to-lung ratio (P<.001). Z-Iodorotenone heart-to-liver ratio is
> equivalent to 99mTc-sestamibi. 7'-Z-Iodorotenone possesses
> distribution characteristics of an improved tracer for SPECT
> perfusion studies.

>
> Publication Types:
>
> * Evaluation Studies <javascript:AL_get(this, 'ptyp',
> 'Evaluation Studies');>
> * Research Support, N.I.H., Extramural <javascript:AL_get(this,
> 'ptyp', 'Research Support, N.I.H., Extramural');>
> * Research Support, U.S. Gov't, Non-P.H.S.
> <javascript:AL_get(this, 'ptyp', 'Research Support, U.S.
> Gov\'t, Non-P.H.S.');>
>
>
> PMID: 17210467 [PubMed - indexed for MEDLINE]
>
> ---
>
> *3: *Nuklearmedizin. <javascript:AL_get(this, 'jour',
> 'Nuklearmedizin.');> 1999;38(6):189-91. Related Articles
>
<http://www.ncbi.nlm.nih.gov/sites/entrez?Db=pubmed&DbFrom=pubmed&Cmd=Link&LinkName=pubmed_pubmed&LinkReadableName=Related%20Articles&IdsFromResult=10510802&ordinalpos=3&itool=EntrezSystem2.PEntrez.Pubmed.Pubmed_ResultsPanel.Pubmed_RVAbstract>,
> Links <javascript:PopUpMenu2_Set(Menu10510802);>
>
>
> *Myocardial uptake of technetium-99m-furifosmin (Q12) versus
> technetium-99m-sestamibi (MIBI).*
>
> *Bangard M*
>
<http://www.ncbi.nlm.nih.gov/sites/entrez?Db=pubmed&Cmd=Search&Term=%22Bangard%20M%22%5BAuthor%5D&itool=EntrezSystem2.PEntrez.Pubmed.Pubmed_ResultsPanel.Pubmed_RVAbstract>,
> *Bender H*
>
<http://www.ncbi.nlm.nih.gov/sites/entrez?Db=pubmed&Cmd=Search&Term=%22Bender%20H%22%5BAuthor%5D&itool=EntrezSystem2.PEntrez.Pubmed.Pubmed_ResultsPanel.Pubmed_RVAbstract>,
> *Grünwald F*
>
<http://www.ncbi.nlm.nih.gov/sites/entrez?Db=pubmed&Cmd=Search&Term=%22Gr%C3%BCnwald%20F%22%5BAuthor%5D&itool=EntrezSystem2.PEntrez.Pubmed.Pubmed_ResultsPanel.Pubmed_RVAbstract>,
> *Hümmelgen M*
>
<http://www.ncbi.nlm.nih.gov/sites/entrez?Db=pubmed&Cmd=Search&Term=%22H%C3%BCmmelgen%20M%22%5BAuthor%5D&itool=EntrezSystem2.PEntrez.Pubmed.Pubmed_ResultsPanel.Pubmed_RVAbstract>,
> *Willkomm P*
>
<http://www.ncbi.nlm.nih.gov/sites/entrez?Db=pubmed&Cmd=Search&Term=%22Willkomm%20P%22%5BAuthor%5D&itool=EntrezSystem2.PEntrez.Pubmed.Pubmed_ResultsPanel.Pubmed_RVAbstract>,
> *Palmedo H*
>
<http://www.ncbi.nlm.nih.gov/sites/entrez?Db=pubmed&Cmd=Search&Term=%22Palmedo%20H%22%5BAuthor%5D&itool=EntrezSystem2.PEntrez.Pubmed.Pubmed_ResultsPanel.Pubmed_RVAbstract>,
> *Lüderitz B*
>
<http://www.ncbi.nlm.nih.gov/sites/entrez?Db=pubmed&Cmd=Search&Term=%22L%C3%BCderitz%20B%22%5BAuthor%5D&itool=EntrezSystem2.PEntrez.Pubmed.Pubmed_ResultsPanel.Pubmed_RVAbstract>,

> *Biersack HJ*
>
<http://www.ncbi.nlm.nih.gov/sites/entrez?Db=pubmed&Cmd=Search&Term=%22Biersack%20HJ%22%5BAutho
r%5D&itool=EntrezSystem2.PEntrez.Pubmed.Pubmed_ResultsPanel.Pubmed_RVAbstract>.
>
> Klinik für Nuklearmedizin, Universitätsklinik Bonn, Deutschland.
> bangard@mailer.meb.uni-bonn.de
>
> AIM: This study was performed to compare the myocardial uptake of
> Tc-99m-furifosmin (Q12) versus Tc-99m-sestamibi (MIBI) in
> correlation to the whole-body uptake under resting conditions.
> METHODS: 21 patients with coronary artery disease and no rest
> ischemia were examined. A whole-body scan was performed 60 min. p.i.
> under resting conditions. A quantification of the uptake
> (whole-body, heart and right lung) was done by ROI technique.
> RESULTS: The heart-to-lung ratio of Q12 (1.56 +/- 0.191) was
> significantly lower as compared to MIBI (1.94 +/- 0.197; $p < 0.01$).
> In contrast, the heart-to-whole-body ratios (Q12 versus MIBI: 0.027
> +/- 0.012 versus 0.026 +/- 0.004; $p < 0.76$) did not differ. The
> lung-to-whole-body ratio (Q12 versus MIBI: 0.018 +/- 0.009 versus
> 0.013 +/- 0.002; $p < 0.17$) were different, but did not reach
> significance. CONCLUSION: **These data show that under resting**
> conditions the total myocardial uptake of Q12 does not differ
> significantly from that of MIBI. However, the pulmonary uptake of
> Q12 is slightly higher, resulting in a significant lower
> heart-to-lung ratio. These findings imply a lower image quality of
> Q12 compared to MIBI.
>
> Publication Types:
>
> * Comparative Study <javascript:AL_get(this, 'ptyp',
> 'Comparative Study');>
>
>
> PMID: 10510802 [PubMed - indexed for MEDLINE]
>
> ----------
>
> *4: *Kaku Igaku. <javascript:AL_get(this, 'jour', 'Kaku Igaku.');> 1991
> Oct;28(10):1133-42. Related Articles
>
<http://www.ncbi.nlm.nih.gov/sites/entrez?Db=pubmed&DbFrom=pubmed&Cmd=Link&LinkName=pubmed_pub
med&LinkReadableName=Related%20Articles&IdsFromResult=1839318&ordinalpos=4&itool=EntrezSystem2.PE
ntrez.Pubmed.Pubmed_ResultsPanel.Pubmed_RVAbstract>,
> Links <javascript:PopUpMenu2_Set(Menu1839318);>
>
>
> *[Phase I clinical study on 99mTc-MIBI]*
>
> [Article in Japanese]
>
> *Kubo A*
>
<http://www.ncbi.nlm.nih.gov/sites/entrez?Db=pubmed&Cmd=Search&Term=%22Kubo%20A%22%5BAuthor%5
D&itool=EntrezSystem2.PEntrez.Pubmed.Pubmed_ResultsPanel.Pubmed_RVAbstract>,
> *Nakamura K*

>
<http://www.ncbi.nlm.nih.gov/sites/entrez?Db=pubmed&Cmd=Search&Term=%22Nakamura%20K%22%5BAuthor%5D&itool=EntrezSystem2.PEntrez.Pubmed.Pubmed_ResultsPanel.Pubmed_RVAbstract>,
> *Sanmiya T*
>
<http://www.ncbi.nlm.nih.gov/sites/entrez?Db=pubmed&Cmd=Search&Term=%22Sanmiya%20T%22%5BAuthor%5D&itool=EntrezSystem2.PEntrez.Pubmed.Pubmed_ResultsPanel.Pubmed_RVAbstract>,
> *Shimizu S*
>
<http://www.ncbi.nlm.nih.gov/sites/entrez?Db=pubmed&Cmd=Search&Term=%22Shimizu%20S%22%5BAuthor%5D&itool=EntrezSystem2.PEntrez.Pubmed.Pubmed_ResultsPanel.Pubmed_RVAbstract>,
> *Hashimoto S*
>
<http://www.ncbi.nlm.nih.gov/sites/entrez?Db=pubmed&Cmd=Search&Term=%22Hashimoto%20S%22%5BAuthor%5D&itool=EntrezSystem2.PEntrez.Pubmed.Pubmed_ResultsPanel.Pubmed_RVAbstract>,
> *Iwanaga S*
>
<http://www.ncbi.nlm.nih.gov/sites/entrez?Db=pubmed&Cmd=Search&Term=%22Iwanaga%20S%22%5BAuthor%5D&itool=EntrezSystem2.PEntrez.Pubmed.Pubmed_ResultsPanel.Pubmed_RVAbstract>,
> *Handa S*
>
<http://www.ncbi.nlm.nih.gov/sites/entrez?Db=pubmed&Cmd=Search&Term=%22Handa%20S%22%5BAuthor%5D&itool=EntrezSystem2.PEntrez.Pubmed.Pubmed_ResultsPanel.Pubmed_RVAbstract>,
> *Torizuka K*
>
<http://www.ncbi.nlm.nih.gov/sites/entrez?Db=pubmed&Cmd=Search&Term=%22Torizuka%20K%22%5BAuthor%5D&itool=EntrezSystem2.PEntrez.Pubmed.Pubmed_ResultsPanel.Pubmed_RVAbstract>.
>
> Department of Radiology, Keio University Hospital, Tokyo.
>
> A phase I clinical study on 99mTc-hexakis 2-methoxy
> isobutylisonitrile (99mTc-MIBI) was carried out in 6 normal
> volunteers. There was no significant change in vital signs and
> laboratory parameters attributing to the reagent other than
> complaint of slight and transient metallic taste immediately after
> the injection in 4 volunteers. The highest dosimetry was calculated
> as 1.1 mGy/37 MBq at lower large intestine, which was within the
> acceptable range. 99mTc-MIBI was rapidly cleared from the blood and
> accumulated in the heart immediately after the injection with 1.4%
> dose and 1.8% dose at 5 min at rest and at stress, respectively. The
> retention of radioactivity in the heart well continued for at least
> several hours. **The heart-to-lung ratio was over 2.00 at 5 min and**
> heart-to-liver ratio was over 1.00 at 60 min. Myocardial planar and
> SPECT images were obtained with high quality. In conclusion,
> 99mTc-MIBI is a useful myocardial perfusion imaging agent.
>
> Publication Types:
>
> * Clinical Trial <javascript:AL_get(this, 'ptyp', 'Clinical
> Trial');>
> * English Abstract <javascript:AL_get(this, 'ptyp', 'English
> Abstract');>
>
>
> PMID: 1839318 [PubMed - indexed for MEDLINE]
>

> ----------
>
> *5: *Eur J Nucl Med. <javascript:AL_get(this, 'jour', 'Eur J Nucl
> Med.');> 1990;16(8-10):705-11. Related Articles
>
<http://www.ncbi.nlm.nih.gov/sites/entrez?Db=pubmed&DbFrom=pubmed&Cmd=Link&LinkName=pubmed_pubmed&LinkReadableName=Related%20Articles&IdsFromResult=2384106&ordinalpos=5&itool=EntrezSystem2.PEntrez.Pubmed.Pubmed_ResultsPanel.Pubmed_RVAbstract>,
> Links <javascript:PopUpMenu2_Set(Menu2384106);>
>
>
> *Segmental analysis of SPECT 99mTc-methoxy isobutyl isonitrile and
> 201Tl myocardial imaging in ischaemic heart disease.*
>
> *Hassan IM*
>
<http://www.ncbi.nlm.nih.gov/sites/entrez?Db=pubmed&Cmd=Search&Term=%22Hassan%20IM%22%5BAuthor%5D&itool=EntrezSystem2.PEntrez.Pubmed.Pubmed_ResultsPanel.Pubmed_RVAbstract>,
> *Mohammed MM*
>
<http://www.ncbi.nlm.nih.gov/sites/entrez?Db=pubmed&Cmd=Search&Term=%22Mohammed%20MM%22%5BAuthor%5D&itool=EntrezSystem2.PEntrez.Pubmed.Pubmed_ResultsPanel.Pubmed_RVAbstract>,
> *Constantinides C*
>
<http://www.ncbi.nlm.nih.gov/sites/entrez?Db=pubmed&Cmd=Search&Term=%22Constantinides%20C%22%5BAuthor%5D&itool=EntrezSystem2.PEntrez.Pubmed.Pubmed_ResultsPanel.Pubmed_RVAbstract>,
> *Sadek S*
>
<http://www.ncbi.nlm.nih.gov/sites/entrez?Db=pubmed&Cmd=Search&Term=%22Sadek%20S%22%5BAuthor%5D&itool=EntrezSystem2.PEntrez.Pubmed.Pubmed_ResultsPanel.Pubmed_RVAbstract>,
> *Nair M*
>
<http://www.ncbi.nlm.nih.gov/sites/entrez?Db=pubmed&Cmd=Search&Term=%22Nair%20M%22%5BAuthor%5D&itool=EntrezSystem2.PEntrez.Pubmed.Pubmed_ResultsPanel.Pubmed_RVAbstract>,
> *Belani N*
>
<http://www.ncbi.nlm.nih.gov/sites/entrez?Db=pubmed&Cmd=Search&Term=%22Belani%20N%22%5BAuthor%5D&itool=EntrezSystem2.PEntrez.Pubmed.Pubmed_ResultsPanel.Pubmed_RVAbstract>,
> *Yousef AM*
>
<http://www.ncbi.nlm.nih.gov/sites/entrez?Db=pubmed&Cmd=Search&Term=%22Yousef%20AM%22%5BAuthor%5D&itool=EntrezSystem2.PEntrez.Pubmed.Pubmed_ResultsPanel.Pubmed_RVAbstract>,
> *Abdel-Dayem HM*
> <http://www.ncbi.nlm.nih.gov/sites/entrez?Db=pubmed&Cmd=Search&Term=%22Abdel-Dayem%20HM%22%5BAuthor%5D&itool=EntrezSystem2.PEntrez.Pubmed.Pubmed_ResultsPanel.Pubmed_RVAbstract>.
>
> Department of Nuclear Medicine, Kuwait University.
>
> To study the potential usefulness of 99mTc-methoxy isobutyl
> isonitrile (99mTc-MIBI) as a substitute for 201Tl in assessing
> patients with ischaemic heart disease, 24 patients underwent 1 day
> rest and exercise 99mTc-MIBI single photon emission computerised
> tomography (SPECT) 1 week after SPECT exercise 201Tl. All patients
> were catheterized within 1 month after myocardial imaging. In 17
> patients, resting first pass radionuclide angiography (FPRNA) was

> performed with 99mTc-MIBI. The heart to lung ratio for 99mTc-MIBI
> and 201Tl was calculated both at rest and exercise. The segmental
> analysis for myocardial perfusion reveals that 87/96 segments (91%)
> were correctly classified by SPECT 201Tl and 84/96 segments (88%)
> were correctly classified by 99mTc-MIBI. A significant correlation
> was present between LVEF measured by 99mTc-MIBI FPRNA and contrast
> ventriculography (r = 0.85, P less than 0.0001). **The heart to lung**
> **ratio both at rest and exercise for 99mTc-MIBI is significantly**
> **higher than 201Tl (P less than 0.01 and less than 0.001**
> **respectively).** We conclude that 99mTc-MIBI is a promising agent for
> simultaneous evaluation of myocardial perfusion and cardiac function.
>
> Publication Types:
>
> * Comparative Study <javascript:AL_get(this, 'ptyp',
> 'Comparative Study ');>
> * Research Support, Non-U.S. Gov't <javascript:AL_get(this,
> 'ptyp', 'Research Support, Non-U.S. Gov\'t ');>
>
>
> PMID: 2384106 [PubMed - indexed for MEDLINE]
>
>
>

FW:

From: **RM Fleming** (rmfmd7@hotmail.com)
Sent: Thu 8/23/07 7:06 PM
To: Mike Hansen PD corrected (mike_hansen@fd.org)
Mike,

Everything being equal, everything ISN"T equal.

Yours,

Dr. Fleming

From: rmfmd7@hotmail.com
To: rmfmd7@hotmail.com
Subject:
Date: Wed, 22 Aug 2007 14:30:54 -0700

article

http://www.jhc.org/cgi/content/full/50/10/1351

FW: MPI washout

From: **RM Fleming** (rmfmd7@hotmail.com)
Sent: Thu 8/23/07 7:08 PM
To: Mike Hansen PD corrected (mike_hansen@fd.org)

Mike,

Regarding all the washout information:
>
"CONCLUSIONS: The myocardial washout rate of MIBI is
> thought to be a novel marker for the diagnosis of myocardial damage or
> dysfunction, providing prognostic information in patients with
> congestive heart failure."
>
>
> J Nucl Cardiol. 2007 Apr;14(2):215-20.Click here to read Links
> A novel clinical indicator using Tc-99m sestamibi for evaluating
> cardiac mitochondrial function in patients with cardiomyopathies.
> Matsuo S, Nakae I, Tsutamoto T, Okamoto N, Horie M.
>
> Department of Cardiovascular and Respiratory Medicine, Shiga
> University of Medical Science, Shiga, Japan. smatsuo@belle.shiga-med.ac.jp
>
> BACKGROUND: Technetium 99m sestamibi (MIBI) is a technetium-labeled
> myocardial perfusion agent that is taken up by the myocardial cell in
> proportion to myocardial regional blood flow and remains fixed in the
> myocardial cell over a long period of time. Previous studies have
> suggested that MIBI shows very slow myocardial clearance after its
> initial uptake in an animal model, which is related to mitochondrial
> function. This study was designed to test the hypothesis that MIBI
> washout can be used to evaluate the severity of congestive heart failure
> in comparison to other clinical parameters in patients with
> cardiomyopathies. METHODS AND RESULTS: After administration of MIBI, 61
> patients with nonischemic congestive heart failure (49 with dilated
> cardiomyopathy and 12 with other cardiomyopathies) and 7 normal control
> subjects were examined by electrocardiography-gated myocardial perfusion
> single photon emission computed tomography and planar data acquisition
> in the early and delayed phases (interval of 3 hours). Myocardial MIBI
> washout rates were calculated from the early and delayed planar images.
> Left ventricular function (systolic and diastolic) was analyzed by use
> of QGS data. Plasma levels of B-type natriuretic peptide and iodine 123
> metaiodobenzylguanidine (MIBG) parameters were also measured. Patients
> were followed up for a mean of 12 months (range, 1-19 months). As the
> severity of the New York Heart Association (NYHA) functional class
> advanced, the washout rate of MIBI increased (21.6% +/- 2.4% in those
> with NYHA class I [n = 23], 28% +/- 4% in those with NYHA class II [n =
> 27], and 35% +/- 5% in those with NYHA class III [n = 10]; P < .05,
> analysis of variance). The washout rate of MIBI was positively
> correlated with the level of B-type natriuretic peptide (r = 0.31, P <
> .05), end-diastolic volume (r = 0.396, P < .01), and end-systolic volume
> (r = 0.496, P < .01) and was negatively correlated with left ventricular
> ejection fraction (r = 0.523, P < .01), peak filling rate (r = 0.444, P
> < .01), and first-third ejection fraction (r = 0.414, P < .01). The
> parameters of MIBG scintigraphy were calculated as the heart-mediastinum

> count ratio (1.9 +/- 3) and washout rate (38% +/- 4%). We found a
> significant relationship between the washout rate of MIBI and the
> heart-mediastinum count ratio of MIBG (r = 0.51, P < .01). Patients with
> a higher washout rate of MIBI had a higher cardiac event rate (> or
> =28%) than those with a lower washout rate (<28%) (P < .05).
> CONCLUSIONS: **The myocardial washout rate of MIBI is thought to be a**
> **novel marker for the diagnosis of myocardial damage or dysfunction,**
> **providing prognostic information in patients with congestive heart failure.**
>
> PMID: 17386384 [PubMed - indexed for MEDLINE]
>
> --

FW: Use of two SPECT images with sestamibi - references for court - complete set

From: **RM Fleming** (rmfmd7@hotmail.com)
Sent: Tue 8/28/07 1:19 PM
To: Mike Hansen PD corrected (mike_hansen@fd.org)

3 attachments

ANM20-5-0...pdf (54.9 KB), ANM16-4-0...pdf (38.9 KB), 272.pdf (139.5 KB)

Mike,

The contention that sestamibi immediately sticks to the heart and does not change over time shows an elementary understanding of how this isotope (or any for that matter) works. Sestamibi requires blood flow (again, like any isotope, drug, et cetera) to deliver it to the target (in this case the heart and/or thymus). Once there it is taken across cell membranes into the mitochondria. Apparently (as you will see from these published papers), it does not remain STUCK. These papers CLEARLY demonstrate that changes over time not only occur; but, are important in detecting heart disease and subsequently treatment. Evidence bases medicine is so much better than voodoo!

> To organize dribs and drabs, here in one place as one complete set for
> the case are:
> 1. two full text research articles supporting diagnostic uses of a
> second image (attachments ANM*),
> 2. five additional abstracts (1-5 below) supporting diagnostic use of a
> second image,
> 3 four additional abstracts (6-9) on sestamibi kinetics (changes over time),
> 4 one full text article with graphics of sestamibi kinetics (attachment
> 272).
> .
> A. SECOND IMAGE USE
>
> 1.*** Diagnostic use of second image - full text not available in my
> library ***
> J Nucl Cardiol. 2007 Apr;14(2):215-20.Click here to read Links
> A novel clinical indicator using Tc-99m sestamibi for evaluating
> cardiac mitochondrial function in patients with cardiomyopathies.
> Matsuo S, Nakae I, Tsutamoto T, Okamoto N, Horie M.
>
> Department of Cardiovascular and Respiratory Medicine, Shiga
> University of Medical Science, Shiga, Japan. smatsuo@belle.shiga-med.ac.jp
>
> BACKGROUND: Technetium 99m sestamibi (MIBI) is a technetium-labeled
> myocardial perfusion agent that is taken up by the myocardial cell in
> proportion to myocardial regional blood flow and remains fixed in the
> myocardial cell over a long period of time. Previous studies have
> suggested that MIBI shows very slow myocardial clearance after its
> initial uptake in an animal model, which is related to mitochondrial
> function. This study was designed to test the hypothesis that MIBI
> washout can be used to evaluate the severity of congestive heart failure
> in comparison to other clinical parameters in patients with
> cardiomyopathies. METHODS AND RESULTS: After administration of MIBI, 61
> patients with nonischemic congestive heart failure (49 with dilated
> cardiomyopathy and 12 with other cardiomyopathies) and 7 normal control
> subjects were examined by electrocardiography-gated myocardial perfusion
> single photon emission computed tomography and planar data acquisition

> in the early and delayed phases (interval of 3 hours). Myocardial MIBI
> washout rates were calculated from the early and delayed planar images.
> Left ventricular function (systolic and diastolic) was analyzed by use
> of QGS data. Plasma levels of B-type natriuretic peptide and iodine 123
> metaiodobenzylguanidine (MIBG) parameters were also measured. Patients
> were followed up for a mean of 12 months (range, 1-19 months). As the
> severity of the New York Heart Association (NYHA) functional class
> advanced, the washout rate of MIBI increased (21.6% ± 2.4% in those with
> NYHA class I [n = 23], 28% ± 4% in those with NYHA class II [n = 27],
> and 35% ± 5% in those with NYHA class III [n = 10]; P < .05, analysis of
> variance). The washout rate of MIBI was positively correlated with the
> level of B-type natriuretic peptide (r = 0.31, P < .05), end-diastolic
> volume (r = 0.396, P < .01), and end-systolic volume (r = 0.496, P <
> .01) and was negatively correlated with left ventricular ejection
> fraction (r = 0.523, P < .01), peak filling rate (r = 0.444, P < .01),
> and first-third ejection fraction (r = 0.414, P < .01). The parameters
> of MIBG scintigraphy were calculated as the heart-mediastinum count
> ratio (1.9 ± 3) and washout rate (38% ± 4%). We found a significant
> relationship between the washout rate of MIBI and the heart-mediastinum
> count ratio of MIBG (r = 0.51, P < .01). Patients with a higher washout
> rate of MIBI had a higher cardiac event rate (> or =28%) than those with
> a lower washout rate (<28%) (P < .05). CONCLUSIONS: The myocardial
> washout rate of MIBI is thought to be a novel marker for the diagnosis
> of myocardial damage or dysfunction, providing prognostic information in
> patients with congestive heart failure.
>
> PMID: 17386384 [PubMed - indexed for MEDLINE]
>
> 2.*** Diagnostic use of second image - full text not available in my
> library ***
> J Nucl Cardiol. 1998 Mar-Apr;5(2):119-27. Related Articles, Links
> Click here to read
> Comment in:
>
> * J Nucl Cardiol. 1998 Mar-Apr;5(2):202-5.
>
>
> Prediction of functional recovery in acute myocardial infarction:
> comparison between sestamibi reverse redistribution and sestamibi/BMIPP
> mismatch.
>
> Fujiwara S, Takeishi Y, Atsumi H, Yamaki M, Takahashi N, Yamaoka M,
> Tojo T, Tomoike H.
>
> First Department of Internal Medicine, Yamagata University School of
> Medicine, Iida-Nishi, Japan. sfujiwar@med.id.yamagata-u.ac.jp
>
> BACKGROUND: It has been known that Tc 99m sestamibi/iodine 123
> betamethyliodophenylpentadecanoic (123I-BMIPP) (sestamibi/BMIPP)
> mismatch is an indicator of viable myocardium in acute myocardial
> infarction (AMI). We have reported that reverse redistribution of
> sestamibi in AMI indicates the patency of infarct-related artery and a
> preserved left ventricular function in the chronic stage. In this study
> we investigated the relationship between reverse redistribution of
> sestamibi and sestamibi/BMIPP mismatch in patients with AMI. METHODS:
> Twenty-three patients with AMI who received direct percutaneous

> transluminal coronary angioplasty underwent both BMIPP and sestamibi
> SPECT within 2 weeks after onset. Sestamibi images were obtained 1 hour
> (early) and 3 hours (delayed) after injection of sestamibi. BMIPP
> imaging was carried out 30 minutes after injection. The left ventricle
> was divided into 17 segments, and regional myocardial uptakes of the
> tracers in each segment were scored from 0 (normal) to 3 (no activity).
> A reverse redistribution pattern was defined as an increase of > or =1
> in the regional score at the delayed images. More reduced BMIPP uptake
> than sestamibi uptake in each segment was determined as sestamibi/BMIPP
> mismatch. Contrast left ventriculography was performed soon after
> revascularization and repeated 1 month later. RESULTS: Of 15 patients
> with sestamibi reverse redistribution, sestamibi/BMIPP mismatch was
> observed in 14 patients (93%), whereas mismatch was seen in only one of
> seven patients (14%) without reverse redistribution ($p < 0.01$). In
> patients with sestamibi reverse redistribution, regional scores of BMIPP
> agreed with those of early and delayed images of sestamibi in 51
> segments (46%) and in 92 segments (83%), respectively. In the chronic
> stage, both regional wall motion and left ventricular ejection fraction
> improved in patients with sestamibi reverse redistribution (wall motion
> score: 6.7 ± 2.4 vs 2.7 ± 2.1, $p < 0.01$; ejection fraction: $56\% \pm 7\%$ vs
> $64\% \pm 8\%$, $p < 0.01$), but not in those without reverse redistribution.
> CONCLUSION: Both reverse redistribution of sestamibi and sestamibi/BMIPP
> mismatch reflect the recovery of left ventricular function and thus
> imply myocardial viability in AMI. Because the presence of reverse
> redistribution of sestamibi agreed with that of sestamibi/BMIPP
> mismatch, additional BMIPP images can be replaced by the delayed images
> after a single injection of sestamibi.
>
> Publication Types:
>
> * Comparative Study
> * Research Support, Non-U.S. Gov't
>
>
> PMID: 9588663 [PubMed - indexed for MEDLINE] .
>
> 3. *** Diagnostic use of second image - full text not available in my
> library ***
> J Nucl Cardiol. 2006 Jan-Feb;13(1):64-8. Related Articles, Links
> Click here to read
> Usefulness of Tc-99m methoxyisobutylisonitrile scintigraphy for
> evaluating congestive heart failure.
>
> Sugiura T, Takase H, Toriyama T, Goto T, Ueda R, Dohi Y.
>
> Department of Internal Medicine, Enshu General Hospital, Hamamatsu,
> and Department of Internal Medicine and Molecular Science, Graduate
> School of Medical Sciences, Nagoya City University, Japan.
>
> BACKGROUND: Evidence is accumulating that technetium 99m
> methoxyisobutylisonitrile (MIBI) is not retained in the impaired
> myocardium. The purpose of this study was to determine whether the
> severity of congestive heart failure (CHF) can be evaluated by use of
> the washout rate (WR) of MIBI. METHODS AND RESULTS: Seventeen patients
> with CHF and ten healthy volunteers were enrolled in this study. MIBI
> and iodine 123 metaiodobenzylguanidine (MIBG) scintigraphy techniques

> were performed, and the WR was calculated. The blood was also sampled
> for the measurement of levels of brain natriuretic peptide, which is a
> powerful predictor of the severity of CHF. The WR of MIBI was higher in
> CHF patients (31.2%+/-6.3%) than in healthy volunteers (25.2%+/-4.7%)
> (P<.05). There were positive correlations between the WR of MIBI and
> brain natriuretic peptide levels (r=0.723, P<.0001) and a negative
> correlation between the WR of MIBI and the left ventricular ejection
> fraction (r=-0.545, P<.01). The WR of MIBI was correlated with that of
> MIBG (r=0.603, P<.01). CONCLUSIONS: MIBI scintigraphy is useful in
> evaluating the severity of congestive heart failure.
>
> Publication Types:
>
> * Comparative Study
> * Controlled Clinical Trial
>
>
> PMID: 16464718 [PubMed - indexed for MEDLINE]
>
> 4. *** Diagnostic use of second image - English full text not available ***
> Kaku Igaku. 2002 May;39(2):117-24. Related Articles, Links
>
> [Rest delayed images on 99mTc-MIBI myocardial SPECT as a noninvasive
> screen for the diagnosis of vasospastic angina pectoris]
>
> [Article in Japanese]
>
> Ono S, Yamaguchi H, Takayama S, Kurabe A, Heito T.
>
> Department of Radiology, Yamagata Prefectural Shinjo Hospital.
>
> Diagnostic usefulness of 99mTc-MIBI myocardial SPECT at rest was
> examined in 39 cases of coronary vasospastic angina pectoris who were
> diagnosed by a positive reaction to ergonovine provocation. SPECT was
> performed 45 minutes (early image) and 3 hours (delayed image) after the
> intravenous injection of approximately 600 MBq of MIBI. Decrease in
> accumulation was ranked by four defect scores (0: normal; 1: slight
> decrease; 2: moderate decrease; 3: severe decrease) and the total defect
> score was evaluated semiquantitatively. The washout rate between the
> normal area and the spasm area was also evaluated quantitatively using
> bull's eye. As a result, 15 cases (15/39; 38.4%) showed decreased
> accumulation in the early image and 27 cases (27/39; 69.2%) showed
> decreased accumulation in the delayed image. All of the cases which
> showed decreased accumulation in the early image had decreased
> accumulation in the delayed image as well. In 6 cases (6/34; 17.6%)
> showed ST wave changes during exercise ECG and 16 cases (16/34: 47%)
> showed decreased accumulation in the exercise myocardial SPECT. The
> washout rate of MIBI in the decreased accumulation area was
> significantly higher than that of the normal area. Of 32 ergonovine
> induced vasospastic area, 23 areas (72%) exhibited decreased
> accumulation in the delayed image for the same area. Decreased
> accumulation in the delayed image in MIBI was due to the enhanced
> washout, which, in turn, indicated declined retention of MIBI by
> mitochondrial membrane. In coronary vasospastic angina pectoris, spasm
> induced ischemia was thought to have an effect on the mitochondria. This
> study suggested that even with a normal exercise ECG and exercise

> myocardial SPECT, there's a strong possibility of coronary vasospastic
> angina pectoris if a decreased accumulation was found in the delayed
> image in the MIBI myocardial SPECT at rest. Hence, in diagnosing
> coronary vasospastic angina pectoris, the delayed image in the MIBI
> myocardial SPECT at rest was believed to be useful.
>
> Publication Types:
>
> * English Abstract
>
>
> PMID: 12058420 [PubMed - indexed for MEDLINE]
>
> 5. *** Diagnostic use of second image - full text not available in my
> library ***
> *J Nucl Cardiol. <javascript:AL_get(this, 'jour', 'J Nucl Cardiol.');>
> 2001 Nov-Dec;8(6):677-86. Related Articles
>
<http://www.ncbi.nlm.nih.gov/sites/entrez?Db=pubmed&DbFrom=pubmed&Cmd=Link&LinkName=pubmed_pubmed&LinkReadableName=Related%20Articles&IdsFromResult=11725264&ordinalpos=26&itool=EntrezSystem2.PEntrez.Pubmed.Pubmed_ResultsPanel.Pubmed_RVAbstract>,
> Links <javascript:PopUpMenu2_Set(Menu11725264);>
>
> Click here to read
>
> <http://www.ncbi.nlm.nih.gov/entrez/utils/fref.fcgi?PrId=3048&itool=Abstract-def&uid=11725264&db=pubmed&url=http://linkinghub.elsevier.com/retrieve/pii/S1071-3581%2801%2954260-9>
>
> *Detection of myocardial viability in ischemic-reperfused rat hearts
> by Tc-99m sestamibi kinetics.*
>
> *Liu Z*
>
>
<http://www.ncbi.nlm.nih.gov/sites/entrez?Db=pubmed&Cmd=Search&Term=%22Liu%20Z%22%5BAuthor%5D&itool=EntrezSystem2.PEntrez.Pubmed.Pubmed_ResultsPanel.Pubmed_RVAbstract>,
> *Johnson G 3rd*
>
>
<http://www.ncbi.nlm.nih.gov/sites/entrez?Db=pubmed&Cmd=Search&Term=%22Johnson%20G%203rd%22%5BAuthor%5D&itool=EntrezSystem2.PEntrez.Pubmed.Pubmed_ResultsPanel.Pubmed_RVAbstract>,
> *Beju D*
>
>
<http://www.ncbi.nlm.nih.gov/sites/entrez?Db=pubmed&Cmd=Search&Term=%22Beju%20D%22%5BAuthor%5D&itool=EntrezSystem2.PEntrez.Pubmed.Pubmed_ResultsPanel.Pubmed_RVAbstract>,
> *Okada RD*
>
>
<http://www.ncbi.nlm.nih.gov/sites/entrez?Db=pubmed&Cmd=Search&Term=%22Okada%20RD%22%5BAuthor%5D&itool=EntrezSystem2.PEntrez.Pubmed.Pubmed_ResultsPanel.Pubmed_RVAbstract>.
>
> William K. Warren Medical Research Institute of the University of
> Oklahoma Health Sciences Center, Tulsa , USA. zliu@u.arizona.edu
>
> BACKGROUND: The purpose of this study was to evaluate technetium 99m

> sestamibi (MIBI) kinetics in assessing myocardial viability in
> hearts subjected to different ischemia-reperfusion treatments,
> resulting in graded severity of injury. METHODS AND RESULTS: Sixteen
> isolated Krebs-Henseleit-perfused rat hearts were divided into 3
> groups: control (flow, 12 mL/min; n = 5), ischemic-reperfused with
> glucose (IR+G, n = 6), and ischemic-reperfused without glucose
> (IR-G, n = 5). MIBI (11.1 mBq [300 microCi]) was infused for 60
> minutes (uptake), followed by a 60-minute clearance. MIBI uptake
> (percent injected dose per gram) was significantly decreased in the
> IR+G (2.07 ± 0.31) and IR-G groups (2.03 ± 0.23; P = not
> significant with IR+G) compared with the control group (3.06 ±
> 0.25, P <.05). Fractional washout of MIBI was more rapid in the IR-G
> group (72.7% ± 3.9%, P <.05) than in the control (21.9% ± 1.9%)
> and IR+G groups (20.3% ± 1.7%). End retention (percent injected
> dose per gram) of MIBI in the IR-G (0.60 ± 0.12) and IR+G groups
> (1.60 ± 0.18) was significantly less than in the control group
> (2.30 ± 0.11, P <.05), respectively. The retention in the IR-G
> group was less than in the IR+G group (P <.05). Creatine kinase
> assay, triphenyltetrazolium chloride staining, and transmission
> electron microscopy analysis demonstrated more serious myocardial
> damage in the IR-G group than in the IR+G group. End MIBI activity
> was highly correlated with myocardial viability determined by
> triphenyltetrazolium chloride staining (r = 0.94; P <.05) and
> creatine kinase assay (r = -0.86; P <.05). CONCLUSIONS: Clearance of
> Tc-99m sestamibi is sensitive to metabolic states and may be used
> for assessment of ongoing myocardial damage.
>
> PMID: 11725264 [PubMed - indexed for MEDLINE]
>
> B. SESTAMIBI KINETICS
>
> 6. *** Rat study of sestamibi kinetics - full text not available in my
> library ***
> J Nucl Cardiol. 2001 Nov-Dec;8(6):677-86. Related Articles, Links
> Click here to read
> Detection of myocardial viability in ischemic-reperfused rat hearts
> by Tc-99m sestamibi kinetics.
>
> Liu Z, Johnson G 3rd, Beju D, Okada RD.
>
> William K. Warren Medical Research Institute of the University of
> Oklahoma Health Sciences Center, Tulsa , USA. zliu@u.arizona.edu
>
> BACKGROUND: The purpose of this study was to evaluate technetium 99m
> sestamibi (MIBI) kinetics in assessing myocardial viability in hearts
> subjected to different ischemia-reperfusion treatments, resulting in
> graded severity of injury. METHODS AND RESULTS: Sixteen isolated
> Krebs-Henseleit-perfused rat hearts were divided into 3 groups: control
> (flow, 12 mL/min; n = 5), ischemic-reperfused with glucose (IR+G, n =
> 6), and ischemic-reperfused without glucose (IR-G, n = 5). MIBI (11.1
> mBq [300 microCi]) was infused for 60 minutes (uptake), followed by a
> 60-minute clearance. MIBI uptake (percent injected dose per gram) was
> significantly decreased in the IR+G (2.07 ± 0.31) and IR-G groups (2.03
> ± 0.23; P = not significant with IR+G) compared with the control group
> (3.06 ± 0.25, P <.05). Fractional washout of MIBI was more rapid in the
> IR-G group (72.7% ± 3.9%, P <.05) than in the control (21.9% ± 1.9%) and

> IR+G groups (20.3% ± 1.7%). End retention (percent injected dose per
> gram) of MIBI in the IR-G (0.60 ± 0.12) and IR+G groups (1.60 ± 0.18)
> was significantly less than in the control group (2.30 ± 0.11, P <.05),
> respectively. The retention in the IR-G group was less than in the IR+G
> group (P <.05). Creatine kinase assay, triphenyltetrazolium chloride
> staining, and transmission electron microscopy analysis demonstrated
> more serious myocardial damage in the IR-G group than in the IR+G group.
> End MIBI activity was highly correlated with myocardial viability
> determined by triphenyltetrazolium chloride staining (r = 0.94; P <.05)
> and creatine kinase assay (r = -0.86; P <.05). CONCLUSIONS: Clearance of
> Tc-99m sestamibi is sensitive to metabolic states and may be used for
> assessment of ongoing myocardial damage.
>
> PMID: 11725264 [PubMed - indexed for MEDLINE]
>
> 7. *** Sestamibi kinetics - full text not available in my library***
> Eur J Nucl Med. 2000 Nov;27(11):1632-40. Related Articles, Links
> Click here to read
> A comparison of the overall first-pass kinetics of thallium-201 and
> technetium-99m MIBI in normoxic and low-flow ischaemic myocardium.
>
> Ayalew A, Marie PY, Menu P, Mertes PM, Hassan N, Danchin N, Olivier
> P, Karcher G, Bertrand A.
>
> Department of Nuclear Medicine, UPRES EA 2403, CHU-Nancy, France.
>
> The specific impact of ischaemia on the myocardial kinetics of
> thallium-201 and technetium-99m 2-methoxy-2-isobutylisonitrile (MIBI)
> remains a matter of debate. Using an isolated heart model perfused with
> red blood cell-enhanced perfusate, we compared the overall first-pass
> kinetics of 201Tl and MIBI under haemodynamically stable conditions of
> low-flow ischaemia (> 50% reduction in normal coronary flow and a > or =
> 20 mmHg fall in systolic contraction pressure, n = 10) and normoxia (n =
> 11). For both 201Tl and MIBI, we found that under ischaemic conditions
> (as compared with normoxia) there was a higher initial net extraction
> fraction (201Tl: 0.78 ± 0.03 vs 0.72 ± 0.06, P = 0.006; MIBI: 0.49 ±
> 0.10 vs 0.39 ± 0.11, P = 0.03), a lower clearance rate in the 30 min
> following extraction (% decrease in cardiac uptake: 201Tl: 30 ± 12 vs 47
> ± 14, P = 0.02; MIBI: 5 ± 5 vs 13 ± 11, P = 0.02) and a higher retention
> fraction at 30 min (201Tl: 0.54 ± 0.10 vs 0.39 ± 0.12, P = 0.004; MIBI:
> 0.46 ± 0.08 vs 0.33 ± 0.12, P = 0.01). Multivariate analyses, however,
> revealed that all myocardial kinetic parameters of both tracers were
> dependent only on coronary flow rates, without any additional
> significant impact of the presence of ischaemia or states of
> contractility or oxidative metabolism. We conclude that the myocardial
> fractional retention of both 201Tl and MIBI is strongly correlated with
> the decrease in coronary flow during ischaemia. This inverse
> relationship with coronary flow derives from both the flow-dependent
> increase in the initial myocardial extraction and the decrease in the
> subsequent myocardial washout of the tracers.
>
> Publication Types:
>
> * Comparative Study
> * Research Support, Non-U.S. Gov't
>

>
> PMID: 11105819 [PubMed - indexed for MEDLINE]
>
> 8. *** Sestamibi kinetics - full text not avilable in my library ***
> Eur J Nucl Med. 1995 Jan;22(1):49-55. Related Articles, Links
>
> Washout and redistribution between immediate and two-hour myocardial
> images using technetium-99m sestamibi.
>
> Richter WS, Cordes M, Calder D, Eichstaedt H, Felix R.
>
> Universitätsklinikum Rudolf Virchow, Freie Universität Berlin, Germany.
>
> The aim of this study was to assess whether a clinically relevant
> change in myocardial sestamibi activity could be documented within the
> first 120 min following injection (p.i.). In 17 patients planar anterior
> imaging of the heart was performed 5 min and 120 min p.i. During this
> time interval, mean decay-corrected myocardial activity declined to
> 77.9% ± 9.7% after stress and to 85.7% ± 7.9% after injection at rest (P
> < 0.05). In 19 patients with angiographically documented coronary artery
> disease, single-photon emission tomography was performed 5 min and 120
> min after injection at maximum stress. For analysis, sestamibi activity
> was scored semiquantitatively in six left ventricular segments.
> Furthermore, sestamibi uptake was assessed quantitatively using a
> circumferential profile method. In 35 of 114 segments the score improved
> within 120 min p.i. (early fill-in); in these segments relative
> sestamibi activity rose from 69.9% ± 22.5% to 74.5% ± 20.8% (P < 0.01).
> In five patients this early fill-in was the only sign of
> exercise-induced hypoperfusion. In 7 of 114 segments the score
> deteriorated 120 min p.i. (early tracer washout); in these segments
> relative sestamibi activity declined from 85.6% ± 9.9% to 80.1% ± 10.7%
> (P < 0.02). In three of four patients with early tracer washout the
> corresponding coronary artery was significantly narrowed. In conclusion,
> a global myocardial sestamibi washout was registered within the first
> 120 min after injection. A fill-in of initial defects as well as an
> early tracer loss could be detected in a relevant number of patients
> with chronic coronary artery disease during the first 2 h p.i.(ABSTRACT
> TRUNCATED AT 250 WORDS)
>
> Publication Types:
>
> * Comparative Study
>
>
> PMID: 7698155 [PubMed - indexed for MEDLINE]
>
>
> 9. ***Rat study of sestamibi kinetics - full text not yet available from
> publisher***
> Ann Nucl Med. 2007 Jul;21(5):267-73. Epub 2007 Jul 25. Related
> Articles, Links
> Click here to read
> Myocardial kinetics of (201)Thallium, (99m)Tc-tetrofosmin, and
> (99m)Tc-sestamibi in an acute ischemia-reperfusion model using isolated
> rat heart.
>

> Fukushima K, Momose M, Kondo C, Kusakabe K, Kasanuki H.
>
> Department of Cardiology, Tokyo Women's Medical University, Tokyo, Japan.
>
> OBJECTIVE: (201)Thallium (TL), (99m)Tc-tetrofosmin (TF), and
> (99m)Tc-sestamibi (MIBI) are extensively used as myocardial perfusion
> agents. The objective of the present study was to evaluate their
> kinetics under acute ischemia-reperfusion. METHODS: Isolated rat hearts,
> perfused by the Langendorff method at a constant flow rate of 10 ml/min,
> were allotted to normal control, mild ischemia, and severe ischemia
> groups, in which 20-min tracer wash-in was conducted followed by a
> 25-min tracer washout. No-flow ischemia (15 min for mild ischemia
> groups; 30 min for severe ischemia groups) was induced before conducting
> wash-in and washout in the ischemia groups. Whole-heart radioactivity
> was determined with an external gamma detector. Myocardial flow rate (K
> (1), ml/min) and clearance rate (k (2), min(-1)) were calculated.
> RESULTS: K (1TL), K (1TF), and K (1MIBI) decreased according to the
> severity of ischemia (K (1TL) 5.32 ± 0.53, 4.76 ± 0.70, and 1.44 ± 0.59;
> K (1TF) 3.80 ± 0.70, 2.73 ± 0.99, and 1.09 ± 0.45; and K (1MIBI) 3.45 ±
> 1.10, 2.15 ± 0.82, and 1.05 ± 0.13, in the normal control, mild, and
> severe ischemia groups, respectively). K (1) was significantly higher
> for TL than for the (99m)Tc tracers ($P < 0.05$), but the (99m)Tc tracers
> had equivalent K (1) values. k (2TL) increased significantly ($P < 0.05$)
> in the ischemia groups (k (2TL) 0.062 ± 0.013, 0.11 ± 0.045, and 0.12 ±
> 0.035), but showed no significant difference between the ischemia
> groups. k (2MIBI) and k (2TF) were significantly ($P < 0.05$) lower than k
> (2TL) and increased significantly ($P < 0.05$) in the severe ischemia
> group (k (2TF) 0.0056 ± 0.0022, 0.0037 ± 0.0015, and 0.024 ± 0.015; and
> k (2MIBI) 0.00072 ± 0.0011, 0.00038 ± 0.00076, and 0.042 ± 0.034). k
> (2MIBI) was significantly ($P < 0.05$) lower than k (2TF) in the normal
> control and mild ischemia groups. CONCLUSIONS: Tracer extraction was
> higher for TL than for the (99m)Tc tracers and all tracers decreased
> according to the severity of ischemia-reperfusion in the three tracer
> groups. The clearance kinetics of not only MIBI but also TF is possibly
> useful for the evaluation of the severity of ischemia, and the
> Langendorff method and a methodological approach by continuous
> determinations of radioactivity may serve for the quantitative analysis
> of tracer kinetic profiles.
>
> PMID: 17634844 [PubMed - in process]
>
> --

Yours truly,

Dr. Richard M. Fleming

a published paper documenting benefit of 4 minute and 60 minute post stress sestamibi

From: **RM Fleming** (rmfmd7@hotmail.com)
Sent: Wed 9/19/07 1:39 PM
To: Mike Hansen PD corrected (mike_hansen@fd.org)

1 attachment Windows Live OneCare

4 minuts ...pdf (1189.4 KB)

Dear Mike,

Let me know when we can talk to review the images I have. Please let me know if you received the Calkins letter. The attached article (published paper) shows benefit of 4 minute planar and 60 minute SPECT imaging of sestamibi following 'stress'.

Yours,

Dr. Fleming

Re:

From: **Gordon DePuey** (gdepuey@chpnet.org)
Sent: Mon 9/24/07 7:09 AM
To: RM Fleming (rmfmd7@hotmail.com)

1 attachment

Tc99m Ses...ppt (27.0 KB)

Attached is the slide on liver washout rates with Tc-99m sestamibi and apadenoson that I presebnted at the meeting in Arizona. Please note this is unpublished data. We have not pursued this research any further since BMS dropped their development this agent and associated clinical trials.
The Japanese have done quite a bit of research on myocardial redistribution of MIBI in patients with cardiomyopathy. However, to my knowledge, this concept has not taken hold in the U.S.. So you might include the Japanese journals in you literature search.

>>> RM Fleming <rmfmd7@hotmail.com> 9/14/2007 12:05 PM >>>

Dear Dr. DePuey,
Thank you for taking my telephone call a few minutes ago and for the updated email. I will try to briefly summarize my questions to you as well as our previous meeting.On August 8, 2006 at the Apadenoson 305 Investigator Meeting in Chandler, AZ you presented interesting research findings demonstrating changes in heart to liver uptake of sestamibi over a 90 minute period of time. Recently I have been reading information on washout kinetics of sestamibi comparing changes in isotope uptake by myocardial cells at 5 minutes and 2 hours post stress. We have seen this and would appreciate your thoughts on why the images show different uptake and the potential meaning of these different uptakes over time following dipyridamole, adenosine or other forms of cardiac stress. I have also been running across information on heart to lung ratios and cardiomyopathy. Unfortunately our VA is not doing a lot of research in this area and I feel like we am missing out on new developments. I can find most of the slides from the apadenoson talk, but not yours with the bar graphs. Do you have these slides and would you please email these to me. Do you also have thoughts on why images taken 5 minutes post stress may have different findings from those take 1 or 2 hours later as well as any other thoughts you might have on sestamibi.Appreciatively,Dr. Richard Fleming

Tc^{99m} Sestamibi Liver Washout with Apadenoson

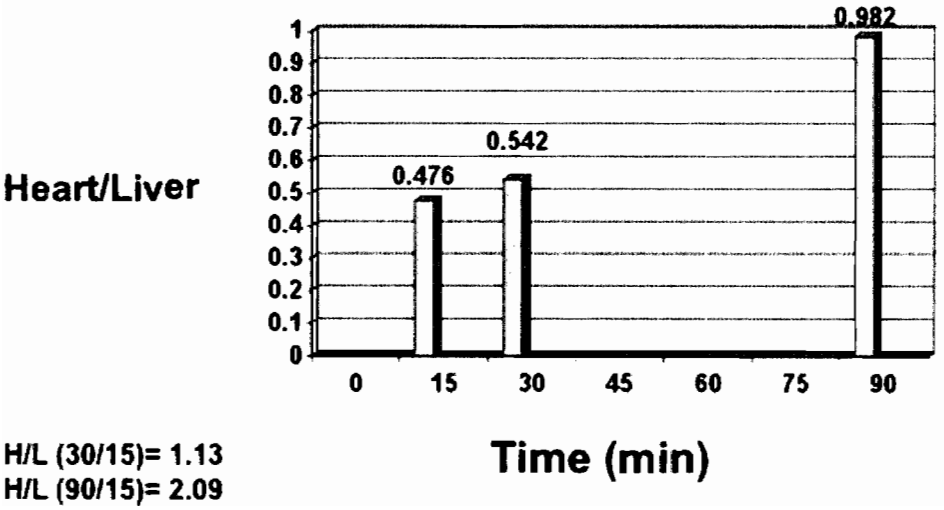

H/L (30/15)= 1.13
H/L (90/15)= 2.09

slide 21

From: **RM Fleming** (rmfmd7@hotmail.com)
Sent: Sat 5/31/08 2:17 PM
To: Mike Hansen PD corrected (mike_hansen@fd.org)
1 attachment
BMS 203 T...ppt (118.1 KB)

FYI.

The government was shown slide #21 from a research meeting a couple of years ago which showed increased sestamibi uptake by the heart over time (not in the first few minutes). They just wanted to ignore it.

Dr. Fleming

FW: Blumgart

From: **RM Fleming** (rmfmd7@hotmail.com)
Sent: Wed 7/09/08 6:09 PM
To: Mike Hansen PD corrected (mike_hansen@fd.org)

1 attachment

BlumgartY...pdf (824.1 KB)

Dear Mike,

Here is the original paper of Dr. Blumgart from 1925. Do I need to be in Lincoln on July 17th and have you confirmed Victoria's work dates showing she was only in the office for the first 2 weeks of the study. I am working on further publications on the Nuclear and its use with Cardiologists from the Berlin meeting.

Yours,

Dr. Fleming

P.S. Did you receive the email on Diane's arrest for child abuse sent to you yesterday?

RMF

Ghee!!!!!!!!!!!!!!!!!

From: **RM Fleming** (rmfmd7@hotmail.com)
Sent: Fri 8/29/08 8:00 PM
To: Mike Hansen PD corrected (mike_hansen@fd.org)
Cc: Gordon Harrington (gordon.harrington@uni.edu)
Bcc: rmfmd7@hotmail.com
Dear Mike & Gordon,

Ghee, I guess these guys are just as stupid as I am. Note their conclusion: "Conclusion Our proposed protocol demonstrates good correlation and agreement with standard method and even is superior in some cases especially for estimation of viability after MI. Regarding no need for the rest phase radiotracer injection and imaging, this protocol can be more convenient (except the need for close monitoring of the patient during LDD infusion), less time-consuming, less expensive and moreover with less radiation burden to the patients and personnel." In other words, when the did two sets of images after stress with (in this case dobutamine), they get better results than with the stress and rest approach. Go figure!!!!!!!!!

Dr. Fleming

http://www.ncbi.nlm.nih.gov/pubmed/18563624?ordinalpos=1&itool=EntrezSystem2.PEntrez.Pubmed.Pubmed_ResultsPanel.Pubmed_RVDocSum

1: Int J Cardiovasc Imaging. 2008 Jun 18. [Epub ahead of print] Links

Single Tc99m Sestamibi injection, double acquisition gated SPECT after stress and during low-dose dobutamine infusion: a new suggested protocol for evaluation of myocardial perfusion.

Fallahi B, **Beiki D**, **Gholamrezanezhad A**, **Mahmoudian B**, **Ansari Gilani K**, **Eftekhari M**, **Fard-Esfahani A**, **Mohseni Z**, **Saghari M**.
Research Institute for Nuclear Medicine, Tehran University of Medical Sciences, Shariati Hospital, North Kargar Ave., 14114, Tehran, Iran.

Background The ability of low dose dobutamine (LDD) has been established in exploiting the reserved contractility of ischemic myocardium. This study was designed to assess the value of a new protocol, with an additional stress imaging during LDD infusion instead of the rest images, for evaluation of coronary artery disease (CAD) and perfusion reversibility. Methods A total of 51 patients (42 men, 9 women; 57.2 +/- 11.3 years) were included in the study and underwent three sequential steps of imaging; the first step-stress gated SPECT with Tc-99m sestamibi, immediately followed by the second step-gated SPECT during constant infusion of 7.5 mug/kg/min dobutamine and finally the third step-rest phase scan following trinitroglycerine administration in the next day. The findings were interpreted using the images in three sets of display; first vs. second step-single injection-double acquisition gated SPECT before and during LDD (SIDAGS-LDD), first vs. third step-standard stress/rest protocol, and only first step-gated stress-only SPECT. In all cases, the Visual perfusion index of each protocols were calculated by summating the premeditated 5-point scale (5: normal, 4: completely reversible, 3: partially reversible, 2: nontransmural fixed and 1: transmural fixed defects) of 17 standard myocardial segments. The accuracy as well as the correlation and agreement of protocols for detecting perfusion abnormality and corresponding reversibility were statistically analyzed. Results Calculated sensitivity, specificity, positive predictive value, negative predictive value and accuracy regarding the presence of CAD in both SIDAGS-LDD and standard

protocols were 90.9% (40/44), 71.4% (5/7), 95.2% (40/42), 55.6% (5/9) and 88.2% (45/51), respectively. The extent and localization of perfusion abnormality with the new protocol were correlated well with standard method. The estimation of reversibility, however, was considerably improved by SIDAGS-LDD, especially in those with history of previous myocardial infarction (MI). Conclusion Our proposed protocol demonstrates good correlation and agreement with standard method and even is superior in some cases especially for estimation of viability after MI. Regarding no need for the rest phase radiotracer injection and imaging, this protocol can be more convenient (except the need for close monitoring of the patient during LDD infusion), less time-consuming, less expensive and moreover with less radiation burden to the patients and personnel.

PMID: 18563624 [PubMed - as supplied by publisher]

More, say it isn't so!

From: **RM Fleming** (rmfmd7@hotmail.com)
Sent: Fri 8/29/08 8:05 PM
To: Mike Hansen PD corrected (mike_hansen@fd.org)
Cc: Gordon Harrington (gordon.harrington@uni.edu)
Bcc: rmfmd7@hotmail.com

Again, all I can say is Ghee and these guys aren't even Iranian. These idiots are from Hartford, CT. Well their conclusion can't possible be right (Attenuation correction applied to studies **with stress-only** Tc-99m ECG-gated single photon emission computed tomography images **significantly increases the ability to interpret studies** as definitely normal or abnormal and **reduces the need for rest imaging**. These findings **may improve laboratory efficiency and diagnostic accuracy**.), because Kathy Palmer would be wrong and well that just can't be. Say it isn't so!

http://www.ncbi.nlm.nih.gov/pubmed/15173774?ordinalpos=3&itool=EntrezSystem2.PEntrez.Pubmed.Pubmed_ResultsPanel.Pubmed_RVDocSum

J Nucl Cardiol. 2004 May-Jun;11(3):273-81. Links
Comment in:
J Nucl Cardiol. 2004 May-Jun;11(3):239-41.

Clinical value of attenuation correction in stress-only Tc-99m sestamibi SPECT imaging.

Heller GV, Bateman TM, Johnson LL, Cullom SJ, Case JA, Galt JR, Garcia EV, Haddock K, Moutray KL, Poston C, Botvinick EH, Fish MB, Follansbee WP, Hayes S, Iskandrian AE, Mahmarian JJ, Vandecker W.
Nuclear Cardiology Laboratory, Hartford Hospital, CT 06102-5037, USA. gheller@harthosp.org

BACKGROUND: Attenuation artifact remains a substantial limitation to confident interpretation of images and reduces laboratory efficiency by requiring comparison of stress and rest image sets. Attenuation-corrected stress-only imaging has the potential to ameliorate these limitations. METHODS AND RESULTS: Ten experienced nuclear cardiologists independently interpreted 90 stress-only electrocardiography (ECG)-gated technetium 99m sestamibi images in a sequential fashion: myocardial perfusion imaging (MPI) alone, MPI plus ECG-gated data, and attenuation-corrected MPI with ECG-gated data. Images were interpreted for diagnostic certainty (normal, probably normal, equivocal, probably abnormal, abnormal, and perceived need for rest imaging). With stress MPI data alone, only 37% of studies were interpreted as definitely normal or abnormal, with a very high perceived need for rest imaging (77%). The addition of gated data did not alter the interpretations. However, attenuation-corrected data significantly increased the number of studies characterized as definitely normal or abnormal (84%, P <.005) and significantly reduced the perceived need for rest imaging (43%, P <.005). These results were confirmed by use of a nonsequential consensus interpretation of three readers. CONCLUSION: Attenuation correction applied to studies with stress-only Tc-99m ECG-gated single photon emission computed tomography images significantly increases the ability to interpret studies as definitely normal or abnormal and reduces the need for rest imaging. These findings may improve laboratory efficiency and diagnostic accuracy.

PMID: 15173774 [PubMed - indexed for MEDLINE]

rity of myocardial ischemia in patients with coronary artery stenosis. METHODS: Forty-three angina pectoris with coronary stenosis of greater than 75% were enrolled in this study. Myocardial perfusion SPECT images were obtained 1 and 6 hours after an intravenous injection of MIBI at rest. Stress myocardial perfusion SPECT images were also acquired after the injection of MIBI. And myocardial fatty acid metabolism images were obtained 30 minutes after the injection of BMIPP at rest. Myocardial perfusion SPECT images were divided into 20 segments which were semiquantitatively assessed according to a 4-level defect score scale: score 0 (normal) to score 3 (severely); then the extent score (ES) and severity score (SS) were calculated. RESULTS: The sensitivity for myocardial ischemia showed the highest rate at 88.3% with MIBI delayed SPECT. According to the coronary angiography findings, MIBI stress SPECT and MIBI delayed SPECT detected the severity and extent of ischemia with more sensitivity than MIBI early SPECT in 12 patients (group A) with stenosis of more than 75% but less than 90% ($p < 0.01$). Even though MIBI stress SPECT detected the severity and extent of ischemia in 31 patients (group B) with stenosis of more than 90% but less than 100%, there was no significant difference between MIBI stress SPECT and MIBI delayed SPECT. BMIPP SPECT revealed significant differences between group A and group B regarding the severity of myocardial ischemia. MIBI reverse redistribution was observed in 33 patients and no significant difference existed between groups A and B. CONCLUSIONS: Myocardial washout of MIBI was frequently observed in patients with angina pectoris and the detection accuracy for ischemia was high. MIBI imaging is considered useful for assessment not only of myocardial perfusion but also mitochondrial function. The imagings with BMIPP and delayed MIBI could serve to determine the severity of myocardial ischemia more accurately.
PMID: 16878707 [PubMed - indexed for MEDLINE]

Related Articles

- Detection of stunned myocardium in post-reperfusion cases of acute myocardial infarction. [Ann Nucl Med. 2003]
- Dipyridamole stress echocardiography and ultrasonic myocardial tissue characterization in predicting myocardial ischemia, in comparison with dipyridamole stress Tc-99m MIBI SPECT myocardial imaging. [Jpn Heart J. 2004]
- [Rest delayed images on 99mTc-MIBI myocardial SPECT as a noninvasive screen for the diagnosis of vasospastic angina pectoris] [Kaku Igaku. 2002]
- ReviewAn automatic approach to the analysis, quantitation and review of perfusion and function from myocardial perfusion SPECT images. [Int J Card Imaging. 1997]
- ReviewCardiac imaging with technetium 99m-labeled isonitriles. [J Thorac Imaging. 1990]

» See Reviews... » See All...

Display Show

- Write to the Help Desk
- NCBI | NLM | NIH
- Department of Health & Human Services
- Privacy Statement | Freedom of Information Act | Disclaimer

(hidden) (hidden) (hidden) (hidden) (hidden) (hidden)

--Forwarded Message Attachment--

NCBI
PubMed A service of the U.S. National Library of Medicine
and the National Institutes of Health

1: Ann Nucl Med. 2007 Jul;21(5):267-73. Epub 2007 Jul 25.

Myocardial kinetics of (201)Thallium, (99m)Tc-tetrofosmin, and (99m)Tc-sestamibi in an acute ischemia-reperfusion model using isolated rat heart.

Fukushima K, **Momose M**, **Kondo C**, **Kusakabe K**, **Kasanuki H**.
Department of Cardiology, Tokyo Women's Medical University, Tokyo, Japan.

OBJECTIVE: (201)Thallium (TL), (99m)Tc-tetrofosmin (TF), and (99m)Tc-sestamibi (MIBI) are extensively used as myocardial perfusion agents. The objective of the present study was to evaluate their kinetics under acute ischemia-reperfusion. METHODS: Isolated rat hearts, perfused by the Langendorff method at a constant flow rate of 10 ml/min, were allotted to normal control, mild ischemia, and severe ischemia groups, in which 20-min tracer wash-in was conducted followed by a 25-min tracer washout. No-flow ischemia (15 min for mild ischemia groups; 30 min for severe ischemia groups) was induced before conducting wash-in and washout in the ischemia groups. Whole-heart radioactivity was determined with an external gamma detector. Myocardial flow rate (K (1), ml/min) and clearance rate (k (2), min(-1)) were calculated. RESULTS: K (1TL), K (1TF), and K (1MIBI) decreased according to the severity of ischemia (K (1TL) 5.32 +/- 0.53, 4.76 +/- 0.70, and 1.44 +/- 0.59; K (1TF) 3.80 +/- 0.70, 2.73 +/- 0.99, and 1.09 +/- 0.45; and K (1MIBI) 3.45 +/- 1.10, 2.15 +/- 0.82, and 1.05 +/- 0.13, in the normal control, mild, and severe ischemia groups, respectively). K (1) was significantly higher for TL than for the (99m)Tc tracers ($P < 0.05$), but the (99m)Tc tracers had equivalent K (1) values. k (2TL) increased significantly ($P < 0.05$) in the ischemia groups (k (2TL) 0.062 +/- 0.013, 0.11 +/- 0.045, and 0.12 +/- 0.035), but showed no significant difference between the ischemia groups. k (2MIBI) and k (2TF) were significantly ($P < 0.05$) lower than k (2TL) and increased significantly ($P < 0.05$) in the severe ischemia group (k (2TF) 0.0056 +/- 0.0022, 0.0037 +/- 0.0015, and 0.024 +/- 0.015; and k (2MIBI) 0.00072 +/- 0.0011, 0.00038 +/- 0.00076, and 0.042 +/- 0.034). k (2MIBI) was significantly ($P < 0.05$) lower than k (2TF) in the normal control and mild ischemia groups. CONCLUSIONS: Tracer extraction was higher for TL than for the (99m)Tc tracers and all tracers decreased according to the severity of ischemia-reperfusion in the three tracer groups. The clearance kinetics of not only MIBI but also TF is possibly useful for the evaluation of the severity of ischemia, and the Langendorff method and a methodological approach by continuous determinations of radioactivity may serve for the quantitative analysis of tracer kinetic profiles.

PMID: 17634844 [PubMed - indexed for MEDLINE]

Related Articles

- 99mTc-sestamibi kinetics predict myocardial viability in a perfused rat heart model. [Eur J Nucl Med Mol Imaging. 2008]
- (201)Tl and (99m)Tc-MIBI retention in an isolated heart model of low-flow ischemia and stunning: evidence of negligible impact of myocyte metabolism on tracer kinetics. [J Nucl Med. 2002]
- Effects of acute ischemia and reperfusion on the myocardial kinetics of technetium 99m-labeled tetrofosmin and thallium-201. [J Nucl Cardiol. 1997]
- ReviewExperimental studies of the physiologic properties of technetium-99m agents: myocardial transport of perfusion imaging agents. [Am J Cardiol. 1990]
- ReviewExperimental studies of the physiologic properties of technetium-99m isonitriles. [Am J Cardiol. 1990]

» See Reviews... » See All...

Display Show

- Write to the Help Desk
- NCBI | NLM | NIH
- Department of Health & Human Services
- Privacy Statement | Freedom of Information Act | Disclaimer

(hidden) (hidden) (hidden) (hidden) (hidden) (hidden)

--Forwarded Message Attachment--

NCBI
PubMed A service of the U.S. National Library of Medicine
and the National Institutes of Health

My NCBI

1: Nucl Med Commun. 2008 Aug;29(8):686-9.

Preliminary clinical investigation of 99mTc-methoxyisobutylisonitrile washout rate in hypertrophic cardiomyopathy.

Sun M, Li Y, Li N, Liu H, Yin Y, Li D.

Nuclear Medicine Department, the No. 1 Hospital of China Medical University, Shenyang, Liaoning, China.

OBJECTIVE: The aim of this study was to investigate the changes in early and late washout rates of 99mTc-methoxyisobutylisonitrile (MIBI) in hypertrophic cardiomyopathy (HCM), and to analyze the relationships between early and late washout rates and the hypertrophic thickness of left ventricular (LV) wall. METHODS: The patients who were clinically diagnosed as positive for HCM underwent 99mTc-MIBI static planar and gated single-photon emission computed tomography (SPECT) imaging. Early (90 min after the intravenous injection) and late (4 h after the intravenous injection) washout rates of 99mTc-MIBI between HCM group and normal control group were compared. Linear correlation analysis was made between early and late washout rates and the hypertrophic thickness of LV wall measured by gated SPECT. RESULTS: The early and late washout rates of 99mTc-MIBI in normal control group were (18.90+/-3.70) and (31.27+/-4.04)%, respectively; and the washout rates in HCM group were (27.77+/-2.60) and (42.66+/-3.30)%, respectively. Significant statistical differences were observed in the early and late washout rates of 99mTc-MIBI between HCM group and normal control group ($t=-7.320$ and $t=-8.069$, both $P<0.01$). Correlations between early and late washout rates and the maximal hypertrophic thickness of LV wall obtained by gated SPECT were excellent ($r=0.611$, $P<0.05$; $r=0.873$, $P<0.01$, respectively). CONCLUSION: The early and late washout rates of 99mTc-MIBI in HCM group were significantly higher than those in normal control group, and both the early and late washout rates correlated well with the hypertrophic thickness of LV wall.

PMID: 18753820 [PubMed - indexed for MEDLINE]

Related Articles

- [Regional left ventricular contraction kinetics in patients with hypertrophic cardiomyopathy: investigation by ECG-gated myocardial SPECT with 99mTc-MIBI] [Kaku Igaku. 1996]
- Enhanced washout of 99mTc-tetrofosmin in hypertrophic cardiomyopathy: quantitative comparisons with regional 123I-BMIPP uptake and wall thickness determined by MRI. [Eur J Nucl Med Mol Imaging. 2003]
- Comparison of myocardial fatty acid metabolism with left ventricular function and perfusion in cardiomyopathies: by 123I-BMIPP SPECT and 99mTc-tetrofosmin electrocardiographically gated SPECT. [Ann Nucl Med. 2003]
- Sympathetic nervous function in patients with hypertrophic cardiomyopathy assessed by [123I]-MIBG: relationship with left ventricular perfusion and function. [Q J Nucl Med Mol Imaging. 2004]
- Comparison of cardiac sympathetic nervous function with left ventricular function and perfusion in cardiomyopathies by (123)I-MIBG SPECT and (99m)Tc-tetrofosmin electrocardiographically gated SPECT. [J Nucl Med. 2001]

» See All...

Display Show

- Write to the Help Desk
- NCBI | NLM | NIH
- Department of Health & Human Services
- Privacy Statement | Freedom of Information Act | Disclaimer

washout

From: **RM Fleming** (rmfmd7@hotmail.com)
Sent: Thu 11/27/08 1:28 PM
To: rmfmd7@hotmail.com

http://www.nuclearmed.com/pt/re/cnra/abstract.00003072-200804000-00003.htm;jsessionid=JvQGD8PLJQDY8L7XM2C1Rqv07YrGZjs2GsGG4kPg0S0qPLhGfRyG!-611447371!181195628!8091!-1

http://www.springerlink.com/content/j512324770724640/